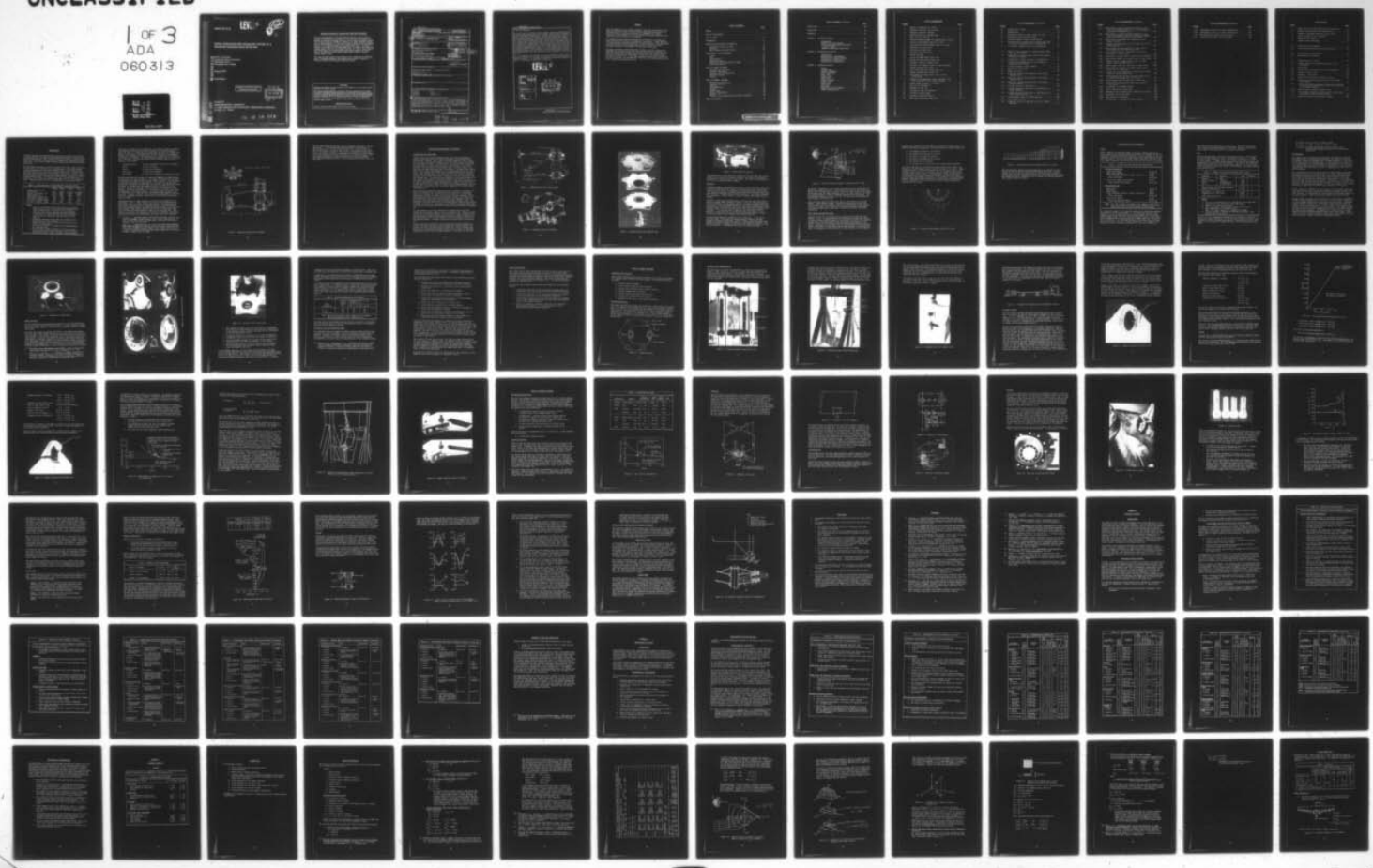
AD-A060 313 KAMAN AEROSPACE CORP BLOOMFIELD CONN F/G 1/3
DESIGN, FABRICATION AND LABORATORY TESTING OF A HELICOPTER COMP--ETC(U)
AUG 78 R J MAYERJAK DAAJ02-75-C-0013

UNCLASSIFIED USARTL-TR-78-16 NL

1 OF 3
ADA
060313



USARTL-IR-78-16

LEVEL II

DESIGN, FABRICATION AND LABORATORY TESTING OF A HELICOPTER COMPOSITE MAIN ROTOR HUB

Robert J. Mayerjak
Kaman Aerospace Corporation
Old Windsor Road
Bloomfield, Conn. 06002

August 1978

Final Report

AD A060313

Approved for public release;
distribution unlimited.

DDC
RECEIVED
OCT 24 1978
D

Prepared for

APPLIED TECHNOLOGY LABORATORY
U. S. ARMY RESEARCH AND TECHNOLOGY LABORATORIES (AVRADCOM)
Fort Eustis, Va. 23604

DDC FILE COPY

78 10 19 049

APPLIED TECHNOLOGY LABORATORY POSITION STATEMENT

This report was prepared by the Kaman Aerospace Corporation under the terms of Contract DAAJ02-75-C-0013. The objective of this effort was to demonstrate the feasibility of a helicopter composite main rotor hub by analysis and laboratory testing. This was achieved using the CH-54B as a baseline by the design, fabrication, measurement of radar detectability on a radar range, component testing, and 1/2-scale assembly testing of a hub consisting primarily of three graphite-epoxy plates. The hub was subjected to both static limit and fatigue design loads. The resultant hub design offers a weight savings of 24% and a cost savings of 52% with no credit for lower weight or 78% if weight savings are considered; demonstrates damage tolerance; and offers a reduction in radar cross section of 38% by shaping alone or 93% if a spray-on magnetic absorber is used.

This report has been reviewed by this Laboratory and is considered to be technically sound. The technical manager for this program was Mr. George T. Singley, III, Structures Technical Area, Aeronautical Technology Division.

DISCLAIMERS

The findings in this report are not to be construed as an official Department of the Army position unless so designated by other authorized documents.

When Government drawings, specifications, or other data are used for any purpose other than in connection with a definitely related Government procurement operation, the United States Government thereby incurs no responsibility nor any obligation whatsoever; and the fact that the Government may have formulated, furnished, or in any way supplied the said drawings, specifications, or other data is not to be regarded by implication or otherwise as in any manner licensing the holder or any other person or corporation, or conveying any rights or permission, to manufacture, use, or sell any patented invention that may in any way be related thereto.

Trade names cited in this report do not constitute an official endorsement or approval of the use of such commercial hardware or software.

DISPOSITION INSTRUCTIONS

Destroy this report when no longer needed. Do not return it to the originator.

UNCLASSIFIED

SECURITY CLASSIFICATION OF THIS PAGE (When Data Entered)

REPORT DOCUMENTATION PAGE

READ INSTRUCTIONS BEFORE COMPLETING FORM

1. REPORT NUMBER: USARTL-TR-78-16	2. GOVT ACCESSION NO.
3. RECIPIENT'S CATALOG NUMBER	
4. TITLE (and Subtitle): DESIGN, FABRICATION AND LABORATORY TESTING OF A HELICOPTER COMPOSITE MAIN ROTOR HUB	5. TYPE OF REPORT & PERIOD COVERED: FINAL REPORT
6. PERFORMING ORG. REPORT NUMBER	
7. AUTHOR(s): Robert J. Mayerjak	8. CONTRACT OR GRANT NUMBER(s): DAAJ02-75-C-0013
9. PERFORMING ORGANIZATION NAME AND ADDRESS: Kaman Aerospace Corporation, Old Windsor Road, Bloomfield, Connecticut 06002	10. PROGRAM ELEMENT, PROJECT, TASK AREA & WORK UNIT NUMBERS: 62209A 1F262209AH76 00 036 EK
11. CONTROLLING OFFICE NAME AND ADDRESS: Applied Technology Laboratory, U. S. Army Research and Technology Laboratories, Fort Eustis, Virginia 23604 (AVRADCOM)	12. REPORT DATE: August 1978
	13. NUMBER OF PAGES: 210
14. MONITORING AGENCY NAME & ADDRESS (if different from Controlling Office)	15. SECURITY CLASS. (of this report): Unclassified
	15a. DECLASSIFICATION/DOWNGRADING SCHEDULE

16. DISTRIBUTION STATEMENT (of this Report)

Approved for public release; distribution unlimited.

217 p.

17. DISTRIBUTION STATEMENT (of the abstract entered in Block 20, if different from Report)

18. SUPPLEMENTARY NOTES

19. KEY WORDS (Continue on reverse side if necessary and identify by block number)

Helicopter	Hub
Composites	CH-54B
Structures	Graphite-Epoxy
Main Rotor	

20. ABSTRACT (Continue on reverse side if necessary and identify by block number)

A new graphite-epoxy rotor hub was designed for the CH-54B helicopter, and a 1/2-scale structural model was fabricated. The hub consisted of three composite plates, which cooperated well to provide efficient load paths. The composite plates were simple and readily fabricated. As a result, the new hub promises improvements in cost, weight, damage tolerance, radar detectability, and maintainability when compared to conventional metal hubs.

DD FORM 1 JAN 73 1473 EDITION OF 1 NOV 65 IS OBSOLETE

UNCLASSIFIED

SECURITY CLASSIFICATION OF THIS PAGE (When Data Entered)

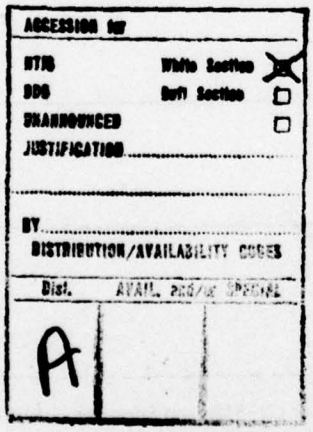
404 362
78 10 19 049

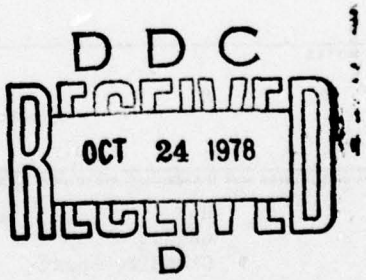
20. Abstract (continued)

Laboratory testing of the model and three component specimens demonstrated that the composite hub possessed good fatigue strength, static strength, tolerance to damage, and stiffness characteristics. Low radar detectability was also established by range testing. The component specimens were destructively tested to establish failure strengths. The strength tests upon the 1/2-scale assembly model were performance demonstration tests in which the model was first subjected to 1,000,000 cycles of the fatigue design load and then to a subsequent static test to limit loads. The model survived the tests without failure of its composite components or composite joints. However, midway through the fatigue test, a titanium fitting cracked and then several attachment bolts severed. The incident provided a demonstration of crack arrest by the composite material and of the damage tolerance of the hub assembly. It is concluded that the cracking of the titanium fittings can be prevented by local detail improvements at the bolt holes with negligible affect upon the weight and cost advantages of the new composite hub.

This report describes: the rationale for the configuration, the features of the design, the fabrication of the model, the results of the tests, and the advantages of the design. It is believed that helicopters of all weight classes can benefit from plate hubs of appropriate configurations.

LEVEL II





PREFACE

This investigation of an improved composite rotor hub was performed under Contract DAAJ02-75-C-0013, from the Applied Technology Laboratory, U. S. Army Research and Technology Laboratories (AVRADCOM), Fort Eustis, Virginia. George Singley, III, of the Applied Technology Laboratory, provided technical direction for the program.

The design work and structural testing were performed at the Kaman Aerospace Corporation facilities in Bloomfield, Connecticut. Robert Mayerjak of Kaman Aerospace Corporation was the principal engineer. The radar detection analyses and tests were performed by John Carver at the Tulsa, Oklahoma, Division of the Rockwell International Corporation.

The author gratefully acknowledges the foresight of Arthur Gustafson of AVRADCOM, who recognized early the potential advantages of composite rotor hubs and initiated the program; the contributions to the design, fabrication, and testing made by Frank Clark, Richard Hollrock, Howard Krauss, and Hector Pelletier, all of the Kaman Aerospace Corporation; and the work of Robert Gilchrist, who prepared the reliability and maintainability analyses presented as Appendices A and B.

TABLE OF CONTENTS

	PAGE
PREFACE	3
LIST OF ILLUSTRATIONS	7
LIST OF TABLES	11
INTRODUCTION	12
DESCRIPTION AND MECHANICS OF BEHAVIOR	16
Configuration and Load Paths	16
Materials	19
Metal Laminae Reinforced Joints	20
CHARACTERISTICS AND PERFORMANCE	23
Weight	23
Cost	24
Producibility	25
Damage Tolerance	26
Reliability and Maintainability (R&M)	29
Radar Detectability	31
TESTS OF ELEMENT SPECIMENS	32
Rationale and Objectives	32
Specimen Description	32
Apparatus and Instrumentation	33
Ultimate Strength	36
Fatigue	38
TESTS OF ASSEMBLY SPECIMEN	45
Rationale and Objectives	45
Loading Conditions	45
Apparatus	47
Instrumentation	48
Fatigue	50
Static Limit	54
Dynamic Compatibility	55
Strains	57
Effect of Test Results Upon Performance Estimates	60
OTHER APPLICATIONS	60

PRECEDING PAGE BLANK-NOT FILMED

TABLE OF CONTENTS (continued)

		PAGE
FUTURE PLANS		60
CONCLUSIONS		62
REFERENCES		63
APPENDIX A	RELIABILITY REPORT	65
	INTRODUCTION	65
	RELIABILITY DESIGN FEATURES	65
	FAILURE MODES AND EFFECTS CRITICALITY ANALYSIS (FMECA)	66
	INHERENT FAILURE RATE PREDICTIONS	73
APPENDIX B	MAINTAINABILITY REPORT	74
	INTRODUCTION	74
	MAINTAINABILITY REQUIREMENTS	74
	MAINTAINABILITY DESIGN FEATURES	75
	MAINTAINABILITY PREDICTION	75
	REPAIRABILITY CONSIDERATIONS	82
APPENDIX C	STRUCTURAL ANALYSIS	83
	SUMMARY	83
	INTRODUCTION	84
	MATERIAL PROPERTIES	85
	DESIGN CONDITIONS	95
	BLADE LOADS	97
	BEARING LOADS	102
	JOINT LOADS	105
	ELEMENT SPECIMEN	107
	TYPICAL JOINT	137
	UPPER PLATE	160
	LOWER PLATE	191
	PAN PLATE	194
	ROTOR SHAFT AND ATTACHMENTS	197
	DYNAMIC COMPATIBILITY	202

LIST OF ILLUSTRATIONS

FIGURE		PAGE
1	Existing titanium hub for CH-54B.	14
2	Composite plate hub, cross section.	17
3	Composite plate hub, assembly	17
4	Composite plate hub, exploded view.	18
5	Model ready for testing	19
6	Typical ultimate strength for graphite-epoxy, 0/$\pm$ 60. . .	20
7	In-plane finite-element model for a joint	21
8	Cross-sectional finite-element model for a joint.	22
9	Components for lower plate.	26
10	Construction of pan plate	27
11	Pan plate, after final cure	28
12	Element specimen.	32
13	Element specimen during static test	33
14	Element specimen during fatigue test.	34
15	Alignment clevis for element tests.	35
16	Procedure for aligning clevis on element specimen	36
17	Element specimen after static test.	37
18	Load versus deflection during static test	39
19	Element specimen after fatigue test	40
20	Relationship of fatigue test to S-N curve for titanium hub.	41
21	Position of specimen while under compressive load after failure of rod in loading cylinder.	43
22	Damage caused by impact of clevises	44
23	Test S-N for titanium hub	46
24	Schematic of test rig	47
25	Principle of test rig linkages.	48
26	Location of strain gages.	49
27	Location of deflection gages.	49
28	Plan view of pan plate with crack	50

LIST OF ILLUSTRATIONS (continued)

FIGURE		PAGE
29	Closeup view of crack	51
30	Severed bolts	52
31	Alternating strains at gages closest to crack	53
32	Deflections during limit load test.	56
33	Free-body diagram of lugs at lead-lag pin	57
34	Strain (μin./in.) versus time for twelve gages shown in Figure 26 during one cycle of fatigue test	58
35	An alternate composite plate hub configuration.	61
C-1	Typical ultimate strength for graphite epoxy, 0/±60, with τ_{xy} as ordinate.	89
C-2	Comparison of constant stress contours and constant stress-ratio contours	90
C-3	Presentation of margin of safety on strength plot	91
C-4	Typical finite-element used in joint analysis to determine bond stresses	92
C-5	Free-body diagram of rotor assembly	95
C-6	Geometry for blade loads.	98
C-7	Damper inclination.	99
C-8	Radial and vertical forces applied to hub during condition TW7F1	100
C-9	Radial and vertical forces applied to hub during condition TW7F2	100
C-10	Radial and vertical forces applied to hub during fatigue condition	101
C-11	Free-body diagram of lead-lag pin	102
C-12	Free-body diagram of hub plates at lead-lag pin for flight conditions	105
C-13	Free-body diagram of hub plates at lead-lag pin for static droop condition.	105
C-14	Finite-element model for element specimen	109
C-15	Local geometry at lug	127
C-16	Tangential stress at inner edge of hole for element specimen.	127

LIST OF ILLUSTRATIONS (continued)

FIGURE		PAGE
C-17	Relationship of axes for material properties to the local finite-element axes at point of calculation of stresses at outer edge of lug	129
C-18	Relationship of axes for material properties to the local finite-element axes for the composite elements around the edge of the largest steel lamina	130
C-19	Radial forces at perimeter of reinforced area for element specimen.	131
C-20	Composite stresses during static ultimate test of the element specimen.	132
C-21	Bond stresses and steel stresses for axial load of 4.24 kips/inch on prototype-sized joint	137
C-22	Finite-element model for calculation of bond-line stresses at a typical joint	139
C-23	Load pattern for upper plate, condition TW7F1 ultimate.	160
C-24	Finite-element model for lead-lag joints in upper plate	161
C-25	Tangential stress at inner edge of hole for upper plate, condition TW7F1 ultimate	186
C-26	Finite-element model for center hole in upper plate	188
C-27	Deflections and stresses for uniform radial load at center hole of upper plate.	189
C-28	Stresses and force intensities at center hole of upper plate for fatigue design loads.	189
C-29	Finite-element model of upper plate for prediction of strains during fatigue test of model hub.	190
C-30	Finite-element model for analysis of lower plate.	191
C-31	Allowable alternating stress versus mean stress for steel laminae	192
C-32	Lug geometry at scalloped flanges	193
C-33	Lug at lead-lag pin of pan plate.	194
C-34	Membrane forces in conical shell loaded at its vertex	196
C-35	Attachment lug on rotor shaft	199
C-36	Cone at top of rotor shaft.	201
C-37	Deformations of titanium hub from head moment	202

LIST OF ILLUSTRATIONS (continued)

FIGURE		PAGE
C-38	Approximate sections for present titanium hub	203
C-39	Approximate I_x and I_y for arm of titanium hub	205
C-40	Deformations of titanium hub from torque.	207
C-41	Torque in rotor shaft for titanium hub.	208

LIST OF TABLES

TABLE		PAGE
1	Weight and Cost of Rotor Hubs for Large Helicopters . . .	12
2	Weights, Existing Hub and New Composite Hub	23
3	Summary of Estimated Production Costs in 1976	24
4	Fatigue Performance of HT Graphite.	29
5	Design and Test Loads	46
6	Summary of Hub Stiffnesses.	55
A-1	Reliability Design Features	67
A-2	Failure Modes and Effects Criticality Analysis.	69
B-1	Maintainability Design Features	76
B-2	Maintainability Prediction.	78
C-1	Minimum Margins of Safety	83
C-2	Laminate Analysis for Graphite-Epoxy with 0 $\pm$ 60 Orientation	88
C-3	Design Loads.	95
C-4	Vertical Forces on Hub from Thrust and Head Moment. . . .	98
C-5	Summary of Bearing Loads.	104
C-6	Summary of Joint Loads.	106
C-7	Finite-Element Analysis of Element Specimen	111
C-8	Stresses in Composite Around the Edge of the Largest Steel Lamina.	130
C-9	Stresses and Margins of Safety in Composite at Locations of High Stress at the Ultimate Load in the Static Test of the Element Specimen	133
C-10	Finite-Element Analysis of Typical Joint.	141
C-11	Finite-Element Analysis of Lead-Lag Joint in Upper Plate for Ultimate Loads of Condition TW7F1	163
C-12	Margins of Safety for Rotor Shaft, Fatigue.	199

INTRODUCTION

The Army's efforts to reduce helicopter costs and to exploit the benefits of structures made from composite materials have lead to the search for an improved composite rotor hub. Composite rotor hubs appear to offer improvements in the following characteristics in comparison to conventional metal rotor hubs: cost, weight, damage tolerance, radar detectability, and maintainability.

The high costs and weights of large helicopter rotor hubs, shown in Table 1, were the impetus for the R&D effort reported herein. The trend in metal rotor-hub materials has been toward titanium alloys, which provide high strength-to-weight ratios and good corrosion resistances. Although lighter than their steel counterparts, titanium-alloy hubs are more costly. Conventional metal hubs are machined from large forgings, and they are plagued by high machining waste. For example, the CH-47C hub was machined in 77 operations from a 790-lb 4340-steel forging with over 80 percent machining waste. Composite materials offer the opportunity to avoid such losses.

TABLE 1. WEIGHT AND COST OF ROTOR HUBS FOR LARGE HELICOPTERS

	CH-46F	CH-47C	CH-54B	HLH
Number of Main Rotors	2	2	1	2
Hub Material	Steel	Steel	Titanium	Titanium
Design Gross Weight, lbs	21519	33000	47000	118000
Empty Weight, lbs	13435	20085	19685	64878
Hub Weight, Housing, lbs	100	225	345	1847
Hub Weight, Assembly, lbs	1002	1496	1799	7034
Hub Cost, Housing, $1000s	8.4	20.2	34.0	112.1
Hub Cost, Assembly, $1000s	109.9	102.4	144.6	511.2

NOTES:

1. Costs for the CH-46F, CH-47C and CH-54B were developed from the prices last paid for the items adjusted to the value of 1976 dollars. The HLH costs are estimates based upon HLH prototype aircraft experience adjusted to 1976 dollars. The CH-46F, CH-47C, and the CH-54B costs are for the 600th hub; the HLH costs, for the 250th hub.
2. Weights are measured values taken from weight and balance reports for each aircraft.
3. Weights and costs for the tandem rotor helicopters are totals for both rotors.
4. The rotor hub housing is defined as the finish-machined hub forgings alone.
5. The rotor hub assembly includes all rotor head components between the root-end fittings of the rotor blades and the rotor shaft, except for blade folding hardware.

Although it is believed that helicopters of all weight classes can benefit from composite rotor hubs, the need is greatest for large helicopters, where the size of a conventional hub approaches the limits of forging feasibility. Accordingly, the CH-54B rotor hub was selected as the baseline. The CH-54B is a heavy-lift helicopter that has a single main rotor with six articulated rotor blades. Its titanium-alloy main rotor hub is 5 feet wide and 1 foot high. The following partial list of design loads provides a measure of its strength:

Centrifugal force	82 tons (ultimate) from each of six blades
Thrust	64 tons (ultimate)
Torque	142 foot-tons (ultimate)
Head moment	94 foot-tons (ultimate)
Head moment	$\pm$ 33 foot-tons (fatigue) for millions of cycles

The existing production hub has two structural elements, an upper hub and a lower plate, as shown in Figure 1. The upper hub consists of six cantilevered beams that radiate from a hollow central cylinder. The lower plate is similarly star-shaped but much thinner. The upper hub and the lower plate share the support of centrifugal force and the transmission of torque. The beams of the upper hub alone support shears from lift and control moments. The hub is connected to the drive shaft by splines for torque transfer, cone seats for moment, and a threaded nut for axial force. This configuration is efficient in metal. It provides compact load paths that are appropriate for a dense material that exhibits high strength in any direction of loading. However, these conventional load paths are not well-suited for composite materials, which have low interlaminar tensile and shear strengths.

Pioneering efforts to apply composites to the CH-54B hub began in 1971 (References 1 and 2). These designs investigated the conventional load path, which can be called the center-beam concept. The design featured many narrow, continuous loops of composite material, each of which connected two opposite blades. The loops passed by the sides of a hollow central cylinder. When stacked together and enclosed by shear webs, these loops formed radial beams similar to those of the production hub. This concept is attractive in principle but difficult to implement efficiently. After detailed study, the investigators concluded that such a composite

---

1. Levenetz, B., COMPOSITE-MATERIAL HELICOPTER ROTOR HUBS, Whittaker Corporation; USAAMRDL Technical Report 73-14, Eustis Directorate, U. S. Army Air Mobility Research and Development Laboratory, Fort Eustis, Virginia, July 1973, AD 771973.

2. Faiz, R. L., A DESIGN ANALYSIS OF A CH-54B MAIN ROTOR HUB FABRICATED FROM COMPOSITE MATERIALS, Sikorsky Aircraft Division, United Aircraft Corporation; USAAMRDL Technical Report 73-49, Eustis Directorate, U. S. Army Air Mobility Research and Development Laboratory, Fort Eustis, Virginia, October 1973, AD 771966.

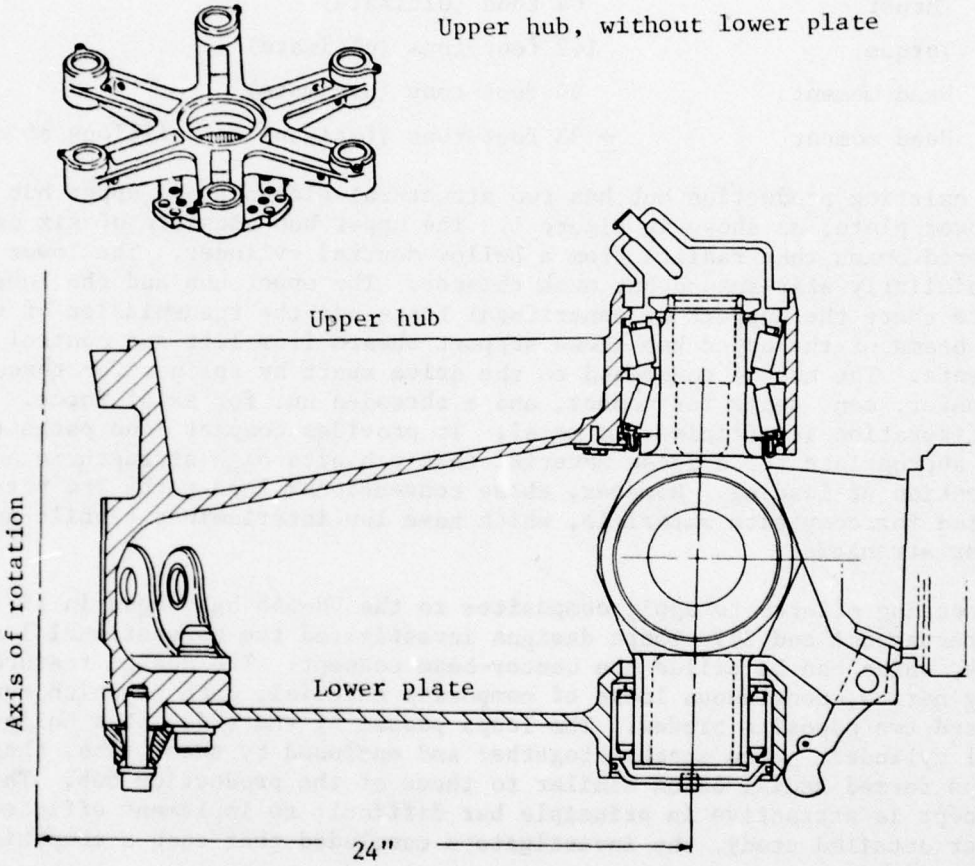


Figure 1. Existing titanium hub for CH-54B.

upper hub would weigh 270 lbs more than its titanium counterpart; 122 percent heavier. It is believed that the high weight is attributable in unknown proportions to at least three factors: the inherently low capacity of the concept to transfer shear forces, the parasitic weight introduced by the spacers required to accommodate the geometrical interferences of the loops, which must overlap each other at the central cylinder, and the design requirement that the hub should mate to existing hardware. These problems stimulated efforts to find an alternative concept for a composite hub.

DESCRIPTION AND MECHANICS OF BEHAVIOR

Configuration and Load Paths

Figures 2 and 3 show the new composite hub, which has been designed to match or exceed the static and fatigue strengths of the present CH-54B titanium hub. Figures 4 and 5 show a 1/2-scale structural model of this hub. The hub is called the composite plate hub (CPH) because it consists of three composite plates: an upper plate, a pan plate, and a lower plate. Both the upper and lower plates are flat except in areas of local reinforcement. The pan plate is cone-shaped, with a circular flange at its center and six lugs projecting from its perimeter. The upper plate and the pan plate are joined semipermanently by six bearing housing and nut assemblies. Each lead-lag pin is held into a bearing housing by the tapered-roller upper bearings and by the retaining nut at the top end of the lead-lag pin. The straight-roller lower bearings are free to float axially on the lead-lag pins. The lower plate is supported at its center by the bolts that connect the pan plate and the lower plate to the main rotor shaft. The dampers are supported by six bolts between the pan and the lower plates. In order to present the maximum information in a single view, the cross section shown in Figure 2 shows the center bolts as being coplanar with the damper bolts. Each center bolt is actually displaced 15° from the respective damper bolt.

Major loads are transmitted primarily by direct stresses and shears in the planes of the plates that lie along efficient load paths. Centrifugal forces are bridged by the lead-lag pins to the planes of the upper and lower plates. There, the loads are introduced into the composite plies by interleaved metal shims, which provide durable surfaces for contact with the housing and large areas of bond surface for the composite. Once in the plates, the loads spread out, following highly redundant paths. Load diffusion is fostered by the pattern of reinforcement, which provides equal-stiffness load paths for centrifugal forces in both a hexagonal ring direction from pin to adjacent pin and in a radial direction from pin to opposite pin.

The hub provides a new direct load path for torque without using the splines and the central cylinder of the conventional hub. Torque is transferred from a scalloped flange on the drive shaft to metal fittings in the pan and the lower plates by twelve bolts, which are loaded in double shear. Balanced-stiffness scarf joints transfer the torque from the fittings to the composite plates. The upper plate does not participate in the torque path.

Vertical shears are produced at the lead-lag pins by blade flapping and coning. The upper and the pan plates support the vertical shears by the truss action of the in-plane forces in each plate. Vertical shears also produce local interlaminar shearing stresses in the lugs of the pan plate. The lugs are thick to control these stresses. At the center of the hub,

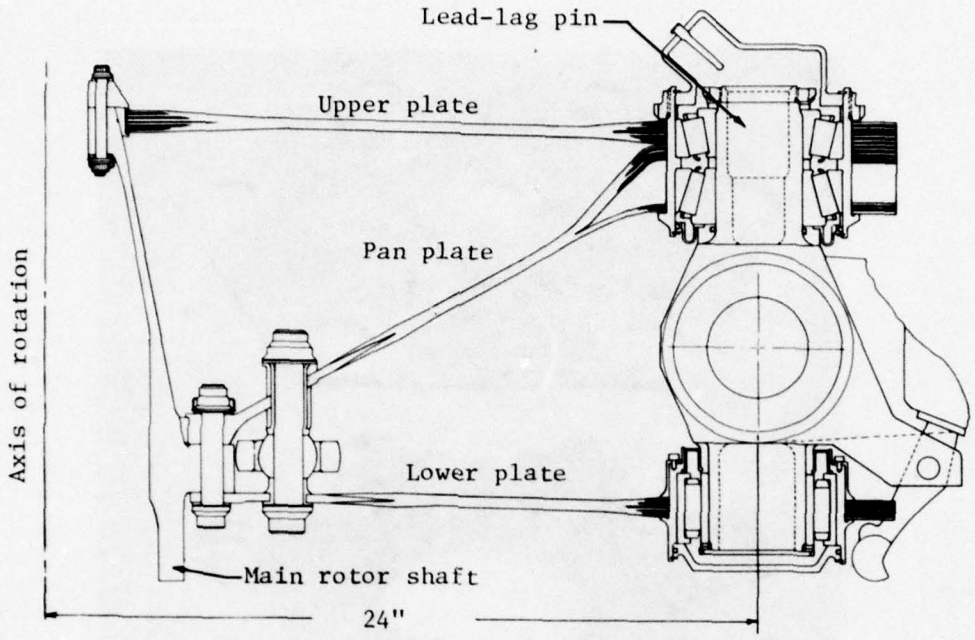


Figure 2. Composite plate hub, cross section.

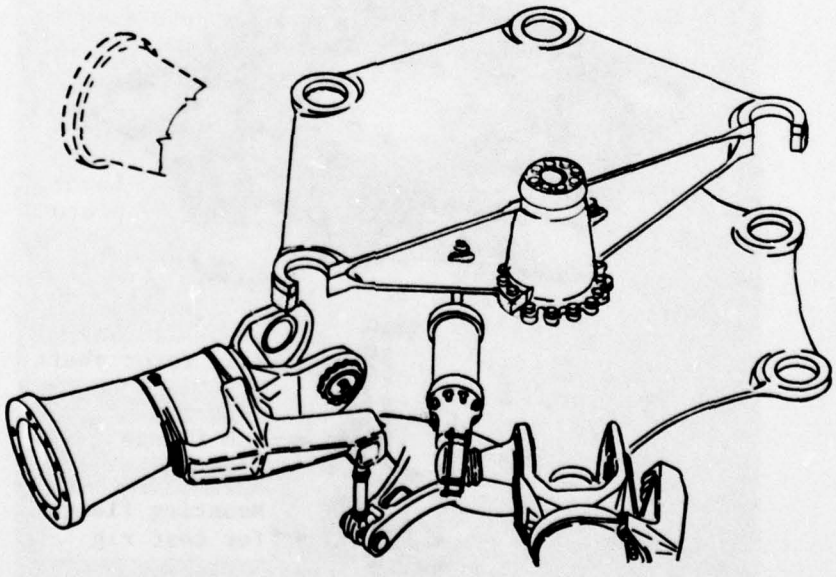


Figure 3. Composite plate hub, assembly.

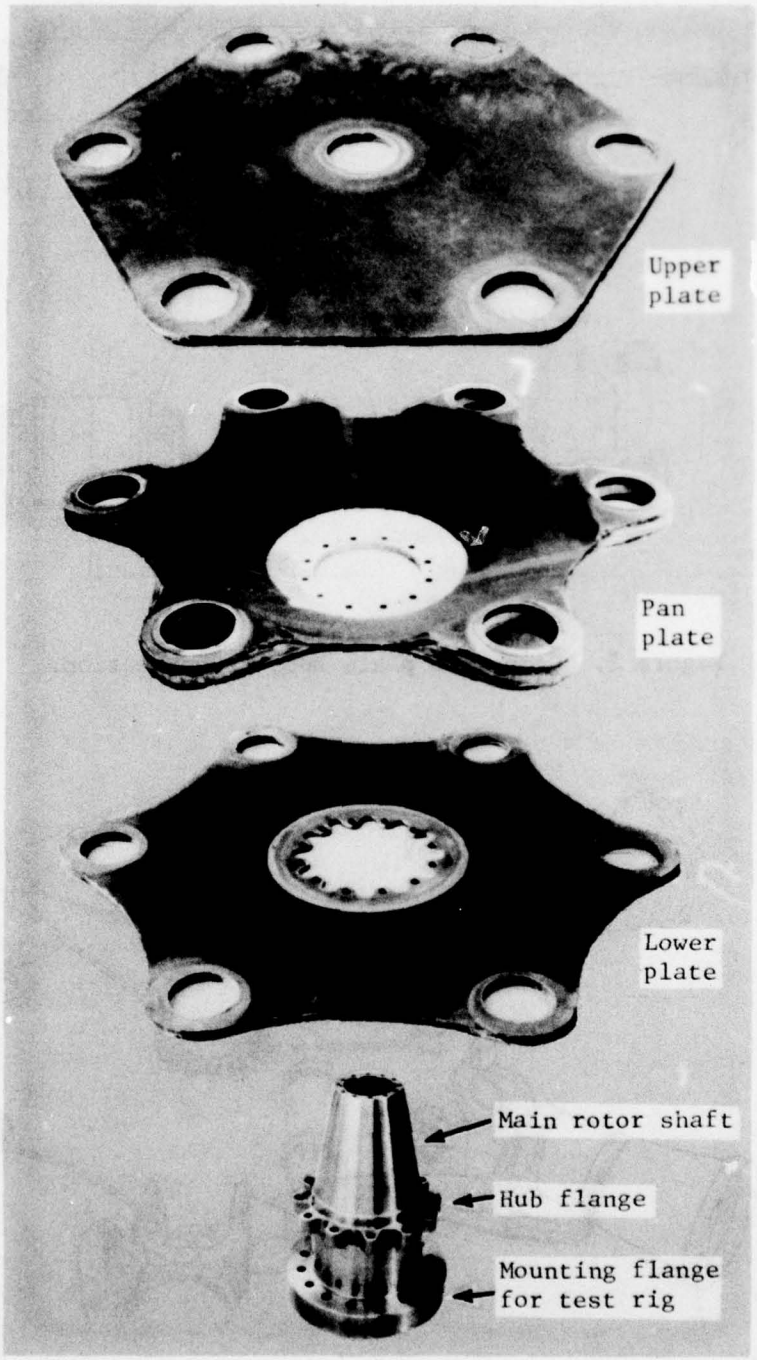


Figure 4. Composite plate hub, exploded view.

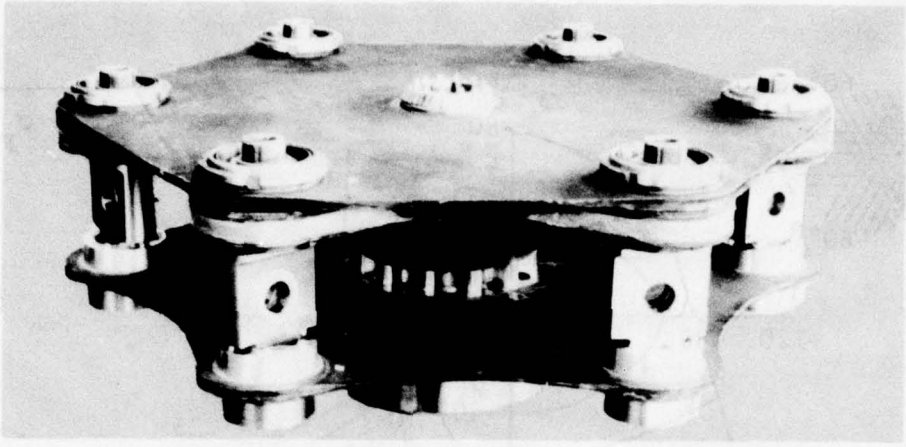


Figure 5. Model ready for testing.

three-quarters of the hub moment is transferred from the upper and the pan plates to the rotor shaft by radial forces at the cones; the remainder is transferred by vertical shears to the flange. The cones are preloaded as the bolts are tightened during assembly.

Materials

A constant-thickness construction with fibers in the 0 and $\pm$ 60° directions (0/$\pm$ 60) is used throughout because it provides multiaxial strength and economical fabrication. The orientation is appropriate for a six-bladed rotor because it produces a symmetrical pattern of reinforcement that coincides with the hexagonal-ring and center load paths. Four fiber materials were considered: S-glass, Kevlar, a blend of Kevlar and alumina, and all graphite.

Initially, S-glass was favored because of its low cost, low radar detectability, and high impact strength. However, glass was eliminated because of its low modulus, low fatigue strength in the quasi-isotropic state, and high density. Stress analysis showed that significant compressions (11 ksi, ultimate) would be developed in the plates under maneuver conditions; thus, buckling became a design consideration, and the low modulus of glass, a liability. It is believed that a composite hub using glass could be designed to weigh less than the existing titanium hub; however, a glass hub would be heavier than one made from advanced materials.

Of the advanced materials, graphite is most attractive. In the quasi-isotropic layup, it provides the highest absolute strength, specific strength, and specific stiffness. Figure 6 shows a calculated interaction diagram for typical ultimate strengths of a graphite-epoxy laminate. The ultimate strength was defined as the stress that causes the failure of the most critical ply. A limiting-strain theory of failure was used.

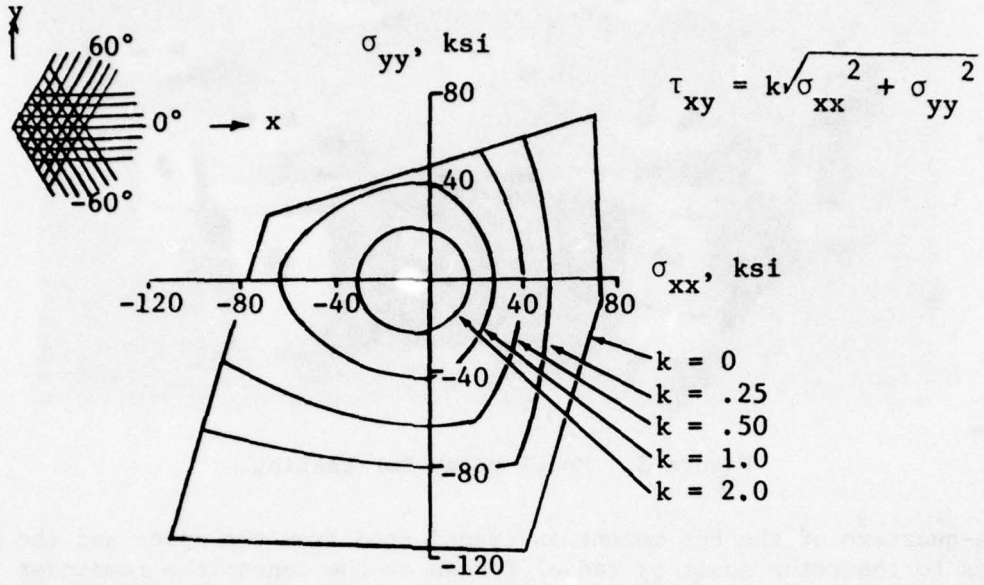


Figure 6. Typical ultimate strength for graphite-epoxy, 0/±60.

The metallic components of the new hub were selected with consideration to performance, weight, and cost. Titanium 6Al4V is used for the larger elements: the retaining ring at the top of the rotor shaft, the disc fittings, the housings, and the large retaining nuts at the upper housing. The cones are aluminum-bronze in order to minimize fretting of the drive shaft. The reinforcement laminae are steel, 17-7 PH. The fasteners and bushings are high-strength, low-alloy steel.

Glass cloth and adhesive doublers are used at each surface of the steel laminae. These doublers inhibit corrosion by isolating the steel from direct contact with the graphite, reduce local micro-kinks in the graphite fibers at the edges of the doublers by providing smoother, draped edges, and lower the edge peaks in the shear stresses by providing low modulus transitions.

Metal Laminae Reinforced Joints

Nineteen of the holes in the new hub are reinforced with multiple metal laminae. The metal laminae provide local multiaxial strength that allows the use of simple, low-cost layups for the plates and narrow edge distances at the holes. The metal laminae also provide wear resistance to local chafing, both in the holes and on the contacting faces adjacent to the holes. In addition, at the center hole of the top plate, the metal plates provide resistance to creep, which assures the retention of an initial preload. The integrity of these joints was a prime concern, and the program

included both analytical and experimental evaluations of these joints. Six modes of failure were considered. They were static and fatigue failures of:

1. The composite adjacent to the doublers
2. The composite at the edge of each hole
3. The metal at the edge of each hole
4. The bond of the composite to the metal
5. The tapered tip of the metal
6. The bearing surface within each hole (interlaminar splitting).

The first three modes of failure were analyzed using linear-elastic, two-dimensional, finite-element models lying in the plane of the plate. Figure 7 shows a portion of the finite-element model for the upper plate in the vicinity of the outer joint. The fourth and fifth modes of failure were analyzed using a linear-elastic, two-dimensional, finite-element model of a unit-width cross section through the thickness, as shown in Figure 8. The sixth mode, interlaminar splitting, is not amenable to direct analysis. However, the design inhibits splitting by subjecting the interlaminar surfaces to compressive preloads produced by initial clamp-up through the thickness at each joint.

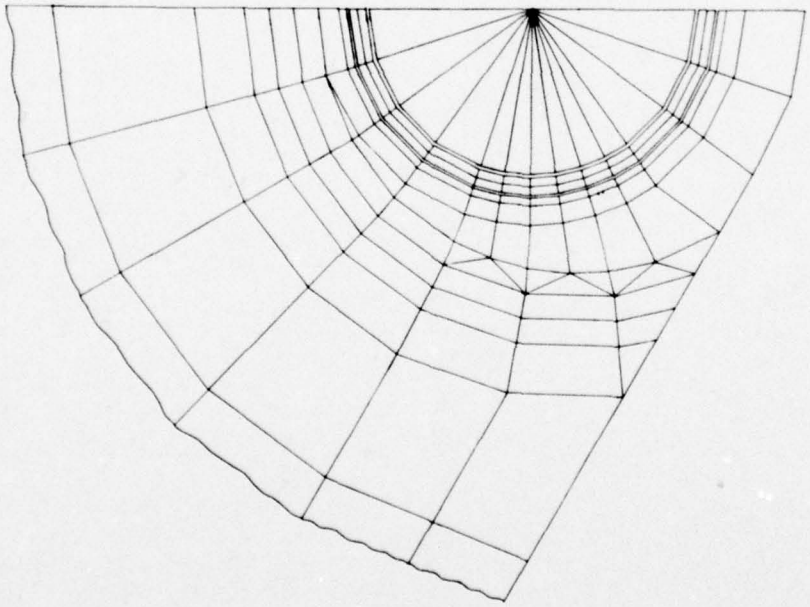


Figure 7. In-plane finite-element model for a joint.

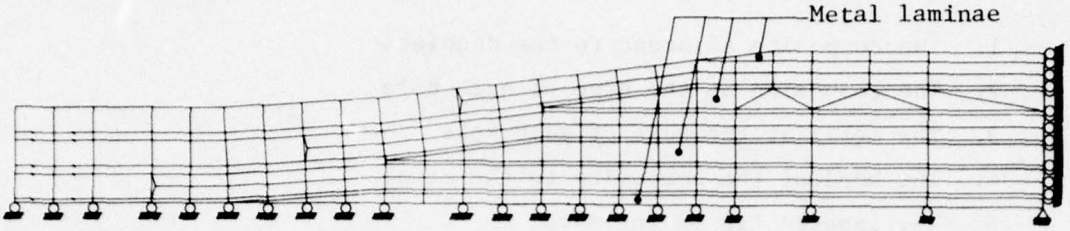


Figure 8. Cross-sectional finite-element model for a joint.

The finite-element analyses provided knowledge of the biaxial states of stress for both the static and the fatigue design conditions. Corresponding data to predict the strength of the materials when subjected to such stresses were not considered reliable, and the program included static and fatigue testing to determine failure strengths and working allowables under similar states of stress.

CHARACTERISTICS AND PERFORMANCE

Weight

Table 2 compares the estimated weight of the new composite hub and the actual weight of the existing CH-54B titanium hub. The weights for the new design were calculated from detail drawings. The new composite hub and its attachments are 99.30 lbs or 24 percent lighter than their existing production counterparts. The new rotor shaft is also lighter by 22.19 lbs. The total weight saving for the hub and rotor shaft is 121.49 lbs or 24 percent.

TABLE 2. WEIGHTS, EXISTING HUB AND NEW COMPOSITE HUB

EXISTING TITANIUM HUB	
Upper hub assembly	221.80 lbs
Lower plate assembly	70.50
Other (brackets, fasteners, rings, cones, etc.)	111.90
TOTAL, HUB PROPER	404.20 lbs
Rotor shaft segment (calculated)	97.03
TOTAL, HUB AND ROTOR SHAFT	501.23 lbs
NEW COMPOSITE HUB	
Upper plate	63.23 lbs
Pan plate	98.36
Lower plate	56.79
Other (housings, fasteners, rings, cones, etc.)	86.52
TOTAL, HUB PROPER	304.90 lbs
Rotor shaft segment	74.84
TOTAL, HUB AND ROTOR SHAFT	379.74 lbs

NOTE: The table includes the weight of the segment of shaft above Water Line 250.95 to provide a valid comparison because the shafts above that level are different in each design.

The calculated weights of the composite plates were confirmed by weighing the plates for the 1/2-scale model. It was found that the sum of the weights for the three plates was only 6 percent higher than the corresponding weight scaled from the calculated weight in Table 2. This difference is primarily due to excess resin in the model that would not be present in production. The individual weights of the upper, pan, and lower plates were 8.25, 13.20, and 7.45 lbs, respectively. The weight for the pan plate includes a calculated adjustment of 1.07 lbs to account for

differences between the model and the prototype. The model used glass-epoxy, rather than graphite-epoxy, for the filler blocks at the lugs and also 12 spacer rings that would not be needed in production.

Cost

Detailed estimates were prepared for the average price in a total production run of 1000 assemblies. Table 3 summarizes the results. It shows that the initial acquisition price is $17,144 per assembly with no credit for lower weight. If weight savings were valued at only $50 per pound, the adjusted price would be $11,070 per assembly. These prices are based upon a 1976 quotation of $35/lb for graphite-epoxy prepregs. If the cost were $20/lb (a projected future cost stated in 1976 dollars), the weight-adjusted price would be $7,712.

TABLE 3. SUMMARY OF ESTIMATED PRODUCTION COSTS IN 1976

Component	Material	Cost	See Note
Doublers	CRES	$ 171	1
Center Fittings	Titanium	1,088	
Plates	Graphite-Epoxy	5,140	2
Other	Miscellaneous	1,208	
TOTAL Material and Purchased Components		$ 7,607	
Material Burden Factor		x 1.524	3
Through Price for Materials		$11,593	4
Production Labor, 246.7 hrs.		5,551	5
TOTAL Production Price		$17,144	6

NOTES:

1. All costs are average costs for a production run of 1000 hubs.
2. Using 1976 prices, $35/lb for 5209 T-300 system.
3. Typical for a competitive company.
4. Price to customer, including all burdens and 12% profit.
5. Hours based upon an 87% learning curve.
   Rate = $22.50/hr, typical for a competitive company.
6. Price to customer, including all materials and labor, fully burdened with a 12% profit.

The price for the corresponding titanium hub is estimated to be $36,000. (This price includes $34,000 for the hub housing, as shown in Table 1, plus $2,000 for 59 lbs of fasteners and supports.) Based upon this price, the composite hub provides the following savings in initial acquisition costs alone:

52 percent, with no credit for weight savings

69 percent, if weight savings were valued at $50/lb

78 percent, if weight savings were valued at $50/lb, and if graphite were available at $20/lb in the acquisition time period.

Producibility

The composite hub is designed for uncomplicated and efficient production using hand layups of preimpregnated materials. The layups are exceptionally simple, permitting placement with a minimum of handling. Each plate is basically uniform in thickness; thus, a large steel-rule die can be used to cut the pattern, including the holes, in one operation. The plies and local reinforcements can then be stacked in sequence to achieve the desired interleaving. The bonding tool can have a standing plug at each hole to assist placement.

Such procedures were used to make the model for this program. They worked well on the first try, and no plates had to be remade. One fabrication technique that helped was the use of what can be called midplane tooling. Very simple tooling was used because each plate was made in two steps. First, one half was layed up and partially cured against a flat surface for the top and bottom plates and against a circular cone for the pan plate. Then, the other half was layed up upon the partially cured first half. This procedure also assured good alignment of fibers at the edges of the doublers and may be a significant contributor to the strength of the plates.

Figure 9 shows the components for the layup of the first half of the lower plate (the doublers for only one lug are shown). The graphite plies appear to be white in this figure because the protective handling surfaces are still in place. It can be seen that large steel-rule dies were used to cut the entire pattern. These patterns were handled and placed with ease.

Figure 10 shows the steps in the fabrication of the pan plate. Photograph A shows the bare midplane tool. The center titanium fitting was bolted to it, and a premade fiberglass block was placed at each corner. Photograph B shows a typical corner block. Photograph C shows the plate after the layup of the first graphite plies. It can be seen that the steel-rule die pattern covered only one-third of the total surface. This smaller pattern was used to insure the ease of handling during layup. The joints between the patterns were staggered. Photograph D is a closeup view of a corner showing a typical fiberglass-adhesive doubler and a steel lamina. Photograph E shows the start of the second layup using the partially cured first half as the mold. Figure 11 shows the completed pan plate.

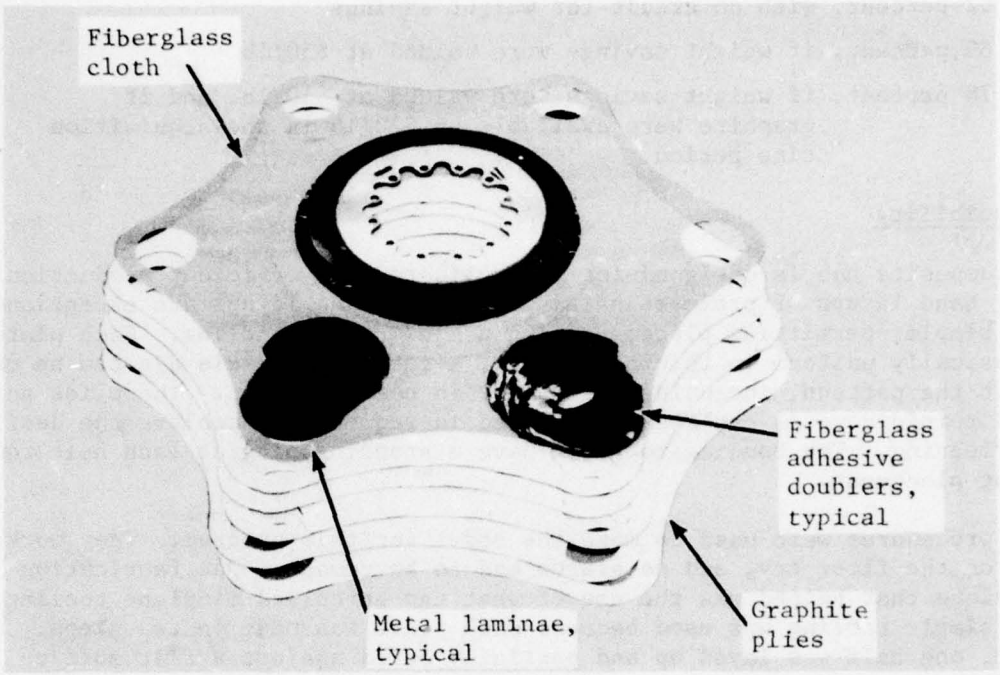


Figure 9. Components for lower plate.

Damage Tolerance

The new composite hub provides damage tolerance, in full accordance with Reference 3, which requires that no failure of a single structural element cause catastrophic failure or preclude safe, continuous flight to a normal destination.

The plate hub concept has inherent redundancy. Each plate can be envisioned as many closely spaced elements that provide multiple and alternative load paths. Such plates can survive arbitrarily located ballistically-induced holes. Olster and Roy performed tests to determine the ballistic survivability of graphite composites and observed that failure will not occur upon impact if the stress at the time of impact is below a characteristic threshold strength and that failure will not occur upon subsequent loadings of the damaged plate if the stresses are below a characteristic residual strength (Reference 4). Their conclusions included the following:

3. STRUCTURAL DESIGN REQUIREMENTS (HELICOPTERS), AR-56, Naval Air Systems Command, Department of the Navy, Washington, D. C., 1970.

4. Olster, E. F., and Roy, P. A., TOLERANCE OF ADVANCED COMPOSITES TO BALLISTICS DAMAGE, presented at the Third Conference on Composite Materials: Testing and Design; ASTM STP 546, American Society for Testing and Materials, Philadelphia, Pennsylvania, 1973.

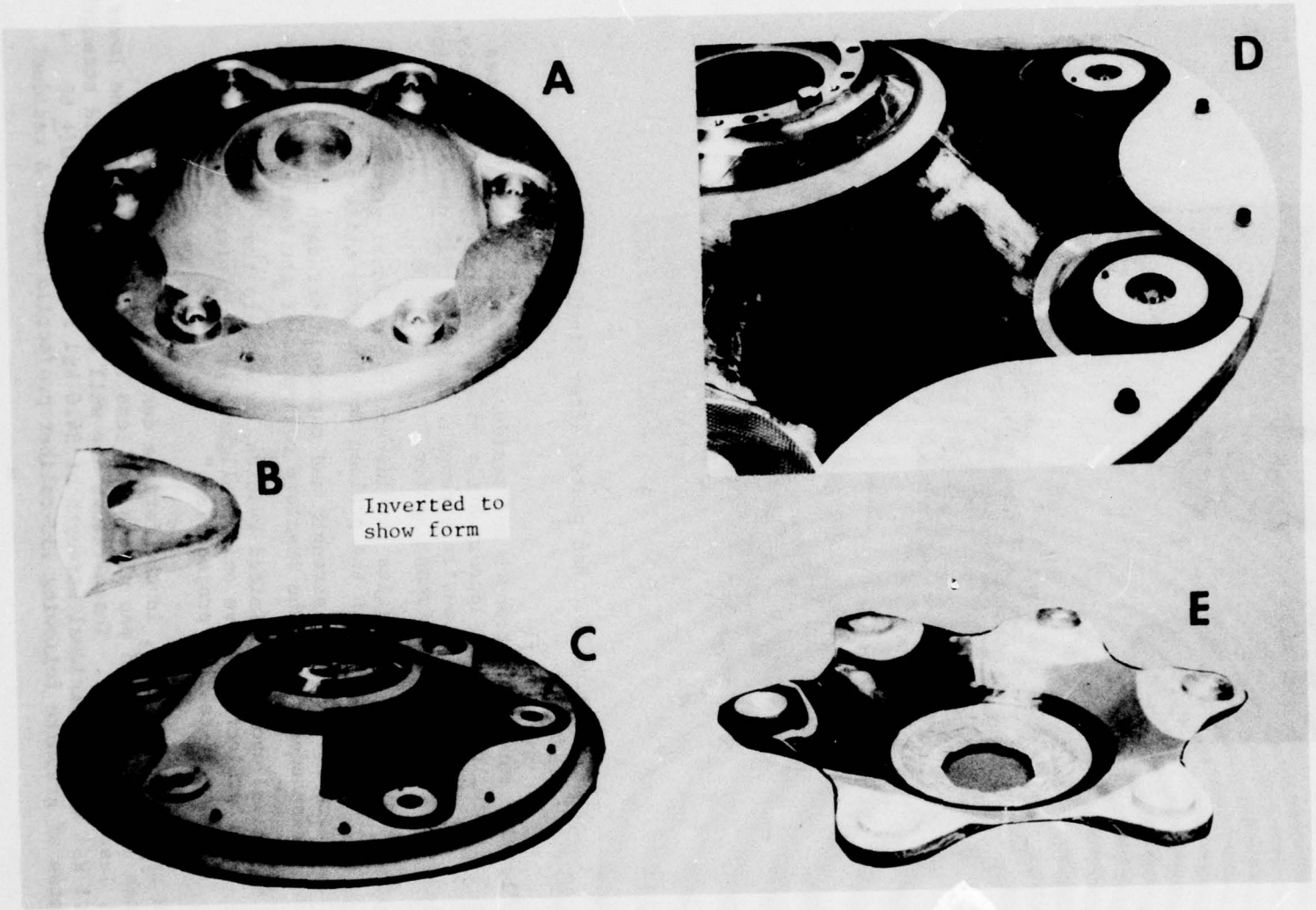


Figure 10. Construction of pan plate.

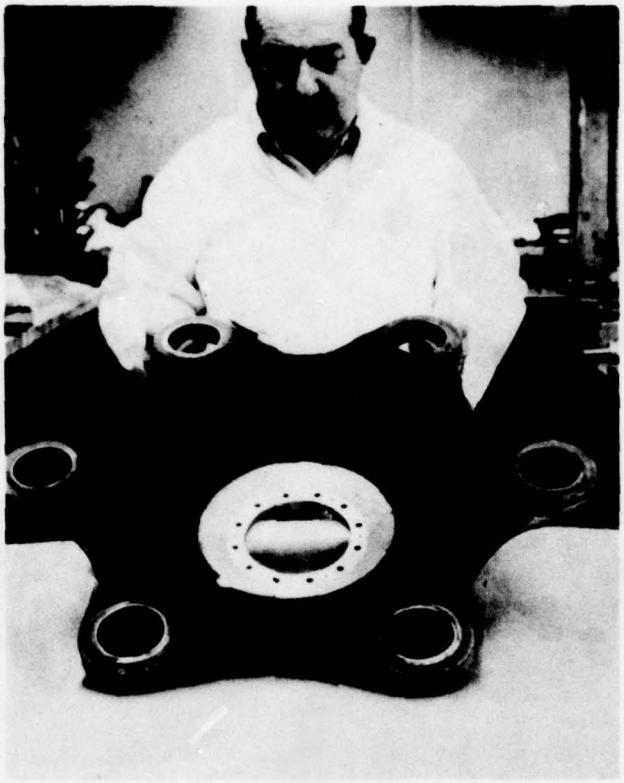


Figure 11. Pan plate, after final cure.

"1. The threshold strength and residual strength of the laminates were found to be approximately 55 and 62 percent, respectively, of the ultimate tensile strength, implying that ply orientation is the most significant factor.

2. For the two velocities considered, the residual strength was independent of both the preload and the projectile velocity.

3. Both the residual strength and threshold strength show a correspondence with the fracture toughness of the laminates.

4. Based upon very limited results, it appears that .50-caliber AP projectiles have only a slightly more detrimental effect than .30-caliber projectiles."

Stress analyses show that, in the fatigue design condition, the peak stresses in the upper and pan plates are less than 11 ksi and, in the lower plate, less than 13 ksi. These values are well below the threshold strength of 30.1 ksi and the residual strength of 34.6 ksi reported for 0/$\pm$ 60 laminates of graphite following .30-caliber projectile hits. A residual

strength of 29.4 ksi was reported following a .50-caliber hit. Thus, it is concluded that the plates will be ballistics tolerant even to multiple hits.

In addition, it is believed that there exists a significant survival probability following a 23-mm HE attack, but no convincing analysis is possible. Experimental verification would be necessary to establish 23-mm survivability.

It is also expected that significant fatigue performance will still be available following .30- or .50-caliber attack. Freeman and Kuebeler have shown that graphite structures exhibit fatigue strengths that are exceptionally large fractions of their static strengths, even in the presence of sharp notches (Reference 5). For example, high tensile strength (HT) graphite, with various fiber orientations, exhibits the fatigue performance shown in Table 4.

TABLE 4. FATIGUE PERFORMANCE OF HT* GRAPHITE

Fiber Orientation	Static Ultimate Stress ksi	Maximum Stress, R = 0.1 Notched K_t = 3	
		10^4 cycles	10^7 cycles
0	165	70	60
0, 90	110	63	60
0, 90, $\pm$ 45	58	32	30

*HT = High tensile strength, high elongation, intermediate modulus, intermediate cost, graphite fiber.

The expectation of good damage tolerance has been supported by experiences that are reported herein in sections describing the tests of the element specimens and the assembly specimen.

Reliability and Maintainability (R&M)

The composite plates are rugged and simple and have highly redundant load paths and low notch sensitivity. They are inherently reliable and maintainable. Therefore, the design efforts concentrated upon the joint details, where R&M had a great influence upon the final configuration. The simplicity, low parts count, and producibility of the composite design

5. Freeman, W. T., and Kuebeler, G. C., MECHANICAL AND PHYSICAL PROPERTIES OF ADVANCED COMPOSITES, presented at the Third Conference on Composite Materials: Testing and Design; ASTM STP 546, American Society for Testing and Materials, Philadelphia, Pennsylvania, 1973.

joints are, in large measure, the results of repeated design changes to improve reliability and maintainability. A desirable consequence was a corresponding lowering of cost.

The maintainability requirements were stated as the following qualitative goals and objectives:

1. Minimize the maintenance manhours per flight-hour for both scheduled maintenance and unscheduled corrective maintenance
2. Minimize the probability of maintenance being required above field level
3. Ensure the simplicity of installation and removal
4. Ensure that there are positive removal procedures, even in the presence of extensive corrosion or fretting
5. Ensure that the installation and removal of the hub assembly requires no disassembly of hub components
6. Ensure the ease of inspection of critical parts
7. Provide maximum accessibility to mounting hardware
8. Ensure that all components subject to corrosion, fretting, or wear can be refurbished or replaced
9. Ensure that the maintenance manpower requirements will be compatible with the maintenance program for the CH-54B
10. Ensure that the skill levels required for field repairs are compatible with the training of the Army personnel.

The hub is installed and removed as a complete unit, with no buildup or disassembly at the Direct Support level. For installation, first the damper bolts are loosened two turns, then the hub is lowered over the drive shaft until the bottom plate approaches the flange on the drive shaft. The hub is turned to align the scallops, lowered to rest on the cone seats, and turned again to align the bolt holes, and then, the lower bolts are inserted. The ring at the top of the shaft is positioned, and the upper bolts are inserted. All bolts are then torqued to standard levels. As the bolts tighten, they draw the aluminum-bronze cones down to positive stops and induce a tight preload.

The removal of the hub is also easy. The upper and lower cone seats are cut at an angle of 14 degrees, which will normally allow self-release. In the event of abnormal seizing due to corrosion or fretting, positive removal is still assured by provisions for forcing the separation by applying hydraulic pressure to the upper cone and a mechanical jack to the lower cone. Assembly and removal require only common hand tools. The mounting bolts are all easily accessible.

More detailed information about the maintainability and reliability of the composite plate hub is presented in Appendices A and B.

Radar Detectability

Radar cross section (RCS) measurements were made using 1/2-scale models of the present production hub and several versions of the new plate hub. These versions included hubs constructed from bare, nonconducting fiberglass composites; from nonconducting composites selectively coated with a magnetic absorber; and from a conducting composite. The latter was simulated by covering the fiberglass model with aluminum foil. The magnetic absorber material is a special paint.

The new plate hub provides reduced radar detectability to the following extents:

1. A 38-percent reduction in RCS was achieved by shape alone, comparing the current hub and the plate hub covered with aluminum.
2. A 76-percent reduction in RCS was achieved through the combination of shape and the use of nonconducting composites.
3. A 93-percent reduction in RCS was achieved through the combination of shape, nonconducting composite materials, and the application of the magnetic absorber.
4. The use of conductive (graphite) composites will change the RCS treatments required. It will be necessary to cover larger areas with the magnetic absorber.

TESTS OF ELEMENT SPECIMENS

Rationale and Objectives

Three element specimens were tested to destruction to verify the strength of a typical joint reinforced by metal laminae. The objectives were to determine:

1. Ultimate static strength
2. Static failure modes and characteristics
3. Failure and survivable static ultimate stresses
4. Fatigue strength and variability
5. Fatigue failure modes and characteristics
6. Failure and survivable fatigue stresses
7. Adequacy of the joint for the loads of the hub.

Specimen Description

The element specimens were large flat plates, 20.4 inches long and 15 inches wide. Both ends of the specimens were test areas that contained a duplication (in 1/2 scale of the prototype for the CH-54B) of the lag-pin joint in the top plate. The planform of a specimen is shown in Figure 12, superimposed over the top plate of the composite hub. Finite-element analyses showed that the stresses in the vicinity of the joints of the element specimen are generally similar in pattern and magnitude to those in the hub for scaled loads.

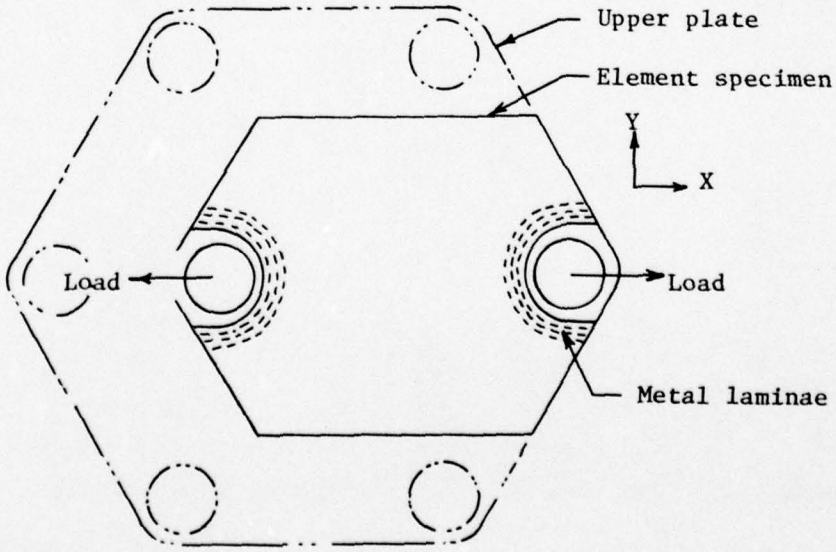


Figure 12. Element specimen.

Apparatus and Instrumentation

The static test to failure was performed in a universal testing machine. Figure 13 shows the setup. The rate of loading was held constant by the automatic platen motion system of the machine. The loads and platen motions were recorded using the automatic plotting system. A contact microphone was attached to the loading clevis, and acoustic emissions were amplified and recorded.

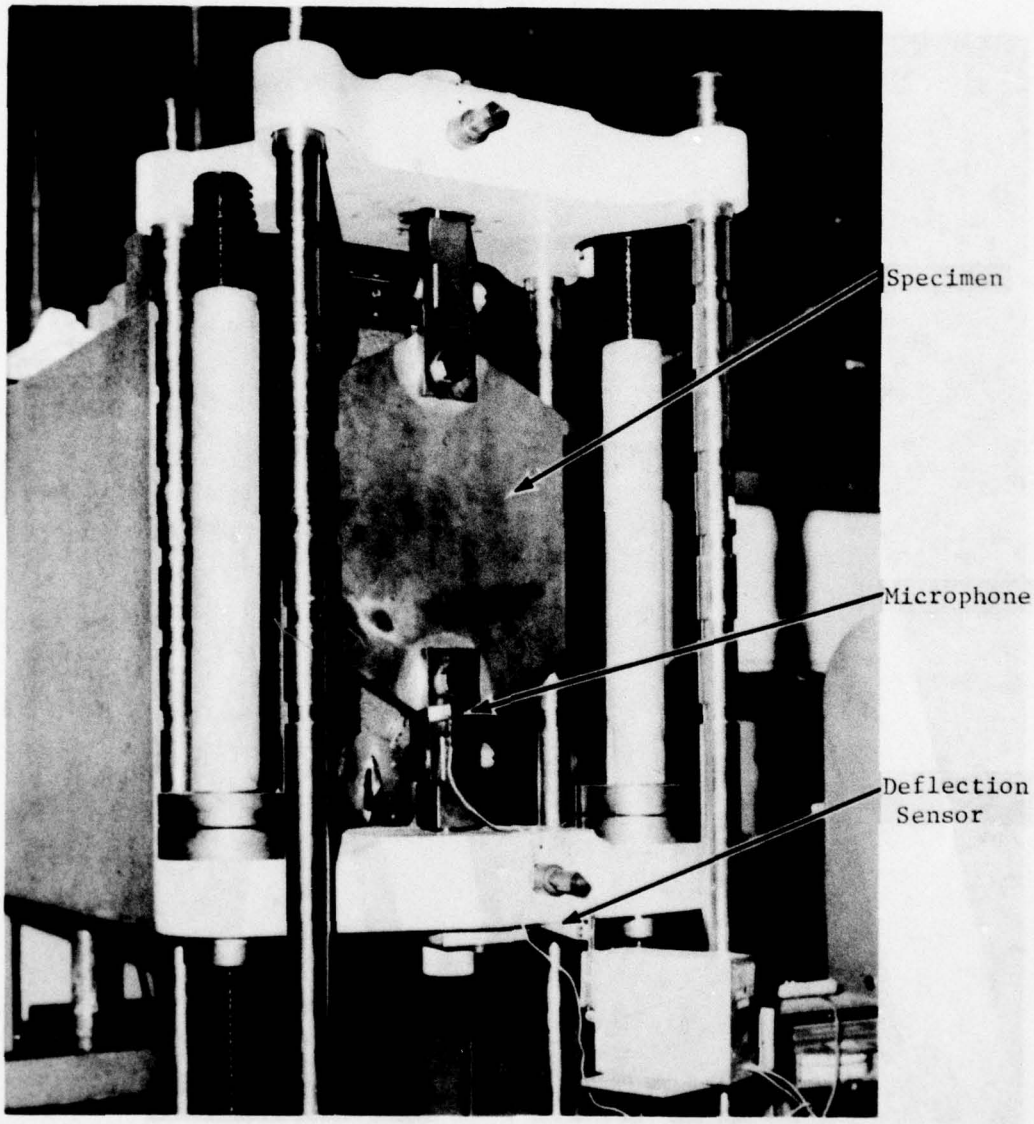


Figure 13. Element specimen during static test.

A custom test rig was used for the fatigue tests. The rig was a frame that coaxially supported the specimen, a load cell, and a hydraulic cylinder. The load cell was a strain-gaged, calibrated load link. The loads were controlled by a hydraulic system, which employed a Moog servo valve. The rig was efficient because it was stiff and had low moving masses. Testing rates of 12 Hz were achieved. The loads were monitored and recorded periodically on an oscillograph. Figure 14 shows a fatigue specimen in the rig. Interestingly, in this figure, the specimen appears to be wrinkling under load.

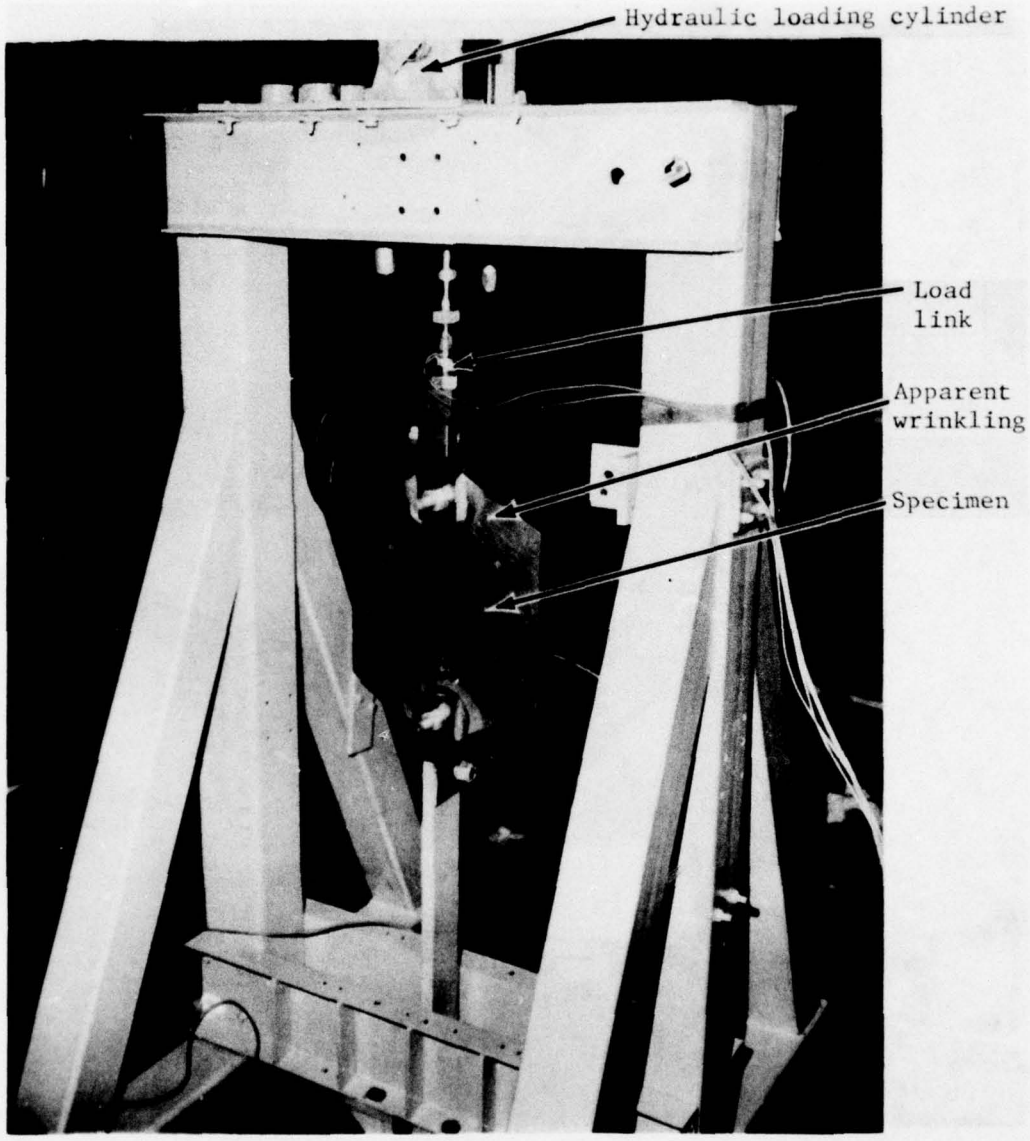


Figure 14. Element specimen during fatigue test.

This is an illusion. The apparent wrinkling is the result of lighting conditions which exaggerated surface waves that were produced during fabrication by puckering of the bleeder plies while heat and pressure were being applied in the autoclave. In subsequent components, a reinforced silicone rubber pad and a thin fiberglass caul plate were used to provide a more attractive surface. The wrinkling was a cosmetic detraction and had no effect upon the test results.

Considerable care was taken to align the load with the local midplane of the plate at each end of the specimen and thus assure that bending was negligible at the test joints. A double-pinned clevis, shown in Figure 15, was used at each end to achieve alignment.

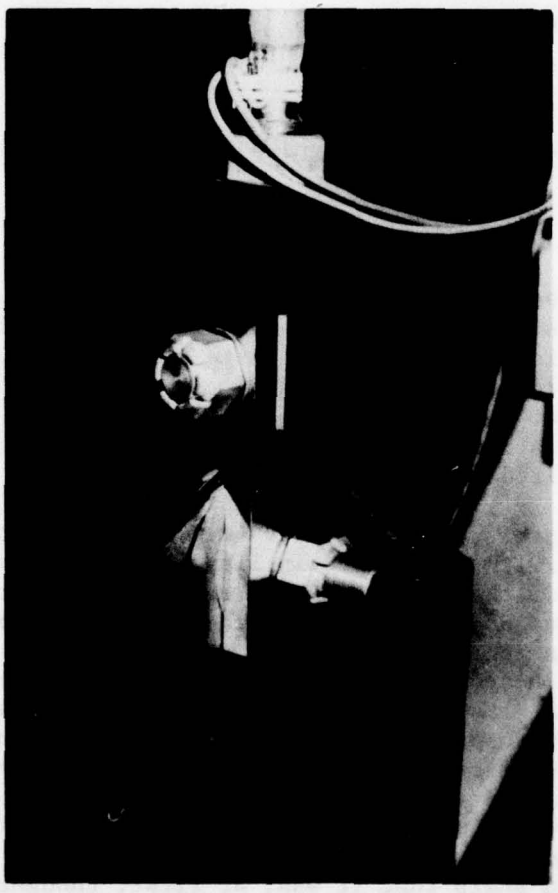


Figure 15. Alignment clevis for element tests.

The double-pinned clevis was shimmed into proper position on an individual basis for each specimen. The following procedure was used. The clevises were clamped to the specimen with trial shims. Then, the alignment was checked by supporting the plate on three balls on a flat stone table and measuring the height of the pin from the table. The specimen was turned over and remeasured. The process was repeated with appropriate adjustment to the shims until the measurements were the same. Figure 16 shows a schematic of the setup.

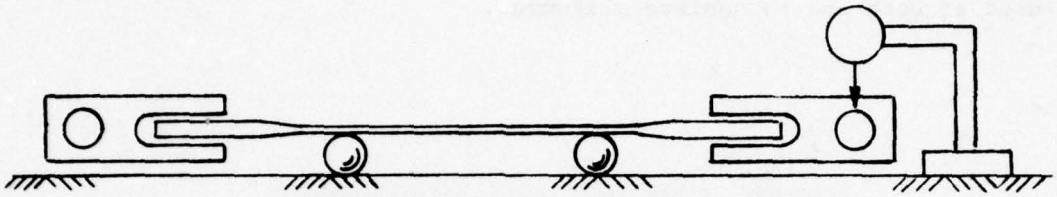


Figure 16. Procedure for aligning clevis on element specimen.

Ultimate Strength

The first element specimen was tested statically to its ultimate rupture. Both the strength and mode of failure were as planned and were satisfactory. The test indicated that the ultimate strength of a full-sized joint would be 4 x 44 = 176 kips, which is 1.95 times the required ultimate strength for the most critical loading. The high margin of safety (+ .95) on static strength is a consequence of providing sufficient reinforcement to provide the required fatigue strength.

The test was uneventful up to a load of 41.8 kips. During this initial period, an engineer with experience in listening to composites under test monitored sounds from the microphone and expressed qualitative judgments that the specimen was unusually quiet with only occasional pings. He interpreted the sounds as indicating that the specimen was well fabricated and had few defects, such as resin pockets or misaligned fibers, which could fail and emit sounds. No increase in sound level was discernable as the loads increased. Our experience in previous tests of composite structures has been that the level of sounds increased significantly as the failure load was approached, and thus, acoustic monitoring could provide a forewarning of composite failure. The element specimen provided little in the form of low-level sounds, but suddenly at 41.8 kips, the specimen gave out a report so loud and sharp that it was, at first, thought to be total failure of the specimen. However, the specimen continued to support steadily increasing loads for an additional .65 minutes of testing. Three additional

reports were heard before final failure. In all, reports were heard at 93, 95, 97, 99, and 100 percent of the failure load. It is believed that these sounds correspond to the failure of individual steel lamina or groups of composite laminae. The fact that the specimen repeatedly survived the failure shock, arrested the failure, and supported increased loads is a demonstration of a significant tolerance to damage.

Figure 17 shows that the bonds transferred the load from the steel laminae to the composite and that the composite supported the load with no signs of distress. The failure was in the lug itself. This was the desirable mode of failure since the basic concept is to use only the minimum weight of steel laminae that will provide the required strength.

Figure 17 also shows that the mode of failure was complex. There were broken laminae at point A, which is close to the minimum cross section of the lug, and at point B, which is at the inner edge of the hole transverse to the direction of loading. These results are consistent with the stress analysis of the specimen, which is presented in Appendix C. It indicates that the lug was balanced in strength. Both the steel and the composite at points A and B were near, or at, their corresponding failure stresses.

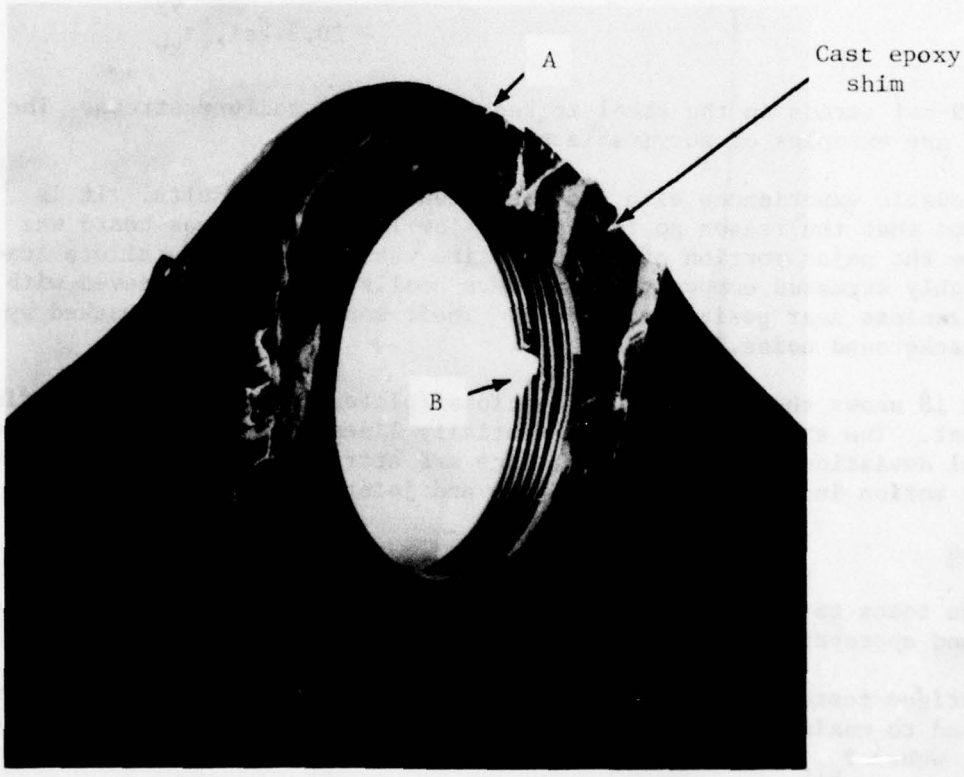


Figure 17. Element specimen after static test.

In such a case, it is difficult to say with confidence what triggered the failure. However, it is believed that the origin was at point A because the other end of the specimen had slightly larger dimensions (and thus, lower stresses) at the corresponding section, and it did not fail.

The following stresses were calculated using the elastic finite-element model and the final failure load:

Composite adjacent to doublers	35.9 ksi, σ_{xx}
	.6 ksi, σ_{yy}
	17.2 ksi, τ_{xy}
Composite at inner edge of hole	58.9 ksi
Metal at inner edge of hole	229.0 ksi
Bond of composite to metal	2.0 ksi
Tapered tip of metal	61.5 ksi
Metal at failure origin, A	194.0 ksi
Composite at failure origin, A	10.3 ksi, σ_{xx}
	39.6 ksi, σ_{yy}
	- 20.2 ksi, τ_{xy}

The 229-ksi stress in the steel is regarded as the failure stress. The others are examples of survivable static stresses.

The acoustic experiences also are consistent with the results. It is believed that the reason no increase in low-level sounds was heard was because the major portion of the composite was not near its failure load. The highly stressed composite areas were small volumes interleaved with the steel laminae near positions A and B. Their sonic output was masked by general background noise.

Figure 18 shows the loads and deflections (platen motion) recorded during the test. The specimen behaved essentially linearly up to failure. The initial deviations from a straight line are attributed to the fact that platen motion includes seating of pins and joints in the load path.

Fatigue

Fatigue tests to failure showed that the joint fatigue strength was consistent and appropriate for use on the CH-54B.

The fatigue tests were conducted using R = .1, where R is the ratio of minimum load to maximum load. The first specimen was subjected to the following loads, where P_{ult} is the static failure load:

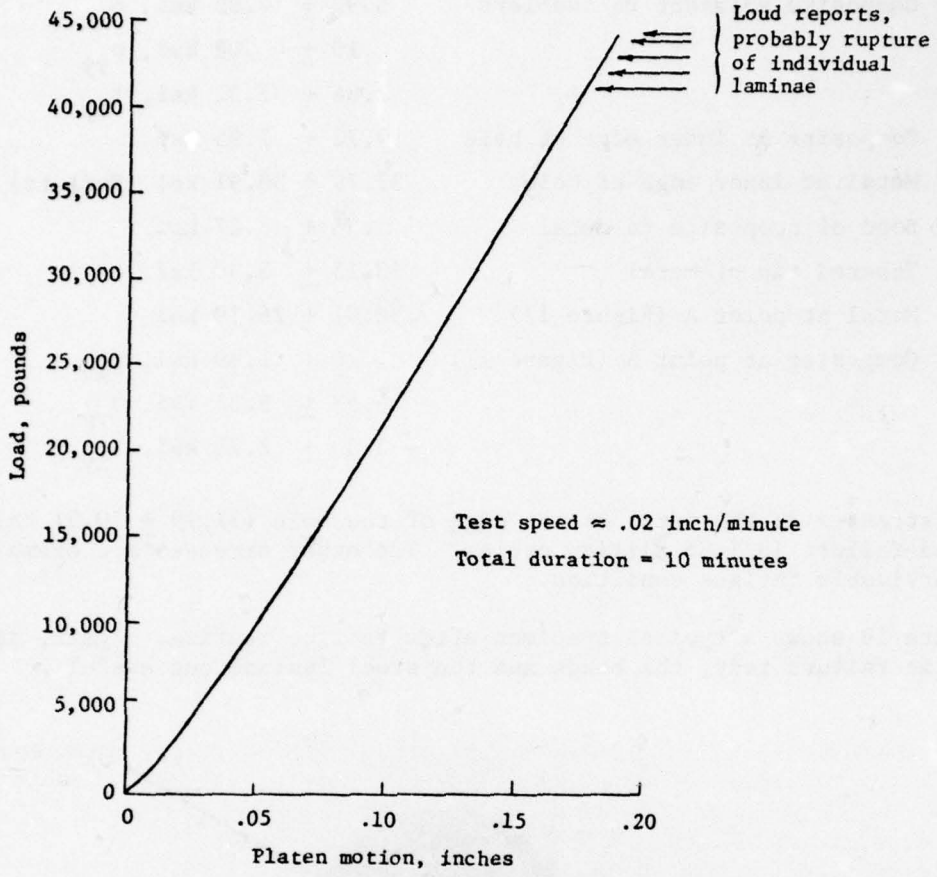


Figure 18. Load versus deflection during static test.

1.00 million cycles, maximum load = .250 P_{ult}

1.00 million cycles, maximum load = .307 P_{ult}

.26 million cycles, maximum load = .386 P_{ult}

The second specimen was subjected to:

1.85 million cycles, maximum load = .300 P_{ult}

The stresses corresponding to these loads are directly proportional to the stresses shown for the static test. For example, the stresses during the second fatigue test were:

Composite adjacent to doublers	5.92 ± 4.85 ksi, σ_{xx}
	$.10 \pm .08$ ksi, σ_{yy}
	2.84 ± 2.32 ksi, τ_{xy}
Composite at inner edge of hole	9.72 ± 7.95 ksi
Metal at inner edge of hole	37.79 ± 30.91 ksi (Failure)
Bond of composite to metal	$.33 \pm .27$ ksi
Tapered tip of metal	10.15 ± 8.30 ksi
Metal at point A (Figure 17)	32.01 ± 26.19 ksi
Composite at point A (Figure 17)	1.70 ± 1.39 ksi, σ_{xx}
	6.53 ± 5.35 ksi, σ_{yy}
	-3.33 ± 2.73 ksi, τ_{xy}

The stresses in the metal at the edge of the hole (37.79 ± 30.91 ksi) produced failure in 1.85 million cycles. The other stresses are examples of a survivable fatigue condition.

Figure 19 shows a typical specimen after fatigue testing. Again, as in static failure test, the bonds and the steel laminae successfully

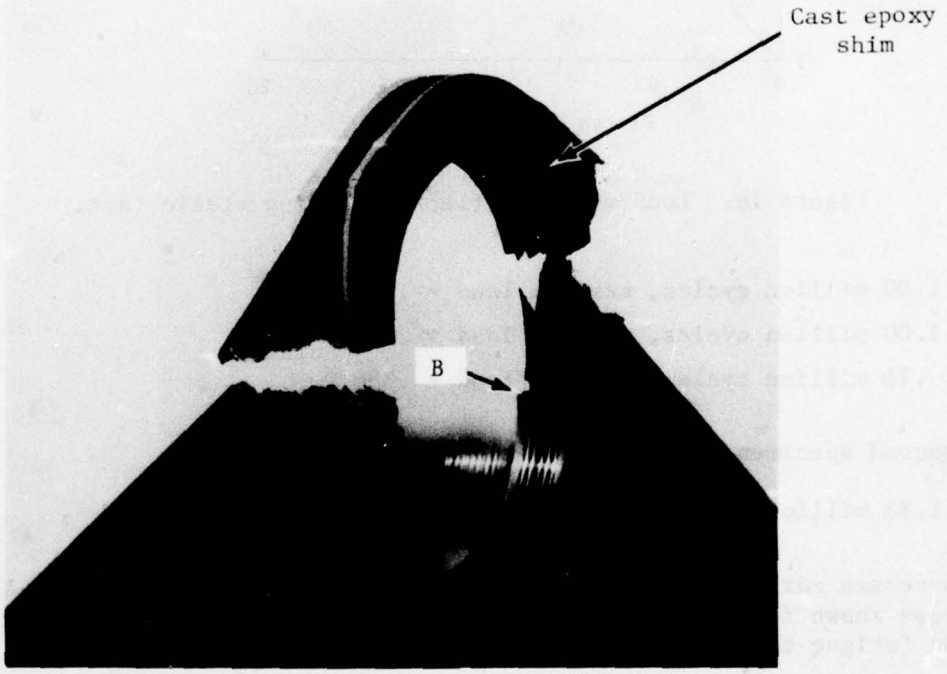


Figure 19. Element specimen after fatigue test.

transferred the fatigue loads into the composite. The composite supported the loads with no signs of distress. The mode of failure was a fatigue failure of the steel laminae at the inner edge of the hole at position B in Figure 19, which is approximately transverse to the direction of loading. This was the preferred mode of failure.

The following comparisons show that the fatigue strength of the composite joints exceeded that required to match the fatigue strength of the existing titanium hub by 7 percent for the first specimen and 14 percent for the second. The actual margin of safety may be somewhat greater than shown, however, because these comparisons are based on calculated loads and tests of the model hub assembly indicated that the actual loads were lower than calculated. Figure 20, taken in part from Reference 2, summarizes the comparisons; it shows:

1. Two test points and the estimated mean S-N curve for the existing titanium hub (solid line curve, spline mode)
2. Test conditions (3 steps) for the first composite element fatigue test and the S-N curve for the composite hub (dashed lines) derived from this test
3. Test point for the second composite element specimen (∇).

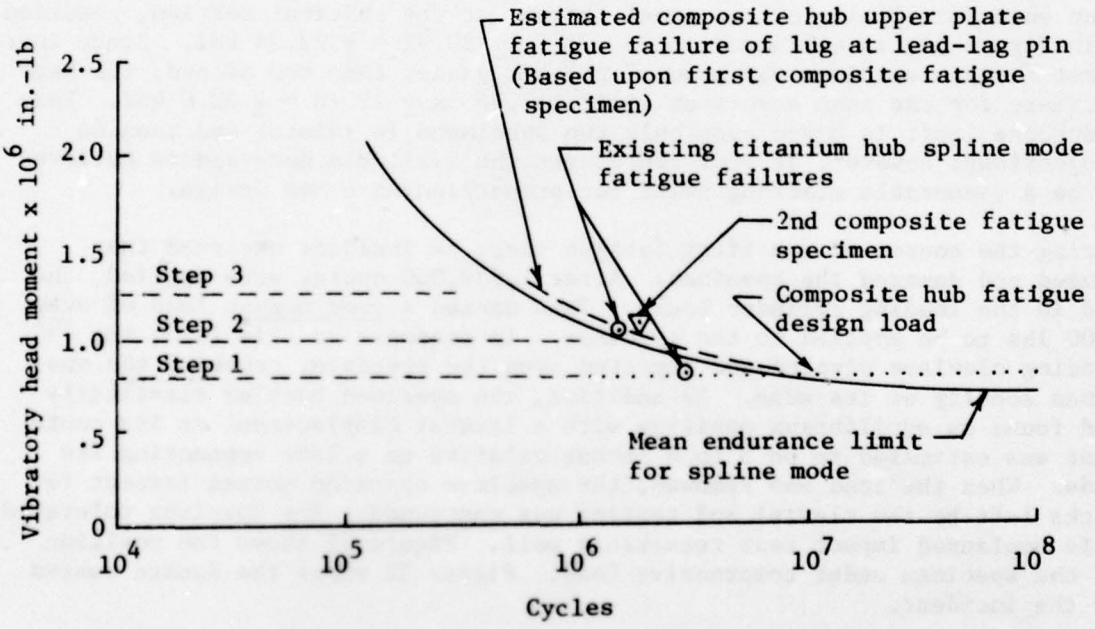


Figure 20. Relationship of fatigue test to S-N curve for titanium hub.

Using the test data and the S-N curve for the composite hub, Miner's Rule provides the following summation:

For failure:

$$\frac{n_1}{N_1} + \frac{n_2}{N_2} + \frac{n_3}{N_3} = 1 \quad \text{(Miner's Rule)}$$

For first fatigue specimen:

$$\frac{1}{9} + \frac{1}{2} + \frac{.26}{.67} = 1.00$$

Thus, the dashed S-N curve is in agreement with Miner's rule and the three load steps of the first fatigue test. The curve lies about 7 percent higher than the S-N curve for the existing titanium hub.

The failure point for the second composite fatigue specimen lies about 14 percent above the S-N curve for the existing titanium hub. The strength of the second specimen is consistent with that of the first. The fatigue strength shows a very desirable low scatter.

Using the curve for the existing titanium hub, shown in Figure 20, the mean endurance limit (mean strength for infinite life) can be projected as .7/.95 = .737 times the fatigue strength at 1.85 million cycles. Applying this factor to the calculated stress during the second fatigue test, the mean endurance limit for the steel laminae at the critical section, position B in Figure 19, is estimated to be .737 x $\pm$ 30.91 = $\pm$ 22.78 ksi. Since the first fatigue specimen was about 7 percent weaker than the second, the best estimate for the mean endurance limit is .965 x $\pm$ 22.78 = $\pm$ 22.0 ksi. This endurance limit is based upon only two specimens (4 joints) and tenuous projections; however, it best represents the available data and is believed to be a reasonable starting point for proportioning a new design.

During the course of the first fatigue test, an incident occurred that abused and damaged the specimen. After 1,630,000 cycles were applied, the rod in the loading cylinder broke. This caused a compressive load of over 3000 lbs to be applied to the specimen. In response to this load, the loading clevises pivoted and impacted upon the specimen, crushing the specimen locally at its edge. In addition, the specimen buckled elastically and found an equilibrium position with a lateral displacement at its center that was estimated to be 3 to 4 inches relative to a line connecting its ends. When the load was removed, the specimen appeared normal (except for nicks left by the clevis) and testing was continued. The specimen tolerated this unplanned impact test remarkably well. Figure 21 shows the position of the specimen under compressive load. Figure 22 shows the damage caused by the incident.

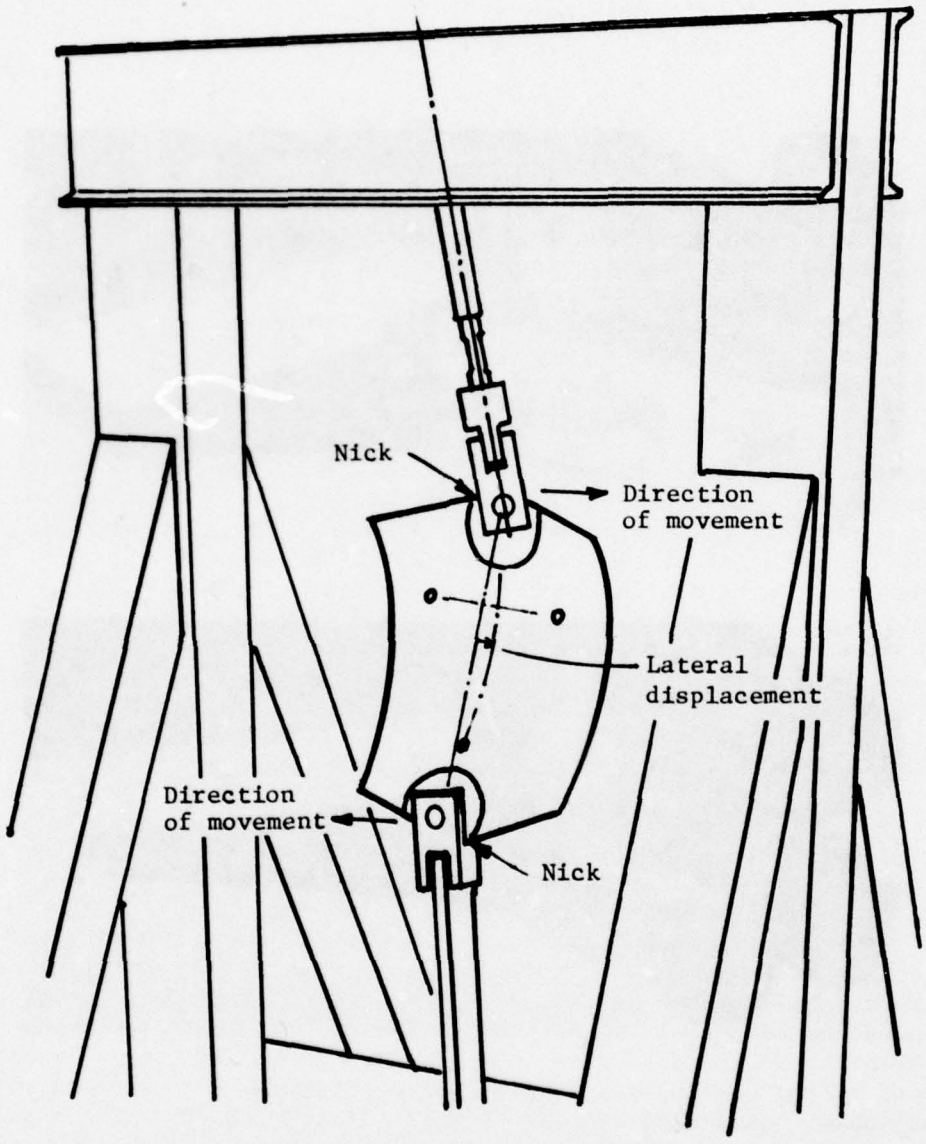


Figure 21. Position of specimen while under compressive load after failure of rod in loading cylinder.

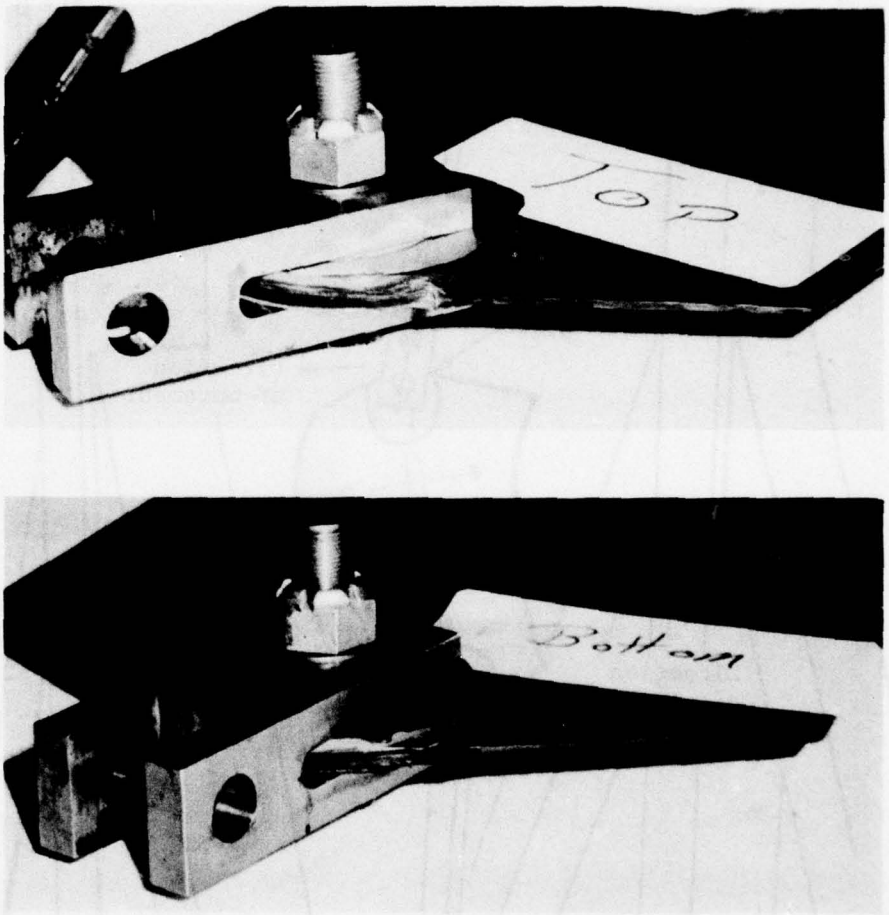


Figure 22. Damage caused by impact of clevises.

TESTS OF ASSEMBLY SPECIMEN

Rationale and Objectives

The tests were planned cautiously, recognizing that only a single specimen existed. The plan was to demonstrate high levels of structural integrity, but yet to avoid destruction of the specimen, which would have precluded further testing. Since the greatest need was to demonstrate fatigue strength or to find areas of fatigue weakness, the test program subjected the model first to the fatigue design loads and then to static limit loads. The specific test objectives were:

1. To demonstrate fatigue strength sufficient to survive 1 million cycles of the fatigue design loads.
2. To demonstrate a residual strength after fatigue testing sufficient to support the most critical flight loads.
3. To demonstrate adequate stiffness for dynamic compatibility with the rotor controls and drive train.
4. To verify partially the calculations of internal loads.
5. To determine the importance of secondary bending in the plates.

These objectives were accomplished and, as it turned out, a sixth objective was also achieved:

6. To demonstrate damage tolerance.

Loading Conditions

Table 5 shows the design loads for the CH-54B prototype, the actual test loads for the 1/2-scale model, and the test loads as a percentage of the scaled loads. In general, the model used scaled loads with only two exceptions, for which the loads were approximately 4 percent higher than true scale. The use of these slightly higher loads allowed a single alignment of loading apparatus to be used for both the static and fatigue tests.

The fatigue design loads are described in Reference 2, which shows that the fatigue design head moment is higher than 95.5 percent of the head moments specified in the mission spectrum for the CH-54B. It is also 14 percent higher than the mean endurance limit for the present titanium hub. Figure 23 shows the relationship of the composite hub fatigue demonstration to the S-N curve for the present titanium hub. Survival of the fatigue test demonstrated that the composite hub had at least 74 percent of the strength of the present hub.

The static limit loads were taken from References 2 and 3. The loads correspond to flight condition TW7F1, which is a symmetrical dive and pullout with power on. This condition is critical because it includes both high torque and high head moment.

TABLE 5. DESIGN AND TEST LOADS				
CONDITION	LOADING	CH-54B PROTOTYPE	MODEL TEST	$\frac{\text{TEST}}{\text{SCALED}} \times 100\%$
FATIGUE	Head Moment, in.-kip	± 800.	± 100.	100.0
DESIGN	C.F. , kip	83.	21.64	104.3
LOADS	Torque , in.-kip	2075.	259.4	100.0
	Thrust , kip	38.	9.5	100.0
STATIC	Head Moment, in.-kip	1314.	164.25	100.0
LIMIT	C.F. , kip	99.	24.75	100.0
	Torque , in.-kip	2272.	296.60	104.4
TW7F1	Thrust , kip	85.8	21.45	100.0

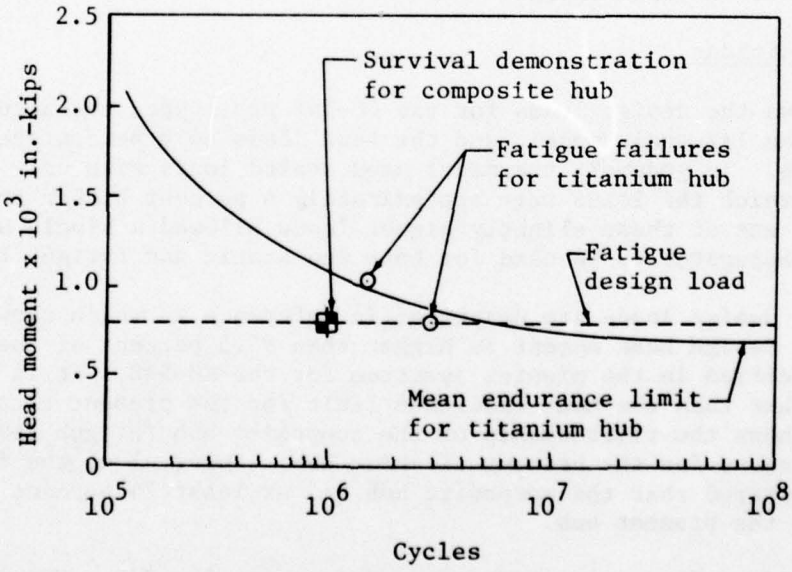
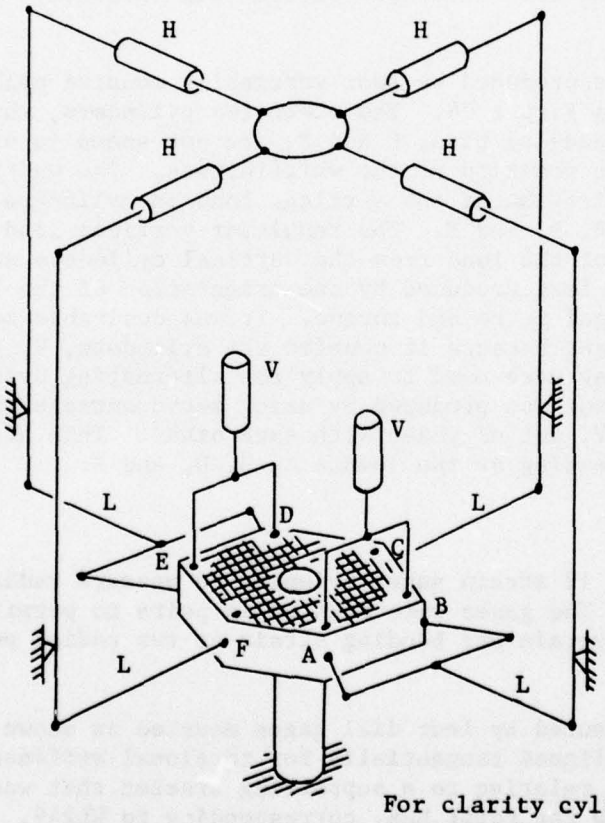


Figure 23. Test S-N for titanium hub.

Apparatus

Figure 24 shows a line schematic of the composite hub in the loading rig. The specimen was mounted upon a cantilevered shaft, and the loads were applied to the six lead-lag pins, A through F. The steady loads of centrifugal force and torque were produced by the hydraulic cylinders, H, and measured by strain-gaged links in the bars, L. The loading bars were oriented to provide components of force appropriate for the loading condition at each lead-lag pin. The linkages and pivots of the rig were designed to apply the centrifugal force and torque without inhibiting the deflections of the hub and its mounting shaft that occur in response to alternating head moment, thus permitting a valid test of the hub, the attachments of the hub to the shaft, and the shaft. Figure 25 shows, in exaggeration, how the loading linkage rocks to accommodate the deflections of the hub and its mounting shaft.



For clarity cylinders, V, at C and F are not shown.

Figure 24. Schematic of test rig.

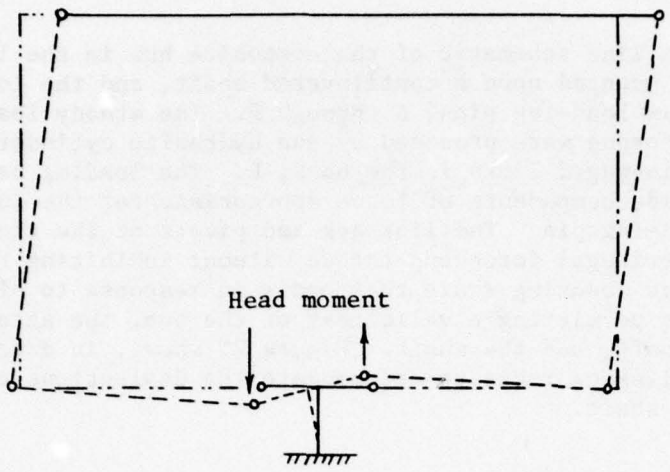


Figure 25. Principle of test rig linkages.

The steady thrust was produced by four vertically mounted cylinders, two of which are shown in Figure 24. The other two cylinders, which were connected directly to lead-lag pins, C and F, are not shown in order to indicate more clearly the position of the whiffletrees. The whiffletrees in the vertical plane distributed the vertical load in cylinders, V, equally to lead-lag pins A, B, D, and E. The resultant vertical load at each lead-lag pin was the sum of the load from the vertical cylinders and a component of downward vertical load produced by the orientation of the links, L, that applied the centrifugal force and torque. It was desirable to introduce this downward component because it enabled the cylinders, V, to operate in tension only when they were used to apply the alternating head moment. The alternating head moment was produced by using servocontrols that cycled the loads in cylinders, V, out of phase with each other. This arrangement provided simultaneous testing of the joints A, B, D, and E.

Instrumentation

The specimen carried 12 strain gages oriented to measure radial strains, as shown in Figure 26. The gages were mounted in pairs to permit the calculation of extensional strain and bending strain at two radial positions on each plate.

Deflections were measured by four dial gages mounted as shown in Figure 27. Gages 1 and 2 were aligned tangentially for torsional stiffness calculations. The deflections were relative to a supporting bracket that was attached to the rotor shaft below the rotor hub, corresponding to WL249.

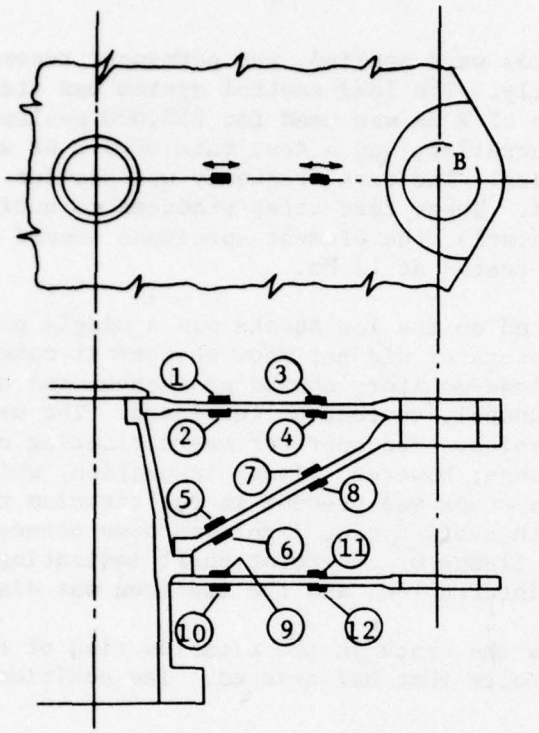


Figure 26. Location of strain gages.

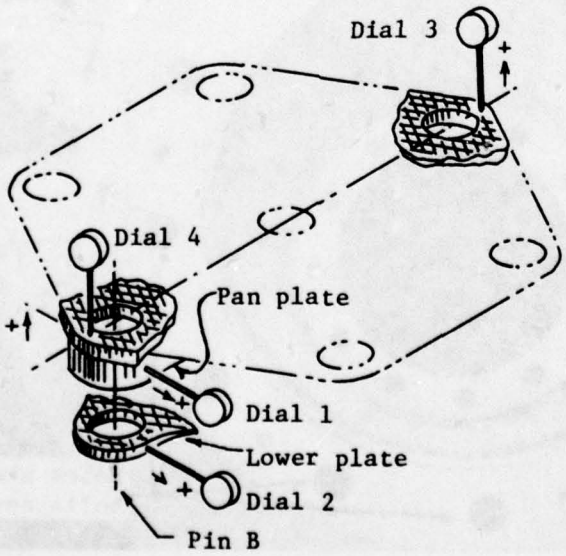


Figure 27. Location of deflection gages.

Fatigue

The fatigue design loads were applied, and permanent records of loads and strains were made hourly. The load control system was stable and the test ran well. A test rate of 2 Hz was used for 258,000 cycles. Then, a larger pump and motor were installed, and a test rate of 3.5 Hz was used for the remaining 742,000 cycles. The test frequency was similar to the CH-54B rotor speed of 3.1 rps. These test rates produced no noticeable heating of the specimen. Similarly, the element specimens showed no noticeable temperature rise when tested at 12 Hz.

The first incident noted on the log sheets was a single pop heard after 376,000 cycles. The operator did not know whether it came from the specimen or the rig. The load monitors showed no change, and a visual inspection showed nothing unusual, so testing continued. The second incident occurred at 601,800 cycles. The operator heard clicking noises. The load monitors showed no change; however, visual inspection, while the test was running, showed that a crack was present in the titanium ring at the center of the pan plate. With every cycle, light was seen between the flange of the pan plate and the flange of the rotor shaft indicating that bolts had broken. Testing was interrupted, and the specimen was disassembled.

Figures 28 and 29 show the crack in the titanium ring of the pan plate. Figure 30 shows four bolts that had severed. The positions of the broken

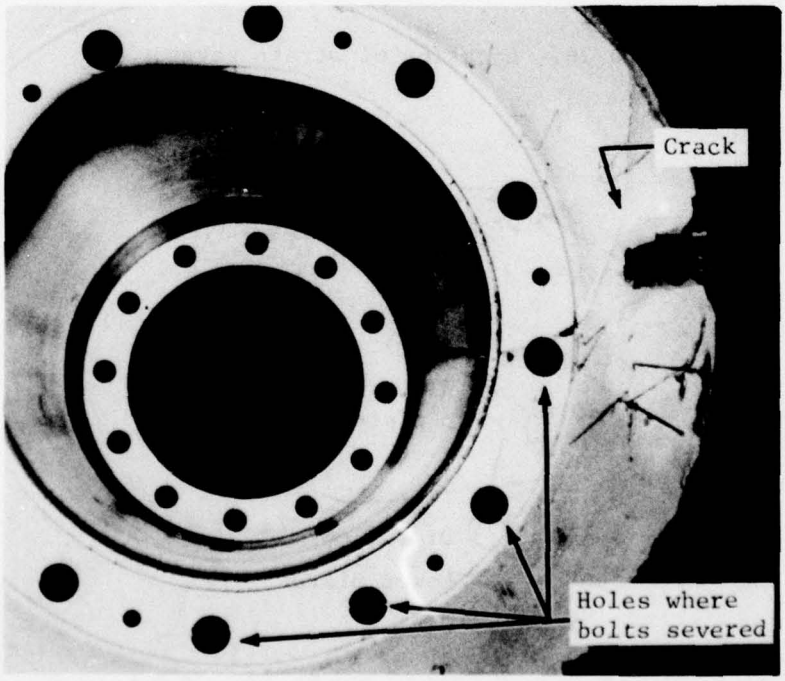


Figure 28. Plan view of pan plate with crack.



Figure 29. Closeup view of crack.

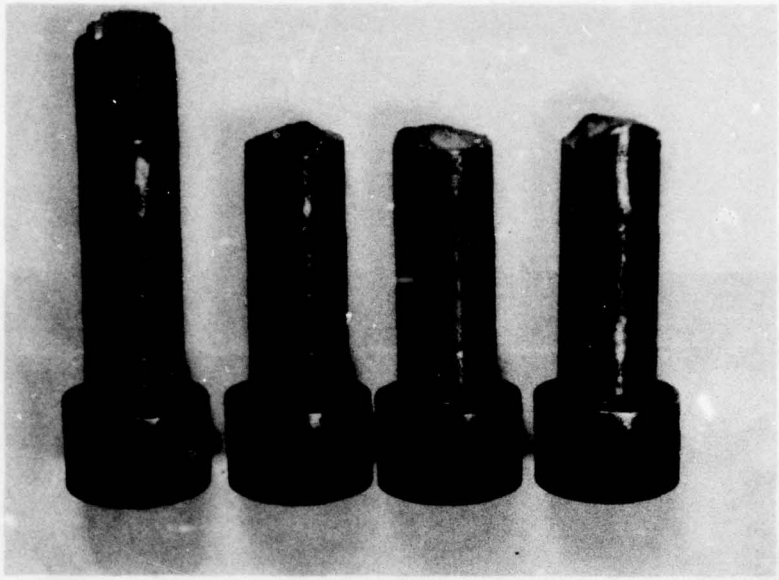


Figure 30. Severed bolts.

bolts are indicated in Figure 28. Since initially there were only 12 bolts, the pan plate was operating at the time of interruption with no attachment over an arc of 120°. Figures 28 and 29 also show that strain gages 5 and 6 were in good position to record the growth of the crack. This was a fortunate placement of gages because the crack had equal likelihood of starting at three other symmetrically located sites that had no gages. The strains at gages 5 and 6 are shown versus cycles in Figure 31. The following is believed to be the sequence of events:

1. A crack ran from the bolt hole to the center hole. Probably this was the pop heard at 376,000 cycles.
2. The crack grew gradually outward until it was arrested by the composite.
3. The crack changed the support of loading, causing the bolts to be loaded by horizontal shears at the joint between the pan plate and the hub.
4. The bolts were overloaded by these shears and eventually broke. The fracture surface of one bolt shows evidence of a fatigue origin. The others are characteristic of a relatively low-cycle, static failure. Probably, the first bolt broke at 572,000 cycles, 3.1 hours before the tests were suspended, corresponding to the abrupt change in the shape of the strain-cycle curves for gages 5 and 6, as seen in Figure 31.

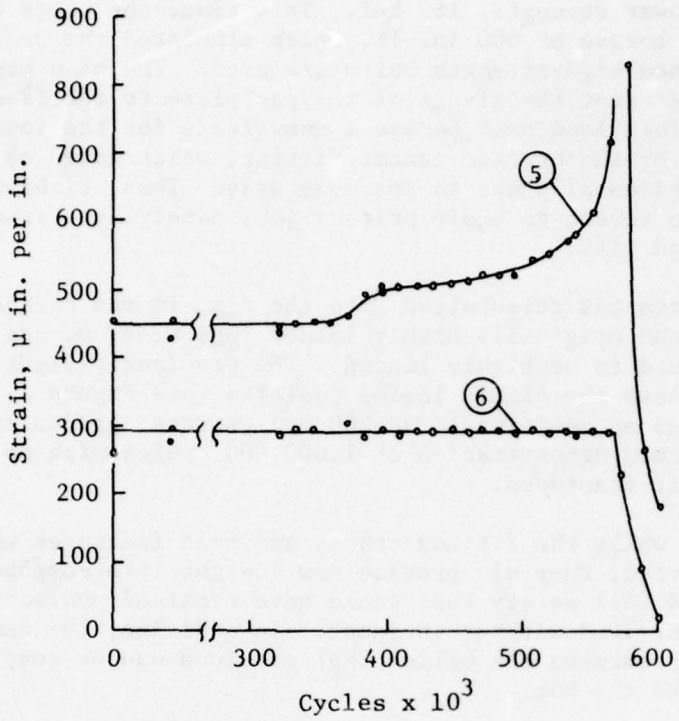


Figure 31. Alternating strains at gages closest to crack.

In hindsight, there were several easily avoidable factors that contributed to the cracking. The simple local improvements noted below should be effective in preventing future cracking:

1. The test bolts were inadequately tightened. For reasons of cost, the lower and pan plates were assembled to the rotor shaft using 190 ksi, commercial-grade bolts. These bolts had a black-oxide coating, which has greater friction than usual aircraft coatings. The bolts were tightened only to 300 in.-lb; a normal value for cadmium-plated aircraft bolts. Later, it was noted that the manufacturer recommended 500 in.-lb for black-oxide bolts. The significance of tight bolts is discussed in the next paragraph.
2. The test bolts had a coating that aggravated fretting. A Sermetel-W coating is planned for use in service.
3. The holes in the test titanium fitting had no preparation to improve their fatigue performance. It is now planned that the edges of the holes will be provided with a radius and the hole will be shotpeened.

The specimen was reassembled with no repairs using available NAS bolts. They were of lower strength, 160 ksi. This time, the bolts were fully tightened to a torque of 500 in.-lb, which simulated the preload that will be available when high-strength bolts are used. The plan was to transfer horizontal shear from the flange of the pan plate to the flange on the hub by friction. This load path became a substitute for the load path originally provided by the cracked center fitting, which acted as a large lug tranferring horizontal shear to the cone seat. Thus, tightening the bolts allowed them to revert to their primary job, namely, the transmission of drive torque and lift.

When the specimen was reinstalled into the rig, it was rotated 60°. This meant that of the originally highly loaded lugs A, B, D, and E, only lugs A and D continued to be highly loaded. The previously lightly loaded lugs C and F moved into the highly loaded position (see Figure 24). The testing was resumed, and an additional 398,200 cycles were applied to complete the originally planned demonstration of 1,000,000 cycles with no additional cracking or bolt fractures.

In retrospect, while the fitting cracks and bolt fractures were unwelcome when they occurred, they did provide new insight into component criticality, load paths, and fail safety that would have remained undiscovered if the specimen had survived without incident. In addition, the damage tolerance demonstrated encourages the belief that missions can be completed after battle damage to the hub.

The good fatigue performance of the hub, even in a cracked state, after the bolts were tightened implies that just tightening the bolts would be adequate to avoid cracking. However, it is recommended that the holes be strengthened as described in order to provide an additional margin of safety.

Static Limit

The specimen supported the limit loads in Table 5 without incident or damage. The hub was also silent. The audible creaking usually associated with composite assemblies was absent in all testing in this program. The loads were applied in three stages:

STAGE 1. The cylinders, H, in Figure 24 were energized in progressive steps to apply the limit centrifugal force and torque to the specimen. Concurrently, a downward thrust was also applied as a consequence of the orientations of the load links. This downward load enabled the vertical cylinders, V, to operate in tension when the head moment was added in Stage 3.

STAGE 2. The cylinders, V, and two other vertical cylinders (not shown in Figure 24) added limit thrust.

STAGE 3. The cylinders, V, were adjusted to add the limit head moment.

Figure 32 shows the deflections measured during the limit load tests. These deflections indicate that the specimen remained elastic. Upon release of the load, gages 2 and 3 returned to their original position within .002 inch. Gages 1 and 4 showed a residual displacement of about .015 inch. Figure 27 shows that dial gage 1 measured tangential motions of the pan plate, and dial gage 4, vertical motions. These dial gages were closest to the crack in the center ring of the pan plate. It is believed that under load, the crack opened a little, thus permitting slight shifts in the position that the pan plate was clamped to the flange of the rotor shaft. These shifts of position were recorded by dial gages 1 and 4.

Dynamic Compatibility

There were two concerns for dynamic compatibility:

1. The moment stiffness and thrust stiffness should be great enough so that deflections of the hub do not have a significant effect upon the control inputs to the pitch arm.
2. The torque stiffness should be great enough to avoid torsional resonances in the drive train.

Table 6 shows that the composite hub is from 28 to 183 percent stiffer than the present titanium hub, and thus it is concluded that the composite hub is compatible and would have no adverse effects upon the behavior or controllability of the rotor system.

TABLE 6. SUMMARY OF HUB STIFFNESSES

Type of Stiffness	TI-Hub	CPH	$\frac{\text{CPH}}{\text{TI-Hub}}$
Moment, in.-kips/degree	4218	5416	1.28
Thrust, kips/in.	1010	2228	2.21
Torque, in.-kips/degree	9279	27227	2.93

Theoretically, the higher stiffnesses of the CPH are beneficial because they reduce interaction of the hub deflection with control inputs and raise the torsional natural frequencies of the drive train further above the operating speed. However, the hub stiffnesses under consideration are so high that dynamic compatibility is insensitive to changes in stiffness. For example, if a new hub were only one-half as stiff as the present titanium hub, the maximum vertical deflection of the full-scale hub at the lead-lag pin would increase by only .20 inch at the limit load, and the increase in torsional windup would be equivalent to that produced by only a 13-inch increase in the length of the rotor shaft.

Stage	Moment In.-kip	C. F. Kip	Torque In.-kip	Thrust Kip
3	164.25	24.75	296.60	21.45
2	0	24.75	296.60	21.45
1	0	24.75	296.60	-11.87

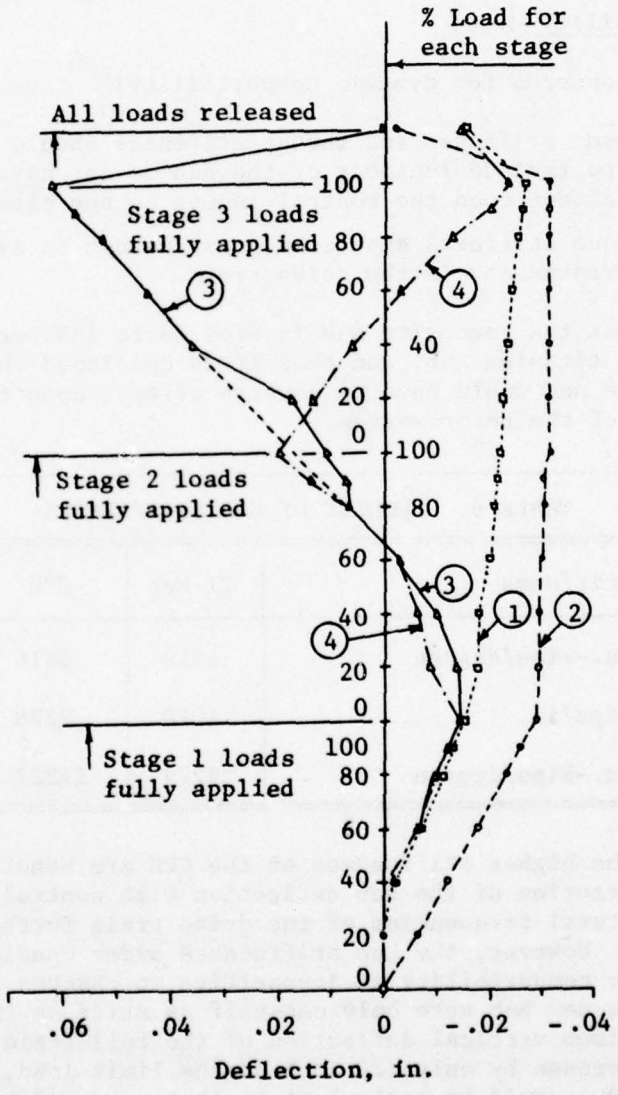


Figure 32. Deflections during limit load test.

The stiffnesses shown in Table 6 for the present titanium hub are theoretical stiffnesses calculated using approximate dimensions scaled from the manufacturer's assembly drawings. The stiffnesses for the CPH are the measured stiffnesses of the model during the limit load test scaled up to full size. The stiffnesses for the titanium hub were calculated relative to the shaft just below the hub at WL249. This position corresponds to the measuring technique used to determine the experimental stiffnesses of the model of the CPH, and thus stiffnesses are on a common basis and can be compared directly.

Strains

The design of the plates was based upon loads found using the statically determinate free-body diagram shown in Figure 33. In effect, simple truss action was assumed with the support for the blade loads being supplied solely by axial forces lying along the midplane of each plate. Bending and transverse shears were considered secondary events, which were a consequence of deflections of the primary load path provided by axial forces.

Strain gages were positioned to find out how closely the actual behavior resembled that assumed and to discover the magnitude of the bending strains. It would have been desirable also to place strain gages at critical sites where failures would originate. However, in the composite hub, these sites are at the inside edges of loaded holes or at interlaminar bond lines, which are unsuitable for gage application.

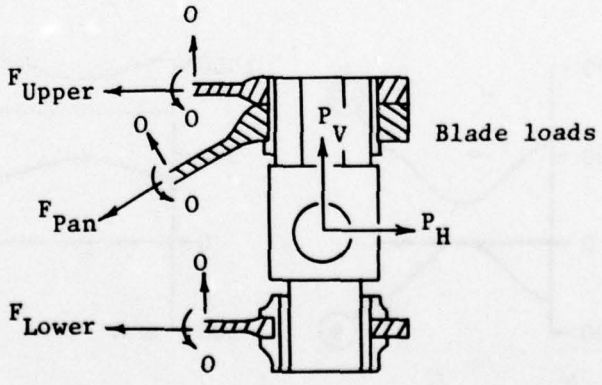


Figure 33. Free-body diagram of lugs at lead-lag pin.

Figure 34 shows the strains during a typical cycle of loading in the fatigue test. The values indicated at the peaks are the averages of nine readings taken during the first 260,000 cycles. The strains showed little variation from reading to reading. For any set of nine readings, the typical difference between the highest and lowest alternating strains was 36 μin./in.

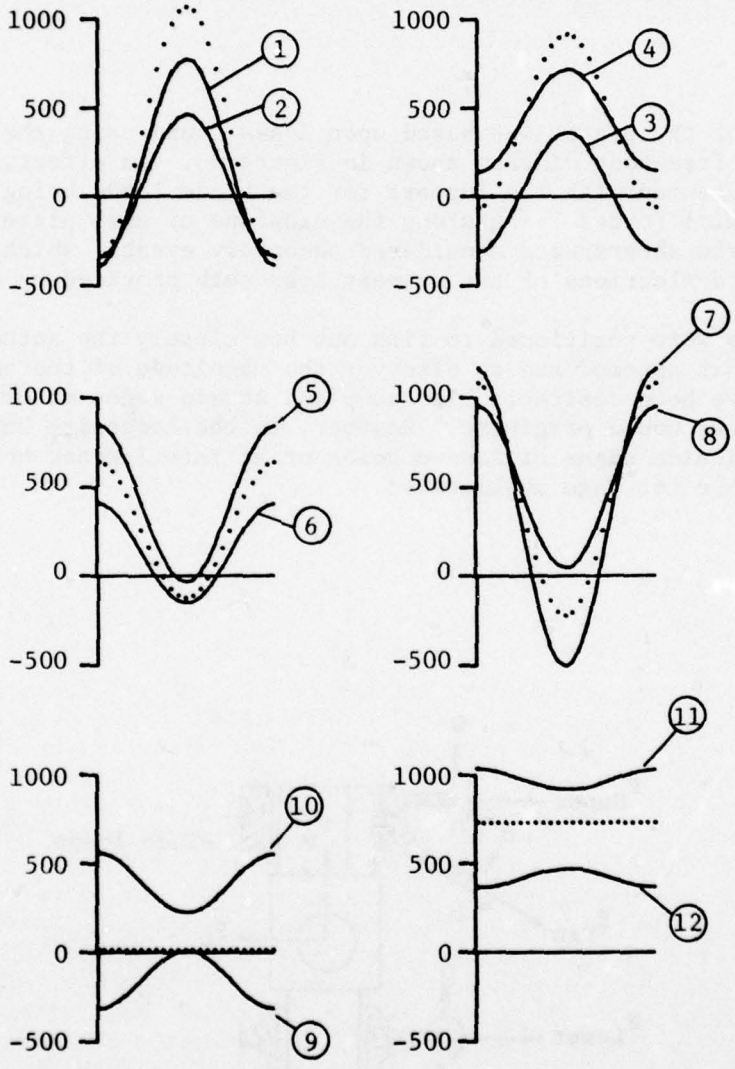


Figure 34. Strain (μin./in.) versus time for twelve gages shown in Figure 26 during one cycle of fatigue test.

which could be attributed, in part, to data collection and reduction, as well as a variation in specimen response. Several observations can be made from the strain gage data:

1. The strains are consistent with the assumed truss action indicated in the free-body diagram of Figure 33. At the peak loads, the line of action of the axial forces was quite close to the midplane; for the upper and pan plates, the line of action of the axial forces was within 6 percent of the thickness of being directly on the midplane. The lower plate is a special case and is discussed in observation 5.

2. The bending strains, represented by one-half the difference between the strains for the gages at a station, were typically appreciable fractions of the axial strain; however, in absolute value, the bending strains were small and had no significance to the strength of the hub. The critical strains were at the inner boundaries of the holes. These strains were analyzed using finite-element models described in Appendix C.

3. The strains measured in the composite were low, indicating high tolerance to damage in the large open areas of the hub, away from the joints. For example, the highest strain measured was 1166 μin./in. (about 8.7 ksi); the highest alternating strain was $\pm$ 835 μin./in. (about $\pm$ 6.3 ksi).

4. The strains measured on the titanium fittings (gages 5, 6, 9, and 10) were also low. The highest strain measured at gage 5 was 848 μin./in. (about 13.7 ksi); the highest alternating strain was $\pm$ 441 μin./in. (about $\pm$ 7.1 ksi).

5. The strains measured by gages 9 and 10 on the lower plate reveal a special feature of detail design. The primary loads on the lower plate are equal radial forces at the six lead-lag pins. The plate is redundant and can support these loads by internal hoop forces from adjacent pin to adjacent pin and/or by radial forces from pin to opposing pin. The hoop path is preferred for normal levels of load because it relieves the scalloped lugs on the center fitting and the bolts from the task of transferring the radial load. The bolt holes were positioned and sized to allow the hoop path to operate without restraint. Thus, the analysis indicated an axial strain of only 2 μin./in. The finite-element analysis of the lower plate indicates that the tangential stress at the location of gages 9 and 10 would be 15 ksi.

6. The strains measured in the upper plate were lower than expected. At least two factors may have contributed to this difference. First, it was assumed that centrifugal force was supported by the upper and lower plates alone. Actually, the pan plate can assist the upper plate, and thus reduce the

loads upon the upper plate. Secondly, it was assumed that the upper plate did not contribute to the support of torque. Actually, friction at the center hole may have allowed the upper plate to share in the support of torque. If it did, it could lower the strains at the points measured.

Effect of Test Results Upon Performance Estimates

The expected strengths and stiffnesses were verified by the testing program with only one exception, that of the holes in the titanium fitting in the pan plate. Changes to increase the strength of the titanium fitting added no weight and only $30 (or 0.17 percent) to the price of a hub assembly. The damage tolerance shown during the fatigue test and subsequent static limit load testing exceeded expectations.

OTHER APPLICATIONS

In the design for the CH-54B, the pan plate, which provides the load path for transverse shear, is located in the intermediate position. This is not the only possible configuration. The pan plate could also be located either above or below the flat plates. Figure 35 shows a sketch of an alternate design (for a four-bladed rotor) in which the pan plate (2) is on top. In addition, the plates (1 and 3) are also shown with a shallow cone, corresponding to the steady 1-g cone angle of the blade. The load paths in this design are similar to those described earlier except for the transmission of torque, which, in this design, is shared by plates 1 and 3.

The principal advantage of this configuration is the clear envelope it provides inboard of the bearings. The entire annular space between plates 1 and 3 is open. Figure 35 shows an elastomeric articulation in this space. A spherical bearing (4) provides for the lead-lag and flapping motions; a chevron-stack thrust bearing (5) allows feathering motions. The outboard end of the spherical bearing receives attachment bolts that hold it to the hub. The rotor blade shank (6) extends inboard for contact with flapping stops and the attachment of a damper.

FUTURE PLANS

The present program has been completed and a new program to develop the concept further is in progress. The Applied Technology Laboratory of the U. S. Army Research and Technology Laboratories is supporting a program to investigate the feasibility of applying the composite plate hub concept to medium utility helicopters using the UH-60A as a baseline. The decision to shift future development from the CH-54B to the UH-60A was based upon cost-benefit analyses. A dominant factor in the analyses was the fact that the helicopters of the UH-60A weight class will be procured in large numbers, and thus this weight class offers the greatest opportunity to realize large total cost, weight, and performance benefits from the successful application of a composite plate hub.

Key

1 - Nearly flat plate
2 - Pan plate
3 - Nearly flat plate
4 - Spherical bearing
5 - Chevron-stack thrust bearing
6 - Rotor blade shank

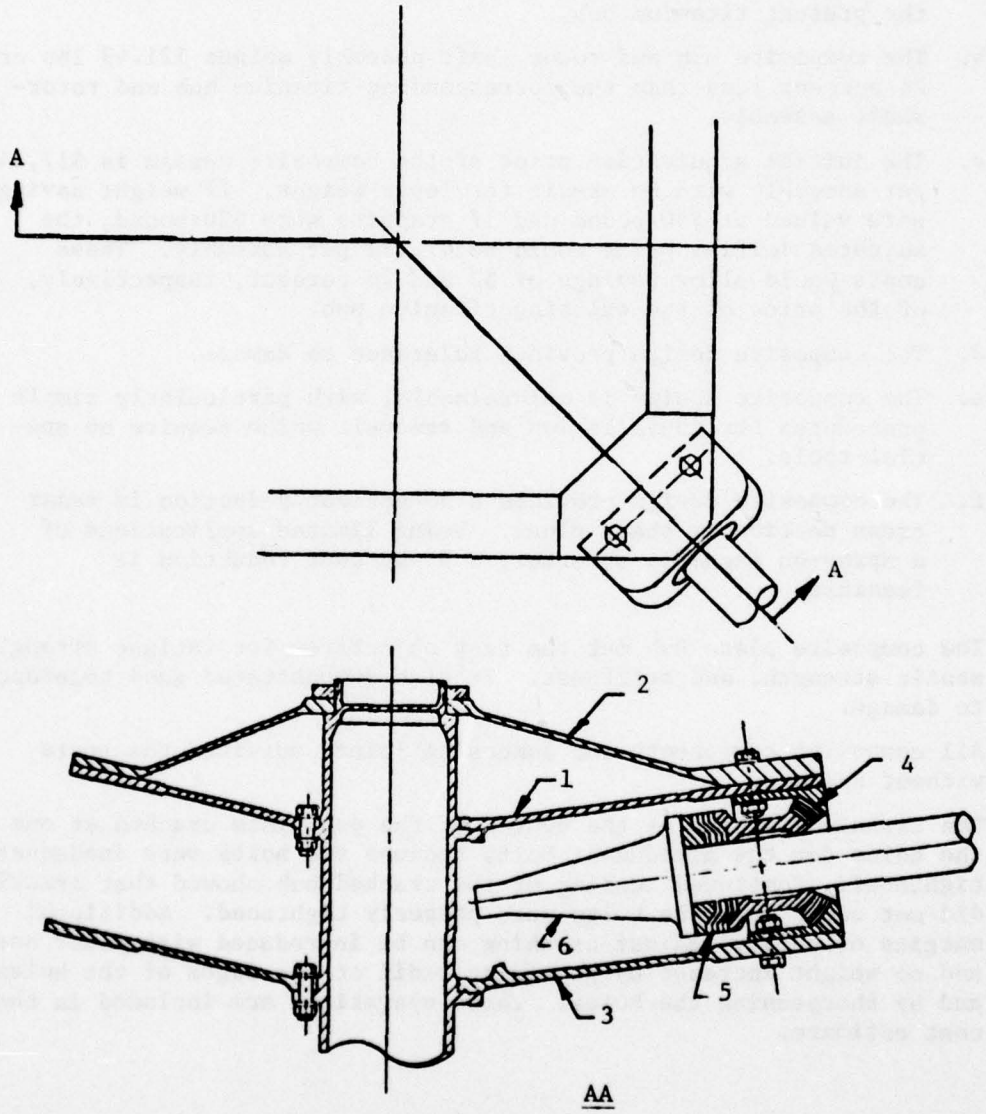


Figure 35. An alternate composite plate hub configuration.

CONCLUSIONS

1. The composite plate hub is structurally efficient and readily producible.

2. The composite hub designed for the CH-54B has the following characteristics:

   a. The composite hub weighs 99.30 lbs or 24 percent less than the present titanium hub.

   b. The composite hub and rotor shaft assembly weighs 121.49 lbs or 24 percent less than the corresponding titanium hub and rotor-shaft assembly.

   c. The initial acquisition price of the composite design is $17,144 per assembly with no credit for lower weight. If weight savings were valued at $50/pound and if graphite were $20/pound, the adjusted initial price would be $7,712 per assembly. These costs would allow savings of 52 and 78 percent, respectively, of the price of the existing titanium hub.

   d. The composite design provides tolerance to damage.

   e. The composite design is maintainable, with particularly simple procedures for installation and removal, which require no special tools.

   f. The composite design provides a 38-percent reduction in radar cross section by shape alone. Using limited applications of a spray-on magnetic absorber, a 93-percent reduction is feasible.

3. The composite plate hub met the test objectives for fatigue strength, static strength, and stiffness. It also demonstrated good tolerance to damage.

4. All composite components and composite joints survived the tests without failure.

5. The titanium fitting at the center of the pan plate cracked at one of the holes for the attachment bolts because the bolts were inadequately tightened. Continued testing of the cracked hub showed that cracking did not occur when the bolts were properly tightened. Additional margins of safety against cracking can be introduced with minor cost and no weight increase by providing radii at the edges of the holes and by shotpeening the holes. These operations are included in the cost estimate.

REFERENCES

1. Levenetz, B., COMPOSITE-MATERIAL HELICOPTER ROTOR HUBS, Whittaker Corporation; USAAMRDL Technical Report 73-14, Eustis Directorate, U. S. Army Air Mobility Research and Development Laboratory, Fort Eustis, Virginia, July 1973, AD 771973.

2. Faiz, R. L., A DESIGN ANALYSIS OF A CH-54B MAIN ROTOR HUB FABRICATED FROM COMPOSITE MATERIALS, Sikorsky Aircraft Division, United Aircraft Corporation; USAAMRDL Technical Report 73-49, Eustis Directorate, U. S. Army Air Mobility Research and Development Laboratory, Fort Eustis, Virginia, October 1973, AD 771966.

3. STRUCTURAL DESIGN REQUIREMENTS (HELICOPTERS), AR-56, Naval Air Systems Command, Department of the Navy, Washington, D. C., 1970.

4. Olster, E. F., and Roy, P. A., TOLERANCE OF ADVANCED COMPOSITES TO BALLISTICS DAMAGE, presented at the Third Conference on Composite Materials: Testing and Design; ASTM STP 546, American Society for Testing and Materials, Philadelphia, Pennsylvania, 1973.

5. Freeman, W. T., and Kuebeler, G. C., MECHANICAL AND PHYSICAL PROPERTIES OF ADVANCED COMPOSITES, presented at the Third Conference on Composite Materials: Testing and Design; ASTM STP 546, American Society for Testing and Materials, Philadelphia, Pennsylvania, 1973.

6. AVIATION UNIT AND INTERMEDIATE MAINTENANCE MANUAL: ARMY MODEL CH-54B HELICOPTER, TM 55-1520-217-23-2-1, -2, -3, Department of the Army, Washington D. C., 1977.

7. Cook, T. N., Young, R. L., and Starses, F. E., MAINTAINABILITY ANALYSIS OF MAJOR HELICOPTER COMPONENTS, Kaman Aerospace Corporation; USAAMRDL Technical Report 73-43, Eustis Directorate, U. S. Army Air Mobility Research and Development Laboratory, Fort Eustis, Virginia, August 1973, AD 769941.

8. MILITARY STANDARDIZATION HANDBOOK, METALLIC MATERIALS AND ELEMENTS FOR AEROSPACE VEHICLE STRUCTURES, MIL-HDBK-5B, U. S. Government Printing Office, Washington, D. C., 1 September 1971.

9. AEROSPACE STRUCTURAL METALS HANDBOOK, Mechanical Properties Data Center, Traverse City, Michigan; AFML Technical Report 65-115, Volume 2, U. S. Air Force Materials Laboratory, Wright-Patterson AFB, Ohio, 1975.

10. Greszczuk, L. B., and Chao, H., INVESTIGATION OF BRITTLE FRACTURES IN GRAPHITE-EPOXY COMPOSITES SUBJECTED TO IMPACT, McDonnell-Douglas Astronautics Company; USAAMRDL Technical Report 75-15, Eustis Directorate, U. S. Army Air Mobility Research and Development Laboratory, Fort Eustis, Virginia, May 1975, AD 12269.

11. NARMCO RIGIDITE 5209 CARBON FIBER PREPREG SYSTEMS, Narmco Materials, Inc., Celanese Corporation, Costa Mesa, California, undated.

12. Ashton, J. E., Halpin, J. C., and Petit, P. H., PRIMER ON COMPOSITE MATERIALS: ANALYSIS, Stamford, Connecticut, Technomic Publishing Co., Inc., 1969.

13. PLASTICS FOR AEROSPACE VEHICLES, PART 1, REINFORCED PLASTICS, MIL-HDBK-17A, U. S. Government Printing Office, Washington, D. C., January 1971.

14. Pipes, R. B., INTERLAMINAR SHEAR FATIGUE CHARACTERISTICS OF FIBER-REINFORCED COMPOSITE MATERIALS, presented at the Third Conference on Composite Materials: Testing and Design; ASTM STP 546, American Society for Testing and Materials, Philadelphia, Pennsylvania, 1973.

15. Nagle, R., PERSONAL LETTER To Mr. Mark White, B. F. Goodrich General Products Company, Akron, Ohio, 30 January 1973.

16. SUMMARY WEIGHT STATEMENT, ACTUAL, SER-64316, Sikorsky Aircraft Division, United Aircraft Corporation, Stratford, Connecticut, 1970.

17. Mayerjak, R. J., FATIGUE STRENGTH OF LUGS CONTAINING LINERS, VOLUME II - COMPUTER PROGRAM USED FOR ANALYSIS, USAAVLABS Technical Report 70-49B, U. S. Army Aviation Materiel Laboratories, Fort Eustis, Virginia, November 1970, AD 880290.

18. Melcon, M. A., and Hoblit, F. M., DEVELOPMENTS IN THE ANALYSIS OF LUGS AND SHEAR PINS, Product Engineering, June 1953.

19. Flugge, W., STRESSES IN SHELLS, Berlin, Springer-Verlag, 1960.

20. Newmark, N. M., NUMERICAL PROCEDURE FOR COMPUTING DEFLECTIONS, MOMENTS AND BUCKLING LOADS, Transactions of the American Society of Civil Engineers, New York, 1943.

21. Drawings Number 65100-11000, Sheet 4, and 65103-11000, Sheet 5, Sikorsky Aircraft Division, United Aircraft Corporation, Stratford, Connecticut, 1963.

APPENDIX A

RELIABILITY REPORT

INTRODUCTION

The composite plate hub (CPH) was designed with careful monitoring of the design effort from a reliability standpoint. Since the CPH concept intrinsically embodies basic reliability advantages, such as diffuse and redundant load paths, high ballistic damage tolerance, and large areas of primary bonding, the reliability goals focused on maintaining high reliability at the shaft-to-hub and hub-to-hinge interfaces. The design simplicity, low parts count, producibility, and ease of inspection are the results of those efforts. Reliability criteria clearly influenced the design effort in these areas, but for the most part, the basic design requirements of a rotor hub, such as long fatigue life, ballistics tolerance, and fail safety, ensure the very qualities which reliability demands. Reliability goals did not impose fundamentally new or unique requirements on this design, but rather, tended to complement other design objectives.

The results of the reliability analyses are presented primarily in two tables. The first summarizes the reliability design features by which tolerance to damage or prevention of damage from typical inherent or induced failures is achieved. The second table presents a failure modes and effects criticality analysis, which examines the consequences of failures. The inherent failure rates are also discussed and a prediction of a retirement life is made.

RELIABILITY DESIGN FEATURES

The tests of the composite plate hub assembly and elements have demonstrated a greater tolerance to damage than that of a conventional metal hub. The same features that provided the damage tolerance also work to improve reliability. The improvements arise from a complementary combination of favorable configuration and material. The plate configuration provides reliability by maximizing primary bond areas, diffusing the load paths, and ensuring redundant or "standby" load-carrying capability. The use of advanced composite materials permits the plates to achieve strength, stiffness, and resistance to buckling with lower weight than possible using metal construction. In addition, and perhaps most important to reliability and cost, the CPH is highly producible, even in very large sizes.

The following maintenance characteristics also contribute to reliability by reducing the probability of induced failures because of improper maintenance:

1. The hub can be installed and removed without disassembly of hub components.

2. The hub is attached to the rotor shaft with standard fasteners using standard tightening procedures.

3. Assembly and maintenance can be performed with standard tools.

Table A-1 identifies the methods of achieving tolerance to, or prevention of, damages resulting from both inherent or induced failures.

FAILURE MODES AND EFFECTS CRITICALITY ANALYSIS (FMECA)

The FMECA is a systematic analysis of each major component of the hub to determine the possible modes and sources of failure, and the effect and criticality of each mode. The results of the analysis are used to identify failure modes of potential safety concern, and to assess the effect of each failure mode on mission reliability and maintenance. The FMECA is also used to:

1. Identify the need for more reliable materials

2. Identify requirements for redundancy, alternative load paths, or other forms of fail-safe design

3. Indicate areas wherein manufacturing processes and quality control may require special attention

4. Ensure that future test procedures encompass all of the critical failure modes.

The Reliability Group worked closely with the Stress Group in developing the FMECA since the failure modes of a structural element such as the hub can only be identified by an in-depth understanding of material properties and stress analysis. Where failure modes posed a potential hazard to safety, the System Safety Group was asked to participate in the analysis.

Table A-2 presents the FMECA for the composite plate hub considering inherent and induced failure modes. For every component, possible failure modes are identified. For each failure mode, the FMECA states the effect, the most likely time of occurrence, and the criticality rating. The criticality rating provides a qualitative measure of significance for the potential effect of each identified failure mode according to the following criteria:

Minor - Condition such that failure effect will not result in a threat to equipment or personnel, but will normally precipitate a maintenance action.

Major - Condition such that failure effect may result in degraded performance, but can be counteracted or controlled without major system damage or injury to personnel.

Critical - Condition such that failure effect will degrade or precipitate degraded performance, damage equipment, or result in condition requiring immediate corrective action for personnel or equipment survival.

TABLE A-1. RELIABILITY DESIGN FEATURES

TYPE OF DAMAGE/METHOD OF ACHIEVING DAMAGE TOLERANCE OR PREVENTION
FATIGUE CRACKS AND DELAMINATION
a. Plate configurations are inherently multidirectional, providing highly redundant and diffuse load paths.
b. The basic material, graphite-epoxy, provides exceptionally high fatigue strength and low notch sensitivity.
c. Generous sizing provides conservative levels of stress below the endurance limits.
d. The + 60/0°/- 60° orientation of the graphite aligns the reinforcement efficiently with basic radial and perimeter load paths, and also provides good shear strength.
e. Loads are introduced into the composite material via many interleaved metal laminae, which can tolerate high bearing loads and can diffuse these loads into the composite over large bond areas.
f. All bonds are high-integrity, primary bonds, co-cured at initial fabrication.
g. Glass fabric used over the metal laminae reduces local stresses in the graphite at the edges of the metal laminae.
h. High-interference fits are used at the cone seat joints to increase fatigue life.
i. Steel liner is used to allow interference assembly of the cone seat into the composite upper plates without damage to edges of laminae.
j. Long-term retention of interference fits at cone seats is assured by the creep resistance provided by the metal laminae and metal fittings.
k. The major vibratory load, the hub moment, is transferred from the hub to the rotor mast through interference-fitted cone seats, which minimize vibratory stress ranges.
l. Micro-buckling and interlaminar splitting at composite bearing surfaces are inhibited by transverse clamp-up pressures and mechanical entrapment provided at every joint.
m. Steel bushings at damper bolt locations provide several benefits, including interference fits for improved fatigue performances, increased bearing areas, machinable surfaces for final fabrication of close-tolerance fits, machinable and replaceable components for refurbishing the assembly.

TABLE A-1. RELIABILITY DESIGN FEATURES (continued)

TYPE OF DAMAGE/METHOD OF ACHIEVING DAMAGE TOLERANCE OR PREVENTION
FATIGUE CRACKS AND DELAMINATION (continued)
n. Lug geometry at attachment of hub to mast provides flexibility that promotes uniform sharing of the mast torque to each bolt.
CORROSION
a. Corrosion-resistant materials are used for metal fittings and bearing housings.
b. Sermetel-W coating is used on all metal components, except laminae.
FRETTING AND WEAR
a. Sermetel-W coating is used on all metal components, except laminae.
b. Dissimilar metal cone seats provide low fretting and wear against the steel mast. The relative softness of the seat in comparison to the cone will tend to limit fretting and wear to the seat rather than the cone. The seat is more easily refurbished.
c. Components subject to fretting and wear are replaceable.
FOREIGN OBJECT OR BATTLE DAMAGE
a. Diffuse load paths provide tolerance to random damage locations.
b. Low notch-sensitive materials provide either crack arrest or slow crack propagation.
c. Conservative sizing provides residual strength after damage that is sufficient for normal flight.
d. Thick composite plates provide inherent ruggedness.
e. Sacrificial glass fabric outer lamination provides scuffing and snagging protection.
f. Upper and lower plates provide a measure of protection to the center pan plate.

TABLE A-2. FAILURE MODES AND EFFECTS CRITICALITY ANALYSIS

COMPONENT/FAILURE MODE	EFFECT	TIME OF FAILURE	CRITICALITY
UPPER PLATE			
a. Cracks or delamination around center hole. b. Cracks or delamination around hinge bearing retention hole. c. Cracks at doubler edges. d. Buckling. e. Fracture. f. Ballistic damage.	a,b,c. Increased stress in surrounding plate areas may eventually precipitate secondary failure. d,e,f. Increased loads in pan plate. Partial loss of reaction to vibratory hub moment may result in diminished control of blade pitch with corresponding changes of lift and increased vibration. f. May cause notch effect on adjacent laminate material causing reduction of fatigue performance.	a,b,c,e,f. All. d. Autorotative flareout or high-g maneuver.	a,b,c,d. Minor e. Major or Critical f. Minor, Major or Critical
UPPER PLATE CONE SEAT			
a. Fretting. b. Corrosion. c. Crack or fracture. d. Ballistic damage.	a,b. Negligible. c,d. May precipitate secondary failure by increased fretting of steel liner with eventual failure of liner and plate material. Change in preload; increase in vibratory stress of upper plate.	a,b,c,d. All.	a,b,c,d. Minor
UPPER PLATE RETAINING RING			
a. Corrosion. b. Loosening of bolts. c. Crack or fracture. d. Ballistic damage.	a. Negligible. b,c,d. May allow vertical motion of cone seat resulting in change of radial stress on upper plate.	a,b,c,d. All.	a. Minor b,c,d. Minor or Major
PAN PLATE			
a. Cracks around attachment bolt holes. b. Cracks around damper bolt. c. Cracks or delamination around hinge bearing retention holes. d. Cracks at doubler edges. e. Fracture. f. Ballistic damage.	a,b,c,d. Increased stress in surrounding plate areas. May eventually precipitate secondary failures of bolts and plate. e,f. Increased loads on upper and lower plate. Partial loss of reaction to vibratory hub moment may result in diminished control of blade pitch with corresponding changes of lift and increased vibration. f. May cause notch effect on adjacent laminate material causing reduction in fatigue performance.	a,b,c,d,e,f. All.	a,b,c,d. Minor e. Major or Critical f. Minor, Major or Critical
PAN PLATE CONE SEAT			
a. Fretting.	a,b. Negligible.	a,b,c,d. All.	a,b. Minor

TABLE A-2. FAILURE MODES AND EFFECTS CRITICALITY ANALYSIS (continued)

COMPONENT/FAILURE MODE	EFFECT	TIME OF FAILURE	CRITICALITY
PAN PLATE CONE SEAT (continued)			
b. Corrosion. c. Cracks or fracture. d. Ballistic damage.	c,d. May precipitate secondary failure by increased fretting or eventual fracture of the titanium center fitting in pan plate. Change in plate preload causing increase of vibratory stress of pan plate.		c,d. Minor or Major
LOWER PLATE			
a. Cracks or delamination around attachment bolt holes. b. Cracks or delamination around damper bolt holes. c. Cracks or delamination around hinge bearing retention holes. d. Cracks at doubler edges. e. Buckling. f. Fracture. g. Ballistic damage.	a,b,c,d. Increased stress in surrounding plate areas may eventually precipitate secondary failures. e. If buckling results in loss of blade support over large plate area, will result in uncontrolled blade droop and loss of blade. f,g. Increased loads on pan and upper plates. If outer plate section separated, could lead to loss of blade. g. May cause notch effect on adjacent laminate material causing reduction of fatigue performance.	a,b,c,d. All. e. Startup, shutdown or taxiing. f,g. All.	a,b,c,d. Minor e. Major or Critical f. Major or Critical g. Minor, Major or Critical
STEEL LINER AT UPPER AND PAN PLATE CENTER HOLE			
a. Corrosion. b. Fretting. c. Fracture. d. Ballistic damage.	a,b. Negligible. May precipitate secondary failures. c,d. May cause notch effect on adjacent laminate material. Reduction of fatigue performance.	a,b,c,d. All.	a,b. Minor c,d. Minor or Major
BUSHING AT DAMPER BOLT LOWER PLATE			
a. Corrosion. b. Fretting. c. Fracture. d. Ballistic damage.	a,b. Negligible. May make bolt removal difficult. May precipitate secondary failure. c,d. May cause notch effect on adjacent laminate material. Reduction of fatigue performance.	a,b,c,d. All.	a,b. Minor c,d. Minor or Major
LOWER WEDGE BLOCK FOR DAMPER BOLT			
a. Corrosion. b. Fretting. c. Fracture. d. Ballistic damage.	a,b. Negligible. c,d. May allow bushing to move with respect to pan plate causing wear at hole. May precipitate secondary failure.	a,b,c,d. All.	a,b. Minor c,d. Minor

TABLE A-2. FAILURE MODES AND EFFECTS CRITICALITY ANALYSIS (continued)

COMPONENT/FAILURE MODE	EFFECT	TIME OF FAILURE	CRITICALITY
UPPER WEDGE BLOCK FOR DAMPER BOLT			
a. Corrosion.	a,b. Negligible.	a,b,c,d,e. All.	a,b,e. Minor
b. Fretting.	c,d. May cause notch effect in pan plate reducing fatigue strength.		c,d. Minor or Major
c. Fracture.			
d. Ballistic damage.	c,d,e. May prevent damper bolt removal unless hub is removed from aircraft.		
e. Loosening.			
DAMPER BOLT NUT RETAINER			
a. Corrosion.	a. Negligible.	a,b,c,d. All.	a,b,c,d. Minor
b. Fracture.	b,c,d. May prevent proper tightening or loosening of damper bolt. May require removal of hub from aircraft.		
c. Loosening.			
d. Ballistic damage.			
ATTACHMENT BOLT NUT RETAINER			
a. Corrosion.	a. Negligible.	a,b,c,d. All.	a,b,c,d. Minor
b. Fracture.	b,c,d. May prevent proper tightening or loosening of attachment bolts. May require disassembly of upper plate to achieve hub removal.		
c. Loosening.			
d. Ballistic damage.			
BUSHING FOR DAMPER BOLT PAN PLATE			
a. Corrosion.	a,b. Negligible.	a,b,c,d. All.	a,b,c,d. Minor
b. Fretting.	c,d. May permit upper wedge block to separate and become loose part which impedes removal and prevents reinstallation of damper bolt. May require removal of hub.		
c. Fracture.			
d. Ballistic damage.			
COLLAR FOR BEARING HOUSING IN LOWER PLATE			
a. Corrosion.	a,b. Negligible.	a,b,c,d. All	a,b. Minor
b. Fretting.	c,d. Elimination of clampup of lower plate may increase potential for interlaminar splitting or micro-buckling.		c,d. Minor or Major
c. Fracture.			
d. Ballistic damage.			
BEARING HOUSING LOWER PLATE			
a. Corrosion.	a,b. Negligible.	a,b,c,d. All.	a. Minor
b. Fretting.	b. May precipitate eventual fracture.		b. Minor or Major
c. Fracture.			
d. Ballistic damage.	c,d. Possible loss of lubrication or contamination of lubrication may precipitate bearing failure. May cause increased stresses at lower hinge retention hole.		c,d. Major or Critical

TABLE A-2. FAILURE MODES AND EFFECTS CRITICALITY ANALYSIS (continued)

COMPONENT/FAILURE MODE	EFFECT	TIME OF FAILURE	CRITICALITY
COLLAR FOR BEARING HOUSING IN UPPER PLATE			
a. Corrosion.	a,b. Negligible.	a,b,c,d. All.	a,b. Minor
b. Fretting.	c,d. Elimination of clampup of upper and pan plates may increase potential for interlaminar splitting or microbuckling.		c,d. Minor or Major
c. Fracture.			
d. Ballistic damage.			
BEARING HOUSING AT UPPER PLATE			
a. Corrosion.	a. Negligible.	a.b. All.	a. Minor
b. Fretting.	b. May precipitate eventual fracture.	c,d. All.	b. Minor or Major
c. Fracture.			
d. Ballistic damage.	c,d. Possible loss of lubrication or contamination of lubrication may precipitate bearing failure. May cause increased stresses at upper hinge retention hole.		c,d. Major or Critical
ATTACHMENT BOLT AT HUB			
a. Corrosion.	a,b. Negligible.	a,b,c,d,e. All.	a,b. Minor
b. Fretting.	c,d,e. May lead to cracking of fitting in pan plate and bolt fractures.		c,d,e. Major or Critical
c. Loosening.			
d. Fracture.			
e. Ballistic damage.			
ATTACHMENT BOLT AT DAMPER			
a. Corrosion.	a,b. Negligible.	a,b,c,d. All.	a,b,c,d. Minor
b. Fretting.	c,d. Reduction of margin of safety against ground resonance. After swing of approximately 6°, the loose end of damper will be restrained by the adjacent damper and bottom plate.		
c. Fracture.			
d. Ballistic damage.			

INHERENT FAILURE RATE PREDICTIONS

Inherent modes of failure for a rotor hub are basically of two types:

1. Stress- or fatigue-generated failures, such as cracks and bond separations.
2. Environment-generated failure, such as corrosion.

Stress- or fatigue-generated failures would be critical and deadly events in a conventional metal rotor hub. In practice, they are effectively precluded from occurrence by the establishment of a retirement life. The retirement life is determined by probability of occurrence calculations which use as input laboratory-determined S-N curves, measured flight loads, and assumed usages (mission profiles and times). A typical theoretical failure rate allowed at the retirement life is .0005. The actual failure rate is generally even lower because conservative approximations are used in the theoretical calculations. The retirement life for the present titanium hub is an adequate 21,675 hours (Reference 6). The composite plate rotor hub was designed to provide strengths equal to or greater than the present hub. Thus, for the same service usage, the retirement life for the CPH is greater than 21,675 hours.

The traditional basis for predicting rate of inherent failure for environment-generated failures is the statistical experience of other helicopters of similar design used under similar conditions. No such data are available for the composite plate hub because it is quite unlike existing hubs in materials and configuration. However, it is anticipated that failure rates from corrosion will be of minor importance because of the provisions that have been made to protect the metallic components and the inherent noncorrodibility of the composite materials.

6. AVIATION UNIT AND INTERMEDIATE MAINTENANCE MANUAL: ARMY MODEL CH-54B HELICOPTER, TM 55-1520-217-23-2-1, -2, -3, Department of the Army, Washington, D. C., 1977.

APPENDIX B

MAINTAINABILITY REPORT

INTRODUCTION

Maintainability was a major consideration throughout the design cycle. Maintainability goals were established that provided persistent pressure upon the design. Their effect is evident in the overall simplicity of the design and particularly in the simplicity of the procedures for installation and removal. The final design achieved all major maintainability objectives.

This report presents an analysis of the composite plate hub for the CH-54B helicopter to assess the maintainability characteristics of the design, and to make initial estimates of maintenance requirements. In addition, the details of the maintenance plan, installation/removal procedures, and maintainability features are also provided.

MAINTAINABILITY REQUIREMENTS

The maintainability requirements were stated as the following qualitative goals:

1. Minimize maintenance manhours per flight-hour for both scheduled maintenance and unscheduled corrective maintenance
2. Minimize the probability for maintenance being required above field level
3. Ensure simplicity of installation and removal
4. Ensure positive removal procedures even in the presence of extensive corrosion and/or fretting
5. Ensure installation and removal requires no disassembly of hub components
6. Ensure ease of inspection of critical parts
7. Provide maximum accessibility to mounting hardware
8. Ensure that all components subject to corrosion, fretting, or wear can be refurbished or replaced
9. Ensure that maintenance manpower requirements will be compatible with the maintenance program for the CH-54B
10. Ensure skill levels required for field repairs are compatible with the training of Army personnel
11. Estimate requirements for special tools.

MAINTAINABILITY DESIGN FEATURES

A summary of the maintainability features of the pan plate hub is given in Table B-1.

MAINTAINABILITY PREDICTION

The data in Table B-2 are organized by major components of the hub and by type of failure or damage necessitating maintenance or repair. The maintainability prediction identifies possible maintenance actions and estimated manhours for corrective action. Each action requires an initial decision either to scrap or to repair the hub on or off the aircraft. Technical manuals would provide guidelines and procedures to assess the reliability, safety, and economics of the contemplated repair.

For each damage or failure event scheduled for repair, a brief statement of the repair task is entered in the column headed Maintenance Action. The appropriate maintenance level is assigned and the decision is made to effect the repair on the aircraft or to remove the hub for repair.

The next step in the analysis assigns a repair time to each task. The repair-time allocation reflects the initial engineering estimate of the elapsed time required for the typical Army mechanic to perform specified types of repairs on the hub. It encompasses the time required to isolate and correct the fault, including any adhesive cure time, and to replace the aircraft in an operational readiness status. It attempts to reflect expected performance under field maintenance conditions and the resources available to the field mechanic. It is an estimate of productive maintenance time, and does not account for supply delays, administrative time, etc.

Hub replacement time of 26.7 hours was estimated based on the differences in installation between the composite plate hub and the present CH-54B titanium hub. Reference 7 lists the Main Rotor Head Assembly replacement time as 28.7 hours, apportioned by task element as follows: Fault Isolate, 1.1; Remove/Install Other Components, 19.6; Remove/Install Component, 4.7; Drain/Lube Service, .8; Adjust/Align, etc., 1.0; Inspect/Test, 1.5. The simplification of pan hub-to-shaft attachment and the elimination of complicated iterative torquing procedures reduced the remove and install component time from 4.7 to 2.7 hours. Since the pan hub design will not significantly affect any of the other task elements, the total replacement time is, therefore, reduced by 2 hours from 28.7 to 26.7 hours.

---

7. Cook, T. N., Young, R. L., and Starses, F. E., MAINTAINABILITY ANALYSIS OF MAJOR HELICOPTER COMPONENTS, Kaman Aerospace Corporation; USAAMRDL Technical Report 73-43, Eustis Directorate, U. S. Army Air Mobility Research and Development Laboratory, Fort Eustis, Virginia, August 1973, AD 769941.

TABLE B-1. MAINTAINABILITY DESIGN FEATURES

MAINTENANCE ACTION/METHOD OF ACHIEVING GOOD MAINTAINABILITY
DAILY, INTERMEDIATE, AND PERIODIC INSPECTION (PMD, PMI, PMP)
a. Extensive use of composite materials reduces corrosion inspection efforts.
b. Slow crack propagation rate and diffuse load paths reduce consequences of undiscovered cracks in incipient stages.
c. Large plate surfaces provide ease of inspection for cracks, dents, nicks, and security.
d. Simplified hub-to-shaft attachment increases inspectability of critical parts.
BLEND NICKS AND SCRATCHES IN METAL COMPONENTS
a. Exposed metal parts have high fracture toughness and low notch sensitivity.
BLEND NICKS AND SCRATCHES IN COMPOSITE COMPONENTS
a. All exterior surfaces are covered by woven ply of E-glass providing protective layer that becomes sacrificial material in blending process.
b. Superficial nicks and scratches can be ignored since outer glass layer is sacrificial.
c. Repair of most nicks and scratches can be performed on the aircraft.
REFURBISH FRETTING-CORROSION
a. Use of composite material reduces overall corrosion potential.
b. Sermetel-W coating on metal components, except laminae.
c. All components susceptible to corrosion are replaceable at DS, GS, or depot level.
d. The geometry of the pan plate provides openings at its perimeter. Any moisture accumulation in the interior of the hub will be expelled by centrifugal force through these openings. The openings also permit inspection of the interior of the hub without disassembly.

TABLE B-1. MAINTAINABILITY DESIGN FEATURES (continued)

MAINTENANCE ACTION/METHOD OF ACHIEVING GOOD MAINTAINABILITY
TIGHTEN ATTACHMENT HARDWARE
a. Self-locking upper cone seat retention bolts.
b. Lock nuts and nut retainers on hub attachment bolts and damper bolts.
c. Self-locking nuts on rotating scissors attachment lug bolts.
HUB REPLACEMENT
a. Upper and lower cone seats are cut at angles that normally will allow self-release and ease of removal. In the event of abnormal seizing due to corrosion or fretting, positive and sure removal is assured by provisions to apply hydraulic pressure and mechanical jacking to force separation.
b. All mounting bolts are easily accessible.
c. Removal and replacement requires only common hand tools.
d. Simplified hub attachment requires only 24 standard fasteners; 12 to secure the upper cone seat retaining ring and 12 to secure hub to mast flange.
e. Hub is replaceable as complete assembly and does not require any buildup or disassembly at direct support level.
f. Nut retainers on hub attachment bolts and damper bolts assist bolt extraction.
g. Potential for shaft damage is reduced by eliminating external threads on shaft.
h. Hub replacement procedure does not require torque stabilization procedures.
HUB PLATE REPAIR/REPLACEMENT
a. Anticipated high level of repairability of ballistic damage.
b. Hub plates are individually replaceable.
REMOVAL/REPLACEMENT OF LEAD-LAG HINGE ASSEMBLY
a. Simplified hub removal procedures.
b. Disassembly of lower plate requires no special tools or procedures.

TABLE B-2. MAINTAINABILITY PREDICTION

HUB ELEMENT/ DAMAGE DESCRIPTION	INHERENT	INDUCED	MAINTENANCE ACTION	MAINT. LEVEL					MANHOURS			NUMBER OF MEN
				ORG.	D.S. & G.S.	DEPOT	ON AIRCRAFT	OFF AIRCRAFT	REMOVE AND INSTALL HUB ASSEMBLY	REPAIR	TOTAL	
UPPER PLATE												
a. Cracks or Delamination	x		Replace Hub		x		x		26.7			2
			Replace Plate			x		x		30.0	56.7	1
b. Buckling or Fracture	x		Replace Hub		x		x		26.7			2
			Replace Plate			x		x		30.0	56.7	1
c. Ballistic Damage (Critical)		x	Replace Hub		x		x		26.7			2
			Replace Plate			x		x		30.0	56.7	1
d. Ballistic Damage (Marginal)		x	Replace Hub		x		x		26.7			2
			Repair Plate		x			x		3.0	29.7	1
e. Ballistic Damage (Noncritical)		x	Replace Hub		x		x		26.7			2
			Repair Plate		x			x		1.0	27.7	1
UPPER PLATE CONE SEAT												
a. Fretting	x		Polish Cone Surface	x				x	Note 1	.3	.3	1
b. Corrosion	x		Treat/Refinish	x				x	Note 1	.5	.5	1
c. Crack or Fracture	x		Replace Hub		x		x		26.7			1
			Replace Cone			x		x		2.5	29.2	1
d. Ballistic Damage		x	Replace Hub		x		x		26.7			1
			Replace Cone			x		x		2.5	29.2	1
UPPER PLATE RETAINING RING												
a. Corrosion	x		Treat/Refinish	x			x			.6	.6	1
b. Loosening of Bolts	x		Tighten or Replace Bolts	x			x			.4	.4	1
c. Crack or Fracture	x		Replace Ring		x		x			.4	.4	1
d. Ballistic Damage		x	Replace Ring		x		x			.4	.4	1
PAN PLATE												
a. Cracks or Delaminations	x		Replace Hub		x		x		26.7			2
			Replace Plate			x		x		30.0	56.7	1
b. Fracture	x		Replace Hub		x		x		26.7			2
			Replace Plate			x		x		30.0	56.7	1
c. Battle Damage (Critical)		x	Replace Hub		x		x		26.7			2
			Replace Plate			x		x		30.0	56.7	1
d. Battle Damage (Marginal)		x	Replace Hub		x		x		26.7			2
			Repair Plate			x		x		30.0	56.7	1
e. Battle Damage (Noncritical)		x	Replace Hub		x		x		26.7			2
			Repair Plate		x			x		1.0	27.7	1
PAN PLATE CONE SEAT												
a. Fretting	x		Polish Cone Surface	x				x	Note 1	.3	.3	1
b. Corrosion	x		Treat/Refinish	x				x	Note 1	.5	.5	1
c. Crack or Fracture	x		Replace Hub		x				26.7			2
			Replace Cone			x		x		32.0	58.7	1
d. Ballistic Damage		x	Replace Hub		x			x	26.7			2
			Replace Cone			x				32.0	58.7	1

TABLE B-2. MAINTAINABILITY PREDICTION (continued).

HUB ELEMENT/ DAMAGE DESCRIPTION	INHERENT	INDUCED	MAINTENANCE ACTION	MAINT. LEVEL					MANHOURS			NUMBER OF MEN
				ORG.	D.S. & G.S.	DEPOT	ON AIRCRAFT	OFF AIRCRAFT	REMOVE AND INSTALL HUB ASSEMBLY	REPAIR	TOTAL	
LOWER PLATE												
a. Crack or Delamination	x		Replace Hub		x		x		26.7			2
			Replace Plate			x		x		5.0	31.7	1
b. Buckling or Fracture	x		Replace Hub		x		x		26.7			2
			Replace Plate			x		x		5.0	31.7	1
c. Ballistic Damage (Critical)		x	Replace Hub		x		x		26.7			2
			Replace Plate			x		x		5.0	31.7	1
d. Ballistic Damage (Marginal)		x	Replace Hub		x		x		26.7			2
			Repair Plate			x		x		3.0	29.7	1
e. Ballistic Damage (Noncritical		x	Repair Plate		x		x			1.0	1.0	1
STEEL LINER												
a. All Damage	x	x	Replace Liner			x		x	Note 2	.3	.3	1
BUSHING												
a. Corrosion	x		Treat/Refinish	x				x	Note 1	.3	.3	1
b. Fretting	x		Polish	x				x	Note 1	.5	.5	1
c. Fracture	x		Replace Bushing			x		x	Note 1	5.5	5.5	1
d. Ballistic Damage		x	Replace Bushing			x		x	Note 4	2.0	2.0	1
LOWER WEDGE BLOCK												
a. Corrosion	x		Treat/Refinish	x			x			.3	.3	1
b. Fretting	x		Replace Wedge Block			x		x	Note 3	Note 3		1
c. Fracture	x		Replace Hub		x		x		26.7			2
			Replace Wedge Block			x		x		5.5	32.2	1
d. Ballistic Damage		x	Replace Hub		x		x		26.7			2
			Replace Wedge Block			x		x		5.5	32.2	1
UPPER WEDGE BLOCK												
a. Corrosion	x		Treat/Refinish	x				x	Note 1	.3	.3	1
b. Fretting	x		Replace Wedge Block			x			Note 3			1
c. Fracture	x		Replace Hub		x		x		26.7			2
			Replace Wedge Block			x				5.5	32.2	1
d. Ballistic Damage		x	Replace Hub					x	Note 4	2.0		2
			Replace Wedge Block			x						1
e. Loosening	x		Replace Hub		x				26.7			2
			Replace Securing Bushing							5.5	32.2	1
DAMPER BOLT NUT RETAINER												
a. Corrosion	x		Replace Retainer		x			x	Note 1	.3		1
b. Fracture	x		Replace Hub		x		x		26.7			2
			Replace Retainer		x			x		.3	30.0	1
c. Loosening	x		Replace Hub		x		x		26.7			2
			Replace Retainer		x					.3	30.0	1
d. Ballistic Damage		x	Replace Retainer						Note 4	.3	.3	1

TABLE B-2. MAINTAINABILITY PREDICTION (continued)

HUB ELEMENT/ DAMAGE DESCRIPTION	INHERENT	INDUCED	MAINTENANCE ACTION	MAINT. LEVEL: ORG.	D.S. & G.S.	DEPOT	ON AIRCRAFT	OFF AIRCRAFT	MANHOURS: REMOVE AND INSTALL HUB ASSEMBLY	REPAIR	TOTAL	NUMBER OF MEN
ATTACHMENT BOLT NUT RETAINER												
a. Corrosion	x		Replace Retainer	x				x	Note 1	.3	.3	1
b. Fracture	x		Replace Hub		x		x		27.7			2
			Replace Retainer		x					.3	28.0	1
c. Loosening	x		Replace Hub		x		x		26.7			2
			Replace Retainer		x			x		.3	27.0	1
d. Ballistic Damage		x	Replace Hub		x		x		Note 4			2
			Replace Retainer		x			x		.3	.3	1
BUSHING FOR DAMPER BOLT PAN PLATE												
a. Corrosion	x		Treat/Refinish	x				x	Note 1	.3	.3	1
b. Fretting	x		Polish	x				x	Note 1	.5	.5	1
c. Fracture	x		Replace Bushing			x		x	Note 1	5.5	5.5	1
d. Ballistic Damage		x	Replace Bushing			x		x	Note 4	2.0	2.0	1
COLLAR FOR BEARING HOUSING, LOWER PLATE												
a. Corrosion	x		Treat/Refinish	x		x				.5	.5	1
b. Fretting	x		Polish	x		x			Note 2	.5	.5	1
c. Fracture	x		Replace Hub		x				26.7			2
			Replace Collar			x				5.2	31.9	1
d. Ballistic Damage		x	Replace Hub		x				26.7			2
			Replace Collar			x				5.2	31.9	1
BEARING HOUSING, LOWER PLATE												
a. Corrosion	x		Treat/Refinish	x			x			.6		1
b. Fretting	x		Replace Housing			x		x	Note 3			1
c. Fracture	x		Replace Hub		x		x		26.7			2
			Replace Housing			x		x		7.0	33.7	1
d. Ballistic Damage		x	Replace Hub		x		x		26.7			2
			Replace Housing							7.0	33.7	1
COLLAR FOR BEARING HOUSING, UPPER PLATE												
a. Corrosion	x		Treat/Refinish	x			x			.3	.3	1
b. Fretting	x		Polish	x			x		Note 2			1
c. Fracture	x		Replace Collar		x		x			.5	.5	1
d. Ballistic Damage		x	Replace Collar		x		x			.5	.5	1
BEARING HOUSING UPPER PLATE												
a. Corrosion	x		Treat/Refinish	x			x					1
b. Fretting	x		Replace Housing			x		x				1

TABLE B-2. MAINTAINABILITY PREDICTION (continued)

HUB ELEMENT/ DAMAGE DESCRIPTION	INHERENT	INDUCED	MAINTENANCE ACTION	MAINT. LEVEL: ORG.	D.S. & G.S.	DEPOT	ON AIRCRAFT	OFF AIRCRAFT	MANHOURS: REMOVE AND INSTALL HUB ASSEMBLY	REPAIR	TOTAL	NUMBER OF MEN
BEARING HOUSING UPPER PLATE (continued)												
c. Fracture	x		Replace Hub		x		x		26.7			2
			Replace Housing			x		x		7.5	34.2	1
d. Ballistic Damage		x	Replace Hub		x		x		26.7			2
			Replace Housing			x		x		7.5	34.2	1
ATTACHMENT BOLT, HUB												
a. Corrosion	x		Replace Bolt		x		x			.5	.5	1
b. Fretting	x		Replace Bolt		x		x		Note 3			1
c. Fracture	x		Replace Bolt (Extraction Req'd)		x		x			2.0	2.0	1
d. Ballistic Damage		x	Replace Bolt (Extraction Req'd)		x		x			2.0	2.0	1
ATTACHMENT BOLT, DAMPER												
a. Corrosion	x		Replace Bolt		x		x			.3	.3	1
b. Fretting	x		Replace Bolt		x		x		Note 3			1
c. Fracture	x		Replace Bolt (Extraction Req'd)		x		x			2.0	2.0	1
d. Ballistic Damage		x	Replace Bolt (Extraction Req'd)		x		x			2.0	2.0	1

NOTE 1 Discovered when hub has been removed for other reasons.

NOTE 2 Discovered only after hub removal and plate/parts disassembly.

NOTE 3 Discovered only after parts disassembly. Parts are normally replaced after disassembly. No isolated maintenance time.

NOTE 4 Location of part precludes isolated ballistic damage. Maintenance time, therefore, does not include time to disassemble hub plates.

REPAIRABILITY CONSIDERATIONS

The repairability of minor handling damage and ballistic damage to the composite plate hub was evaluated as part of the maintainability analysis. The evaluation process considered the results of the structural analysis performed on the plates, the anticipated stress concentration factors resulting from ballistic penetration, and damage potential of various areas of each plate, along with Kaman's experience in repair techniques and composite structures. Opinions regarding the anticipated repairability are listed below. Additional structural testing of the composite hub with the proposed repairs would be required to demonstrate their adequacy.

1. Minor blending of surface nicks and scratches can be performed on the aircraft.
2. The surface of each plate can be divided into noncritical, marginal, and critical areas. Identification of such areas on the hub will be provided as a maintenance aid in determining repair disposition or in making repair/scrap decisions.
3. Once damage has been isolated to marginal or noncritical areas, measurement criteria (depth of gouge, hole diameter, hole shape, etc.) would determine repairability and repair technique.
4. Small ballistic holes in noncritical areas can be repaired by a simple plug with upper and lower covering patches. This repair technique would be considered nonstructural. It is anticipated that this repair could be performed at DS or GS levels.
5. Larger damaged areas can be repaired by a double- or single-scarf patching process using low-temperature curing materials. This structural repair would be considered a depot-level activity.
6. Hub manufacturing techniques and tolerance control will allow individual replacement of plates at the depot level. It is anticipated that the lower plate will be replaceable as an assembly, including the lower cartridge housings.
7. All metal parts, including bushings, wedge blocks, cone seats, liners, and housings, will be replaceable in each plate.
8. Skill levels required for all repairs will be consistent with existing maintenance structure.

APPENDIX C

STRUCTURAL ANALYSIS

SUMMARY

The structural analysis is summarized by Table C-1, which presents minimum margins of safety for the components of the composite hub.

TABLE C-1. MINIMUM MARGINS OF SAFETY

Location/Type of Failure	M.S. Fatigue, Ultimate
UPPER PLATE	
Steel Laminae at Lead-Lag Pin	+ .10 , + .95
Steel Laminae at Center Hole	+ .81 , + 1.07
Buckling	N/A , + .24
LOWER PLATE	
Steel Laminae at Lead-Lag Pin	+ 4.50 , + .39
Titanium Lugs on Center Fitting	High , + .31
Buckling	N/A , + .14
PAN PLATE	
Steel Laminae at Lead-Lag Pin	+ .67 , + .14
Composite Interlaminar at Lead-Lag Pin	+ 1.69 , + 1.44
Adhesive Interlaminar at Lead-Lag Pin	+ .07 , + .22
Adhesive at Scarf Joint	+ 1.01 , + 1.12
ROTOR SHAFT AND ATTACHMENTS	
Shaft, Bending	+ .12 , + 2.58
Main Attachment Bolts	High , + .91
Lug, Torque	High , + 2.11
Lug, Bending	+ 3.06 , High
Bolts at Top of Shaft	High , + .54

INTRODUCTION

This appendix presents:

1. Material properties and allowable stresses
2. Design conditions
3. Blade loads for design conditions
4. Internal loads in the form of free-body diagrams of the lead-lag pins, which indicate the loads upon the bearings and the plates (upper, pan, and lower).
5. Stress analyses for the element specimen
6. Stress analyses for a typical joint
7. Stress analyses for each plate using loads from 4, above
8. Stress analyses for the rotor shaft
9. Stiffness analyses to show dynamic compatibility.

Throughout this appendix, the units of length and force are inches and kips, respectively.

MATERIAL PROPERTIES

This section lists the material properties used in the structural analyses. The following notation is used:

Symbols:

ε = normal strain

γ = shear strain

μ = Poisson's ratio, isotropic material

ν = Poisson's ratio, anisotropic material

σ = normal stress

τ = shear stress

E = modulus of elasticity

F = strength

G = shear modulus

Subscripts and Superscripts:

cu = compression, ultimate

e = endurance limit, fatigue

o = denotation for strains at the middle surface of laminate

se = shear, endurance

su = shear, ultimate

tu = tension, ultimate

x, y = reference axes for laminate

1, 2 = reference axes for individual lamina

Double subscripts used with moduli, Poisson's ratios, stresses, and strains correspond to conventional engineering usage.

The following material properties were used in the structural analyses:

1. Ti-6Al-4V, Bars and Forgings, Annealed (Reference 8)

   E = 16200 ksi μ = .31

   G = 6200 ksi

   F_{tu} = 130 ksi

8. MILITARY STANDARDIZATION HANDBOOK, METALLIC MATERIALS AND ELEMENTS FOR AEROSPACE VEHICLE STRUCTURES, MIL-HDBK-5B, U. S. Government Printing Office, Washington, D. C., 1 September 1971.

2. 4340 Steel, All Wrought Forms, Quenched and Tempered (Reference 8)

$E = 2900$ ksi $\quad \mu = .32$

$G = 1100$ ksi

$F_{tu} = 150$ ksi

$F_e = \pm 25$ ksi*

*A fatigue allowable working stress permitted at Kaman for a shot-peened component of simple geometry.

3. 17-7 PH CRES, Sheet, Condition RH950 (Reference 9)

$E = 2900$ ksi $\quad \mu = .32$

$G = 1100$ ksi

$F_{tu} = 210$ ksi

$F_e = \pm 25$ ksi*

*A fatigue allowable working stress at the inside edge of a hole in a steel-lamina-reinforced joint for use with the fatigue design loads. Figure 23 shows the fatigue design load to be 14 percent higher than the endurance limit of the present titanium hub. Tests of element specimens established $\pm$ 22.0 ksi as the mean endurance limit for the laminae. Therefore, an allowable working stress of 1.14 x 22.0 = $\pm$ 25.0 ksi provides a strength that matches the present titanium hub.

4. Thornel 300/Narmco 5209, Carbon Fiber Prepreg System, Inplane Properties

$E_{11} = 19400$ ksi $\quad \nu_{12} = .25$

$E_{22} = 1380$ ksi

$G_{12} = 750$ ksi

$F_{11}^{tu} = 196$ ksi $\quad \varepsilon_{11}^{tu} = .01010$

$F_{11}^{cu} = -200$ ksi $\quad \varepsilon_{11}^{cu} = -.01031$

$F_{22}^{tu} = 9.0$ ksi $\quad \varepsilon_{22}^{tu} = .00652$

$F_{22}^{cu} = -34.0$ ksi $\quad \varepsilon_{22}^{cu} = -.02464$

$F_{12}^{su} = \pm 16.4$ ksi $\quad \gamma_{12}^{su} = \pm .02187$

---

9. AEROSPACE STRUCTURAL METALS HANDBOOK, Mechanical Properties Data Center, Traverse City, Michigan; AFML Technical Report 65-115, Volume 2, U. S. Air Force Materials Laboratory, Wright-Patterson AFB, Ohio, 1975.

The above properties are representative of those presented in the literature for the 5208 or 5209 systems. The stiffness and strength properties of the Thornel 300/Narmco 5208 and Thornel 300/Narmco 5209 are similar at ordinary temperatures. The two resin systems differ at high temperatures where the 5208 system has better retention of its strength and stiffness. The data shown here were taken from References 10 and 11. They correspond to laminate specimens which had the following physical characteristics:

Fiber volume	58.5 percent
Void content	.85 percent
Density	.0557 $lb/inch^3$
Thickness/ply	.00578 inch

In the composite hub, the carbon was used in a symmetrical laminate with equal amounts of reinforcement in the $0/\pm 60$ degree orientations. A typical plate had 30 plies of carbon, two plies of style 120 glass cloth, and one layer of .006-inch adhesive. In the bottom plate, which had the best resin control, this combination averaged .1858 inch in total thickness. Thus, the as-made carbon thickness was $(.1858 - 2 \times .004 - .006)/30 = .00573$ inch/ply.

The properties for the $0/\pm 60$ laminate were calculated using plane stress, orthotropic material, lamination theory, and the maximum strain failure criteria. The calculations followed the composite theory presented in References 12 and 13. The Kaman computer program CMAB (Composite Materials Analysis Version B) was used to make the calculations. Table C-2 shows

---

10. Greszczuk, L. B., and Chao, H., INVESTIGATION OF BRITTLE FRACTURES IN GRAPHITE-EPOXY COMPOSITES SUBJECTED TO IMPACT, McDonnell-Douglas Astronautics Company; USAAMRDL Technical Report 75-15, U. S. Army Air Mobility Research and Development Laboratory, Fort Eustis, Virginia, May 1975, AD A012269.
11. NARMCO RIGIDITE 5209 CARBON FIBER PREPREG SYSTEMS, Narmco Materials, Inc., Celanese Corporation, Costa Mesa, California, undated.
12. Ashton, J. E., Halpin, J. C., and Petit, P. H., PRIMER ON COMPOSITE MATERIALS: ANALYSIS, Stamford, Connecticut, Technomic Publishing Co., Inc., 1969.
13. PLASTICS FOR AEROSPACE VEHICLES, PART 1, REINFORCED PLASTICS, MIL-HDBK-17A, U. S. Government Printing Office, Washington, D. C., January 1971.

TABLE C-2. LAMINATE ANALYSIS FOR GRAPHITE-EPOXY WITH 0/±60 ORIENTATIONS

T300/5209 ULTIMATE U/U/U .3333/.3333/.3333 60/0/-60 PROG...CMAB 5/20/76

MAT.	ALLOWABLE STRESS, UNIAXIAL 11	11	22	22	12	12	MODULI E11	E22	G	NU12
25	-200.0	196.0	-34.0	9.00	-16.40	16.40	19400.	1380.	750.	0.250

LAMINA	1	2	3
MATERIAL	25	25	25
THICKNESS	0.3333	0.3333	0.3333
ANGLE	60.	0.	-60.

A B
B D

8.288E-03	2.494E 03	0.0	0.0	0.0	-4.575E-02
2.494E 03	8.288E 03	0.0	0.0	0.0	-1.284E 03
0.0	0.0	2.897E 03	-4.575E 02	-1.284E 03	0.0
0.0	0.0	-4.575E 02	2.759E 02	2.873E-02	0.0
0.0	0.0	-1.284E 03	2.873E 02	9.461E 02	0.0
-4.575E 02	-1.284E 03	0.0	0.0	0.0	3.209E 02

A* B*
C* D*

1.334E-04	-2.808E-05	0.0	0.0	0.0	7.783E-05
-2.808E-05	3.232E-04	0.0	0.0	0.0	1.253E-03
0.0	0.0	8.844E-04	3.170E-04	1.104E-03	0.0
0.0	0.0	3.170E-04	5.413E-03	-1.213E-03	0.0
0.0	0.0	1.104E-03	-1.213E-03	2.923E-03	0.0
7.783E-05	1.253E-03	0.0	0.0	0.0	8.241E-03

A* B*
C* D*

1.327E-04	-3.992E-05	0.0	0.0	0.0	9.444E-03
-3.992E-05	1.327E-04	0.0	0.0	0.0	1.521E-01
0.0	0.0	3.452E-04	1.579E-01	4.431E-01	0.0
0.0	0.0	-1.579E-01	2.037E 02	8.455E 01	0.0
0.0	0.0	-4.431E-01	8.455E 01	3.772E 02	0.0
-9.444E-03	-1.521E-01	0.0	0.0	0.0	1.213E 02

LAMINATE PROPERTIES	EX	EY	G
K'S UNRESTRAINED	7497.	3094.	1131.
K'S = 0	7539.	7539.	2897.

BEHAVIOR FOR NX= 10.000 NY= 0.0 NXY= 0.0 KX= 0.0 KY= 0.0 KXY= 0.0

LAM. NO.	STRESSES X	Y	XY	STRAINS 11	22	12	11	22	12	M.S. 11	22	12	MIN.
3	2.1	0.0	-0.4	0.9	1.3	1.1	0.000032	0.000895	0.001495	99.00	6.28	13.63	6.28
2	25.7	-0.1	0.0	25.7	-0.1	0.0	0.001327	-0.000399	0.0	6.62	60.72	99.00	6.62
1	2.1	0.0	0.4	0.9	1.3	-1.1	0.000032	0.000895	-0.001495	99.00	6.28	13.63	6.28
ALL	10.0	0.0	0.0				0.001327	-0.000399	0.0				6.28

a typical first page of output which includes the laminate constitutive equations as defined in Reference 13. Since these calculations were carried out for a laminate with a thickness of 1 inch, the matrix [A] that relates the force resultants to the mid-plane strains is also the stress-strain relationship for the laminate and is a required input to the finite-element analyses presented herein.

$$\begin{bmatrix} \sigma_{xx} \\ \sigma_{yy} \\ \tau_{xy} \end{bmatrix} = \begin{bmatrix} 8288. & 2494. & 0. \\ 2494. & 8288. & 0. \\ 0. & 0. & 2897. \end{bmatrix} \begin{bmatrix} \sigma_x^o \\ \sigma_y^o \\ \gamma_{xy}^o \end{bmatrix}$$

The program CMAB calculates margins of safety for each ply for specific loadings. It also includes a provision for systematically varying the loading so that plots showing limiting strength can be developed. Figures 6 and C-1 are such plots for the ultimate strength of graphite-epoxy with 0 $\pm$ 60 orientations.

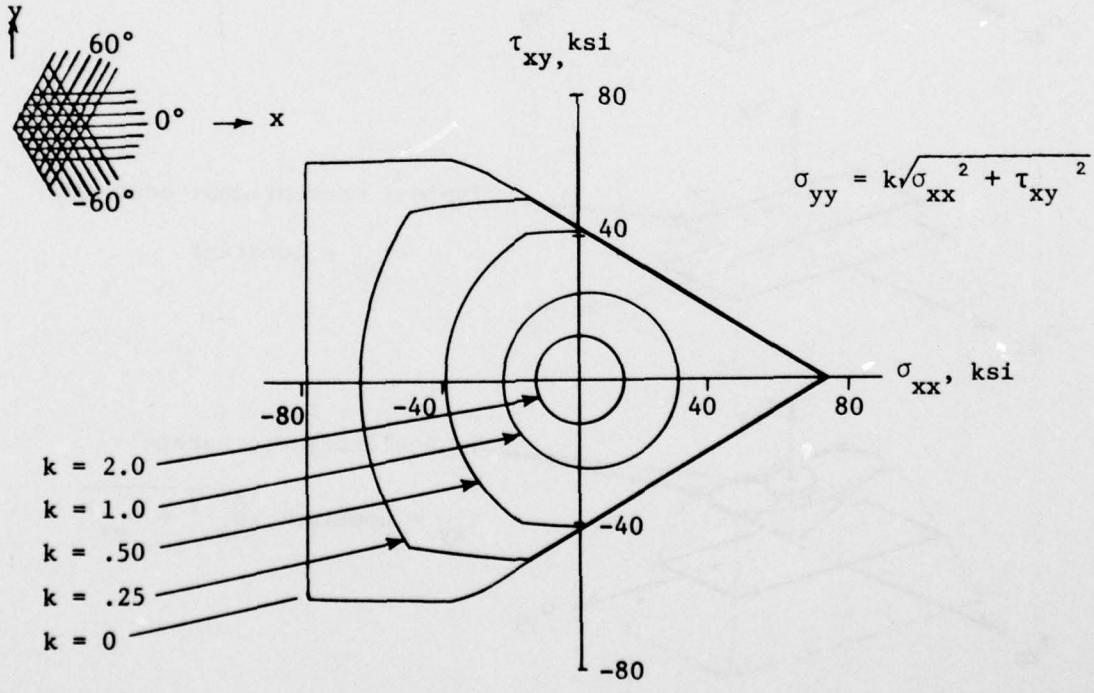


Figure C-1. Typical ultimate strength for graphite-epoxy, 0/$\pm$ 60, with τ_{xy} as ordinate.

The form of presentation in Figures 6 and C-1 is unusual and perhaps original. The following general comments provide a geometrical interpretation of what is being done when the strength contours are plotted as they are herein.

Strength is a function of three stresses, and thus, requires special procedures for its graphical presentation in two dimensions. It is commonly presented as a set of contours that correspond to the intersection of parallel planes with the strength surface. In this report, the contours correspond to the intersection of a cone of constant stress ratio with the limiting strength surface. Figure C-2 compares the two methods.

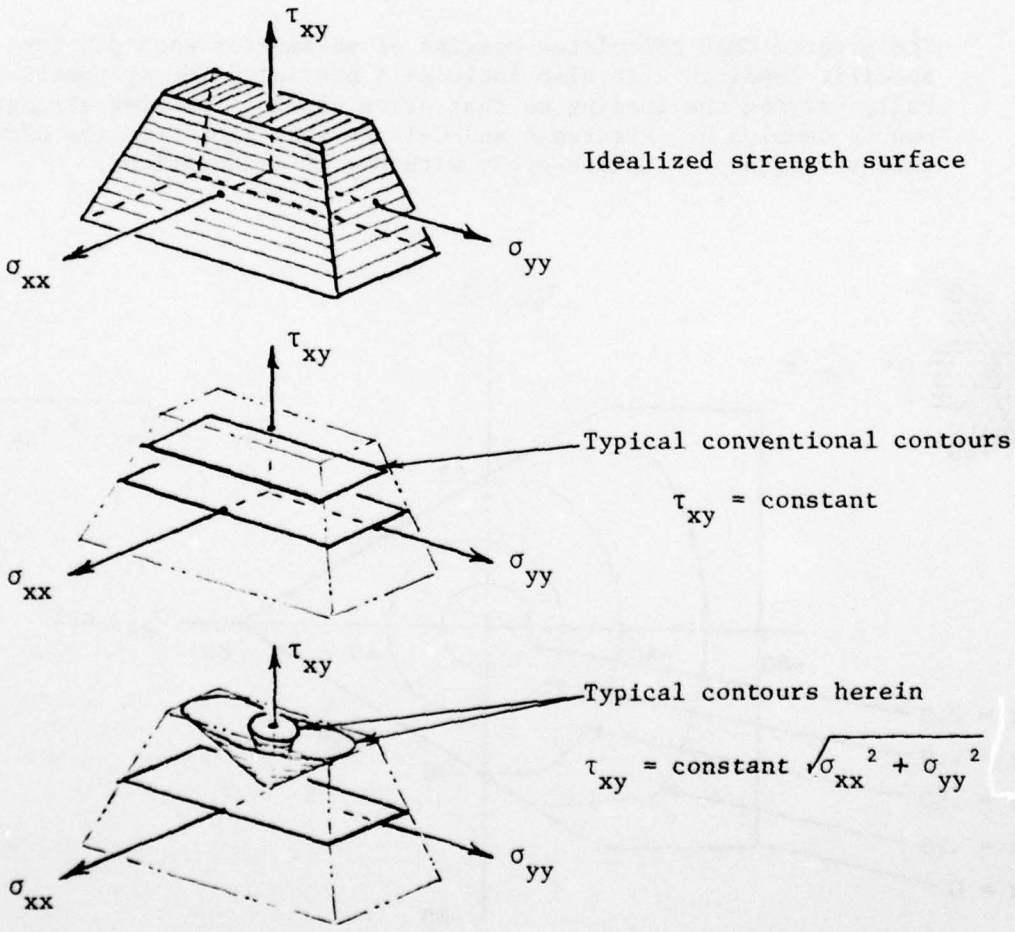


Figure C-2. Comparison of constant stress contours and constant stress-ratio contours.

With a plot of constant stress-ratio contours, it is easy to indicate the margin of safety directly for a given state of stress with radial line segments. In a conventional plot, it requires an iteration to find the end points for the segments and thus, is less convenient. Figure C-3 shows the principle involved.

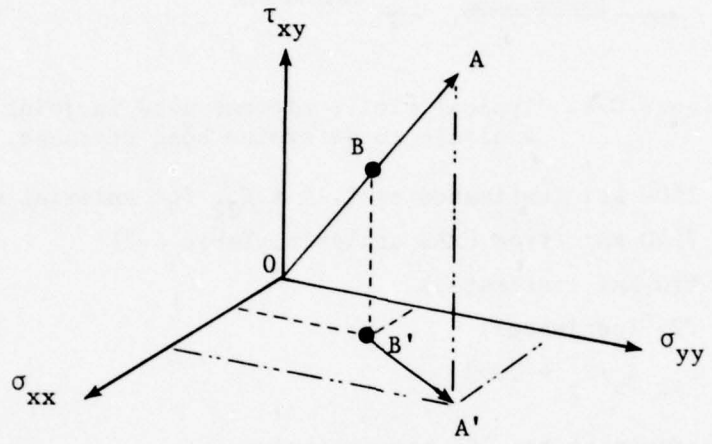


Figure C-3. Presentation of margin of safety on strength plot.

Point B corresponds to the state of stress in the three-dimensional space of σ_{xx}, σ_{yy}, and τ_{xy}. If the loads were proportionally increased to produce failure at point A, the path of stresses would follow the ray OB out to point A. The margin of safety graphically is (OA/OB) - 1. It is also (OA'/OB') - 1 in the projection onto the two-dimensional plane containing the σ_{xx} and σ_{yy} axes. By plotting such line segments onto the two-dimensional plot for several near-critical points in the structure under consideration, it is possible to provide a picture and an aid to understanding of the state of criticality and the regions of the strength surface that were involved.

5. Thornel 300/Narmco 5209, Carbon Fiber Prepreg System, Transverse Properties

The finite-element analysis of a typical joint required as input the stress-strain relationship for an element with the axes and fiber orientations shown in Figure C-4.

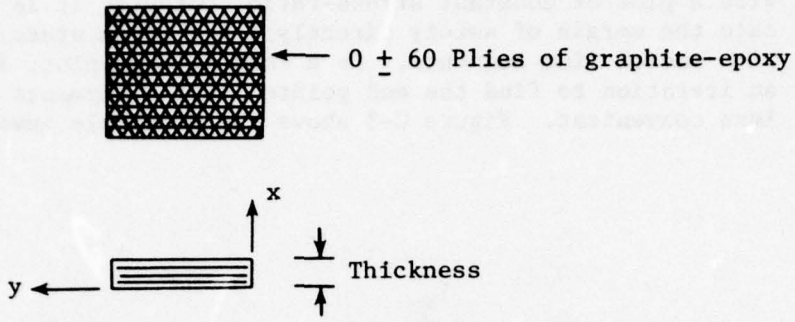


Figure C-4. Typical finite element used in joint analysis to determine bond stresses.

E_x = 1600 ksi (estimated as 1.16 x E_{22} for uniaxial material)

E_y = 7540 ksi (from CMAB analysis, Table C-2)

G_{xy} = 670 ksi (estimated)

ν_{xy} = .25 (estimated)

$\nu_{xy} = \nu_{yx} E_x/E_y = .053$

The elements of the [C] matrix are:

$C_{11} = E_x/(1 - \nu_{xy} \nu_{yx})$

$C_{22} = E_y/(1 - \nu_{xy} \nu_{yx})$

$C_{12} = \nu_{xy} E_x/(1 - \nu_{xy} \nu_{yx})$

$C_{33} = G_{xy}$

$C_{13} = C_{23} = 0$

Thus, the required stress-strain relationship is:

$$\begin{bmatrix} \sigma_{xx} \\ \sigma_{yy} \\ \tau_{xy} \end{bmatrix} = \begin{bmatrix} 1620. & 86. & 0. \\ 86. & 7641. & 0. \\ 0. & 0. & 670. \end{bmatrix} \begin{bmatrix} \varepsilon_x^o \\ \varepsilon_y^o \\ \gamma_{xy}^o \end{bmatrix}$$

6. Composite Materials, Interlaminar Shear Strength

The following data were established by reading and extrapolating curves presented in Figures 3, 13, 15, and 16 of Reference 14:

	BORON-EPOXY	GRAPHITE-EPOXY	S-GLASS EPOXY
F_{su}, ksi	11.5	11.21	10.26
k	x .51	x .49	x .60
peak stress, ksi	5.717	5.635	6.156
F_{se}	3.14 $\pm$ 2.57	3.10 $\pm$ 2.53	3.39 $\pm$ 2.77

where

$$k = \frac{\text{peak stress to cause failure in } 10^8 \text{ cycles with R = .1}}{\text{static ultimate stress}}$$

From these data, it is concluded that the fatigue strength at 10^8 cycles for interlaminar shear is approximately the same for boron-epoxy, graphite-epoxy, or S-glass-epoxy. Calculations of margins of safety herein are based upon the following allowables:

F_{su} = 10.0 ksi

F_{se} = 3.0 $\pm$ 2.5 ksi

7. PL 717 B, Adhesive

G = 16.9 ksi (Reference 15) μ = .35 (Assumed)

E = 45.6 ksi (calculated from G and μ)

F_{su} = 5.0 ksi*

F_{se} = $\pm$ 1.0 ksi*

*An ultimate average shear stress and a fatigue allowable working stress permitted at Kaman for short overlaps, about 1/2 inch. The appropriate allowables for use in finite-element analyses should be higher, but how much higher is a controversial and open question at this time that depends upon the detail of the finite-element model used for the stress analysis.

14. Pipes, R. B., INTERLAMINR SHEAR FATIGUE CHARACTERISTICS OF FIBER-REINFORCED COMPOSITE MATERIALS, presented at the Third Conference on Composite Materials: Testing and Design; ASTM STP 546, American Society for Testing and Materials, Philadelphia, Pennsylvania, 1973.

15. Nagle, R., PERSONAL LETTER To Mr. Mark White, B. F. Goodrich General Products Company, Akron, Ohio, 30 January 1973.

$F_{su,\ scarf} = 4.0$ ksi*

$F_{se,\ scarf} = \pm .8$ ksi*

*Allowables for average shear stress in a balanced-stiffness scarf joint.

DESIGN CONDITIONS

References 1 and 2 define three static limit load conditions and one fatigue condition. For the pan hub, a fifth condition was added which corresponds to a symmetrical static droop. The conditions are summarized in Table C-3.

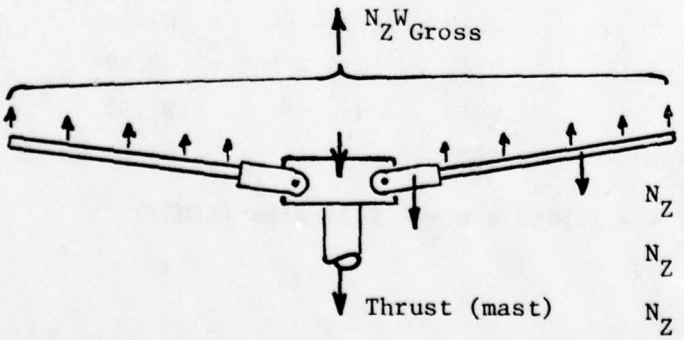
TABLE C-3. DESIGN LOADS

	Static Limit Conditions				Fatigue Design
	TW7F1	TW7F2	Load Burst	Static Droop	
	Symmetrical Dive-Pullout Power-On	Symmetrical Dive-Pullout Autorotation	Engine Restart	Worst Bounce While Towing	Prorated Design Loads
Head Moment, in.-kip	1314.	1500.	0.	0.	800.
C.F., kip	99.	110.	0.	0.	83.
Shaft Torque, in.-kip	2272.	0.	2480.	0.	2075.
Thrust (Mast), in.-kip	85.8	85.8	0.	- 9.39(3)	38.0(1)
Damper Force, kip	± 3.82(2)	± 3.82(2)	0.	0.	± 3.82
Flapping Moment, in.-kip	0.	0.	0.	245.4(3)	0.

NOTES: 1, 2, and 3 described in text.

NOTES FOR TABLE C-3

1. The thrust loading for the fatigue design condition was not stated in References 1 or 2. It was calculated using the equation derived in Figure C-5.



$N_Z W_{Blade}$

$N_Z W_{Hinge\ and\ retention}$

$N_Z W_{Hub}$

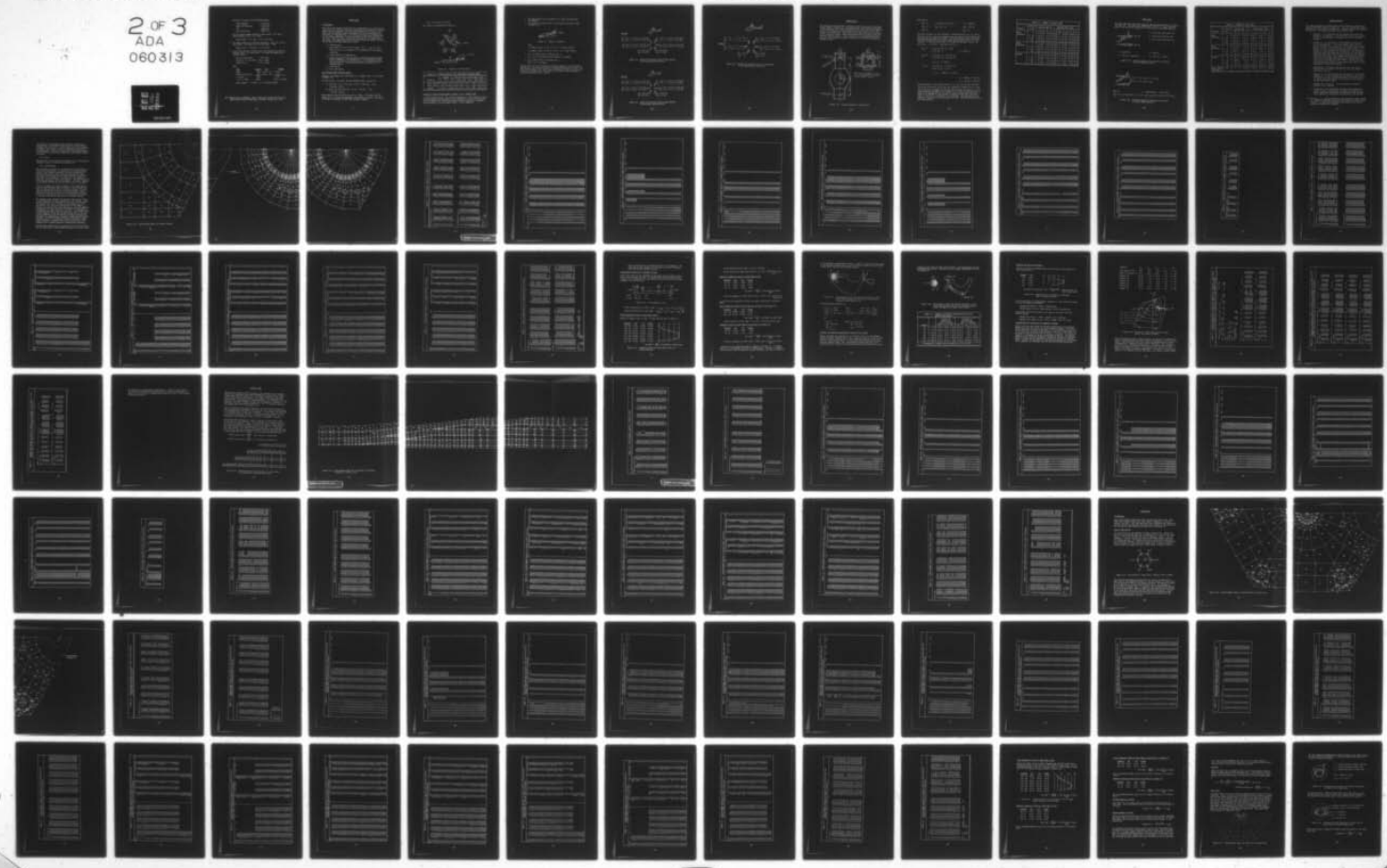
$\Sigma = N_Z W_{Rotor\ head\ total}$

$\therefore$ Thrust (mast) $= N_Z (W_{Gross} - W_{Rotor\ head\ total})$

Figure C-5. Free-body diagram of rotor assembly.

AD-A060 313 KAMAN AEROSPACE CORP BLOOMFIELD CONN F/G 1/3
DESIGN, FABRICATION AND LABORATORY TESTING OF A HELICOPTER COMP--ETC(U)
AUG 78 R J MAYERJAK DAAJ02-75-C-0013
UNCLASSIFIED USARTL-TR-78-16 NL

2 OF 3
ADA
060313



Reference 16 provides the following weights:

Blade Assembly	2.1713 kips
Hinge and Retention	1.3447 kips
Hub	.4539 kip
Rotor Head Total	3.9699 kips

For the fatigue design condition, gross weight = 42.0 kips, from Reference 2; N_z = 1.0. Thus:

Thrust (Mast) = 1.0 (42.0 - 4.0) = 38.0 kips

2. The damper moments are stated in References 1 and 2 as ± 36 in.-kips, limit. The damper arm is 9.412 inches. Thus,

   Damper Force = ± 36/9.412 = ± 3.825 kips

3. Static droop produces a moment about the flapping axis and compression load in the lower plate. The loads and moments were computed using:

   Vertical load factor = 2.67 limit
   Blade c.g. at 5/8 radius = 270.0 inches
   Retention c.g. = 36.9 inches

   Then:

ITEM	WEIGHT	x ARM	= MOMENT
Blade	.3619	x (270 - 24)	= 89.03
Hinge and Retention	.2241	x (36.9 - 24)	= 2.89
1-g static	.5860		91.92
x 2.67 = LIMIT	1.5650		245.4 in.-kips

Thrust (Mast) = - 1.5650 x 6 = - 9.39 kips (LIMIT)

16. SUMMARY WEIGHT STATEMENT, ACTUAL, SER-64316, Sikorsky Aircraft Division, United Aircraft Corporation, Stratford, Connecticut, 1970.

BLADE LOADS

Introduction

Each arm of the present titanium hub acts independently as a cantilevered beam, and thus, only peak loads were considered in its analysis. The composite plate hub, however, is structurally redundant with multiple load paths, and its analysis requires consideration of the total pattern of loads that act simultaneously. Such patterns of loads are developed here for the design conditions. First, out-of-plane loads (those parallel to the axis of the rotor shaft) applied by the blades to the lead-lag pins are found. Then damper forces and centrifugal forces are added. The following symbols and approximations are used:

ψ = azimuth angle

β = flap angle of the root of the blade. Use: $\beta = \beta_0 + \beta_1 \cos \psi$, where β_0 and β_1 are constants to be determined for each design condition.

e = offset distance to flapping pin

P = total force at the root of a blade, including inertial and aerodynamic components. The magnitude of P is approximately equal to the centrifugal force of the blade in its unflapped position. The direction of P is approximately along the blade root, at flapping angle β.

T = rotor thrust

M = rotor head moment

Out-of-Plane Loads (Vertical Loads)

Consider a six-bladed rotor with blade No. 1 aligned with $\psi = 0$, as shown in Figure C-6.

In this position, the thrust and head moments (about Y axis) are:

$$T = [\sin(\beta_0 + \beta_1) + 2\sin(\beta_0 + .5\,\beta_1) + 2\sin(\beta_0 - .5\,\beta_1) + \sin(\beta_0 - \beta_1)]P$$

$$M = [\sin(\beta_0 + \beta_1) + \sin(\beta_0 + .5\,\beta_1) - \sin(\beta_0 - .5\,\beta_1) - \sin(\beta_0 - \beta_1)]Pe$$

These equations were solved for β_0 and β_1, using e = 24 inches, and the values for P, T, and M corresponding to each design condition. The vertical force at each blade (i) was then calculated, using:

$$P_{zi} = P \sin (\beta_0 + \beta_1 \cos \psi_i)$$

The results are summarized in Table C-4.

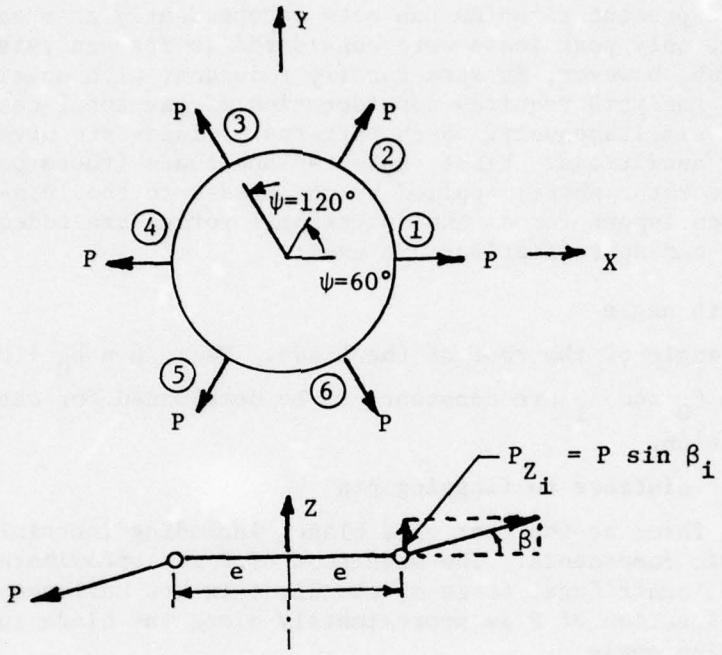


Figure C-6. Geometry for blade loads.

TABLE C-4. VERTICAL FORCES ON HUB FROM THRUST AND HEAD MOMENT

Condition	Degrees		Vertical Force at Blade Root, kips					
	β_0	β_1	P_{Z1}	P_{Z2}	P_{Z3}	P_{Z4}	P_{Z5}	P_{Z6}
TW7F1 (LIMIT)	8.375	10.719	32.38	23.51	5.21	- 4.05	5.21	23.51
TW7F2 (LIMIT)	7.540	11.000	34.98	24.82	3.92	- 6.64	3.92	24.82
FATIGUE	4.392	7.710	17.40	11.91	.78	- 4.80	.78	11.91

Patterns of Load for Head Moment + Thrust + C.F. + Damper Loads

In the preceding section, the vertical components of load produced by thrust and head moment were calculated at each lead-lag pin. Here, the load pattern is completed for vertical and radial loads by adding the components from centrifugal force and damper loads. In this summation:

1. The centrifugal force is assumed to be radial and unreduced by flapping

2. The damper is inclined 9.13° to the plane of the hub as shown in Figure C-7.

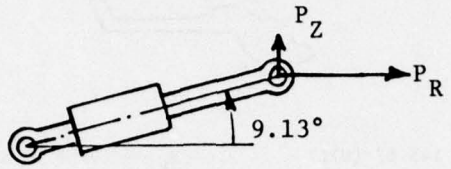


Figure C-7. Damper Inclination.

Thus,

P_Z damper, peak = $\pm$ 3.82 sin 9.13° = $\pm$ .61 kip (LIMIT)

P_R damper, peak = $\pm$ 3.82 cos 9.13° = $\pm$ 3.77 kips (LIMIT)

3. F_{Zi} = Vertical force at lead-lag pin, i.

   F_{Zi} = P_{Zi} (from thrust and head moment) + P_Z damper.

4. F_{Ri} = Radial force at lead-lag pin, i.

   F_{Ri} = C.F. + P_R damper.

Figures C-8, C-9, and C-10 show the resulting patterns of forces acting upon the hub. The views correspond to looking downward upon the hub. The individual components that make up each summation are shown to clarify the origin of the final loads. The signs on the damper loads correspond to the lead-lag motions of the blade.



Forward

F_{R3} = (99 - .5 x 3.77)(1.5) = 145.67 (Ult)
F_{Z3} = (23.51 - .5 x .61)(1.5) = 34.81 (Ult)

F_{R2} = (99 + .5 x 3.77)(1.5) = 151.33 (Ult)
F_{Z2} = (5.21 + .5 x .61)(1.5) = 8.27 (Ult)

F_{R4} = (99 - 3.77)(1.5) = 142.85 (Ult)
F_{Z4} = (32.38 - .61)(1.5) = 47.66 (Ult)

F_{R1} = (99 + 3.77)(1.5) = 154.16 (Ult)
F_{Z1} = (-4.05 + .61)(1.5) = -5.16 (Ult)

F_{R5} = 145.67 (Ult)
F_{Z5} = 34.81 (Ult)

F_{R6} = 151.33 (Ult)
F_{Z6} = 8.27 (Ult)

Figure C-8. Radial and vertical forces in kips applied to hub during condition TW7F1.



Forward

F_{R3} = (110 - .5 x 3.77)(1.5) = 162.17 (Ult)
F_{Z3} = (24.82 - .5 x .61)(1.5) = 36.77 (Ult)

F_{R2} = (110 + .5 x 3.77)(1.5) = 167.83 (Ult)
F_{Z2} = (3.92 + .5 x .61)(1.5) = 6.34 (Ult)

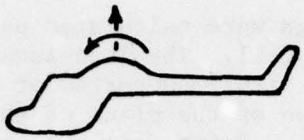
F_{R4} = (110 - 3.77)(1.5) = 159.35 (Ult)
F_{Z4} = (34.98 - .61)(1.5) = 51.56 (Ult)

F_{R1} = (110 + 3.77)(1.5) = 170.66 (Ult)
F_{Z1} =(-6.64 + .61)(1.5) = -9.05 (Ult)

F_{R5} = 162.17 (Ult)
F_{Z5} = 36.77 (Ult)

F_{R6} = 167.83 (Ult)
F_{Z6} = 6.34 (Ult)

Figure C-9. Radial and vertical forces in kips applied to hub during condition TW7F2.



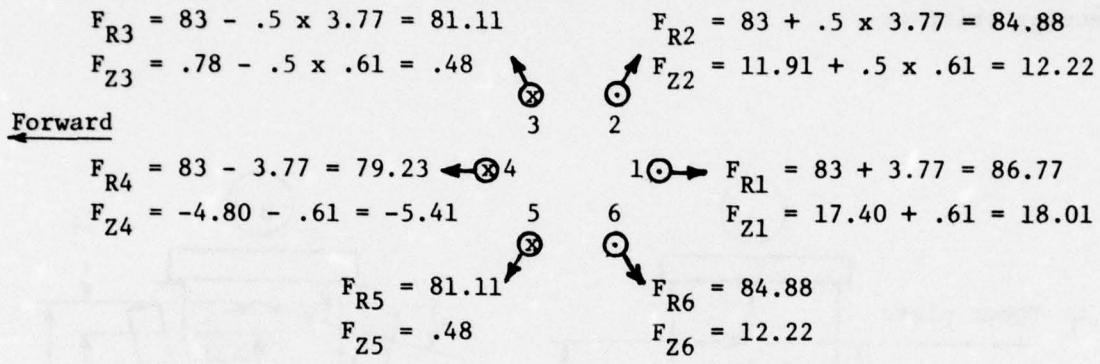
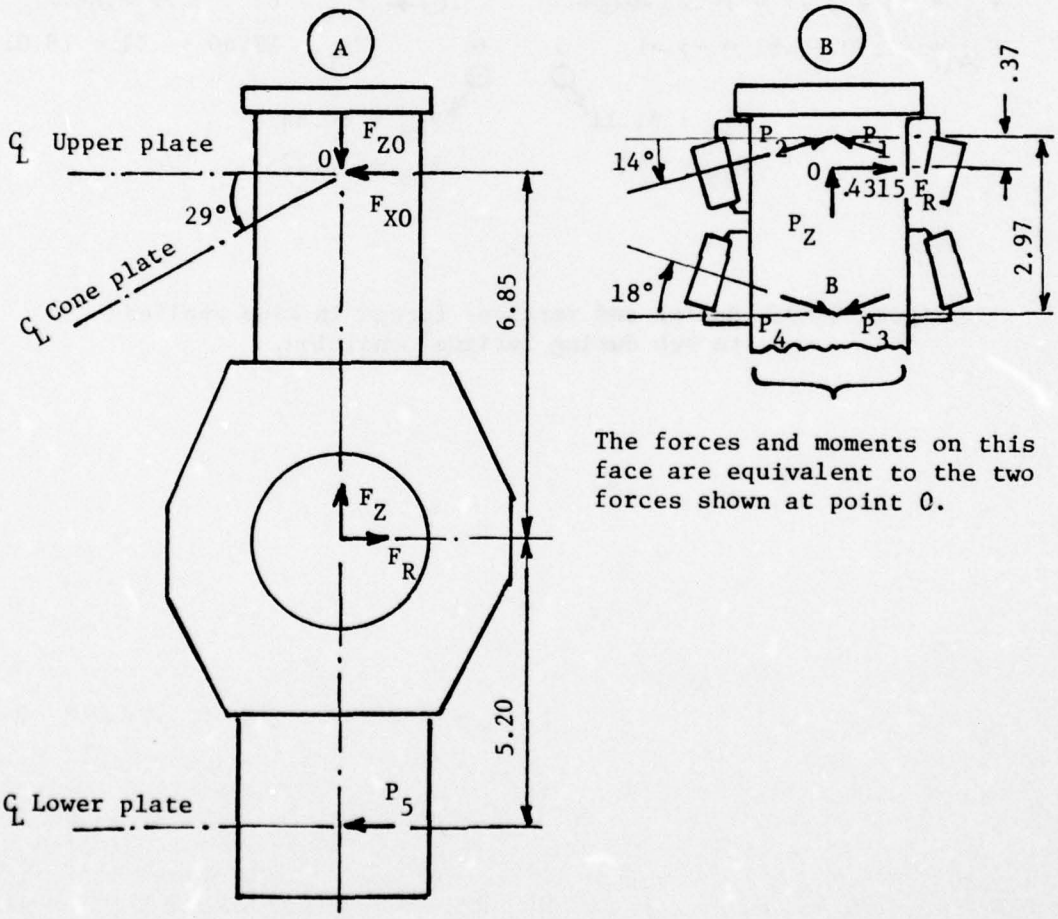


Figure C-10. Radial and vertical forces in kips applied to hub during fatigue condition.

BEARING LOADS

The loads on the bearings were calculated using statics and the free-body diagram (FBD) of Figure C-11. The lead-lag pin is statically determinate. It was considered to be simply supported at the lower plate and at point 0, which is the intersection of the plane of the upper plate and the local "plane" of the pan plate. Point 0 is akin to the vertex of a truss being stiffly supported against translational deflections by membrane forces in the upper and cone plates. Little resistance to rotational deflections exists at either support because the plates are thin with relatively low bending stiffness.



The forces and moments on this face are equivalent to the two forces shown at point 0.

Figure C-11. Free-body diagram of lead-lag pin.

Using FBD A,

$$\Sigma M_0 = 0 \qquad -6.85\ F_R + 12.05\ P_5 = 0 \qquad P_5 = .5685\ F_R$$

$$\Sigma F_X = 0 \qquad F_{X0} = F_R - P_5 \qquad F_{X0} = .4315\ F_R$$

$$\Sigma F_Z = 0 \qquad F_{Z0} = F_Z$$

The force at point 0 is the resultant of bearing forces P_1, P_2, P_3, and P_4. Only zero and (+) values are acceptable for the bearing forces because the bearings are only lightly preloaded. Free-body diagram B shows the geometrical relationships for the forces acting upon the upper end of the lead-lag pin. It is shown herein that for the design conditions, only P_1, P_3 and P_4 act. P_2 is zero. Using FBD B and $P_2 = 0$,

$$\Sigma M_B = 0, \quad -2.97\ (\cos 14°)\ P_1 + 2.60 \times .4315\ F_R = 0 \qquad P_1 = .3893\ F_R$$

$$\Sigma F_X = 0, \quad -(\cos 18°)\ P_3 + (\cos 18°)\ P_4 - (\cos 14°)\ P_1 + .4315\ F_R = 0$$

$$-P_3 + P_4 = -.0565\ F_R$$

$$\Sigma F_Z = 0, \quad -(\sin 18°)\ P_3 - (\sin 18°)\ P_4 + (\sin 14°)\ P_1 + F_Z = 0$$

$$P_3 + P_4 = .3048\ F_R + 3.2361\ F_Z$$

$$P_3 = .1806\ F_R + 1.6181\ F_Z$$

$$P_4 = .1242\ F_R + 1.6181\ F_Z$$

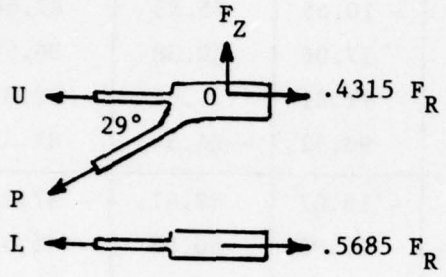
These equations for the bearing loads (P_1, P_2, P_3, and P_4) were used with the radial and vertical forces (F_R, F_Z) presented in Figures C-8, C-9, and C-10 to prepare the summary of bearing loads presented in Table C-5. This table shows that throughout the rotation of the rotor the bearing loads are moderate and appropriate for the applied blade loadings being supported. There is no evidence of high induced or secondary loads that could pose a threat to the life or performance of the bearings. The bearings are consistently loaded and do not go through zero load. They should perform well and conventionally.

TABLE C-5. SUMMARY OF BEARING LOADS

Condition	Position ψ, deg	Forces, kips		Bearing Loads, kips				
		F_R	F_z	P_1	P_2	P_3	P_4	P_5
TW7F1 (Ultimate)	0	154.16	- 5.16	60.01	0	19.49	10.80	87.64
	± 60	151.33	8.27	58.91	0	40.71	32.18	86.03
	± 120	145.67	34.81	56.71	0	82.63	74.42	82.81
	180	142.85	47.66	55.61	0	102.92	94.86	81.21
TW7F2 (Ultimate)	0	170.66	- 9.05	66.44	0	16.18	6.55	97.02
	± 60	167.83	6.34	65.34	0	40.57	31.10	95.41
	± 120	162.17	36.77	63.13	0	88.79	79.64	92.20
	180	159.35	51.56	62.03	0	112.21	103.22	90.59
FATIGUE	0	86.77	18.01	33.78	0	44.81	39.92	49.33
	± 60	84.88	12.22	33.04	0	35.10	30.31	48.25
	± 120	81.11	.48	31.58	0	15.43	10.85	46.11
	180	79.23	- 5.41	30.84	0	5.56	1.09	45.04

JOINT LOADS

The joint loads were calculated using the FBD and equations shown in Figures C-12 and C-13. The results are summarized in Table C-6. These loads were used for the structural analyses of the hub plates in following sections.



U = force upon upper plate lug

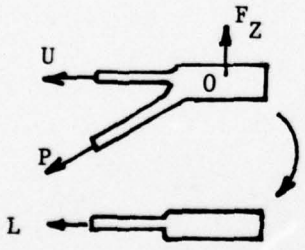
P = force upon pan plate lug

L = force upon lower plate lug

$P = F_Z/\sin 29°$, $\quad P = 2.063\ F_Z$

$U = .4315\ F_R - F_Z/\tan 29°$, $\quad U = .4315\ R_F - 1.804\ F_Z$

Figure C-12. Free-body diagram of hub plates at lead-lag pin for flight conditions.



$F_Z = -9.39 \times 1.5/6 = -2.35$ (ult)

$245.4 \times 1.5 = 368.1$ (ult)

$\Sigma M_0 = 0$, $\quad L = -368.1/12.05 = -30.55$ (ult)

$\Sigma F_X = 0$, $U + P (\cos 29°) + L = 0$, $U = 4.85 (\cos 29°) + 30.55 = 34.79$ (ult)

Figure C-13. Free-body diagram of hub plates at lead-lag for static droop condition.

TABLE C-6. SUMMARY OF JOINT LOADS

Condition	Position ψ, deg	Forces, kips		Joint Loads, kips		
		F_R	F_z	P	U	L
TW7F1 (Ultimate)	0	154.16	- 5.16	- 10.65	75.83	87.64
	± 60	151.33	8.27	17.06	50.38	86.03
	± 120	145.67	34.81	71.81	.06	82.81
	180	142.85	47.66	98.32	- 24.34	81.21
TW7F2 (Ultimate)	0	170.66	- 9.05	- 18.67	89.97	97.02
	± 60	167.83	6.34	13.08	60.98	95.41
	± 120	162.17	36.77	75.86	3.65	92.20
	180	159.35	51.56	106.36	- 24.25	90.59
FATIGUE	0	86.77	18.01	37.15	4.95	49.33
	± 60	84.88	12.22	25.21	14.58	48.25
	± 120	81.11	.48	.99	34.13	46.11
	180	79.23	- 5.41	- 11.16	43.95	45.04
STATIC DROOP (Ultimate)	ALL	0	- 2.35	- 4.85	34.79	- 30.55

ELEMENT SPECIMEN

The element specimen was analyzed using the two-dimensional plane-stress, finite-element model shown in Figure C-14. Since the specimen was doubly symmetric, only one-quarter was analyzed. The model contains 181 nodes and 239 elements. The elements performed the following roles:

1. Elements 1 - 13 represented the pin through which loads were applied to the specimen. In the analysis, 10 kips were applied at node 1, corresponding to 20 kips at each end of the whole specimen.

2. Elements 14 - 39 represented a liner between the pin and the hole in the specimen. In the final design, liners were not used, and elements 14 - 39 were stiffly attached to the pin and became, in effect, part of the pin. In an early stage of the design, the use of a press-fitted interference liner was considered. It was concluded from analyses that, for the geometry considered, which had relatively thin liners, the reduction of vibratory stress was small and not worth the cost and complexity that liners would add. This judgment was based upon analyses using the finite-element model and did not include the beneficial effects in fatigue that might result from less relative motion at the hole because of the liners. Such benefits (which can be established only by testing) may make the use of liners advantageous in other applications.

3. Elements 40 - 53 radially connected the pin to the liner. These elements were made stiff and thus, the liner became an extension of the pin.

4. Elements 54 - 67 radially connected the liner to the specimen. Elements 61 - 67 were assigned very low modulus to permit the natural gap to occur at the unloaded side of the hole. The use of radial connections assumed a frictionless contact between the pin liner and the hole.

5. Elements 68 - 151 and 217 - 239 represented the composite material of the specimen.

6. Elements 152 - 216 represented the steel laminae that reinforced the hole. These laminae overlayed the composite elements. Each steel element had a thickness that was the sum of the thicknesses of the laminae that existed at that position.

---

17. Mayerjak, R. J., FATIGUE STRENGTH OF LUGS CONTAINING LINERS, VOLUME II - COMPUTER PROGRAM USED FOR ANALYSIS, USAAVLABS Technical Report 70-49B, U. S. Army Aviation Materiel Laboratories, Fort Eustis, Virginia, November 1970, AD 880290.

The analyses were performed using the Kaman finite-element program MA2C. This program is very similar to MA2B, which is documented in Reference 17. MA2C differs only by the addition of element types 4 and 5, which are composite triangles and quadrilaterals. The elastic properties for composite elements are defined in the input by a matrix [C], which relates stress to strain:

$$[\sigma] = [C][\varepsilon]$$

The matrix [C] can be found from the matrix [A] of conventional lamination theory as described in Reference 12:

$$[C] = [A]/\text{thickness}$$

The calculation of matrix [A] is presented in this appendix in the section on materials. In general, the [C] matrix corresponds to local element coordinates (defined in Reference 17, and explained further herein) and thus, potentially, could represent a calculation chore if arbitrary fiber orientations were used for each element. Fortunately, in the composite plate hub, only one [C] matrix is required. The quasi-isotropic 0 ± 60 degree laminate is used throughout. For such a laminate, the [C] matrix is the same for any orientation of local axes.

Table C-7 presents the computer analysis. The finite-element structure has dimensions that correspond to the prototype and thus are exactly double those of the test specimen. The analysis is performed for a load of 10 kips per quarter, corresponding to 20 kips at each end of a prototype-sized structure. In the hand calculations that follow, the stresses are scaled to the test load that was applied to the element specimen.

The computer output includes the state of stress at the center of each element in the local coordinates of the element. These local coordinates are established by the order used to define the element. The local y coordinate lies along a line containing the first two node points stated for the element. In general, the elements have been identified so that the STRESS XX corresponds to a radial direction and STRESS YY corresponds to a tangential direction relative to the hole. The stresses taken from the computer output were extrapolated by hand to the edge of the boundaries of the hole and the perimeter of the lug to determine the conditions at the failure origins observed during the tests. The metal laminae stresses so determined are interpretable directly. The composite stresses are given an additional rotation to transform them to the natural axes of the laminate with x oriented along the 0-degree fiber direction.

The bond-line stresses and the stresses in the tips of the laminae are found using a finite-element analysis of a typical joint

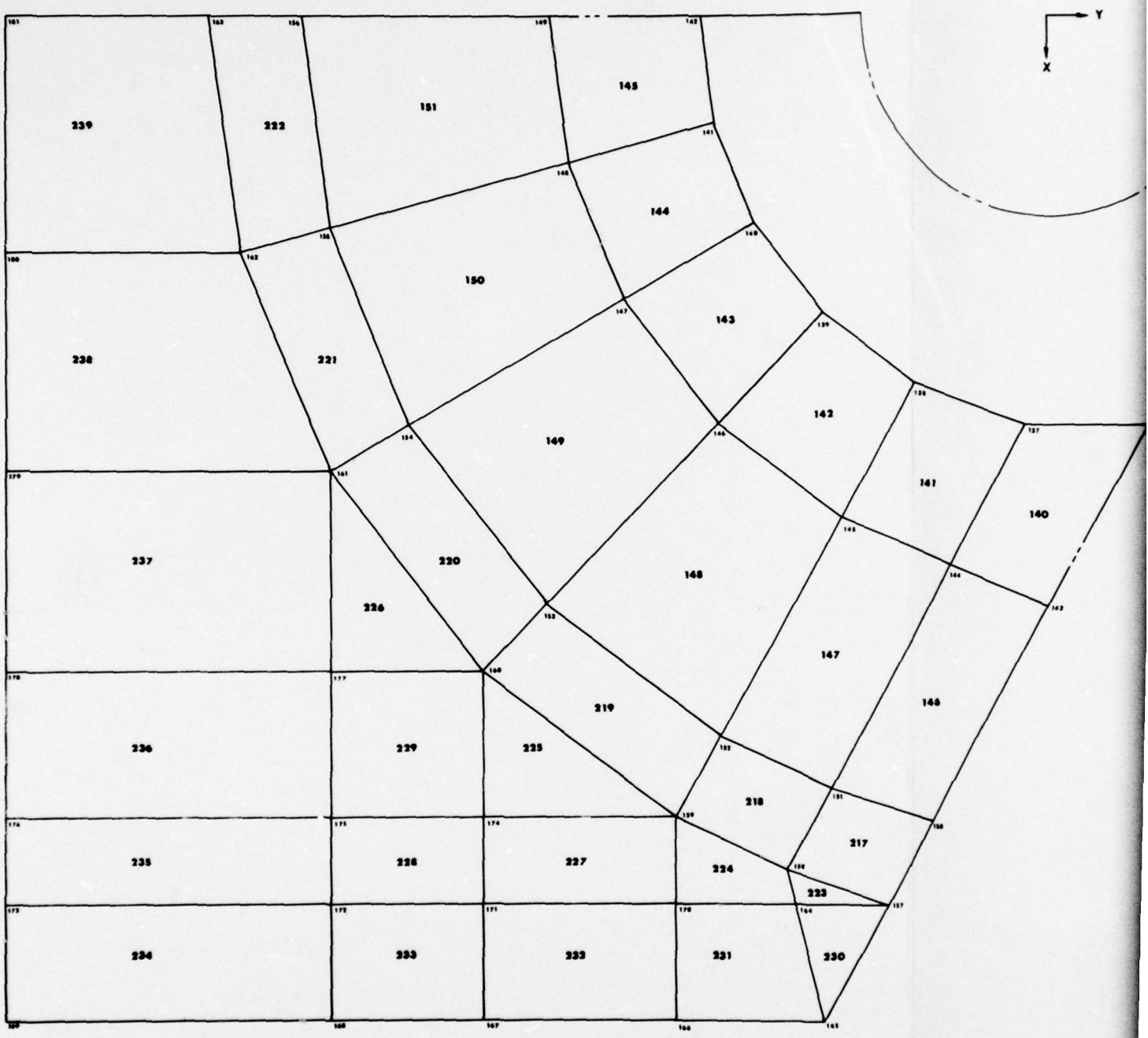
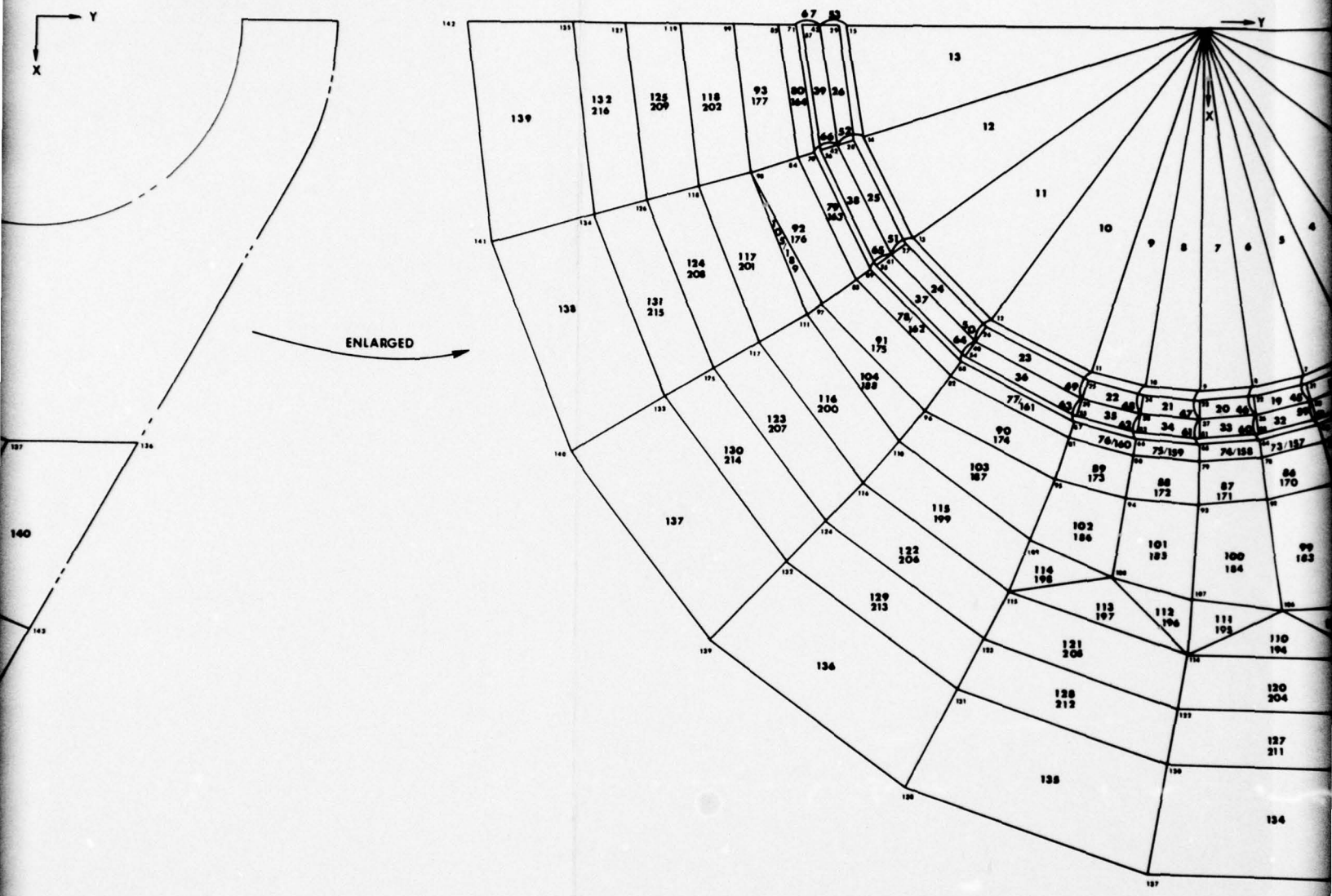


Figure C-14. Finite-element model for element specimen.


Y
X
ENLARGED
Y
X
67
53
13
12
11
10
9
8
7
6
5
4
139
132
216
125
209
118
202
93
177
80
39
36
92
176
124
208
117
201
131
215
138
91
175
104
188
116
200
123
207
130
214
137
90
174
103
187
115
199
122
206
129
213
136
77/161
76/160
75/159
74/158
73/157
89
173
88
172
87
171
86
170
102
186
101
183
100
184
99
183
114
198
113
197
112
196
111
195
110
194
121
208
128
212
120
204
127
211
135
134
140

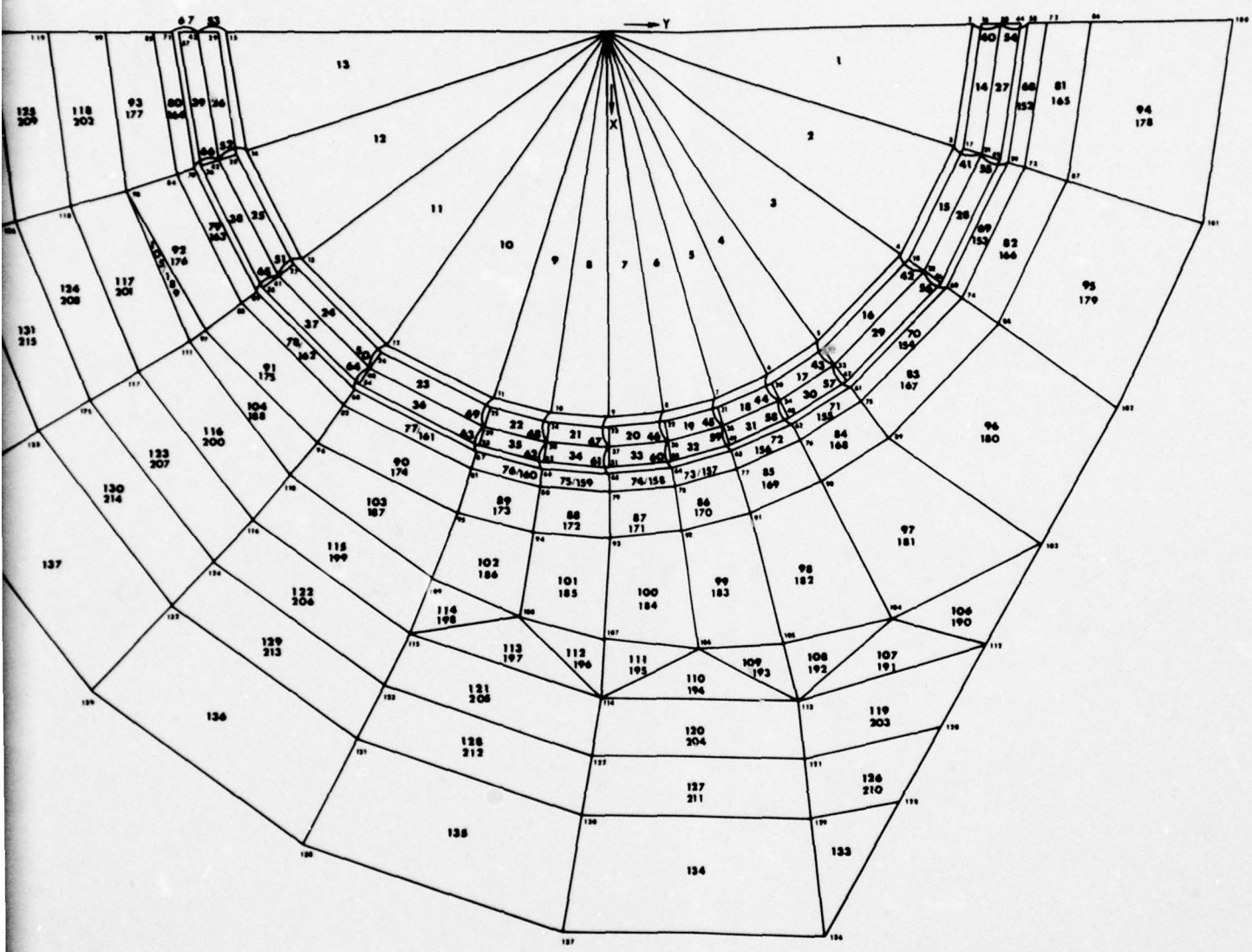

Y
X

TABLE C-7. FINITE-ELEMENT ANALYSIS OF ELEMENT SPECIMEN

X COORDINATES AND SUPPORTS

	1	2	3	4	5	6	7	8	9	10
1	0.0 S	0.0 S	0.8310	1.5800	2.1750	2.3950	2.5560	2.6550	2.6880	2.6550
11	2.5560	2.1750	1.5800	0.8310	0.0 S	0.0 S	0.8310	1.5800	2.1750	2.3950
21	2.5560	2.6550	2.6880	2.6550	2.5560	2.1750	1.5800	0.8310	0.0 S	0.0 S
31	0.8660	1.6480	2.2680	2.4980	2.6670	2.7690	2.8040	2.7690	2.6670	2.2680
41	1.6480	0.8660	0.0 S	0.0 S	0.9020	1.7160	2.3620	2.6020	2.7770	2.8840
51	2.9200	2.8840	2.7770	2.3620	1.7160	0.9020	0.0 S	0.0 S	0.9270	1.7630
61	2.4270	2.6730	2.8530	2.9630	3.0000	2.9630	2.8530	2.4270	1.7630	0.9270
71	0.0 S	0.0 S	0.9700	1.8460	2.5400	2.7980	2.9860	3.1010	3.1400	3.1010
81	2.9860	2.5400	1.8460	0.9700	0.0 S	0.0 S	1.0570	2.0100	2.7670	3.0470
91	3.2530	3.3780	3.4200	3.3780	3.2530	2.7670	2.0100	1.0560	0.0 S	0.0 S
101	1.3700	2.6000	3.5100	4.0000	4.1700	4.2000	4.1200	3.9600	3.7000	2.9900
111	2.0800	4.1900	4.5500	4.5200	4.0700	3.2900	2.2800	1.1700	0.0 S	4.7300
121	4.9500	4.9100	4.4200	3.5700	2.4800	1.3700	0.0 S	5.2400	5.3500	5.3100
131	4.7900	3.8600	2.6800	1.3800	0.0 S	6.1400	6.1000	5.4900	4.4400	3.0900
141	1.5900	0.0 S	8.7800	8.1600	7.4700	6.0800	4.2300	2.1800	0.0 S	11.9300
151	11.5000	10.7300	8.7600	6.1000	3.1500	0.0 S	13.2700	12.7500	11.9700	9.8100
161	6.8000	3.5300	0.0 S	13.2700	15.0000	15.0000	15.0000	15.0000	15.0000	13.2700
171	13.2700	13.2700	13.2700	11.9700	11.9700	11.9700	9.8100	9.8100	6.8000	3.5300
181	0.0 S									

Y COORDINATES AND SUPPORTS

	1	2	3	4	5	6	7	8	9	10
1	0.0	2.6880	2.5560	2.1750	1.5800	1.2200	0.8310	0.4200	0.0	-0.4200
11	-0.8310	-1.5800	-2.1750	-2.5560	-2.6880	2.6880	2.5560	2.1750	1.5800	1.2200
21	0.8310	0.4200	0.0	-0.4200	-0.8310	-1.5800	-2.1750	-2.5560	-2.6880	2.8040
31	2.6670	2.2680	1.6480	1.2730	0.8670	0.4390	0.0	-0.4390	-0.8670	-1.6480
41	-2.2680	-2.6670	-2.8040	2.9200	2.7770	2.3620	1.7160	1.3260	0.9020	0.4570
51	0.0	-0.4570	-0.9020	-1.7160	-2.3620	-2.7770	-2.9200	3.0000	2.8530	2.4270
61	1.7630	1.3620	0.9270	0.4690	0.0	-0.4690	-0.9270	-1.7630	-2.4270	-2.8530
71	-3.0000	3.1400	2.9860	2.5400	1.8460	1.4260	0.9700	0.4910	0.0	-0.4910
81	-0.9700	-1.8460	-2.5400	-2.9860	-3.1400	3.4200	3.2530	2.7670	2.0100	1.5530
91	1.0570	0.5350	0.0	-0.5350	-1.0570	-2.0100	-2.7670	-3.2530	-3.4200	4.4000
101	4.2000	3.5900	3.0400	2.0200	1.2600	0.6500	-0.0400	-0.6500	-1.2400	-2.2100
111	-2.9000	2.6600	1.3600	-0.0700	-1.4000	-2.4700	-3.2500	-3.7000	-3.8500	2.3400
121	1.4000	-0.1400	-1.5800	-2.7500	-3.5800	-4.0900	-4.2500	2.0500	1.4400	-0.2100
131	-1.7700	-3.0300	-3.9400	-4.4800	-4.6500	1.5200	-0.3500	-2.1400	-3.5900	-4.6300
141	-5.2600	-5.4700	0.0	-1.5400	-3.2900	-5.1900	-6.6300	-7.4800	-7.7600	-1.8600
151	-3.4800	-5.1700	-7.8200	-9.8900	-11.1200	-11.5300	-2.5500	-4.1300	-5.8500	-8.7700
161	-11.0800	-12.4400	-12.9200	-4.0000	-3.5500	-5.8500	-8.7700	-11.0800	-16.0000 S	-5.8500
171	-8.7700	-11.0800	-16.0000 S	-8.7700	-11.0800	-16.0000 S	-11.0800	-16.0000 S	-16.0000 S	-16.0000 S
181	-16.0000 S									

LOADS, CASE 1

1	X	0.0
1	Y	10.000

PRECEDING PAGE BLANK-NOT FILMED

TABLE C-7. FINITE-ELEMENT ANALYSIS OF ELEMENT SPECIMEN (continued)

ELEM	P	Q	R	S	TYPE	E	PR	THICK-AREA	ALPHA	TEM 1	TEM 2	TEM 3	TEM 4	TEM 5
1	2	3	1	0	2	29000.	0.3180	0.5000	0.00000560	0.				
2	3	4	1	0	2	29000.	0.3180	0.5000	0.00000560	0.				
3	4	5	1	0	2	29000.	0.3180	0.5000	0.00000560	0.				
4	5	6	1	0	2	29000.	0.3180	0.5000	0.00000560	0.				
5	6	7	1	0	2	29000.	0.3180	0.5000	0.00000560	0.				
6	7	8	1	0	2	29000.	0.3180	0.5000	0.00000560	0.				
7	8	9	1	0	2	29000.	0.3180	0.5000	0.00000560	0.				
8	9	10	1	0	2	29000.	0.3180	0.5000	0.00000560	0.				
9	10	11	1	0	2	29000.	0.3180	0.5000	0.00000560	0.				
10	11	12	1	0	2	29000.	0.3180	0.5000	0.00000560	0.				
11	12	13	1	0	2	29000.	0.3180	0.5000	0.00000560	0.				
12	13	14	1	0	2	29000.	0.3180	0.5000	0.00000560	0.				
13	14	15	1	0	2	29000.	0.3180	0.5000	0.00000560	0.				
14	17	16	30	31	3	29000.	0.3180	0.5000	0.00000560	0.				
15	18	17	31	32	3	29000.	0.3180	0.5000	0.00000560	0.				
16	19	18	32	33	3	29000.	0.3180	0.5000	0.00000560	0.				
17	20	19	33	34	3	29000.	0.3180	0.5000	0.00000560	0.				
18	21	20	34	35	3	29000.	0.3180	0.5000	0.00000560	0.				
19	22	21	35	36	3	29000.	0.3180	0.5000	0.00000560	0.				
20	23	22	36	37	3	29000.	0.3180	0.5000	0.00000560	0.				
21	24	23	37	38	3	29000.	0.3180	0.5000	0.00000560	0.				
22	25	24	38	39	3	29000.	0.3180	0.5000	0.00000560	0.				
23	26	25	39	40	3	29000.	0.3180	0.5000	0.00000560	0.				
24	27	26	40	41	3	29000.	0.3180	0.5000	0.00000560	0.				
25	28	27	41	42	3	29000.	0.3180	0.5000	0.00000560	0.				
26	29	28	42	43	3	29000.	0.3180	0.5000	0.00000560	0.				
27	31	30	44	45	3	29000.	0.3180	0.5000	0.00000560	0.				
28	32	31	45	46	3	29000.	0.3180	0.5000	0.00000560	0.				
29	33	32	46	47	3	29000.	0.3180	0.5000	0.00000560	0.				
30	34	33	47	48	3	29000.	0.3180	0.5000	0.00000560	0.				
31	35	34	48	49	3	29000.	0.3180	0.5000	0.00000560	0.				
32	36	35	49	50	3	29000.	0.3180	0.5000	0.00000560	0.				
33	37	36	50	51	3	29000.	0.3180	0.5000	0.00000560	0.				
34	38	37	51	52	3	29000.	0.3180	0.5000	0.00000560	0.				
35	39	38	52	53	3	29000.	0.3180	0.5000	0.00000560	0.				
36	40	39	53	54	3	29000.	0.3180	0.5000	0.00000560	0.				
37	41	40	54	55	3	29000.	0.3180	0.5000	0.00000560	0.				
38	42	41	55	56	3	29000.	0.3180	0.5000	0.00000560	0.				
39	43	42	56	57	3	29000.	0.3180	0.5000	0.00000560	0.				
40	2	30	0	0	1	29000.	0.3180	0.2300	0.00000560	0.				
41	3	31	0	0	1	29000.	0.3180	0.4600	0.00000560	0.				
42	4	32	0	0	1	29000.	0.3180	0.4600	0.00000560	0.				
43	5	33	0	0	1	29000.	0.3180	0.3450	0.00000560	0.				
44	6	34	0	0	1	29000.	0.3180	0.2300	0.00000560	0.				
45	7	35	0	0	1	29000.	0.3180	0.2300	0.00000560	0.				
46	8	36	0	0	1	29000.	0.3180	0.2300	0.00000560	0.				
47	9	37	0	0	1	29000.	0.3180	0.2300	0.00000560	0.				
48	10	38	0	0	1	29000.	0.3180	0.2300	0.00000560	0.				
49	11	39	0	0	1	29000.	0.3180	0.3450	0.00000560	0.				
50	12	40	0	0	1	29000.	0.3180	0.4600	0.00000560	0.				

TABLE C-7. FINITE-ELEMENT ANALYSIS OF ELEMENT SPECIMEN (continued)

ELEM	P	Q	R	S	TYPE	E	PR	THICK-AREA	ALPHA	TEM 1	TEM 2	TEM 3	TEM 4	TEM 5
51	13	41	0	0	1	29000.	0.3180	0.4600	0.00000560	0.				
52	14	42	0	0	1	29000.	0.3180	0.4600	0.00000560	0.				
53	15	43	0	0	1	29000.	0.3180	0.4600	0.00000560	0.				
54	30	58	0	0	1	29000.	0.3180	0.2300	0.00000560	0.				
55	31	59	0	0	1	29000.	0.3180	0.4600	0.00000560	0.				
56	32	60	0	0	1	29000.	0.3180	0.4600	0.00000560	0.				
57	33	61	0	0	1	29000.	0.3180	0.3450	0.00000560	0.				
58	34	62	0	0	1	29000.	0.3180	0.2300	0.00000560	0.				
59	35	63	0	0	1	29000.	0.3180	0.2300	0.00000560	0.				
60	36	64	0	0	1	29000.	0.3180	0.2300	0.00000560	0.				
61	37	65	0	0	1	1.	0.3180	0.2300	0.00000560	0.				
62	38	66	0	0	1	1.	0.3180	0.2300	0.00000560	0.				
63	39	67	0	0	1	1.	0.3180	0.3450	0.00000560	0.				
64	40	68	0	0	1	1.	0.3180	0.4600	0.00000560	0.				
65	41	69	0	0	1	1.	0.3180	0.4600	0.00000560	0.				
66	42	70	0	0	1	1.	0.3180	0.4600	0.00000560	0.				
67	43	71	0	0	1	1.	0.3180	0.2300	0.00000560	0.				
68	59	58	72	73	5	0.	0.0	0.3420	0.0	0.				
69	60	59	73	74	5	0.	0.0	0.3420	0.0	0.				
70	61	60	74	75	5	0.	0.0	0.3420	0.0	0.				
71	62	61	75	76	5	0.	0.0	0.3420	0.0	0.				
72	63	62	76	77	5	0.	0.0	0.3420	0.0	0.				
73	64	63	77	78	5	0.	0.0	0.3420	0.0	0.				
74	65	64	78	79	5	0.	0.0	0.3420	0.0	0.				
75	66	65	79	80	5	0.	0.0	0.3420	0.0	0.				
76	67	66	80	81	5	0.	0.0	0.3420	0.0	0.				
77	68	67	81	82	5	0.	0.0	0.3420	0.0	0.				
78	69	68	82	83	5	0.	0.0	0.3420	0.0	0.				
79	70	69	83	84	5	0.	0.0	0.3420	0.0	0.				
80	71	70	84	85	5	0.	0.0	0.3420	0.0	0.				
81	73	72	86	87	5	0.	0.0	0.3420	0.0	0.				
82	74	73	87	88	5	0.	0.0	0.3420	0.0	0.				
83	75	74	88	89	5	0.	0.0	0.3420	0.0	0.				
84	76	75	89	90	5	0.	0.0	0.3420	0.0	0.				
85	77	76	90	91	5	0.	0.0	0.3420	0.0	0.				
86	78	77	91	92	5	0.	0.0	0.3420	0.0	0.				
87	79	78	92	93	5	0.	0.0	0.3420	0.0	0.				
88	80	79	93	94	5	0.	0.0	0.3420	0.0	0.				
89	81	80	94	95	5	0.	0.0	0.3420	0.0	0.				
90	82	81	95	96	5	0.	0.0	0.3420	0.0	0.				
91	83	82	96	97	5	0.	0.0	0.3420	0.0	0.				
92	84	83	97	98	5	0.	0.0	0.3420	0.0	0.				
93	85	84	98	99	5	0.	0.0	0.3420	0.0	0.				
94	87	86	100	101	5	0.	0.0	0.3420	0.0	0.				
95	88	87	101	102	5	0.	0.0	0.3420	0.0	0.				
96	89	88	102	103	5	0.	0.0	0.3420	0.0	0.				
97	90	89	103	104	5	0.	0.0	0.3420	0.0	0.				
98	91	90	104	105	5	0.	0.0	0.3420	0.0	0.				
99	92	91	105	106	5	0.	0.0	0.3420	0.0	0.				
100	93	92	106	107	5	0.	0.0	0.3420	0.0	0.				

TABLE C-7. FINITE-ELEMENT ANALYSIS OF ELEMENT SPECIMEN (continued)

ELEM	P	Q	R	S	TYPE	E	PR	THICK-AREA	ALPHA	TEM 1	TEM 2	TEM 3	TEM 4	TEM 5
101	94	93	107	108	5	0.	0.0	0.3420	0.0	0.				
102	95	94	108	109	5	0.	0.0	0.3420	0.0	0.				
103	96	95	109	110	5	0.	0.0	0.3420	0.0	0.				
104	97	96	110	111	5	0.	0.0	0.3420	0.0	0.				
105	98	97	111	0	4	0.	0.0	0.3420	0.0	0.				
106	104	103	112	0	4	0.	0.0	0.3420	0.0	0.				
107	112	113	104	0	4	0.	0.0	0.3420	0.0	0.				
108	105	104	113	0	4	0.	0.0	0.3420	0.0	0.				
109	106	105	113	0	4	0.	0.0	0.3420	0.0	0.				
110	113	114	106	0	4	0.	0.0	0.3420	0.0	0.				
111	107	106	114	0	4	0.	0.0	0.3420	0.0	0.				
112	108	107	114	0	4	0.	0.0	0.3420	0.0	0.				
113	115	114	108	0	4	0.	0.0	0.3420	0.0	0.				
114	109	108	115	0	4	0.	0.0	0.3420	0.0	0.				
115	110	109	115	116	5	0.	0.0	0.3420	0.0	0.				
116	111	110	116	117	5	0.	0.0	0.3420	0.0	0.				
117	98	111	117	118	5	0.	0.0	0.3420	0.0	0.				
118	99	98	118	119	5	0.	0.0	0.3420	0.0	0.				
119	113	112	120	121	5	0.	0.0	0.3420	0.0	0.				
120	114	113	121	122	5	0.	0.0	0.3420	0.0	0.				
121	115	114	122	123	5	0.	0.0	0.3420	0.0	0.				
122	116	115	123	124	5	0.	0.0	0.3420	0.0	0.				
123	117	116	124	125	5	0.	0.0	0.3420	0.0	0.				
124	118	117	125	126	5	0.	0.0	0.3420	0.0	0.				
125	119	118	126	127	5	0.	0.0	0.3420	0.0	0.				
126	121	120	128	129	5	0.	0.0	0.3420	0.0	0.				
127	122	121	129	130	5	0.	0.0	0.3420	0.0	0.				
128	123	122	130	131	5	0.	0.0	0.3420	0.0	0.				
129	124	123	131	132	5	0.	0.0	0.3420	0.0	0.				
130	125	124	132	133	5	0.	0.0	0.3420	0.0	0.				
131	126	125	133	134	5	0.	0.0	0.3420	0.0	0.				
132	127	126	134	135	5	0.	0.0	0.3420	0.0	0.				
133	129	128	136	0	4	0.	0.0	0.3420	0.0	0.				
134	130	129	136	137	5	0.	0.0	0.3420	0.0	0.				
135	131	130	137	138	5	0.	0.0	0.3420	0.0	0.				
136	132	131	138	139	5	0.	0.0	0.3420	0.0	0.				
137	133	132	139	140	5	0.	0.0	0.3420	0.0	0.				
138	134	133	140	141	5	0.	0.0	0.3420	0.0	0.				
139	135	134	141	142	5	0.	0.0	0.3420	0.0	0.				
140	144	137	136	143	5	0.	0.0	0.3420	0.0	0.				
141	145	138	137	144	5	0.	0.0	0.3420	0.0	0.				
142	139	138	145	146	5	0.	0.0	0.3420	0.0	0.				
143	140	139	146	147	5	0.	0.0	0.3420	0.0	0.				
144	141	140	147	148	5	0.	0.0	0.3420	0.0	0.				
145	142	141	148	149	5	0.	0.0	0.3420	0.0	0.				
146	151	144	143	150	5	0.	0.0	0.3420	0.0	0.				
147	152	145	144	151	5	0.	0.0	0.3420	0.0	0.				
148	146	145	152	153	5	0.	0.0	0.3420	0.0	0.				
149	147	146	153	154	5	0.	0.0	0.3420	0.0	0.				
150	148	147	154	155	5	0.	0.0	0.3420	0.0	0.				

TABLE C-7. FINITE-ELEMENT ANALYSIS OF ELEMENT SPECIMEN (continued)

ELEM	P	Q	R	S	TYPE	E	PR	THICK-AREA	ALPHA	TEM 1	TEM 2	TEM 3	TEM 4	TEM 5
151	145	148	155	156	5	0.	0.0	0.3420	0.0	0.				
152	56	58	72	73	3	29000.	0.3180	0.2960	0.00000560	0.				
153	60	59	73	74	3	29000.	0.3180	0.2960	0.00000560	0.				
154	61	60	74	75	3	29000.	0.3180	0.2960	0.00000560	0.				
155	62	61	75	76	3	29000.	0.3180	0.2960	0.00000560	0.				
156	63	62	76	77	3	29000.	0.3180	0.2960	0.00000560	0.				
157	64	63	77	78	3	29000.	0.3180	0.2960	0.00000560	0.				
158	65	64	78	79	3	29000.	0.3180	0.2960	0.00000560	0.				
159	66	65	79	80	3	29000.	0.3180	0.2960	0.00000560	0.				
160	67	66	80	81	3	29000.	0.3180	0.2960	0.00000560	0.				
161	68	67	81	82	3	29000.	0.3180	0.2960	0.00000560	0.				
162	69	68	82	83	3	29000.	0.3180	0.2960	0.00000560	0.				
163	70	69	83	84	3	29000.	0.3180	0.2960	0.00000560	0.				
164	71	70	84	85	3	29000.	0.3180	0.2960	0.00000560	0.				
165	73	72	86	87	3	29000.	0.3180	0.2960	0.00000560	0.				
166	74	73	87	88	3	29000.	0.3180	0.2960	0.00000560	0.				
167	75	74	88	89	3	29000.	0.3180	0.2960	0.00000560	0.				
168	76	75	89	90	3	29000.	0.3180	0.2960	0.00000560	0.				
169	77	76	90	91	3	29000.	0.3180	0.2960	0.00000560	0.				
170	78	77	91	92	3	29000.	0.3180	0.2960	0.00000560	0.				
171	79	78	92	93	3	29000.	0.3180	0.2960	0.00000560	0.				
172	80	79	93	94	3	29000.	0.3180	0.2960	0.00000560	0.				
173	81	80	94	95	3	29000.	0.3180	0.2960	0.00000560	0.				
174	82	81	95	96	3	29000.	0.3180	0.2960	0.00000560	0.				
175	83	82	96	97	3	29000.	0.3180	0.2960	0.00000560	0.				
176	84	83	97	98	3	29000.	0.3180	0.2960	0.00000560	0.				
177	85	84	98	99	3	29000.	0.3180	0.2960	0.00000560	0.				
178	87	86	100	101	3	29000.	0.3180	0.2960	0.00000560	0.				
179	88	87	101	102	3	29000.	0.3180	0.2960	0.00000560	0.				
180	89	88	102	103	3	29000.	0.3180	0.2960	0.00000560	0.				
181	90	89	103	104	3	29000.	0.3180	0.2960	0.00000560	0.				
182	91	90	104	105	3	29000.	0.3180	0.2960	0.00000560	0.				
183	92	91	105	106	3	29000.	0.3180	0.2960	0.00000560	0.				
184	93	92	106	107	3	29000.	0.3180	0.2960	0.00000560	0.				
185	94	93	107	108	3	29000.	0.3180	0.2960	0.00000560	0.				
186	95	94	108	109	3	29000.	0.3180	0.2960	0.00000560	0.				
187	96	95	109	110	3	29000.	0.3180	0.2960	0.00000560	0.				
188	97	96	110	111	3	29000.	0.3180	0.2960	0.00000560	0.				
189	98	97	111	0	2	29000.	0.3180	0.2960	0.00000560	0.				
190	104	103	112	0	2	29000.	0.3180	0.2320	0.00000560	0.				
191	112	113	104	0	2	29000.	0.3180	0.2320	0.00000560	0.				
192	105	104	113	0	2	29000.	0.3180	0.2320	0.00000560	0.				
193	106	105	113	0	2	29000.	0.3180	0.2320	0.00000560	0.				
194	113	114	106	0	2	29000.	0.3180	0.2320	0.00000560	0.				
195	107	106	114	0	2	29000.	0.3180	0.2320	0.00000560	0.				
196	108	107	114	0	2	29000.	0.3180	0.2320	0.00000560	0.				
197	115	114	108	0	2	29000.	0.3180	0.2320	0.00000560	0.				
198	109	108	115	0	2	29000.	0.3180	0.2320	0.00000560	0.				
199	110	109	115	116	3	29000.	0.3180	0.2320	0.00000560	0.				
200	111	110	116	117	3	29000.	0.3180	0.2320	0.00000560	0.				

TABLE C-7. FINITE-ELEMENT ANALYSIS OF ELEMENT SPECIMEN (continued)

ELEM	P	Q	R	S	TYPE	E	PR	THICK-AREA	ALPHA	TEM 1	TEM 2	TEM 3	TEM 4	TEM 5
201	98	111	117	118	3	29000.	0.3180	0.2320	0.00000560	0.				
202	99	98	118	119	3	29000.	0.3180	0.2320	0.00000560	0.				
203	113	112	120	121	3	29000.	0.3180	0.1320	0.00000560	0.				
204	114	113	121	122	3	29000.	0.3180	0.1320	0.00000560	0.				
205	115	114	122	123	3	29000.	0.3180	0.1320	0.00000560	0.				
206	116	115	123	124	3	29000.	0.3180	0.1320	0.00000560	0.				
207	117	116	124	125	3	29000.	0.3180	0.1320	0.00000560	0.				
208	118	117	125	126	3	29000.	0.3180	0.1320	0.00000560	0.				
209	119	118	126	127	3	29000.	0.3180	0.1320	0.00000560	0.				
210	121	120	128	129	3	29000.	0.3180	0.0320	0.00000560	0.				
211	122	121	129	130	3	29000.	0.3180	0.0320	0.00000560	0.				
212	123	122	130	131	3	29000.	0.3180	0.0320	0.00000560	0.				
213	124	123	131	132	3	29000.	0.3180	0.0320	0.00000560	0.				
214	125	124	132	133	3	29000.	0.3180	0.0320	0.00000560	0.				
215	126	125	133	134	3	29000.	0.3180	0.0320	0.00000560	0.				
216	127	126	134	135	3	29000.	0.3180	0.0320	0.00000560	0.				
217	156	151	150	157	5	0.	0.0	0.3420	0.0	0.				
218	155	152	151	158	5	0.	0.0	0.3420	0.0	0.				
219	153	152	159	160	5	0.	0.0	0.3420	0.0	0.				
220	154	153	160	161	5	0.	0.0	0.3420	0.0	0.				
221	155	154	161	162	5	0.	0.0	0.3420	0.0	0.				
222	156	155	162	163	5	0.	0.0	0.3420	0.0	0.				
223	158	157	164	0	4	0.	0.0	0.3420	0.0	0.				
224	159	170	164	158	5	0.	0.0	0.3420	0.0	0.				
225	160	174	159	0	4	0.	0.0	0.3420	0.0	0.				
226	161	177	160	0	4	0.	0.0	0.3420	0.0	0.				
227	174	171	170	159	5	0.	0.0	0.3420	0.0	0.				
228	175	172	174	171	5	0.	0.0	0.3420	0.0	0.				
229	177	175	174	160	5	0.	0.0	0.3420	0.0	0.				
230	157	165	164	0	4	0.	0.0	0.3420	0.0	0.				
231	170	166	165	164	5	0.	0.0	0.3420	0.0	0.				
232	171	167	166	170	5	0.	0.0	0.3420	0.0	0.				
233	172	168	167	171	5	0.	0.0	0.3420	0.0	0.				
234	173	169	168	172	5	0.	0.0	0.3420	0.0	0.				
235	176	173	172	175	5	0.	0.0	0.3420	0.0	0.				
236	178	176	175	177	5	0.	0.0	0.3420	0.0	0.				
237	179	178	177	161	5	0.	0.0	0.3420	0.0	0.				
238	180	179	161	162	5	0.	0.0	0.3420	0.0	0.				
239	181	180	162	163	5	0.	0.0	0.3420	0.0	0.				

TABLE C-7. FINITE-ELEMENT ANALYSIS OF ELEMENT SPECIMEN (continued)

COMPOSITE MATERIAL PROPERTIES									
ELEM	ALPHA 1	ALPHA 2	ALPHA 12	C11	C12	C13	C22	C23	C33
68	0.0	0.0	0.0	8288.0	2494.0	0.0	8288.0	0.0	2897.0
69	0.0	0.0	0.0	8288.0	2494.0	0.0	8288.0	0.0	2897.0
70	0.0	0.0	0.0	8288.0	2494.0	0.0	8288.0	0.0	2897.0
71	0.0	0.0	0.0	8288.0	2494.0	0.0	8288.0	0.0	2897.0
72	0.0	0.0	0.0	8288.0	2494.0	0.0	8288.0	0.0	2897.0
73	0.0	0.0	0.0	8288.0	2494.0	0.0	8288.0	0.0	2897.0
74	0.0	0.0	0.0	8288.0	2494.0	0.0	8288.0	0.0	2897.0
75	0.0	0.0	0.0	8288.0	2494.0	0.0	8288.0	0.0	2897.0
76	0.0	0.0	0.0	8288.0	2494.0	0.0	8288.0	0.0	2897.0
77	0.0	0.0	0.0	8288.0	2494.0	0.0	8288.0	0.0	2897.0
78	0.0	0.0	0.0	8288.0	2494.0	0.0	8288.0	0.0	2897.0
79	0.0	0.0	0.0	8288.0	2494.0	0.0	8288.0	0.0	2897.0
80	0.0	0.0	0.0	8288.0	2494.0	0.0	8288.0	0.0	2897.0
81	0.0	0.0	0.0	8288.0	2494.0	0.0	8288.0	0.0	2897.0
82	0.0	0.0	0.0	8288.0	2494.0	0.0	8288.0	0.0	2897.0
83	0.0	0.0	0.0	8288.0	2494.0	0.0	8288.0	0.0	2897.0
84	0.0	0.0	0.0	8288.0	2494.0	0.0	8288.0	0.0	2897.0
85	0.0	0.0	0.0	8288.0	2494.0	0.0	8288.0	0.0	2897.0
86	0.0	0.0	0.0	8288.0	2494.0	0.0	8288.0	0.0	2897.0
87	0.0	0.0	0.0	8288.0	2494.0	0.0	8288.0	0.0	2897.0
88	0.0	0.0	0.0	8288.0	2494.0	0.0	8288.0	0.0	2897.0
89	0.0	0.0	0.0	8288.0	2494.0	0.0	8288.0	0.0	2897.0
90	0.0	0.0	0.0	8288.0	2494.0	0.0	8288.0	0.0	2897.0
91	0.0	0.0	0.0	8288.0	2494.0	0.0	8288.0	0.0	2897.0
92	0.0	0.0	0.0	8288.0	2494.0	0.0	8288.0	0.0	2897.0
93	0.0	0.0	0.0	8288.0	2494.0	0.0	8288.0	0.0	2897.0
94	0.0	0.0	0.0	8288.0	2494.0	0.0	8288.0	0.0	2897.0
95	0.0	0.0	0.0	8288.0	2494.0	0.0	8288.0	0.0	2897.0
96	0.0	0.0	0.0	8288.0	2494.0	0.0	8288.0	0.0	2897.0
97	0.0	0.0	0.0	8288.0	2494.0	0.0	8288.0	0.0	2897.0
98	0.0	0.0	0.0	8288.0	2494.0	0.0	8288.0	0.0	2897.0
99	0.0	0.0	0.0	8288.0	2494.0	0.0	8288.0	0.0	2897.0
100	0.0	0.0	0.0	8288.0	2494.0	0.0	8288.0	0.0	2897.0
101	0.0	0.0	0.0	8288.0	2494.0	0.0	8288.0	0.0	2897.0
102	0.0	0.0	0.0	8288.0	2494.0	0.0	8288.0	0.0	2897.0
103	0.0	0.0	0.0	8288.0	2494.0	0.0	8288.0	0.0	2897.0
104	0.0	0.0	0.0	8288.0	2494.0	0.0	8288.0	0.0	2897.0
105	0.0	0.0	0.0	8288.0	2494.0	0.0	8288.0	0.0	2897.0
106	0.0	0.0	0.0	8288.0	2494.0	0.0	8288.0	0.0	2897.0
107	0.0	0.0	0.0	8288.0	2494.0	0.0	8288.0	0.0	2897.0
108	0.0	0.0	0.0	8288.0	2494.0	0.0	8288.0	0.0	2897.0
109	0.0	0.0	0.0	8288.0	2494.0	0.0	8288.0	0.0	2897.0
110	0.0	0.0	0.0	8288.0	2494.0	0.0	8288.0	0.0	2897.0
111	0.0	0.0	0.0	8288.0	2494.0	0.0	8288.0	0.0	2897.0
112	0.0	0.0	0.0	8288.0	2494.0	0.0	8288.0	0.0	2897.0
113	0.0	0.0	0.0	8288.0	2494.0	0.0	8288.0	0.0	2897.0
114	0.0	0.0	0.0	8288.0	2494.0	0.0	8288.0	0.0	2897.0
115	0.0	0.0	0.0	8288.0	2494.0	0.0	8288.0	0.0	2897.0
116	0.0	0.0	0.0	8288.0	2494.0	0.0	8288.0	0.0	2897.0
117	0.0	0.0	0.0	8288.0	2494.0	0.0	8288.0	0.0	2897.0

TABLE C-7. FINITE-ELEMENT ANALYSIS OF ELEMENT SPECIMEN (continued)

COMPOSITE MATERIAL PROPERTIES

ELEM	ALPHA 1	ALPHA 2	ALPHA 12	C11	C12	C13	C22	C23	C33
118	0.0	0.0	0.0	8288.0	2494.0	0.0	8288.0	0.0	2897.0
119	0.0	0.0	0.0	8288.0	2494.0	0.0	8288.0	0.0	2897.0
120	0.0	0.0	0.0	8288.0	2494.0	0.0	8288.0	0.0	2897.0
121	0.0	0.0	0.0	8288.0	2494.0	0.0	8288.0	0.0	2897.0
122	0.0	0.0	0.0	8288.0	2494.0	0.0	8288.0	0.0	2897.0
123	0.0	0.0	0.0	8288.0	2494.0	0.0	8288.0	0.0	2897.0
124	0.0	0.0	0.0	8288.0	2494.0	0.0	8288.0	0.0	2897.0
125	0.0	0.0	0.0	8288.0	2494.0	0.0	8288.0	0.0	2897.0
126	0.0	0.0	0.0	8288.0	2494.0	0.0	8288.0	0.0	2897.0
127	0.0	0.0	0.0	8288.0	2494.0	0.0	8288.0	0.0	2897.0
128	0.0	0.0	0.0	8288.0	2494.0	0.0	8288.0	0.0	2897.0
129	0.0	0.0	0.0	8288.0	2494.0	0.0	8288.0	0.0	2897.0
130	0.0	0.0	0.0	8288.0	2494.0	0.0	8288.0	0.0	2897.0
131	0.0	0.0	0.0	8288.0	2494.0	0.0	8288.0	0.0	2897.0
132	0.0	0.0	0.0	8288.0	2494.0	0.0	8288.0	0.0	2897.0
133	0.0	0.0	0.0	8288.0	2494.0	0.0	8288.0	0.0	2897.0
134	0.0	0.0	0.0	8288.0	2494.0	0.0	8288.0	0.0	2897.0
135	0.0	0.0	0.0	8288.0	2494.0	0.0	8288.0	0.0	2897.0
136	0.0	0.0	0.0	8288.0	2494.0	0.0	8288.0	0.0	2897.0
137	0.0	0.0	0.0	8288.0	2494.0	0.0	8288.0	0.0	2897.0
138	0.0	0.0	0.0	8288.0	2494.0	0.0	8288.0	0.0	2897.0
139	0.0	0.0	0.0	8288.0	2494.0	0.0	8288.0	0.0	2897.0
140	0.0	0.0	0.0	8288.0	2494.0	0.0	8288.0	0.0	2897.0
141	0.0	0.0	0.0	8288.0	2494.0	0.0	8288.0	0.0	2897.0
142	0.0	0.0	0.0	8288.0	2494.0	0.0	8288.0	0.0	2897.0
143	0.0	0.0	0.0	8288.0	2494.0	0.0	8288.0	0.0	2897.0
144	0.0	0.0	0.0	8288.0	2494.0	0.0	8288.0	0.0	2897.0
145	0.0	0.0	0.0	8288.0	2494.0	0.0	8288.0	0.0	2897.0
146	0.0	0.0	0.0	8288.0	2494.0	0.0	8288.0	0.0	2897.0
147	0.0	0.0	0.0	8288.0	2494.0	0.0	8288.0	0.0	2897.0
148	0.0	0.0	0.0	8288.0	2494.0	0.0	8288.0	0.0	2897.0
149	0.0	0.0	0.0	8288.0	2494.0	0.0	8288.0	0.0	2897.0
150	0.0	0.0	0.0	8288.0	2494.0	0.0	8288.0	0.0	2897.0
151	0.0	0.0	0.0	8288.0	2494.0	0.0	8288.0	0.0	2897.0
217	0.0	0.0	0.0	8288.0	2494.0	0.0	8288.0	0.0	2897.0
218	0.0	0.0	0.0	8288.0	2494.0	0.0	8288.0	0.0	2897.0
219	0.0	0.0	0.0	8288.0	2494.0	0.0	8288.0	0.0	2897.0
220	0.0	0.0	0.0	8288.0	2494.0	0.0	8288.0	0.0	2897.0
221	0.0	0.0	0.0	8288.0	2494.0	0.0	8288.0	0.0	2897.0
222	0.0	0.0	0.0	8288.0	2494.0	0.0	8288.0	0.0	2897.0
223	0.0	0.0	0.0	8288.0	2494.0	0.0	8288.0	0.0	2897.0
224	0.0	0.0	0.0	8288.0	2494.0	0.0	8288.0	0.0	2897.0
225	0.0	0.0	0.0	8288.0	2494.0	0.0	8288.0	0.0	2897.0
226	0.0	0.0	0.0	8288.0	2494.0	0.0	8288.0	0.0	2897.0
227	0.0	0.0	0.0	8288.0	2494.0	0.0	8288.0	0.0	2897.0
228	0.0	0.0	0.0	8288.0	2494.0	0.0	8288.0	0.0	2897.0
229	0.0	0.0	0.0	8288.0	2494.0	0.0	8288.0	0.0	2897.0
230	0.0	0.0	0.0	8288.0	2494.0	0.0	8288.0	0.0	2897.0
231	0.0	0.0	0.0	8288.0	2494.0	0.0	8288.0	0.0	2897.0
232	0.0	0.0	0.0	8288.0	2494.0	0.0	8288.0	0.0	2897.0

TABLE C-7. FINITE-ELEMENT ANALYSIS OF ELEMENT SPECIMEN (continued)

COMPOSITE MATERIAL PROPERTIES

ELEM	ALPHA 1	ALPHA 2	ALPHA 12	C11	C12	C13	C22	C23	C33
233	0.0	0.0	0.0	8288.0	2494.0	0.0	8288.0	0.0	2897.0
234	0.0	0.0	0.0	8288.0	2494.0	0.0	8288.0	0.0	2897.0
235	0.0	0.0	0.0	8288.0	2494.0	0.0	8288.0	0.0	2897.0
236	0.0	0.0	0.0	8288.0	2494.0	0.0	8288.0	0.0	2897.0
237	0.0	0.0	0.0	8288.0	2494.0	0.0	8288.0	0.0	2897.0
238	0.0	0.0	0.0	8288.0	2494.0	0.0	8288.0	0.0	2897.0
239	0.0	0.0	0.0	8288.0	2494.0	0.0	8288.0	0.0	2897.0

TABLE C-7. FINITE-ELEMENT ANALYSIS OF ELEMENT SPECIMEN (continued)

X DEFLECTION, CASE 1

	1	2	3	4	5	6	7	8	9	10
1	0.0	0.0	-1.137E-05	-5.314E-05	-1.238E-04	-1.485E-04	-1.517E-04	-1.337E-04	-1.179E-04	-1.274E-04
11	-1.506E-04	-1.913E-04	-1.820E-04	-1.111E-04	0.0	0.0	-8.393E-05	-1.674E-04	-2.462E-04	-2.563E-04
21	-2.320E-04	-1.776E-04	-1.213E-04	-9.853E-05	-9.587E-05	-1.036E-04	-9.618E-05	-5.840E-05	0.0	0.0
31	-7.962E-05	-1.603E-04	-2.428E-04	-2.571E-04	-2.344E-04	-1.780E-04	-1.177E-04	-9.521E-05	-9.466E-05	-1.055E-04
41	-1.005E-04	-6.154E-05	0.0	0.0	-7.472E-05	-1.535E-04	-2.384E-04	-2.569E-04	-2.359E-04	-1.779E-04
51	-1.153E-04	-9.228E-05	-9.345E-05	-1.075E-04	-1.046E-04	-6.466E-05	0.0	0.0	6.635E-04	1.073E-03
61	1.095E-03	9.372E-04	6.891E-04	3.473E-04	1.401E-05	-1.847E-04	-3.165E-04	-3.640E-04	-2.766E-04	-1.339E-04
71	0.0	0.0	6.833E-04	1.103E-03	1.100E-03	9.270E-04	6.624E-04	3.137E-04	-1.846E-05	-2.251E-04
81	-3.409E-04	-3.536E-04	-2.319E-04	-9.342E-05	0.0	0.0	7.355E-04	1.166E-03	1.144E-03	9.136E-04
91	6.213E-04	2.664E-04	-6.400E-05	-2.777E-04	-3.823E-04	-3.404E-04	-1.660E-04	-2.873E-05	0.0	0.0
101	9.634E-04	1.612E-03	1.631E-03	1.115E-03	6.211E-04	2.374E-04	-1.444E-04	-3.308E-04	-4.431E-04	-3.329E-04
111	-1.277E-04	1.535E-03	6.663E-04	-1.820E-04	-4.877E-04	-3.210E-04	-6.765E-05	3.655E-05	0.0	1.374E-03
121	6.934E-04	-1.989E-04	-5.154E-04	-3.328E-04	-4.982E-05	4.920E-05	0.0	1.227E-03	7.573E-04	-1.858E-04
131	-5.488E-04	-4.019E-04	-1.290E-04	1.336E-05	0.0	9.093E-04	-1.273E-04	-6.222E-04	-5.946E-04	-3.531E-04
141	-1.398E-04	0.0	3.176E-04	-3.764E-04	-8.398E-04	-9.761E-04	-7.597E-04	-3.993E-04	0.0	-2.673E-04
151	-8.284E-04	-1.215E-03	-1.517E-03	-1.265E-03	-7.323E-04	0.0	-4.096E-04	-1.042E-03	-1.289E-03	-1.743E-03
161	-1.447E-03	-8.901E-04	0.0	-8.099E-04	-7.442E-04	-1.380E-03	-1.703E-03	-2.013E-03	-2.393E-03	-1.370E-03
171	-1.771E-03	-1.991E-03	-2.276E-03	-1.566E-03	-1.962E-03	-2.230E-03	-1.765E-03	-1.789E-03	-1.390E-03	-7.116E-04
181	0.0									

Y DEFLECTION, CASE 1

	1	2	3	4	5	6	7	8	9	10
1	1.206E-02	1.125E-02	1.123E-02	1.118E-02	1.113E-02	1.113E-02	1.115E-02	1.118E-02	1.121E-02	1.125E-02
11	1.130E-02	1.143E-02	1.158E-02	1.169E-02	1.173E-02	1.122E-02	1.122E-02	1.124E-02	1.124E-02	1.127E-02
21	1.131E-02	1.135E-02	1.140E-02	1.144E-02	1.148E-02	1.156E-02	1.164E-02	1.171E-02	1.173E-02	1.123E-02
31	1.123E-02	1.122E-02	1.124E-02	1.128E-02	1.132E-02	1.137E-02	1.141E-02	1.144E-02	1.147E-02	1.155E-02
41	1.164E-02	1.170E-02	1.173E-02	1.123E-02	1.123E-02	1.122E-02	1.124E-02	1.128E-02	1.134E-02	1.139E-02
51	1.142E-02	1.144E-02	1.146E-02	1.154E-02	1.163E-02	1.170E-02	1.173E-02	1.118E-02	1.094E-02	1.027E-02
61	9.307E-03	8.814E-03	8.320E-03	7.832E-03	7.377E-03	6.968E-03	6.585E-03	5.968E-03	5.436E-03	5.058E-03
71	4.916E-03	1.112E-02	1.086E-02	1.017E-02	9.189E-03	8.676E-03	8.182E-03	7.709E-03	7.299E-03	6.941E-03
81	6.607E-03	6.017E-03	5.477E-03	5.066E-03	4.908E-03	1.100E-02	1.073E-02	9.988E-03	8.912E-03	8.440E-03
91	7.942E-03	7.495E-03	7.153E-03	6.866E-03	6.613E-03	6.085E-03	5.536E-03	5.082E-03	4.898E-03	1.073E-02
101	1.038E-02	9.317E-03	8.277E-03	7.467E-03	7.096E-03	6.904E-03	6.744E-03	6.632E-03	6.514E-03	6.112E-03
111	5.557E-03	7.363E-03	6.778E-03	6.513E-03	6.402E-03	6.102E-03	5.575E-03	5.085E-03	4.889E-03	6.712E-03
121	6.412E-03	6.230E-03	6.226E-03	6.007E-03	5.550E-03	5.084E-03	4.865E-03	6.130E-03	5.987E-03	5.857E-03
131	5.502E-03	5.774E-03	5.384E-03	4.986E-03	4.808E-03	5.138E-03	5.080E-03	5.152E-03	5.134E-03	4.939E-03
141	4.686E-03	4.573E-03	3.021E-03	3.367E-03	3.527E-03	3.696E-03	3.741E-03	3.710E-03	3.693E-03	1.450E-03
151	1.582E-03	1.749E-03	2.005E-03	2.060E-03	2.144E-03	2.144E-03	8.616E-04	1.182E-03	1.266E-03	1.513E-03
161	1.485E-03	1.618E-03	1.571E-03	8.520E-04	3.809E-04	4.270E-04	2.682E-04	5.965E-05	0.0	8.923E-04
171	7.522E-04	3.939E-04	0.0	9.269E-04	5.898E-04	0.0	1.117E-03	0.0	0.0	0.0
181	0.0									

TABLE C-7. FINITE-ELEMENT ANALYSIS OF ELEMENT SPECIMEN (continued)

STRESS ELEM	XX	YY	XY	ON	OS	CASE	(TOTAL STRAIN)*1000000. XX	YY	XY	(MECH. STRAIN)*1000000. XX	YY	XY	CASE
1	-9.9100	-3.4212	-0.2044	-4.4437	4.1132	1	-304.	-9.	-19.	-304.	-9.	-19.	1
2	-9.5875	-3.4511	-0.5827	-4.3462	3.9934	1	-293.	-14.	-53.	-293.	-14.	-53.	1
3	-8.7707	-3.4168	-1.3279	-4.0625	3.7689	1	-265.	-22.	-121.	-265.	-22.	-121.	1
4	-7.5230	-3.2018	-2.3982	-3.5749	3.6519	1	-224.	-28.	-218.	-224.	-28.	-218.	1
5	-6.3337	-3.2013	-3.3551	-3.1783	3.7670	1	-183.	-41.	-305.	-183.	-41.	-305.	1
6	-4.7913	-3.1808	-4.0833	-2.6574	3.8831	1	-130.	-57.	-371.	-130.	-57.	-371.	1
7	-3.1048	-3.1845	-3.9888	-2.0965	3.5785	1	-72.	-76.	-363.	-72.	-76.	-363.	1
8	-1.6283	-3.1744	-3.1101	-1.6009	2.8510	1	-21.	-92.	-283.	-21.	-92.	-283.	1
9	-0.4814	-3.1713	-2.3731	-1.2176	2.3878	1	18.	-104.	-216.	18.	-104.	-216.	1
10	0.7567	-3.2012	-1.6217	-0.8148	2.1670	1	61.	-119.	-147.	61.	-119.	-147.	1
11	1.8355	-3.1757	-0.9197	-0.4467	2.2021	1	98.	-130.	-84.	98.	-130.	-84.	1
12	2.4215	-3.1614	-0.4578	-0.2466	2.3163	1	118.	-136.	-42.	118.	-136.	-42.	1
13	2.6768	-3.1556	-0.1439	-0.1596	2.3866	1	127.	-138.	-13.	127.	-138.	-13.	1
14	-0.0880	-2.7537	0.0135	-0.9472	1.2779	1	27.	-94.	1.	27.	-94.	1.	1
15	-0.0697	-2.4360	0.0420	-0.8352	1.1328	1	24.	-83.	4.	24.	-83.	4.	1
16	-0.0476	-2.4783	0.0920	-0.8420	1.1597	1	26.	-85.	8.	26.	-85.	8.	1
17	-0.0272	-2.0747	0.0449	-0.7006	0.9724	1	22.	-71.	4.	22.	-71.	4.	1
18	-0.0339	-1.9990	-0.0137	-0.6766	0.9352	1	21.	-69.	-1.	21.	-69.	-1.	1
19	-0.0460	-2.1421	-0.1130	-0.7293	1.0034	1	22.	-73.	-10.	22.	-73.	-10.	1
20	-0.0626	-2.4253	-0.1785	-0.8293	1.1382	1	24.	-83.	-16.	24.	-83.	-16.	1
21	-0.0689	-2.5325	0.0935	-0.8671	1.1804	1	25.	-87.	8.	25.	-87.	8.	1
22	-0.0798	-2.4199	0.0107	-0.8332	1.1225	1	24.	-83.	1.	24.	-83.	1.	1
23	-0.0613	-2.2772	-0.0051	-0.7795	1.0594	1	23.	-78.	-0.	23.	-78.	-0.	1
24	-0.0619	-2.2395	0.0564	-0.7671	1.0424	1	22.	-77.	5.	22.	-77.	5.	1
25	-0.0412	-2.1882	0.0091	-0.7431	1.0220	1	23.	-75.	1.	23.	-75.	1.	1
26	-0.0446	-2.1504	0.0137	-0.7317	1.0034	1	22.	-74.	1.	22.	-74.	1.	1
27	0.0110	-2.4575	-0.0191	-0.8155	1.1612	1	27.	-85.	-2.	27.	-85.	-2.	1
28	0.0439	-2.1819	0.0341	-0.7127	1.0394	1	25.	-76.	3.	25.	-76.	3.	1
29	0.0455	-2.4390	0.0801	-0.7978	1.1625	1	28.	-85.	7.	28.	-85.	7.	1
30	0.0307	-2.4814	0.0090	-0.8069	1.1843	1	29.	-86.	1.	29.	-86.	1.	1
31	0.0711	-2.4136	-0.0251	-0.7808	1.1551	1	29.	-84.	-2.	29.	-84.	-2.	1
32	0.0527	-2.2412	-0.1150	-0.7295	1.0733	1	26.	-78.	-10.	26.	-78.	-10.	1
33	0.0153	-1.8342	-0.1758	-0.6063	0.8801	1	21.	-63.	-16.	21.	-63.	-16.	1
34	-0.0028	-1.7437	0.0913	-0.5822	0.8247	1	19.	-60.	8.	19.	-60.	8.	1
35	0.0551	-1.8459	0.0042	-0.5969	0.8835	1	22.	-64.	0.	22.	-64.	0.	1
36	0.0105	-2.0617	-0.0010	-0.6837	0.9744	1	23.	-71.	-0.	23.	-71.	-0.	1
37	0.0345	-2.0946	0.0498	-0.6867	0.9965	1	24.	-73.	5.	24.	-73.	5.	1
38	0.0422	-2.1442	0.0056	-0.7007	1.0209	1	25.	-74.	0.	25.	-74.	0.	1
39	0.0453	-2.1423	0.0137	-0.6990	1.0208	1	25.	-74.	1.	25.	-74.	1.	1
40	-6.6142					1	-228.			-228.			1
41	-6.5152					1	-225.			-225.			1
42	-6.7760					1	-234.			-234.			1
43	-7.3789					1	-254.			-254.			1
44	-7.4332					1	-256.			-256.			1
45	-6.1367					1	-212.			-212.			1
46	-2.9833					1	-103.			-103.			1
47	0.0359					1	1.			1.			1
48	0.2156					1	7.			7.			1
49	0.1807					1	6.			6.			1
50	0.1669					1	6.			6.			1

TABLE C-7. FINITE-ELEMENT ANALYSIS OF ELEMENT SPECIMEN (continued)

STRESS ELEM	XX	YY	XY	ON	OS	CASE	(TOTAL STRAIN)*1000000. XX	YY	XY	(MECH. STRAIN)*1000000. XX	YY	XY	CASE
51	0.2007					1	7.			7.			1
52	0.1940					1	7.			7.			1
53	0.0997					1	3.			3.			1
54	-6.8254					1	-235.			-235.			1
55	-6.6584					1	-231.			-231.			1
56	-6.9518					1	-240.			-240.			1
57	-7.5871					1	-262.			-262.			1
58	-7.6310					1	-263.			-263.			1
59	-6.3560					1	-219.			-219.			1
60	-3.1844					1	-110.			-110.			1
61	0.0007					1	672.			672.			1
62	0.0030					1	3028.			3028.			1
63	0.0066					1	6592.			6592.			1
64	0.0156					1	15599.			15599.			1
65	0.0251					1	25075.			25075.			1
66	0.0321					1	32148.			32148.			1
67	0.0348					1	34766.			34766.			1
68	-2.1449	4.8819	-0.0078	0.9123	2.9403	1	-479.	733.	-3.	-479.	733.	-3.	1
69	-2.1838	4.6600	-0.0298	0.8254	2.8544	1	-476.	705.	-10.	-476.	705.	-10.	1
70	-2.2840	4.7906	0.1148	0.8355	2.9495	1	-494.	727.	40.	-494.	727.	40.	1
71	-2.5077	4.5389	0.0976	0.6771	2.9174	1	-514.	702.	34.	-514.	702.	34.	1
72	-2.2791	4.9241	0.0701	0.8817	3.0066	1	-499.	744.	24.	-499.	744.	24.	1
73	-1.5432	5.5901	0.2177	1.3489	3.0695	1	-428.	803.	75.	-428.	803.	75.	1
74	-0.3311	6.2449	0.1782	1.9713	3.0284	1	-293.	842.	62.	-293.	842.	62.	1
75	0.1568	6.2934	-0.1143	2.1501	2.9320	1	-230.	829.	-39.	-230.	829.	-39.	1
76	0.1239	5.9435	0.0063	2.0225	2.7731	1	-221.	784.	2.	-221.	784.	2.	1
77	0.0984	4.3608	-0.1509	1.4864	2.0366	1	-161.	575.	-52.	-161.	575.	-52.	1
78	0.0549	2.4124	-0.2930	0.8224	1.1496	1	-89.	318.	-101.	-89.	318.	-101.	1
79	-0.0227	0.4157	-0.2213	0.1310	0.2707	1	-20.	56.	-76.	-20.	56.	-76.	1
80	-0.0516	-0.7152	-0.0800	-0.2556	0.3322	1	22.	-93.	-28.	22.	-93.	-28.	1
81	-1.7203	4.9315	-0.0548	1.0704	2.8195	1	-425.	723.	-19.	-425.	723.	-19.	1
82	-1.6943	4.6682	-0.0219	0.9913	2.6904	1	-411.	687.	-8.	-411.	687.	-8.	1
83	-1.8638	4.7443	0.0257	0.9602	2.7820	1	-437.	704.	9.	-437.	704.	9.	1
84	-2.0028	3.9607	0.0968	0.6526	2.4792	1	-424.	605.	33.	-424.	605.	33.	1
85	-1.7555	4.6226	0.3257	0.9557	2.7032	1	-417.	683.	112.	-417.	683.	112.	1
86	-1.0748	5.0374	0.3523	1.3209	2.6799	1	-344.	711.	122.	-344.	711.	122.	1
87	-0.0936	5.1059	0.2093	1.6708	2.4353	1	-216.	681.	72.	-216.	681.	72.	1
88	0.4516	5.1084	-0.1466	1.8533	2.3122	1	-144.	660.	-51.	-144.	660.	-51.	1
89	0.3965	4.6942	-0.2396	1.6969	2.1345	1	-135.	607.	-83.	-135.	607.	-83.	1
90	0.3192	3.7182	-0.4742	1.3458	1.7266	1	-106.	481.	-164.	-106.	481.	-164.	1
91	0.1807	2.1197	-0.6218	0.7668	1.0855	1	-61.	274.	-215.	-61.	274.	-215.	1
92	0.0726	0.5598	-0.4797	0.2108	0.4639	1	-13.	71.	-166.	-13.	71.	-166.	1
93	-0.0134	-0.2582	-0.1653	-0.0905	0.1797	1	9.	-34.	-57.	9.	-34.	-57.	1
94	-0.6261	5.2535	-0.0584	1.5425	2.6369	1	-293.	722.	-20.	-293.	722.	-20.	1
95	-0.7062	5.2321	-0.2300	1.5086	2.6553	1	-303.	722.	-79.	-303.	722.	-79.	1
96	-0.3981	4.4714	-0.3635	1.3578	2.2275	1	-231.	609.	-125.	-231.	609.	-125.	1
97	-0.8905	3.4325	-0.1551	0.8473	1.8681	1	-255.	491.	-54.	-255.	491.	-54.	1
98	-0.5695	3.5101	-0.0521	0.9802	1.8045	1	-216.	488.	-18.	-216.	488.	-18.	1
99	-0.1554	3.5316	0.0675	1.1254	1.7035	1	-162.	475.	23.	-162.	475.	23.	1
100	0.2567	3.4222	0.0033	1.2263	1.5563	1	-103.	444.	1.	-103.	444.	1.	1

TABLE C-7. FINITE-ELEMENT ANALYSIS OF ELEMENT SPECIMEN (continued)

STRESS ELEM	XX	YY	XY	ON	OS	CASE	(TOTAL STRAIN)*1000000. XX	YY	XY	(MECH. STRAIN)*1000000. XX	YY	XY	CASE
101	0.6492	3.3774	-0.4476	1.3422	1.5083	1	-49.	422.	-155.	-49.	422.	-155.	1
102	0.7241	3.1245	-0.5520	1.2828	1.4094	1	-29.	386.	-191.	-29.	386.	-191.	1
103	0.5289	2.7259	-0.8692	1.0849	1.3772	1	-39.	341.	-300.	-39.	341.	-300.	1
104	0.2063	1.6939	-0.7884	0.6334	0.9919	1	-40.	216.	-272.	-40.	216.	-272.	1
105	0.1406	0.6326	-0.4206	0.2578	0.4376	1	-7.	78.	-145.	-7.	78.	-145.	1
106	0.6874	3.5846	-1.1228	1.4240	1.8037	1	-52.	448.	-388.	-52.	448.	-388.	1
107	-0.3139	1.7574	-0.7446	0.4812	1.0956	1	-112.	246.	-257.	-112.	246.	-257.	1
108	0.0602	2.4803	-0.3000	0.8468	1.1810	1	-91.	327.	-104.	-91.	327.	-104.	1
109	0.2171	2.1972	-0.7162	0.8048	1.1486	1	-59.	283.	-247.	-59.	283.	-247.	1
110	0.7155	1.7090	-0.5302	0.8081	0.8237	1	27.	198.	-183.	27.	198.	-183.	1
111	0.3310	2.2950	-0.2252	0.8753	1.0295	1	-48.	291.	-78.	-48.	291.	-78.	1
112	0.7209	2.0795	-1.1508	0.9335	1.2752	1	13.	247.	-397.	13.	247.	-397.	1
113	1.4982	1.5372	-0.9107	1.0118	1.0320	1	137.	144.	-314.	137.	144.	-314.	1
114	0.6762	1.9975	-0.6207	0.8912	0.9721	1	10.	238.	-214.	10.	238.	-214.	1
115	1.0323	1.5249	-1.1999	0.8524	1.1677	1	76.	161.	-414.	76.	161.	-414.	1
116	0.8510	1.1661	-1.1559	0.6723	1.0645	1	66.	121.	-399.	66.	121.	-399.	1
117	0.5195	0.5912	-0.8237	0.3702	0.7223	1	45.	58.	-284.	45.	58.	-284.	1
118	0.1753	0.2631	-0.2787	0.1461	0.2525	1	13.	28.	-96.	13.	28.	-96.	1
119	0.3967	1.6344	-0.7566	0.6771	0.9307	1	-13.	201.	-261.	-13.	201.	-261.	1
120	0.7466	1.4748	-0.6836	0.7405	0.8194	1	40.	166.	-235.	40.	166.	-235.	1
121	1.3782	1.2182	-1.1199	0.8655	1.1022	1	134.	107.	-387.	134.	107.	-387.	1
122	1.5535	1.0533	-1.5177	0.8690	1.3982	1	164.	78.	-524.	164.	78.	-524.	1
123	1.2449	0.8871	-1.4702	0.7106	1.3095	1	130.	68.	-507.	130.	68.	-507.	1
124	0.9592	0.8228	-1.1067	0.5940	0.9980	1	94.	71.	-382.	94.	71.	-382.	1
125	0.5650	0.5753	-0.4417	0.3801	0.4498	1	52.	54.	-152.	52.	54.	-152.	1
126	0.7048	1.1607	-0.9267	0.6218	0.8947	1	47.	126.	-320.	47.	126.	-320.	1
127	1.3449	1.2506	-1.2115	0.8652	1.1637	1	129.	112.	-418.	129.	112.	-418.	1
128	2.2579	1.1082	-1.7982	1.1220	1.7336	1	255.	57.	-621.	255.	57.	-621.	1
129	2.6005	1.0110	-2.3012	1.2038	2.1624	1	305.	30.	-794.	305.	30.	-794.	1
130	2.4171	0.9056	-2.3178	1.1076	2.1391	1	285.	24.	-800.	285.	24.	-800.	1
131	1.7025	0.9653	-1.7585	0.8893	1.5961	1	187.	60.	-607.	187.	60.	-607.	1
132	1.5523	0.7603	-0.5898	0.7709	0.7960	1	176.	39.	-204.	176.	39.	-204.	1
133	0.7217	0.9059	-0.8583	0.5425	0.8024	1	60.	91.	-296.	60.	91.	-296.	1
134	1.5387	0.9627	-1.3421	0.8338	1.2664	1	166.	66.	-463.	166.	66.	-463.	1
135	2.6154	1.1431	-1.9620	1.2528	1.9268	1	301.	47.	-677.	301.	47.	-677.	1
136	3.1682	0.9776	-2.5333	1.3819	2.4562	1	391.	3.	-874.	381.	3.	-874.	1
137	3.1338	0.8349	-2.5172	1.3229	2.4454	1	382.	-14.	-869.	382.	-14.	-869.	1
138	2.7757	0.6476	-1.8616	1.1411	1.9277	1	342.	-25.	-643.	342.	-25.	-643.	1
139	2.5693	0.5607	-0.6846	1.0433	1.2366	1	318.	-28.	-236.	318.	-28.	-236.	1
140	0.1436	1.7179	0.3167	0.6205	0.8201	1	-50.	222.	109.	-50.	222.	109.	1
141	0.3311	2.1524	1.0601	0.8279	1.2825	1	-42.	272.	366.	-42.	272.	366.	1
142	2.3670	0.6250	-1.6983	0.9973	1.7105	1	289.	-12.	-586.	289.	-12.	-586.	1
143	2.7654	0.3342	-1.7251	1.0332	1.8716	1	354.	-66.	-595.	354.	-66.	-595.	1
144	2.9042	0.0912	-1.3122	0.9985	1.7219	1	382.	-104.	-453.	382.	-104.	-453.	1
145	2.9658	-0.0919	-0.4804	0.9580	1.4734	1	397.	-131.	-166.	397.	-131.	-166.	1
146	0.0312	0.8083	0.0781	0.2798	0.3793	1	-28.	106.	27.	-28.	106.	27.	1
147	0.1981	1.1145	0.5773	0.4375	0.6766	1	-18.	140.	199.	-18.	140.	199.	1
148	1.4351	0.3277	-0.9957	0.5876	1.0188	1	177.	-14.	-344.	177.	-14.	-344.	1
149	2.0562	0.0433	-1.2362	0.6598	1.3925	1	271.	-76.	-427.	271.	-76.	-427.	1
150	2.5873	-0.3912	-0.9471	0.7320	1.5312	1	359.	-155.	-327.	359.	-155.	-327.	1

TABLE C-7. FINITE-ELEMENT ANALYSIS OF ELEMENT SPECIMEN (continued)

STRESS ELEM	XX	YY	XY	ON	OS	CASE	(TOTAL STRAIN)*1000000. XX	YY	XY	(MECH. STRAIN)*1000000. XX	YY	XY	CASE
151	2.8676	-0.6863	-0.3663	0.7271	1.5680	1	408.	-206.	-126.	408.	-206.	-126.	1
152	-7.9463	18.7394	-0.0298	3.5977	11.1875	1	-479.	733.	-3.	-479.	733.	-3.	1
153	-8.1121	17.8780	-0.1132	3.2553	10.8576	1	-476.	705.	-10.	-476.	705.	-10.	1
154	-8.4907	18.3761	0.4364	3.2952	11.2187	1	-494.	727.	40.	-494.	727.	40.	1
155	-9.3757	17.3855	0.3713	2.6699	11.0913	1	-514.	702.	34.	-514.	702.	34.	1
156	-8.4623	18.8931	0.2664	3.4769	11.4373	1	-499.	744.	24.	-499.	744.	24.	1
157	-5.5641	21.5244	0.8271	5.3201	11.7007	1	-428.	803.	75.	-428.	803.	75.	1
158	-0.8251	24.1478	0.6775	7.7742	11.5960	1	-293.	842.	62.	-293.	842.	62.	1
159	1.0673	24.3711	-0.4336	8.4795	11.2511	1	-230.	829.	-39.	-230.	829.	-39.	1
160	0.9139	23.0145	0.0243	7.9761	10.6403	1	-221.	784.	2.	-221.	784.	2.	1
161	0.6995	16.8862	-0.5731	5.8619	7.8146	1	-161.	575.	-52.	-161.	575.	-52.	1
162	0.3888	9.3414	-1.1126	3.2434	4.4095	1	-89.	318.	-101.	-89.	318.	-101.	1
163	-0.0566	1.6073	-0.8405	0.5169	1.0325	1	-20.	56.	-76.	-20.	56.	-76.	1
164	-0.2512	-2.7723	-0.3039	-1.0078	1.2763	1	22.	-93.	-28.	22.	-93.	-28.	1
165	-6.2986	18.9626	-0.2080	4.2213	10.7375	1	-425.	723.	-19.	-425.	723.	-19.	1
166	-6.2169	17.9454	-0.0832	3.9095	10.2445	1	-411.	687.	-8.	-411.	687.	-8.	1
167	-6.3674	18.2273	0.0975	3.7866	10.5893	1	-437.	704.	9.	-437.	704.	9.	1
168	-7.4623	15.1845	0.3680	2.5741	9.4277	1	-424.	605.	33.	-424.	605.	33.	1
169	-6.4568	17.7645	1.2370	3.7692	10.2909	1	-417.	683.	112.	-417.	683.	112.	1
170	-3.7917	19.4198	1.3378	5.2094	10.2253	1	-344.	711.	122.	-344.	711.	122.	1
171	0.0110	19.7567	0.7949	6.5892	9.3334	1	-216.	681.	72.	-216.	681.	72.	1
172	2.1217	19.8060	-0.5564	7.3092	8.8905	1	-144.	660.	-51.	-144.	660.	-51.	1
173	1.8781	14.1985	-0.9099	6.6922	8.2059	1	-135.	607.	-83.	-135.	607.	-83.	1
174	1.5072	14.4155	-1.8008	5.3076	6.6346	1	-106.	481.	-164.	-106.	481.	-164.	1
175	0.8545	8.2181	-2.3614	3.0242	4.1626	1	-61.	274.	-215.	-61.	274.	-215.	1
176	0.3217	2.1723	-1.8217	0.8313	1.7688	1	-13.	71.	-166.	-13.	71.	-166.	1
177	-0.0710	-1.0003	-0.6276	-0.3571	0.6858	1	9.	-34.	-57.	9.	-34.	-57.	1
178	-2.0392	20.2887	-0.2217	6.0832	10.0809	1	-293.	722.	-20.	-293.	722.	-20.	1
179	-2.3510	20.2001	-0.8737	5.9497	10.1472	1	-303.	722.	-79.	-303.	722.	-79.	1
180	-1.2141	17.2780	-1.3806	5.3546	8.5205	1	-231.	609.	-125.	-231.	609.	-125.	1
181	-3.1957	13.2209	-0.5892	3.3417	7.1227	1	-255.	491.	-54.	-255.	491.	-54.	1
182	-1.9475	13.5450	-0.1977	3.8658	6.8921	1	-216.	488.	-18.	-216.	488.	-18.	1
183	-0.3431	13.6583	0.2564	4.4384	6.5243	1	-162.	475.	23.	-162.	475.	23.	1
184	1.2438	13.2651	0.0125	4.8363	5.9817	1	-103.	444.	1.	-103.	444.	1.	1
185	2.7598	13.1205	-1.7001	5.2934	5.8161	1	-49.	422.	-155.	-49.	422.	-155.	1
186	3.0313	12.1468	-2.0964	5.0594	5.4385	1	-29.	386.	-191.	-29.	386.	-191.	1
187	2.2464	10.5901	-3.3010	4.2788	5.2935	1	-39.	341.	-300.	-39.	341.	-300.	1
188	0.9225	6.5716	-2.9942	2.4580	3.7968	1	-40.	216.	-272.	-40.	216.	-272.	1
189	0.5908	2.4592	-1.5974	1.0167	1.6732	1	-7.	78.	-145.	-7.	78.	-145.	1
190	2.9229	13.9250	-4.2639	5.6160	6.9328	1	-52.	448.	-388.	-52.	448.	-388.	1
191	-1.0864	6.7793	-2.8276	1.8976	4.1764	1	-112.	246.	-257.	-112.	246.	-257.	1
192	0.4146	9.6049	-1.1391	3.3398	4.5298	1	-91.	327.	-104.	-91.	327.	-104.	1
193	1.0011	8.5210	-2.7197	3.1740	4.4038	1	-59.	283.	-247.	-59.	283.	-247.	1
194	2.8944	6.6671	-2.0135	3.1872	3.1866	1	27.	198.	-183.	27.	198.	-183.	1
195	1.4489	8.9075	-0.8552	3.4521	3.9646	1	-48.	291.	-78.	-48.	291.	-78.	1
196	2.9426	8.1020	-4.3701	3.6815	4.8934	1	13.	247.	-397.	13.	247.	-397.	1
197	5.9114	6.0596	-3.4582	3.9903	3.9922	1	137.	144.	-314.	137.	144.	-314.	1
198	2.7633	7.7810	-2.3571	3.5148	3.7519	1	10.	238.	-214.	10.	238.	-214.	1
199	4.1070	5.9779	-4.5569	3.3616	4.4808	1	76.	161.	-414.	76.	161.	-414.	1
200	3.3790	4.5758	-4.3895	2.6516	4.0742	1	66.	121.	-399.	66.	121.	-399.	1

TABLE C-7. FINITE-ELEMENT ANALYSIS OF ELEMENT SPECIMEN (continued)

STRESS ELEM	XX	YY	XY	ON	OS	CASE	(TOTAL STRAIN)*1000000. XX	YY	XY	(MECH. STRAIN)*1000000. XX	YY	XY	CASE
201	2.0540	2.3266	-3.1282	1.4602	2.7572	1	45.	58.	-284.	45.	58.	-284.	1
202	0.6976	1.0315	-1.0584	0.5763	0.9651	1	13.	28.	-96.	13.	28.	-96.	1
203	1.6551	6.3554	-2.8733	2.6702	3.5709	1	-13.	201.	-261.	-13.	201.	-261.	1
204	2.9975	5.7632	-2.5849	2.9202	3.1612	1	40.	166.	-235.	40.	166.	-235.	1
205	5.4237	4.8160	-4.2530	3.4132	4.2362	1	134.	107.	-387.	134.	107.	-387.	1
206	6.0901	4.1908	-5.7637	3.4270	5.3498	1	164.	78.	-524.	164.	78.	-524.	1
207	4.8832	3.5246	-5.5831	2.8026	5.0016	1	130.	68.	-507.	130.	68.	-507.	1
208	3.7728	3.2549	-4.2027	2.3426	3.8162	1	94.	71.	-382.	94.	71.	-382.	1
209	2.2289	2.2683	-1.6774	1.4991	1.7320	1	52.	54.	-152.	52.	54.	-152.	1
210	2.8129	4.5440	-3.5193	2.4523	3.4298	1	47.	126.	-320.	47.	126.	-320.	1
211	5.2973	4.9393	-4.6007	3.4122	4.4670	1	129.	112.	-418.	129.	112.	-418.	1
212	8.8207	4.4547	-6.8288	4.4251	6.6375	1	255.	57.	-621.	255.	57.	-621.	1
213	10.1393	4.1036	-8.7390	4.7476	8.2616	1	305.	30.	-794.	305.	30.	-794.	1
214	9.4216	3.6823	-8.8023	4.3680	8.1660	1	285.	24.	-800.	285.	24.	-800.	1
215	6.6603	3.8608	-6.6779	3.5070	6.0980	1	187.	60.	-607.	187.	60.	-607.	1
216	6.0638	3.0563	-2.2397	3.0400	3.0778	1	176.	39.	-204.	176.	39.	-204.	1
217	-0.0786	0.3228	-0.1146	0.0814	0.1973	1	-23.	46.	-40.	-23.	46.	-40.	1
218	0.1320	0.4808	0.3989	0.2042	0.3837	1	-2.	59.	138.	-2.	59.	138.	1
219	0.9987	0.3464	-0.6129	0.4484	0.6495	1	119.	6.	-212.	119.	6.	-212.	1
220	1.6305	0.0251	-1.1477	0.5519	1.2083	1	215.	-62.	-396.	215.	-62.	-396.	1
221	2.2825	-0.5312	-0.8706	0.5838	1.4125	1	324.	-162.	-301.	324.	-162.	-301.	1
222	2.6445	-0.9968	-0.4150	0.5492	1.5734	1	391.	-238.	-143.	391.	-238.	-143.	1
223	3.5607	0.5866	-0.2028	1.3824	1.5675	1	449.	-64.	-70.	449.	-64.	-70.	1
224	0.9267	1.2507	0.7416	0.7258	0.8047	1	73.	129.	256.	73.	129.	256.	1
225	1.1675	0.9678	0.5110	0.7118	0.6588	1	116.	82.	176.	116.	82.	176.	1
226	1.1564	-0.4492	0.3269	0.2358	0.7271	1	171.	-106.	113.	171.	-106.	113.	1
227	0.4064	-0.7065	0.2751	-0.1001	0.5118	1	82.	-110.	95.	82.	-110.	95.	1
228	1.0108	-0.3726	-0.0103	0.2127	0.5845	1	149.	-90.	-4.	149.	-90.	-4.	1
229	1.3027	0.3558	0.4843	0.5528	0.6772	1	159.	-5.	167.	159.	-5.	167.	1
230	-0.0828	-0.2104	0.0585	-0.0977	0.1181	1	-3.	-25.	34.	-3.	-25.	34.	1
231	-0.2265	-0.2295	-0.0614	-0.1520	0.1186	1	-21.	-21.	-21.	-21.	-21.	-21.	1
232	0.4662	0.2673	0.4355	0.2445	0.4036	1	51.	17.	150.	51.	17.	150.	1
233	1.0499	0.4154	0.3529	0.4884	0.5190	1	123.	13.	122.	123.	13.	122.	1
234	0.2818	-0.2180	0.0842	0.0213	0.2158	1	46.	-40.	29.	46.	-40.	29.	1
235	0.7574	0.0128	0.0556	0.2567	0.3570	1	100.	-29.	19.	100.	-29.	19.	1
236	1.0691	-0.7922	0.2675	0.0923	0.7933	1	173.	-148.	92.	173.	-148.	92.	1
237	1.8947	-0.3285	0.1868	0.5221	0.9916	1	264.	-119.	64.	264.	-119.	64.	1
238	2.6467	-0.5770	0.3755	0.6899	1.4367	1	374.	-182.	130.	374.	-182.	130.	1
239	3.4310	-0.6650	0.1503	0.9220	1.7989	1	482.	-225.	52.	482.	-225.	52.	1

TABLE C-7. FINITE-ELEMENT ANALYSIS OF ELEMENT SPECIMEN (continued)

X FORCE, CASE 1

	1	2	3	4	5	6	7	8	9	10
1	3.884E 00	2.079E 00	-2.441E-04	-4.883E-04	-4.883E-04	0.0	-6.104E-05	-3.052E-05	-3.433E-05	4.578E-05
11	0.0	4.883E-04	4.883E-04	4.883E-04	2.113E 00	1.130E-01	-7.629E-05	-4.578E-04	-4.120E-04	-6.199E-05
21	-3.529E-05	-4.578E-05	3.052E-05	4.578E-05	6.104E-05	1.007E-03	1.099E-03	2.289E-05	5.763E-02	1.409E-01
31	1.984E-04	-2.441E-04	1.373E-04	3.662E-04	4.883E-04	1.526E-05	1.408E-05	-8.153E-05	-7.208E-04	-5.324E-04
41	-4.399E-04	-1.552E-03	1.187E-01	4.373E-02	1.678E-04	4.883E-04	6.409E-04	0.0	1.526E-05	2.098E-05
51	-1.335E-05	-3.052E-05	-3.662E-04	-1.068E-03	-7.782E-04	-3.357E-04	6.630E-02	-3.003E-01	-4.578E-05	-6.104E-05
61	1.259E-04	-4.244E-05	-4.101E-05	2.861E-06	3.052E-05	4.578E-05	6.104E-05	4.578E-05	-1.907E-06	3.147E-05
71	2.574E-01	-1.571E 00	0.0	4.883E-04	-2.670E-05	9.537E-06	7.629E-06	-7.629E-06	1.240E-05	-2.098E-05
81	0.0	7.343E-05	2.575E-05	-9.537E-07	1.972E-01	-5.187E 00	-3.624E-05	-3.815E-06	8.583E-06	2.670E-05
91	1.144E-05	2.193E-05	1.621E-05	-2.575E-05	-4.578E-05	-4.578E-05	-6.104E-05	1.240E-05	1.967E-02	-3.548E 00
101	4.292E-05	4.578E-05	9.537E-06	1.049E-05	-2.098E-05	0.0	0.0	0.0	1.431E-05	4.292E-05
111	-6.676E-06	9.537E-07	-1.335E-05	-4.673E-05	-2.384E-05	-2.003E-05	1.037E-05	-1.907E-05	-1.986E-01	2.861E-05
121	1.335E-05	-4.196E-05	7.629E-06	-4.292E-05	-4.554E-05	-4.768E-06	-2.465E-01	0.0	-9.537E-07	-1.907E-06
131	-2.147E-05	-3.099E-05	-3.630E-05	-1.907E-06	-1.898E-01	3.576E-06	-3.040E-06	1.788E-07	3.755E-06	2.861E-06
141	-9.537E-07	-1.018E-01	-2.272E-07	2.384E-07	-4.590E-06	-5.066E-06	-2.503E-06	1.907E-06	5.537E-01	-2.384E-07
151	1.907E-06	-7.153E-07	-1.371E-06	-2.623E-06	2.384E-06	7.339E-01	-2.384E-07	-1.311E-06	0.0	-9.537E-07
161	-9.537E-07	-1.907E-06	-6.125E-02	-9.537E-07	9.537E-07	0.0	8.345E-07	1.431E-05	0.0	0.0
171	-2.921E-06	0.0	1.717E-05	-9.537E-07	-5.341E-05	2.861E-05	8.583E-06	-1.335E-05	9.537E-07	9.537E-07
181	1.025E 00									

Y FORCE, CASE 1

	1	2	3	4	5	6	7	8	9	10
1	1.000E 01	0.0	-4.883E-04	-4.883E-04	-2.441E-04	3.052E-05	5.341E-04	-1.678E-04	2.441E-04	2.594E-04
11	-1.068E-04	-4.883E-04	-2.441E-04	-4.883E-04	0.0	-5.798E-04	-5.646E-04	-8.850E-04	-5.341E-04	-6.714E-04
21	-2.899E-04	-1.678E-04	-3.052E-05	-2.441E-04	-9.918E-04	-7.172E-04	-7.935E-04	-4.425E-04	-2.441E-04	0.0
31	4.883E-04	4.883E-04	9.308E-04	1.526E-05	-7.629E-05	-4.940E-04	-6.104E-05	1.123E-04	5.569E-04	8.779E-04
41	5.418E-04	8.334E-04	5.784E-04	-6.104E-05	5.951E-04	8.392E-04	6.409E-04	3.815E-04	2.441E-04	3.052E-05
51	7.629E-05	4.578E-05	3.357E-04	5.798E-04	5.951E-04	5.035E-04	2.441E-04	-1.221E-04	0.0	1.831E-04
61	-6.409E-04	-4.578E-05	-6.104E-05	-1.526E-05	-3.052E-05	-4.578E-05	-1.526E-05	-3.662E-04	-6.104E-04	-5.798E-04
71	-1.526E-05	1.984E-04	3.967E-04	3.967E-04	3.023E-04	8.488E-05	6.676E-05	4.482E-05	4.578E-05	4.578E-05
81	1.526E-05	4.272E-04	4.120E-04	5.798E-04	3.052E-05	-3.052E-05	3.471E-04	6.666E-04	-1.459E-04	-4.578E-05
91	4.578E-05	-1.526E-05	7.629E-05	1.526E-05	6.104E-05	1.068E-04	-2.441E-04	4.578E-05	1.526E-05	1.526E-05
101	9.537E-07	3.719E-05	2.956E-05	2.384E-05	7.629E-05	-1.526E-05	0.0	1.526E-05	-1.526E-05	-7.629E-05
111	8.850E-04	4.768E-06	2.098E-05	7.629E-05	1.221E-04	4.578E-05	7.629E-05	3.052E-05	3.052E-05	1.431E-05
121	2.861E-05	9.537E-07	-2.098E-05	3.815E-05	4.387E-05	3.147E-05	0.0	-2.480E-05	1.907E-06	3.910E-05
131	3.338E-05	2.003E-05	2.289E-05	-5.722E-06	2.861E-05	3.815E-06	-9.537E-07	2.766E-05	3.433E-05	2.384E-05
141	2.098E-05	1.907E-06	0.0	-4.768E-06	5.722E-06	-2.861E-06	1.907E-06	9.537E-07	3.397E-06	-3.338E-06
151	-1.907E-06	3.815E-06	9.537E-07	9.537E-07	1.907E-06	9.537E-07	-9.723E-07	2.861E-06	0.0	5.364E-07
161	9.537E-07	0.0	2.980E-07	1.907E-06	-2.861E-06	1.907E-06	0.0	0.0	-8.101E-01	0.0
171	2.027E-06	-9.537E-07	-7.056E-02	0.0	1.907E-06	-1.095E 00	9.537E-07	-1.096E 00	-2.886E 00	-2.609E 00
181	-1.455E 00									

CHECKS, SUM		X-FORCES	Y-FORCES	Z-MOMENTS	CASE
		1.381D-04	-1.771D-02	-1.728D-02	1
NZE	BARK	2896			
	*RMS	2897			
	REDU	2607			

which is described in a following section of this appendix. The input load to that analysis is a load-per-unit width determined from this element specimen analysis.

Extrapolation Formulas for Boundary Stresses

Figure C-15 shows the local geometry of the modes and the element centers for a section through the lug. The extrapolation formulas determine the stresses at the boundaries from the computer-calculated stresses at nearby elements (1st, 2nd, and 3rd).

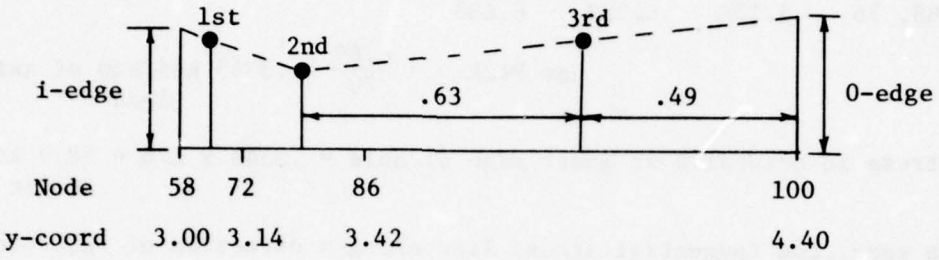


Figure C-15. Local geometry at lug.

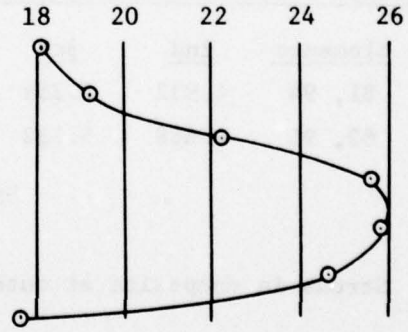
linear extrapolation to edge of hole: $\sigma_{i\text{-edge}} = \sigma_{1st} + (\sigma_{1st} - \sigma_{2nd})/3$

linear extrapolation to outer edge: $\sigma_{0\text{-edge}} = \sigma_{3rd} + (\sigma_{3rd} - \sigma_{2nd}) \frac{.49}{.63}$

Steel Tangential Stress at Inner Edge of Hole

Figure C-16 shows a plot of steel stresses from the data in Table C-7.

Elements	2nd	1st	i-edge
168, 155	15.184	17.385	18.119
169, 156	17.765	18.893	19.269
170, 157	19.420	21.524	22.225
171, 158	19.757	24.148	25.612
172, 159	19.806	24.371	25.893
173, 160	18.199	23.014	24.619
174, 161	14.416	16.886	17.709



Use Peak $\sigma = \frac{26}{20} = 1.30$ ksi/kip of axial load

Figure C-16. Tangential stress at inner edge of hole for element specimen.

Scaled load from static test = 4 x 44 = 176 kips

Stress in metal at inner edge of hole = 1.3 x 176 = 229 ksi in static test

Composite Tangential Stress at Inner Edge of Hole

Elements	2nd	1st	i-edge
86, 73	5.037	5.590	5.774
87, 74	5.106	6.245	6.625
88, 75	5.108	6.293	6.688

Use Peak $\sigma = \frac{6.69}{20} = .3345$ ksi/kip of axial load

Stress in composite at inner edge of hole = .3345 x 176 = 58.9 ksi in static test

In this case, the tangential stress lies along a direction of reinforcement.

Steel Tangential Stress at Outer Edge of Lug (Point A in Figure 17)

Elements	2nd	3rd	0-edge
165, 178	18.963	20.289	21.320
166, 179	17.945	20.200	21.954

Use Peak $\sigma = \frac{22}{20} = 1.1$ ksi/kip of axial load

Stress in metal at outer edge = 1.1 x 176 = 194 ksi in static test

Composite Stress at Outer Edge of Lug (Point A in Figure 17)

Elements	2nd	3rd	0-edge
81, 94	4.932	5.254	5.504
82, 95	4.668	5.232	5.670

Use Peak $\sigma = \frac{5.67}{20} = .2835$ ksi/kip of axial load

Stress in composite at outer edge = .2835 x 176 = 49.9 ksi in static test

In this case, the tangential stress is skewed at an angle of - 27 degrees relative to the 0-degree direction of reinforcement. In order to interpret this stress in terms of properties already calculated and shown in Figure 6,

it is necessary to transform the stress. Figure C-17 shows the relationship of the material property axes (x, y) to the local element axes (X, Y) used in the output from the finite-element program.

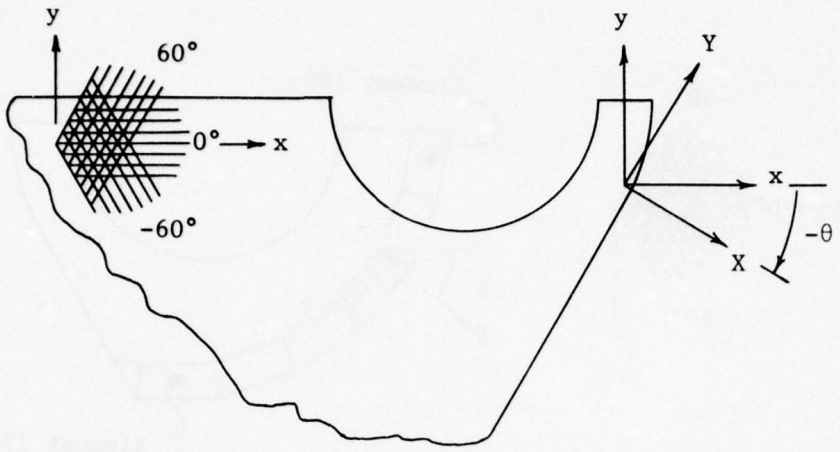


Figure C-17. Relationship of axes for material properties to the local finite-element axes at point of calculation of stresses at outer edge of lug.

The transformation equation is:

$$\begin{bmatrix} \sigma_{xx} \\ \sigma_{yy} \\ \tau_{xy} \end{bmatrix} = \begin{bmatrix} \cos^2\theta & \sin^2\theta & 2\sin\theta\cos\theta \\ \sin^2\theta & \cos^2\theta & -2\sin\theta\cos\theta \\ -\sin\theta\cos\theta & \sin\theta\cos\theta & (\cos^2\theta - \sin^2\theta) \end{bmatrix} \begin{bmatrix} \sigma_{XX} \\ \sigma_{YY} \\ \tau_{XY} \end{bmatrix}$$

For

$\sigma_{XX} = 0$ then, $\sigma_{xx} = 10.3$ ksi

$\sigma_{YY} = 49.9$ ksi $\sigma_{yy} = 39.6$ ksi

$\tau_{XY} = 0$ $\tau_{xy} = -20.2$ ksi

$\theta = -27°$

Stresses in Composite Around Edge of Largest Steel Lamina

Figure C-18 shows the position of the local axes (X, Y) for the elements and the composite material axes (x, y). Table C-8 shows the stress in each composite element (elements 134 - 139) around the perimeter in the local axes and in the material axes. The local axes stress were taken directly from the computer output. The corresponding stresses relative to the material axes for the static test load were found by multiplying the output

stresses by the ratio of scaled loads (176/20 = 8.8) and applying the axis transformation equation. The most critical stresses combination occurred in element 137.

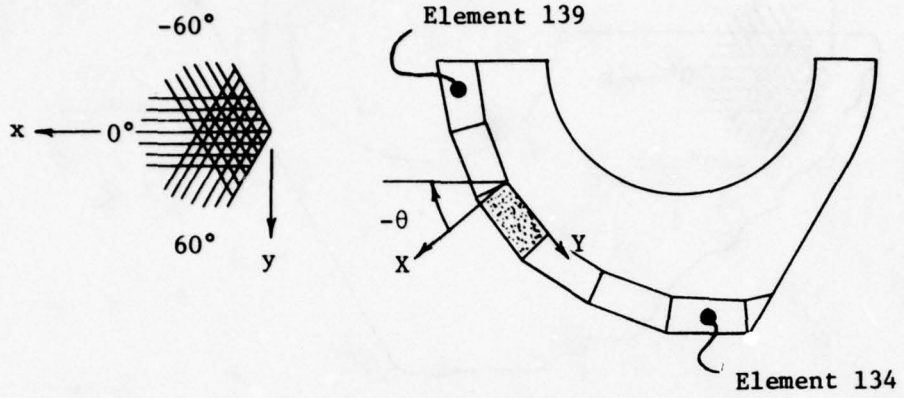


Figure C-18. Relationship of axes for material properties to the local finite-element axes for the composite elements around the edge of the largest steel lamina.

TABLE C-8. STRESSES IN COMPOSITE AROUND THE EDGE OF THE LARGEST STEEL LAMINA

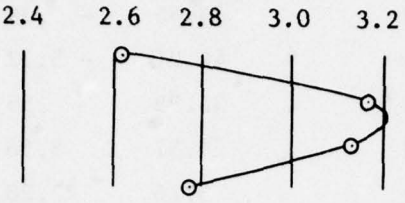
Element	θ	Stresses in Element Axes For P = 20 kips			Stresses in Material Axes For P = 176 kips*		
		XX	YY	XY	xx	yy	xy
134	- 7.5	1.54	.96	- 1.34	16.52	5.50	- 10.75
135	- 23.0	2.62	1.14	- 1.96	33.46	- .39	- 7.33
136	- 38.0	3.17	.98	- 2.53	42.21	- 5.72	3.96
137	- 54.0	3.13	.83	- 2.52	35.95	.55	17.21
138	- 60.0	2.78	.65	- 1.86	24.57	5.56	16.30
139	- 88.5	2.57	.56	- .68	5.26	22.28	6.48

*Corresponds to highest load in static test, 4 x 44 = 176

Adhesive and Steel Tip Stresses

Figure C-19 shows the maximum radial force per inch at the perimeter of the reinforced area.

Element	σ_{xx}
135	2.615
136	3.168
137	3.134
138	2.776



$$\text{Use Peak Load Intensity} = \frac{\sigma t}{P} = \frac{3.21 \times .342}{20} = .05489 \text{ kip/inch per kip of axial load}$$

Figure C-19. Radial forces at perimeter of reinforced area for element specimen.

In the next section, a finite-element analysis of a unit width will establish the following relationships:

maximum bond stress = .20797 x load/inch ksi

maximum stress in tip of steel lamina = 6.369 x load/inch ksi

Using these factors and scaling to the loads of the static test, the stresses become:

maximum bond stress = .20797 x .05489 x 176 = 2.009 ksi

maximum steel stress at tip = 6.369 x .05489 x 176 = 61.53 ksi

Interpretation of Criticality of Composite Stresses

Figure C-20 lists and relates the stresses experienced by the composite during the static test to the calculated ultimate strength. The arrows connect the state of stress in the test to the corresponding failure point if the loads were increased proportionately. The ratio of the length of the arrow to that of the ray from the origin to the tail of the arrow corresponds to the margin of safety, as described on page 91. The negative values of k can be plotted as positive quantities in Figure C-20 because Figure C-1 shows that the strength is the same for positive or negative shears. Figure C-20 and Table C-9 show that the observed lack of distress in the composite is consistent with the predicted strength boundaries.

LOCATION	σ_{xx}	σ_{yy}	τ_{xy}	k	M.S.
Inner edge of hole	58.9	0.0	0.0	0.0	+ .24
Point A in Figure 17	10.3	39.6	- 20.2	.49	+ .35
Element 134	16.52	5.50	- 10.75	- .62	+ 1.10
Element 135	33.46	- .39	- 7.33	- .22	+ .59
Element 136	42.21	- 5.72	3.96	.09	+ .50
Element 137	35.95	.55	17.21	.48	+ .13
Element 138	24.57	5.56	16.30	.65	+ .40
Element 139	5.26	22.28	6.48	.28	+ 1.38

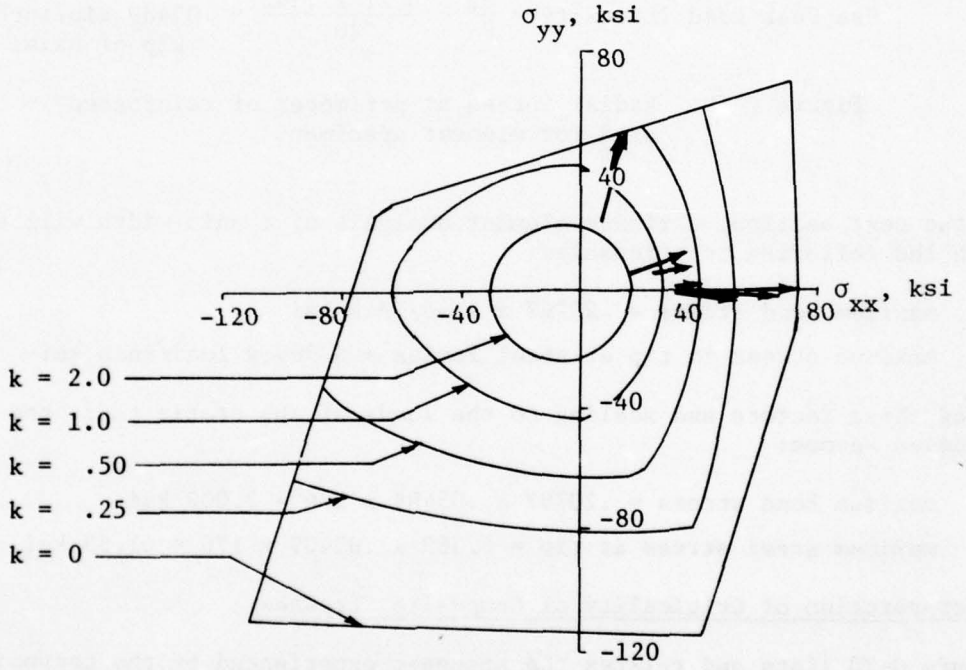


Figure C-20. Composite stresses during static ultimate test of the element specimen.

Table C-9 presents further information about the nature of the margins of safety by identifying the stresses, strains, and margins of safety for each lamina. These data show that in all cases the minimum margin of safety corresponds to a transverse tensile strain (22-strain). Such a mode of failure provides a conservative estimate of strength because typically it does not correspond to rupture of the laminate, but rather to a slope change in the load-deformation relationship. The margin of safety against rupture of the laminate is better indicated by the margin of safety along

TABLE C-9. STRESSES AND MARGINS OF SAFETY IN COMPOSITE AT LOCATIONS OF HIGH STRESS AT THE ULTIMATE LOAD IN THE STATIC TEST OF THE ELEMENT SPECIMEN

T300/5209 ULTIMATE U/U/U .3333/.3333/.3333 60/0/-60 PROG...CMAB

MAT.	ALLOWABLE STRESS, UNIAXIAL 11	11	22	22	12	12	MODULI E11	E22	G	NU12
25	-200.0	196.0	-34.0	9.00	-16.40	16.40	19400.	1380.	750.	0.250

LAMINA	1	2	3
MATERIAL	25	25	25
THICKNESS	0.3333	0.3333	0.3333
ANGLE	60.	0.	-60.

LAMINATE PROPERTIES	EX	EY	G
K'S UNRESTRAINED	7497.	3094.	1131.
K'S = 0	7539.	7539.	2897.

BEHAVIOR FOR NX= 58.900 NY= 0.0 NXY= 0.0 KX= 0.0 KY= 0.0 KXY= 0.0

LAM. NO.	STRESSES X	Y	XY	11	22	12	STRAINS 11	22	12	M.S. 11	22	12	MIN.
3	12.6	0.3	-2.5	5.5	7.4	6.6	0.000190	0.005273	0.008803	52.26	0.24	1.48	0.24
3	12.6	0.3	-2.5	5.5	7.4	6.6	0.000190	0.005273	0.008803	52.26	0.24	1.48	0.24
2	151.5	-0.6	0.0	151.5	-0.6	0.0	0.007814	-0.002351	0.0	0.29	9.48	99.00	0.29
2	151.5	-0.6	0.0	151.5	-0.6	0.0	0.007814	-0.002351	0.0	0.29	9.48	99.00	0.29
1	12.6	0.3	2.5	5.5	7.4	-6.6	0.000190	0.005273	-0.008803	52.26	0.24	1.48	0.24
1	12.6	0.3	2.5	5.5	7.4	-6.6	0.000190	0.005273	-0.008803	52.26	0.24	1.48	0.24
ALL	53.9	0.0	0.0				0.007814	-0.002351	0.0				0.24

BEHAVIOR FOR NX= 10.300 NY= 39.600 NXY=-20.200 KX= 0.0 KY= 0.0 KXY= 0.0

LAM. NO.	STRESSES X	Y	XY	11	22	12	STRAINS 11	22	12	M.S. 11	22	12	MIN.
3	31.1	96.4	-55.2	127.9	-0.4	-0.7	0.006597	-0.001969	-0.000892	0.53	11.51	23.51	0.53
3	31.1	96.4	-55.2	127.9	-0.4	-0.7	0.006597	-0.001969	-0.000892	0.53	11.51	23.51	0.53
2	-2.5	6.6	-5.2	-2.5	6.6	-5.2	-0.000214	0.004842	-0.006972	47.12	0.35	2.14	0.35
2	-2.5	6.6	-5.2	-2.5	6.6	-5.2	-0.000214	0.004842	-0.006972	47.12	0.35	2.14	0.35
1	2.3	15.8	-0.1	12.3	5.8	5.9	0.000560	0.004069	0.007866	17.05	0.60	1.78	0.60
1	2.3	15.8	-0.1	12.3	5.8	5.9	0.000560	0.004069	0.007866	17.05	0.60	1.78	0.60
ALL	10.3	39.6	-20.2				-0.000214	0.004842	-0.006972				0.35

TABLE C-9. STRESSES AND MARGINS OF SAFETY IN COMPOSITE AT LOCATIONS OF HIGH STRESS AT THE ULTIMATE LOAD IN THE STATIC TEST OF THE ELEMENT SPECIMEN (continued)

BEHAVIOR FOR NX= 16.520 NY= 5.500 NXY=-10.750 KX= 0.0 KY= 0.0 KXY= 0.0

LAM. NO.	STRESSES X	Y	XY	11	22	12	STRAINS 11	22	12	M.S. 11	22	12	MIN.
3	13.2	29.3	-19.2	41.9	0.6	2.6	0.002152	-0.000110	0.003503	3.69	99.00	5.24	3.69
3	13.2	29.3	-19.2	41.9	0.6	2.6	0.002152	-0.000110	0.003503	3.69	99.00	5.24	3.69
2	38.5	0.8	-2.8	38.5	0.8	-2.8	0.001972	0.000070	-0.003711	4.12	91.86	4.89	4.12
2	38.5	0.8	-2.8	38.5	0.8	-2.8	0.001972	0.000070	-0.003711	4.12	91.86	4.89	4.12
1	-2.1	-13.6	-10.3	-19.6	3.9	0.2	-0.001061	0.003103	0.000209	8.72	1.10	99.00	1.10
1	-2.1	-13.6	-10.3	-19.6	3.9	0.2	-0.001061	0.003103	0.000209	8.72	1.10	99.00	1.10
ALL	16.5	5.5	-10.3				0.001972	0.000070	-0.003711				1.10

BEHAVIOR FOR NX= 33.460 NY= -0.390 NXY= -7.330 KX= 0.0 KY= 0.0 KXY= 0.0

LAM. NO.	STRESSES X	Y	XY	11	22	12	STRAINS 11	22	12	M.S. 11	22	12	MIN.
3	12.2	14.2	-11.2	23.4	3.0	4.7	0.001168	0.001899	0.006324	7.65	2.43	2.46	2.43
3	12.2	14.2	-11.2	23.4	3.0	4.7	0.001168	0.001899	0.006324	7.65	2.43	2.46	2.43
2	86.3	-0.4	-1.9	86.3	-0.4	-1.9	0.004455	-0.001387	-0.002530	1.27	16.76	7.64	1.27
2	86.3	-0.4	-1.9	86.3	-0.4	-1.9	0.004455	-0.001387	-0.002530	1.27	16.76	7.64	1.27
1	1.8	-15.0	-8.9	-18.5	5.3	-2.8	-0.001023	0.004090	-0.003794	9.08	0.59	4.76	0.59
1	1.8	-15.0	-8.9	-18.5	5.3	-2.8	-0.001023	0.004090	-0.003794	9.08	0.59	4.76	0.59
ALL	33.5	-0.4	-7.3				0.004455	-0.001387	-0.002530				0.59

BEHAVIOR FOR NX= 42.210 NY= -5.720 NXY= 3.960 KX= 0.0 KY= 0.0 KXY= 0.0

LAM. NO.	STRESSES X	Y	XY	11	22	12	STRAINS 11	22	12	M.S. 11	22	12	MIN.
3	4.1	-15.8	7.5	-17.3	5.7	4.9	-0.000968	0.004352	0.006480	9.65	0.50	2.37	0.50
3	4.1	-15.8	7.5	-17.3	5.7	4.9	-0.000968	0.004352	0.006480	9.65	0.50	2.37	0.50
2	112.7	-1.4	1.0	112.7	-1.4	1.0	0.005828	-0.002444	0.001367	0.73	9.08	15.00	0.73
2	112.7	-1.4	1.0	112.7	-1.4	1.0	0.005828	-0.002444	0.001367	0.73	9.08	15.00	0.73
1	9.8	0.0	3.3	5.3	4.5	-5.9	0.000216	0.003169	-0.007847	45.85	1.06	1.79	1.06
1	9.8	0.0	3.3	5.3	4.5	-5.9	0.000216	0.003169	-0.007847	45.85	1.06	1.79	1.06
ALL	42.2	-5.7	4.0				0.005828	-0.002444	0.001367				0.50

BEHAVIOR FOR NX= 35.950 NY= 0.550 NXY= 17.210 KX= 0.0 KY= 0.0 KXY= 0.0

LAM. NO.	STRESSES X	Y	XY	11	22	12	STRAINS 11	22	12	M.S. 11	22	12	MIN.
3	-4.3	-33.4	21.7	-44.9	7.2	1.7	-0.002407	0.005792	0.002320	3.28	0.13	8.43	0.13
3	-4.3	-33.4	21.7	-44.9	7.2	1.7	-0.002407	0.005792	0.002320	3.28	0.13	8.43	0.13
2	92.0	-0.2	4.5	92.0	-0.2	4.5	0.004747	-0.001362	0.005940	1.13	17.09	2.69	1.13
2	92.0	-0.2	4.5	92.0	-0.2	4.5	0.004747	-0.001362	0.005940	1.13	17.09	2.68	1.13
1	20.1	35.3	25.5	53.6	1.8	-6.2	0.002737	0.000648	-0.008261	2.69	9.06	1.65	1.65
1	20.1	35.3	25.5	53.6	1.8	-6.2	0.002737	0.000648	-0.008261	2.69	9.06	1.65	1.65
ALL	36.0	0.6	17.2				0.004747	-0.001362	0.005940				0.13

TABLE C-9. STRESSES AND MARGINS OF SAFETY IN COMPOSITE AT LOCATIONS OF HIGH STRESS AT THE ULTIMATE LOAD IN THE STATIC TEST OF THE ELEMENT SPECIMEN (continued)

BEHAVIOR FOR NX= 24.570 NY= 5.560 NXY= 16.300 KX= 0.0 KY= 0.0 KXY= 0.0

LAM. NO.	STRESSES X	Y	XY	STRAINS 11	22	12	11	22	12	M.S. 11	22	12	MIN.
3	-4.3	-24.5	17.5	-34.6	5.8	0.0	-0.001859	0.004654	0.000027	4.55	0.40	99.00	0.40
3	-4.3	-24.5	17.5	-34.6	5.8	0.0	-0.001859	0.004654	0.000027	4.55	0.40	99.00	0.40
2	59.1	0.7	4.2	59.1	0.7	4.2	0.003038	-0.000243	0.005626	2.33	99.00	2.89	2.33
2	59.1	0.7	4.2	59.1	0.7	4.2	0.003038	-0.000243	0.005626	2.33	99.00	2.89	2.33
1	18.9	40.5	27.2	58.6	0.7	-4.2	0.003013	-0.000218	-0.005655	2.35	99.00	2.87	2.35
1	18.9	40.5	27.2	58.6	0.7	-4.2	0.003013	-0.000218	-0.005655	2.35	99.00	2.87	2.35
ALL	24.6	5.6	16.3				0.003038	-0.000243	0.005626				0.40

BEHAVIOR FOR NX= 5.260 NY= 22.280 NXY= 6.480 KX= 0.0 KY= 0.0 KXY= 0.0

LAM. NO.	STRESSES X	Y	XY	STRAINS 11	22	12	11	22	12	M.S. 11	22	12	MIN.
3	4.7	18.6	-6.6	20.8	2.5	-2.7	0.001043	0.001511	-0.003662	8.68	3.32	4.97	3.32
3	4.7	18.6	-6.6	20.8	2.5	-2.7	0.001043	0.001511	-0.003662	8.68	3.32	4.97	3.32
2	-2.8	3.7	1.7	-2.8	3.7	1.7	-0.000192	0.002746	0.002237	52.83	1.38	8.78	1.38
2	-2.8	3.7	1.7	-2.8	3.7	1.7	-0.000192	0.002746	0.002237	52.83	1.38	8.78	1.38
1	13.9	44.5	24.4	57.9	0.4	1.1	0.002980	-0.000426	0.001425	2.39	56.87	14.34	2.39
1	13.9	44.5	24.4	57.9	0.4	1.1	0.002980	-0.000426	0.001425	2.39	56.87	14.34	2.39
ALL	5.3	22.3	6.5				-0.000192	0.002746	0.002237				1.38

the direction of reinforcement (11-direction). Table C-9 shows that for all locations, other than at the inner edge of the hole, the margin of safety for 11-directions is significantly higher than that for the minimum for the 22-direction.

TYPICAL JOINT

The bond line stresses and the stresses in the tapered tips of the metal laminae were determined using the two-dimensional, plane-stress, finite-element model shown in Figure C-22. This model represents a unit width cross section through the thickness at the edge of the reinforced area. Only one-half of the laminate is analyzed because it is symmetric about the midplane. The model contains 271 nodes and 246 elements. Elements 1 - 47 represented the steel laminae; elements 48 - 159, the graphite composite; and elements 160 - 246, the adhesive layer.

Table C-10 presents the computer analysis. The finite-element structure has dimensions that correspond to the prototype and, thus, are double those of the components fabricated in this program. In this model, the Plastilox 17-7B adhesive layer is .010 inch. However, the elastic modulus of the layer has been increased so that its flexibility corresponds to that of a thickness of only .006 inch. Thus, $E = 45.6 \times .010/.006 = 76.0$ ksi.

The analysis was performed for an axial load of 4.24 kips/inch of width acting upon the full thickness. This corresponds to an average stress of 13.3 ksi in the graphite. Figure C-21 shows the shear stresses applied to steel laminae and also the tensile stress in the laminae. These values were taken directly from the data shown in Table C-10. It is seen that the shear stresses at the tips of the central lamina and the adjacent laminae are equal, and thus, the design provides a balanced sharing of the load to the central three steel laminae. The following relationships hold:

$$\text{maximum bond stress} = \frac{.8818}{4.24} = .208 \text{ ksi/kip of running load}$$

$$\text{maximum steel stress} = \frac{27.01}{4.24} = 6.37 \text{ ksi/kip of running load}$$

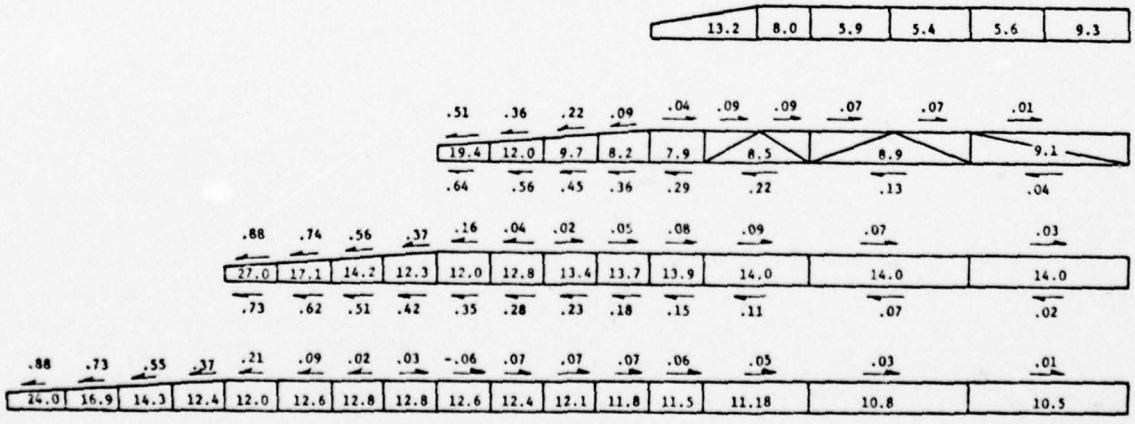


Figure C-21. Bond stresses and steel stresses for axial load of 4.24 kips/inch on prototype-sized joint.

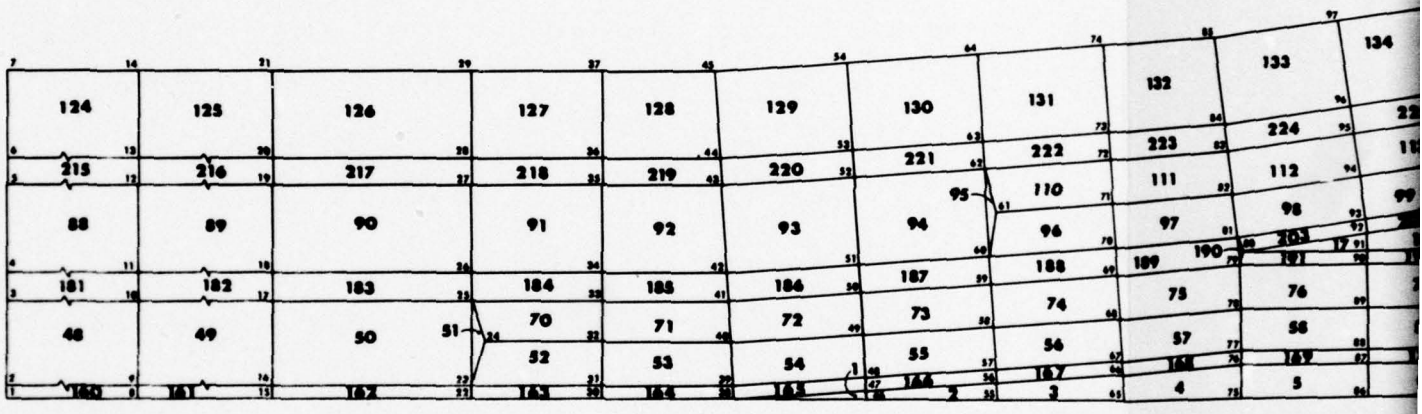
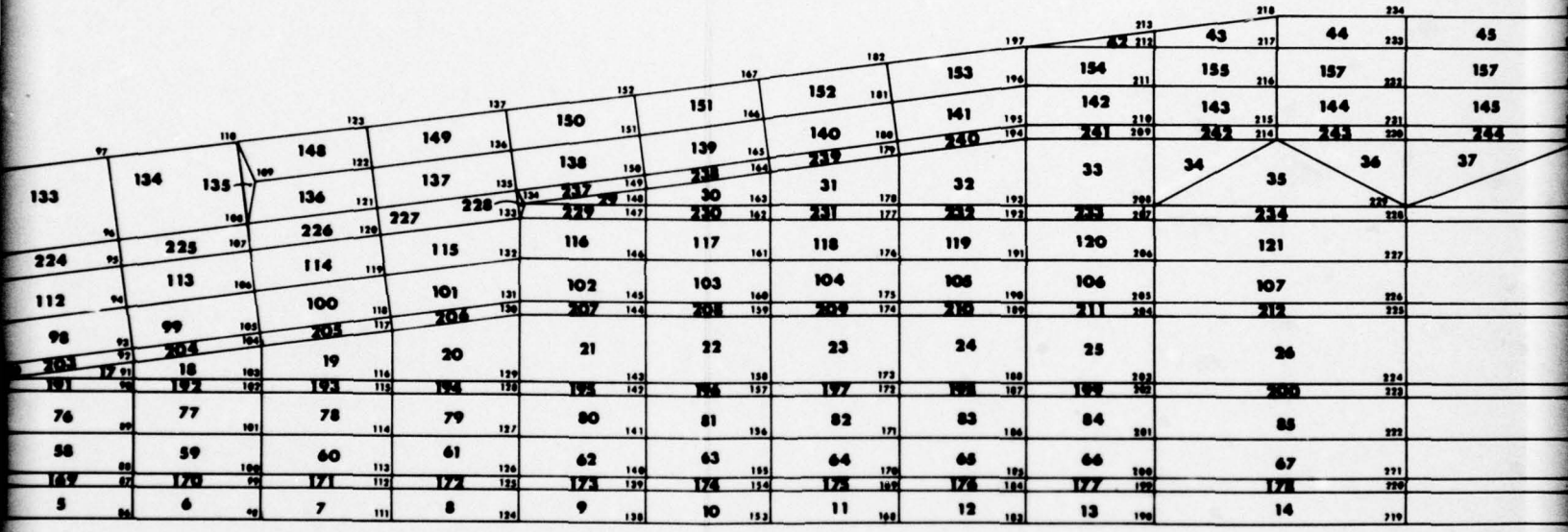


Figure C-22. Finite-element model for calculation of bond-line stresses at a typical joint.

PRECEDING PAGE BLANK-NOT FILMED


133
134
135
148
149
150
151
152
153
154
155
157
157
136
137
138
139
140
141
142
143
144
145
226
227
228
229
230
231
232
33
34
35
36
37
225
115
116
117
118
119
120
121
114
101
102
103
104
105
106
107
113
100
99
204
205
206
207
208
209
210
211
212
98
203
18
19
20
21
22
23
24
25
26
76
77
78
79
80
81
82
83
84
85
58
59
60
61
62
63
64
65
66
67
169
170
171
172
173
174
175
176
177
178
5
6
7
8
9
10
11
12
13
14

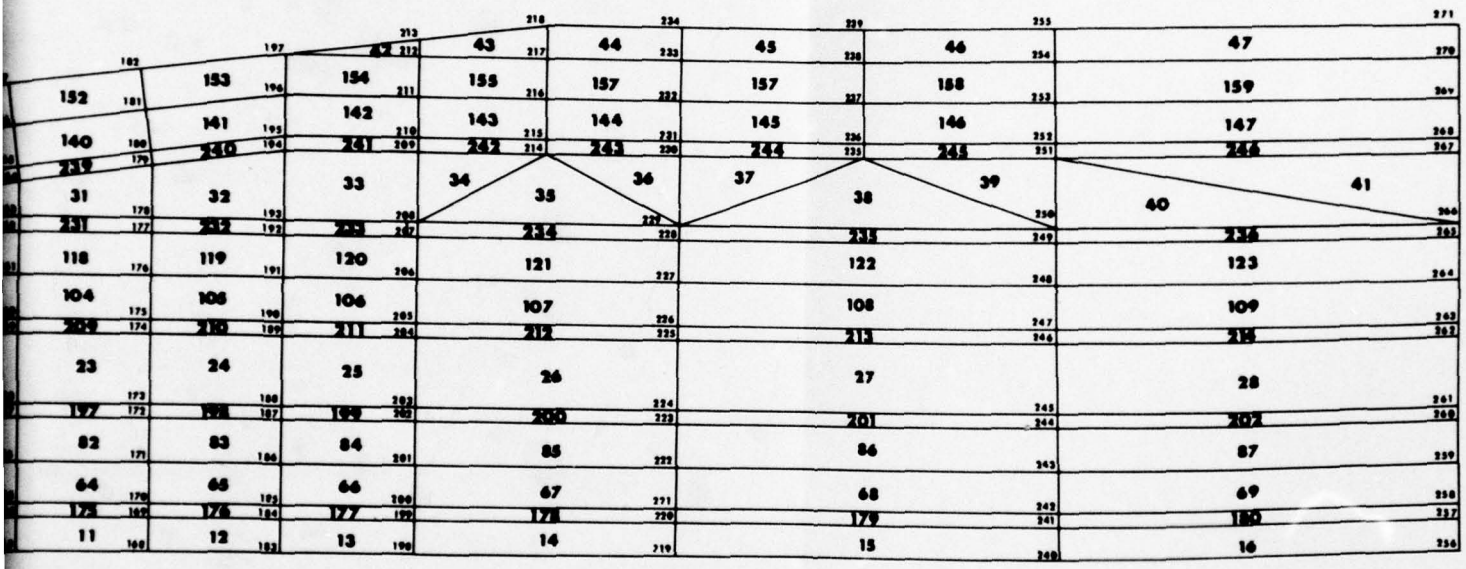

152
153
154
43
44
45
46
47
140
141
142
155
157
157
158
159
143
144
145
146
147
31
32
33
34
35
36
37
38
39
40
41
118
119
120
121
122
123
104
105
106
107
108
109
23
24
25
26
27
28
82
83
84
85
86
87
64
65
66
67
68
69
11
12
13
14
15
16

TABLE C-10. FINITE-ELEMENT ANALYSIS OF TYPICAL JOINT

X COORDINATES AND SUPPORTS

	1	2	3	4	5	6	7	8	9	10
1	0.0 S	0.0100	0.0736	0.0936	0.1572	0.1772	0.2090	0.0 S	0.0100	0.0736
11	0.0936	0.1572	0.1772	0.2090	0.0 S	0.0100	0.0736	0.0936	0.1572	0.1772
21	0.2090	0.0 S	0.0100	0.0418	0.0736	0.0936	0.1572	0.1772	0.2090	0.0 S
31	0.0100	0.0418	0.0736	0.0936	0.1572	0.1772	0.2090	0.0 S	0.0100	0.0418
41	0.0736	0.0936	0.1572	0.1772	0.2090	0.0 S	0.0062	0.0162	0.0479	0.0797
51	0.0996	0.1631	0.1831	0.2148	0.0 S	0.0125	0.0225	0.0542	0.0860	0.1059
61	0.1382	0.1694	0.1894	0.2211	0.0 S	0.0187	0.0287	0.0604	0.0922	0.1121
71	0.1439	0.1756	0.1956	0.2273	0.0 S	0.0250	0.0350	0.0668	0.0986	0.1086
81	0.1185	0.1501	0.1817	0.2016	0.2331	0.0 S	0.0250	0.0350	0.0668	0.0986
91	0.1086	0.1211	0.1310	0.1626	0.1941	0.2140	0.2455	0.0 S	0.0250	0.0350
101	0.0668	0.0986	0.1086	0.1336	0.1435	0.1751	0.2066	0.2265	0.2432	0.2580
111	0.0 S	0.0250	0.0350	0.0668	0.0986	0.1086	0.1461	0.1560	0.1876	0.2191
121	0.2390	0.2547	0.2705	0.0 S	0.0250	0.0350	0.0668	0.0986	0.1086	0.1586
131	0.1686	0.2004	0.2322	0.2422	0.2520	0.2678	0.2834	0.0 S	0.0250	0.0350
141	0.0668	0.0986	0.1086	0.1586	0.1686	0.2004	0.2322	0.2422	0.2547	0.2646
151	0.2804	0.2961	0.0 S	0.0250	0.0350	0.0668	0.0986	0.1086	0.1586	0.1686
161	0.2004	0.2322	0.2422	0.2672	0.2771	0.2929	0.3086	0.0 S	0.0250	0.0350
171	0.0668	0.0986	0.1086	0.1586	0.1686	0.2004	0.2322	0.2422	0.2797	0.2896
181	0.3054	0.3211	0.0 S	0.0250	0.0350	0.0668	0.0986	0.1086	0.1586	0.1686
191	0.2004	0.2322	0.2422	0.2922	0.3022	0.3182	0.3342	0.0 S	0.0250	0.0350
201	0.0668	0.0986	0.1086	0.1586	0.1686	0.2004	0.2322	0.2422	0.2922	0.3022
211	0.3181	0.3340	0.3448	0.2922	0.3022	0.3181	0.3340	0.3554	0.0 S	0.0250
221	0.0350	0.0668	0.0986	0.1086	0.1586	0.1686	0.2004	0.2322	0.2422	0.2922
231	0.3022	0.3181	0.3340	0.3660	0.2922	0.3022	0.3181	0.3340	0.3660	0.0 S
241	0.0250	0.0350	0.0668	0.0986	0.1086	0.1586	0.1686	0.2004	0.2322	0.2422
251	0.2922	0.3022	0.3181	0.3340	0.3660	0.0 S	0.0250	0.0350	0.0668	0.0986
261	0.1086	0.1586	0.1686	0.2004	0.2322	0.2422	0.2922	0.3022	0.3181	0.3340
271	0.3366									

PRECEDING PAGE BLANK-NOT FILMED

TABLE C-10. FINITE-ELEMENT ANALYSIS OF TYPICAL JOINT (continued)

Y COORDINATES AND SUPPORTS

	1	2	3	4	5	6	7	8	9	10
1	3.1000	3.1000	3.1000	3.1000	3.1000	3.1000	3.1000	2.7000	2.7000	2.7000
11	2.7000	2.7000	2.7000	2.7000	2.5500	2.5500	2.5500	2.5500	2.5500	2.5500
21	2.5500	2.4000	2.4000	2.3920	2.4000	2.4000	2.4000	2.4000	2.4000	2.3000
31	2.3000	2.3000	2.3000	2.3000	2.3000	2.3000	2.3000	2.2000	2.2003	2.2013
41	2.2023	2.2029	2.2049	2.2055	2.2065	2.1000	2.1000	2.1006	2.1026	2.1046
51	2.1058	2.1098	2.1111	2.1130	2.0000	2.0000	2.0006	2.0026	2.0046	2.0058
61	1.9996	2.0098	2.0111	2.0130	1.9000	1.9000	1.9006	1.9026	1.9046	1.9058
71	1.9078	1.9098	1.9111	1.9130	1.8000	1.8000	1.8000	1.8000	1.8000	1.7982
81	1.8025	1.8064	1.8104	1.8129	1.8188	1.7000	1.7000	1.7000	1.7000	1.7000
91	1.7000	1.7000	1.7012	1.7052	1.7091	1.7116	1.7156	1.6000	1.6000	1.6000
101	1.6000	1.6000	1.6000	1.6000	1.6012	1.6052	1.6091	1.6116	1.6059	1.6156
111	1.5000	1.5000	1.5000	1.5000	1.5000	1.5000	1.5000	1.5012	1.5052	1.5091
121	1.5116	1.5136	1.5156	1.4000	1.4000	1.4000	1.4000	1.4000	1.4000	1.4000
131	1.4000	1.4000	1.4000	1.3982	1.4025	1.4044	1.4065	1.3000	1.3000	1.3000
141	1.3000	1.3000	1.3000	1.3000	1.3000	1.3000	1.3000	1.3000	1.3000	1.3012
151	1.3032	1.3052	1.2000	1.2000	1.2000	1.2000	1.2000	1.2000	1.2000	1.2000
161	1.2000	1.2000	1.2000	1.2000	1.2012	1.2032	1.2052	1.1000	1.1000	1.1000
171	1.1000	1.1000	1.1000	1.1000	1.1000	1.1000	1.1000	1.1000	1.1000	1.1012
181	1.1032	1.1052	1.0000	1.0000	1.0000	1.0000	1.0000	1.0000	1.0000	1.0000
191	1.0000	1.0000	1.0000	1.0000	1.0000	1.0000	1.0000	0.9000	0.9000	0.9000
201	0.9000	0.9000	0.9000	0.9000	0.9000	0.9000	0.9000	0.9000	0.9000	0.9000
211	0.9000	0.9000	0.9000	0.8000	0.8000	0.8000	0.8000	0.8000	0.7000	0.7000
221	0.7000	0.7000	0.7000	0.7000	0.7000	0.7000	0.7000	0.7000	0.7000	0.7000
231	0.7000	0.7000	0.7000	0.7000	0.5500	0.5500	0.5500	0.5500	0.5500	0.4000
241	0.4000	0.4000	0.4000	0.4000	0.4000	0.4000	0.4000	0.4000	0.4000	0.4000
251	0.4000	0.4000	0.4000	0.4000	0.4000	0.1000 S	0.1000 S	0.1000 S	0.1000 S	0.1000 S
261	0.1000 S	0.1000 S	0.1000 S	0.1000 S	0.1000 S	0.1000 S	0.1000 S	0.1000 S	0.1000 S	0.1000 S
271	0.1000 S									

LOADS, CASE 1

1	X	0.0
1	Y	0.0
2	X	0.0
2	Y	0.424
3	X	0.0
3	Y	0.424
4	X	0.0
4	Y	0.424
5	X	0.0
5	Y	0.424
6	X	0.0
6	Y	0.212
7	X	0.0
7	Y	0.212

TABLE C-10. FINITE-ELEMENT ANALYSIS OF TYPICAL JOINT (continued)

ELEM	P	Q	R	S	TYPE	E	PR	THICK-AREA	ALPHA	TEM 1	TEM 2	TEM 3	TEM 4	TEM 5
1	46	38	47	0	2	18560.	0.3180	1.0000	0.00000560	0.				
2	55	46	47	56	3	18560.	0.3180	1.0000	0.00000560	0.				
3	65	55	56	66	3	18560.	0.3180	1.0000	0.00000560	0.				
4	75	65	66	76	3	18560.	0.3180	1.0000	0.00000560	0.				
5	86	75	76	87	3	18560.	0.3180	1.0000	0.00000560	0.				
6	98	86	87	99	3	18560.	0.3180	1.0000	0.00000560	0.				
7	111	98	99	112	3	18560.	0.3180	1.0000	0.00000560	0.				
8	124	111	112	125	3	18560.	0.3180	1.0000	0.00000560	0.				
9	138	124	125	139	3	18560.	0.3180	1.0000	0.00000560	0.				
10	153	138	139	154	3	18560.	0.3180	1.0000	0.00000560	0.				
11	168	153	154	169	3	18560.	0.3180	1.0000	0.00000560	0.				
12	183	168	169	184	3	18560.	0.3180	1.0000	0.00000560	0.				
13	198	183	184	199	3	18560.	0.3180	1.0000	0.00000560	0.				
14	219	198	199	220	3	18560.	0.3180	1.0000	0.00000560	0.				
15	240	219	220	241	3	18560.	0.3180	1.0000	0.00000560	0.				
16	258	240	241	257	3	18560.	0.3180	1.0000	0.00000560	0.				
17	91	80	92	0	2	29000.	0.3180	1.0000	0.00000560	0.				
18	103	91	92	104	3	29000.	0.3180	1.0000	0.00000560	0.				
19	116	103	104	117	3	29000.	0.3180	1.0000	0.00000560	0.				
20	129	116	117	130	3	29000.	0.3180	1.0000	0.00000560	0.				
21	143	129	130	144	3	29000.	0.3180	1.0000	0.00000560	0.				
22	158	143	144	159	3	29000.	0.3180	1.0000	0.00000560	0.				
23	173	158	159	174	3	29000.	0.3180	1.0000	0.00000560	0.				
24	188	173	174	189	3	29000.	0.3180	1.0000	0.00000560	0.				
25	203	188	189	204	3	29000.	0.3180	1.0000	0.00000560	0.				
26	224	203	204	225	3	29000.	0.3180	1.0000	0.00000560	0.				
27	245	224	225	246	3	29000.	0.3180	1.0000	0.00000560	0.				
28	261	245	246	262	3	29000.	0.3180	1.0000	0.00000560	0.				
29	148	134	149	0	2	29000.	0.3180	1.0000	0.00000560	0.				
30	163	148	149	164	3	29000.	0.3180	1.0000	0.00000560	0.				
31	178	163	164	179	3	29000.	0.3180	1.0000	0.00000560	0.				
32	193	178	179	194	3	29000.	0.3180	1.0000	0.00000560	0.				
33	208	193	194	209	3	29000.	0.3180	1.0000	0.00000560	0.				
34	209	214	208	0	2	29000.	0.3180	1.0000	0.00000560	0.				
35	229	208	214	0	2	29000.	0.3180	1.0000	0.00000560	0.				
36	214	230	229	0	2	29000.	0.3180	1.0000	0.00000560	0.				
37	230	235	229	0	2	29000.	0.3180	1.0000	0.00000560	0.				
38	250	229	235	0	2	29000.	0.3180	1.0000	0.00000560	0.				
39	235	251	250	0	2	29000.	0.3180	1.0000	0.00000560	0.				
40	266	250	251	0	2	29000.	0.3180	1.0000	0.00000560	0.				
41	251	267	266	0	2	29000.	0.3180	1.0000	0.00000560	0.				
42	212	197	213	0	2	29000.	0.3180	1.0000	0.00000560	0.				
43	217	212	213	218	3	29000.	0.3180	1.0000	0.00000560	0.				
44	233	217	218	234	3	29000.	0.3180	1.0000	0.00000560	0.				
45	238	233	234	239	3	29000.	0.3180	1.0000	0.00000560	0.				
46	254	238	239	255	3	29000.	0.3180	1.0000	0.00000560	0.				
47	270	254	255	271	3	29000.	0.3180	1.0000	0.00000560	0.				
48	9	2	3	10	5	0.	0.0	1.0000	0.0	0.				
49	16	9	10	17	5	0.	0.0	1.0000	0.0	0.				
50	23	16	17	25	5	0.	0.0	1.0000	0.0	0.				

TABLE C-10. FINITE-ELEMENT ANALYSIS OF TYPICAL JOINT (continued)

ELEM	P	Q	R	S	TYPE	E	PR	THICK-AREA	ALPHA	TEM 1	TEM 2	TEM 3	TEM 4	TEM 5
51	23	25	24	0	4	0.	0.0	1.0000	0.0	0.				
52	31	23	24	32	5	0.	0.0	1.0000	0.0	0.				
53	39	31	32	40	5	0.	0.0	1.0000	0.0	0.				
54	48	39	40	49	5	0.	0.0	1.0000	0.0	0.				
55	57	48	49	58	5	0.	0.0	1.0000	0.0	0.				
56	67	57	58	68	5	0.	0.0	1.0000	0.0	0.				
57	77	67	68	78	5	0.	0.0	1.0000	0.0	0.				
58	88	77	78	89	5	0.	0.0	1.0000	0.0	0.				
59	100	88	89	101	5	0.	0.0	1.0000	0.0	0.				
60	113	100	101	114	5	0.	0.0	1.0000	0.0	0.				
61	126	113	114	127	5	0.	0.0	1.0000	0.0	0.				
62	140	126	127	141	5	0.	0.0	1.0000	0.0	0.				
63	155	140	141	156	5	0.	0.0	1.0000	0.0	0.				
64	170	155	156	171	5	0.	0.0	1.0000	0.0	0.				
65	185	170	171	186	5	0.	0.0	1.0000	0.0	0.				
66	200	185	186	201	5	0.	0.0	1.0000	0.0	0.				
67	221	200	201	222	5	0.	0.0	1.0000	0.0	0.				
68	242	221	222	243	5	0.	0.0	1.0000	0.0	0.				
69	258	242	243	259	5	0.	0.0	1.0000	0.0	0.				
70	32	24	25	33	5	0.	0.0	1.0000	0.0	0.				
71	40	32	33	41	5	0.	0.0	1.0000	0.0	0.				
72	49	40	41	50	5	0.	0.0	1.0000	0.0	0.				
73	58	49	50	59	5	0.	0.0	1.0000	0.0	0.				
74	68	58	59	69	5	0.	0.0	1.0000	0.0	0.				
75	78	68	69	79	5	0.	0.0	1.0000	0.0	0.				
76	89	78	79	90	5	0.	0.0	1.0000	0.0	0.				
77	101	89	90	102	5	0.	0.0	1.0000	0.0	0.				
78	114	101	102	115	5	0.	0.0	1.0000	0.0	0.				
79	127	114	115	128	5	0.	0.0	1.0000	0.0	0.				
80	141	127	128	142	5	0.	0.0	1.0000	0.0	0.				
81	156	141	142	157	5	0.	0.0	1.0000	0.0	0.				
82	171	156	157	172	5	0.	0.0	1.0000	0.0	0.				
83	186	171	172	187	5	0.	0.0	1.0000	0.0	0.				
84	201	186	187	202	5	0.	0.0	1.0000	0.0	0.				
85	222	201	202	223	5	0.	0.0	1.0000	0.0	0.				
86	243	222	223	244	5	0.	0.0	1.0000	0.0	0.				
87	259	243	244	260	5	0.	0.0	1.0000	0.0	0.				
88	11	4	5	12	5	0.	0.0	1.0000	0.0	0.				
89	18	11	12	19	5	0.	0.0	1.0000	0.0	0.				
90	26	18	19	27	5	0.	0.0	1.0000	0.0	0.				
91	34	26	27	35	5	0.	0.0	1.0000	0.0	0.				
92	42	34	35	43	5	0.	0.0	1.0000	0.0	0.				
93	51	42	43	52	5	0.	0.0	1.0000	0.0	0.				
94	60	51	52	62	5	0.	0.0	1.0000	0.0	0.				
95	60	62	61	0	4	0.	0.0	1.0000	0.0	0.				
96	70	60	61	71	5	0.	0.0	1.0000	0.0	0.				
97	81	70	71	82	5	0.	0.0	1.0000	0.0	0.				
98	93	81	82	94	5	0.	0.0	1.0000	0.0	0.				
99	105	93	94	106	5	0.	0.0	1.0000	0.0	0.				
100	118	105	106	119	5	0.	0.0	1.0000	0.0	0.				

TABLE C-10. FINITE-ELEMENT ANALYSIS OF TYPICAL JOINT (continued)

ELEM	P	Q	R	S	TYPE	E	PR	THICK-AREA	ALPHA	TEM 1	TEM 2	TEM 3	TEM 4	TEM 5
101	131	118	119	132	5	0.	0.0	1.0000	0.0	0.				
102	145	131	132	146	5	0.	0.0	1.0000	0.0	0.				
103	160	145	146	161	5	0.	0.0	1.0000	0.0	0.				
104	175	160	161	176	5	0.	0.0	1.0000	0.0	0.				
105	190	175	176	191	5	0.	0.0	1.0000	0.0	0.				
106	205	190	191	206	5	0.	0.0	1.0000	0.0	0.				
107	226	205	206	227	5	0.	0.0	1.0000	0.0	0.				
108	247	226	227	248	5	0.	0.0	1.0000	0.0	0.				
109	263	247	248	264	5	0.	0.0	1.0000	0.0	0.				
110	71	61	62	72	5	0.	0.0	1.0000	0.0	0.				
111	82	71	72	83	5	0.	0.0	1.0000	0.0	0.				
112	94	82	83	95	5	0.	0.0	1.0000	0.0	0.				
113	106	94	95	107	5	0.	0.0	1.0000	0.0	0.				
114	119	106	107	120	5	0.	0.0	1.0000	0.0	0.				
115	132	119	120	133	5	0.	0.0	1.0000	0.0	0.				
116	146	132	133	147	5	0.	0.0	1.0000	0.0	0.				
117	161	146	147	162	5	0.	0.0	1.0000	0.0	0.				
118	176	161	162	177	5	0.	0.0	1.0000	0.0	0.				
119	191	176	177	192	5	0.	0.0	1.0000	0.0	0.				
120	206	191	192	207	5	0.	0.0	1.0000	0.0	0.				
121	227	206	207	228	5	0.	0.0	1.0000	0.0	0.				
122	248	227	228	249	5	0.	0.0	1.0000	0.0	0.				
123	264	248	249	265	5	0.	0.0	1.0000	0.0	0.				
124	13	6	7	14	5	0.	0.0	1.0000	0.0	0.				
125	20	13	14	21	5	0.	0.0	1.0000	0.0	0.				
126	28	20	21	29	5	0.	0.0	1.0000	0.0	0.				
127	36	28	29	37	5	0.	0.0	1.0000	0.0	0.				
128	44	36	37	45	5	0.	0.0	1.0000	0.0	0.				
129	53	44	45	54	5	0.	0.0	1.0000	0.0	0.				
130	63	53	54	64	5	0.	0.0	1.0000	0.0	0.				
131	73	63	64	74	5	0.	0.0	1.0000	0.0	0.				
132	84	73	74	85	5	0.	0.0	1.0000	0.0	0.				
133	96	84	85	97	5	0.	0.0	1.0000	0.0	0.				
134	108	96	97	110	5	0.	0.0	1.0000	0.0	0.				
135	108	110	109	0	4	0.	0.0	1.0000	0.0	0.				
136	121	108	109	122	5	0.	0.0	1.0000	0.0	0.				
137	135	121	122	136	5	0.	0.0	1.0000	0.0	0.				
138	150	135	136	151	5	0.	0.0	1.0000	0.0	0.				
139	165	150	151	166	5	0.	0.0	1.0000	0.0	0.				
140	180	165	166	181	5	0.	0.0	1.0000	0.0	0.				
141	195	180	181	196	5	0.	0.0	1.0000	0.0	0.				
142	210	195	196	211	5	0.	0.0	1.0000	0.0	0.				
143	215	210	211	216	5	0.	0.0	1.0000	0.0	0.				
144	231	215	216	232	5	0.	0.0	1.0000	0.0	0.				
145	236	231	232	237	5	0.	0.0	1.0000	0.0	0.				
146	252	236	237	253	5	0.	0.0	1.0000	0.0	0.				
147	268	252	253	269	5	0.	0.0	1.0000	0.0	0.				
148	122	109	110	123	5	0.	0.0	1.0000	0.0	0.				
149	136	122	123	137	5	0.	0.0	1.0000	0.0	0.				
150	151	136	137	152	5	0.	0.0	1.0000	0.0	0.				

TABLE C-10. FINITE-ELEMENT ANALYSIS OF TYPICAL JOINT (continued)

ELEM	P	Q	R	S	TYPE	E	PR	THICK-AREA	ALPHA	TEM 1	TEM 2	TEM 3	TEM 4	TEM 5
151	166	151	152	167	5	0.	0.0	1.0000	0.0	0.				
152	181	166	167	182	5	0.	0.0	1.0000	0.0	0.				
153	196	181	182	197	5	0.	0.0	1.0000	0.0	0.				
154	211	196	197	212	5	0.	0.0	1.0000	0.0	0.				
155	216	211	212	217	5	0.	0.0	1.0000	0.0	0.				
156	232	216	217	233	5	0.	0.0	1.0000	0.0	0.				
157	237	232	233	238	5	0.	0.0	1.0000	0.0	0.				
158	253	237	238	254	5	0.	0.0	1.0000	0.0	0.				
159	269	253	254	270	5	0.	0.0	1.0000	0.0	0.				
160	8	1	2	9	3	76.	0.3500	1.0000	0.00003000	0.				
161	15	8	9	16	3	76.	0.3500	1.0000	0.00003000	0.				
162	22	15	16	23	3	76.	0.3500	1.0000	0.00003000	0.				
163	30	22	23	31	3	76.	0.3500	1.0000	0.00003000	0.				
164	38	30	31	39	3	76.	0.3500	1.0000	0.00003000	0.				
165	47	38	39	48	3	76.	0.3500	1.0000	0.00003000	0.				
166	56	47	48	57	3	76.	0.3500	1.0000	0.00003000	0.				
167	66	56	57	67	3	76.	0.3500	1.0000	0.00003000	0.				
168	76	66	67	77	3	76.	0.3500	1.0000	0.00003000	0.				
169	87	76	77	88	3	76.	0.3500	1.0000	0.00003000	0.				
170	99	87	88	100	3	76.	0.3500	1.0000	0.00003000	0.				
171	112	99	100	113	3	76.	0.3500	1.0000	0.00003000	0.				
172	125	112	113	126	3	76.	0.3500	1.0000	0.00003000	0.				
173	139	125	126	140	3	76.	0.3500	1.0000	0.00003000	0.				
174	154	139	140	155	3	76.	0.3500	1.0000	0.00003000	0.				
175	169	154	155	170	3	76.	0.3500	1.0000	0.00003000	0.				
176	184	169	170	185	3	76.	0.3500	1.0000	0.00003000	0.				
177	199	184	185	200	3	76.	0.3500	1.0000	0.00003000	0.				
178	220	199	200	221	3	76.	0.3500	1.0000	0.00003000	0.				
179	241	220	221	242	3	76.	0.3500	1.0000	0.00003000	0.				
180	257	241	242	258	3	76.	0.3500	1.0000	0.00003000	0.				
181	10	3	4	11	3	76.	0.3500	1.0000	0.00003000	0.				
182	17	10	11	18	3	76.	0.3500	1.0000	0.00003000	0.				
183	25	17	18	26	3	76.	0.3500	1.0000	0.00003000	0.				
184	33	25	26	34	3	76.	0.3500	1.0000	0.00003000	0.				
185	41	33	34	42	3	76.	0.3500	1.0000	0.00003000	0.				
186	50	41	42	51	3	76.	0.3500	1.0000	0.00003000	0.				
187	59	50	51	60	3	76.	0.3500	1.0000	0.00003000	0.				
188	69	59	60	70	3	76.	0.3500	1.0000	0.00003000	0.				
189	79	69	70	81	3	76.	0.3500	1.0000	0.00003000	0.				
190	79	81	80	0	2	76.	0.3500	1.0000	0.00003000	0.				
191	90	79	80	91	3	76.	0.3500	1.0000	0.00003000	0.				
192	102	90	91	103	3	76.	0.3500	1.0000	0.00003000	0.				
193	115	102	103	116	3	76.	0.3500	1.0000	0.00003000	0.				
194	128	115	116	129	3	76.	0.3500	1.0000	0.00003000	0.				
195	142	128	129	143	3	76.	0.3500	1.0000	0.00003000	0.				
196	157	142	143	158	3	76.	0.3500	1.0000	0.00003000	0.				
197	172	157	158	173	3	76.	0.3500	1.0000	0.00003000	0.				
198	187	172	173	188	3	76.	0.3500	1.0000	0.00003000	0.				
199	202	187	188	203	3	76.	0.3500	1.0000	0.00003000	0.				
200	223	202	203	224	3	76.	0.3500	1.0000	0.00003000	0.				

TABLE C-10. FINITE-ELEMENT ANALYSIS OF TYPICAL JOINT (continued)

ELEM	P	Q	R	S	TYPE	E	PR	THICK-AREA	ALPHA	TEM 1	TEM 2	TEM 3	TEM 4	TEM 5
201	244	223	224	245	3	76.	0.3500	1.0000	0.00003000	0.				
202	260	244	245	261	3	76.	0.3500	1.0000	0.00003000	0.				
203	92	80	81	93	3	76.	0.3500	1.0000	0.00003000	0.				
204	104	92	93	105	3	76.	0.3500	1.0000	0.00003000	0.				
205	117	104	105	118	3	76.	0.3500	1.0000	0.00003000	0.				
206	130	117	118	131	3	76.	0.3500	1.0000	0.00003000	0.				
207	144	130	131	145	3	76.	0.3500	1.0000	0.00003000	0.				
208	159	144	145	160	3	76.	0.3500	1.0000	0.00003000	0.				
209	174	159	160	175	3	76.	0.3500	1.0000	0.00003000	0.				
210	189	174	175	190	3	76.	0.3500	1.0000	0.00003000	0.				
211	204	189	190	205	3	76.	0.3500	1.0000	0.00003000	0.				
212	225	204	205	226	3	76.	0.3500	1.0000	0.00003000	0.				
213	246	225	226	247	3	76.	0.3500	1.0000	0.00003000	0.				
214	262	246	247	263	3	76.	0.3500	1.0000	0.00003000	0.				
215	12	5	6	13	3	76.	0.3500	1.0000	0.00003000	0.				
216	19	12	13	20	3	76.	0.3500	1.0000	0.00003000	0.				
217	27	19	20	28	3	76.	0.3500	1.0000	0.00003000	0.				
218	35	27	28	36	3	76.	0.3500	1.0000	0.00003000	0.				
219	43	35	36	44	3	76.	0.3500	1.0000	0.00003000	0.				
220	52	43	44	53	3	76.	0.3500	1.0000	0.00003000	0.				
221	62	52	53	63	3	76.	0.3500	1.0000	0.00003000	0.				
222	72	62	63	73	3	76.	0.3500	1.0000	0.00003000	0.				
223	83	72	73	84	3	76.	0.3500	1.0000	0.00003000	0.				
224	95	83	84	96	3	76.	0.3500	1.0000	0.00003000	0.				
225	107	95	96	108	3	76.	0.3500	1.0000	0.00003000	0.				
226	120	107	108	121	3	76.	0.3500	1.0000	0.00003000	0.				
227	133	120	121	135	3	76.	0.3500	1.0000	0.00003000	0.				
228	133	135	134	0	2	76.	0.3500	1.0000	0.00003000	0.				
229	147	133	134	148	3	76.	0.3500	1.0000	0.00003000	0.				
230	162	147	148	163	3	76.	0.3500	1.0000	0.00003000	0.				
231	177	162	163	178	3	76.	0.3500	1.0000	0.00003000	0.				
232	192	177	178	193	3	76.	0.3500	1.0000	0.00003000	0.				
233	207	192	193	208	3	76.	0.3500	1.0000	0.00003000	0.				
234	228	207	208	229	3	76.	0.3500	1.0000	0.00003000	0.				
235	249	228	229	250	3	76.	0.3500	1.0000	0.00003000	0.				
236	265	249	250	266	3	76.	0.3500	1.0000	0.00003000	0.				
237	149	134	135	150	3	76.	0.3500	1.0000	0.00003000	0.				
238	164	149	150	165	3	76.	0.3500	1.0000	0.00003000	0.				
239	179	164	165	180	3	76.	0.3500	1.0000	0.00003000	0.				
240	194	179	180	195	3	76.	0.3500	1.0000	0.00003000	0.				
241	209	194	195	210	3	76.	0.3500	1.0000	0.00003000	0.				
242	214	209	210	215	3	76.	0.3500	1.0000	0.00003000	0.				
243	230	214	215	231	3	76.	0.3500	1.0000	0.00003000	0.				
244	235	230	231	236	3	76.	0.3500	1.0000	0.00003000	0.				
245	251	235	236	252	3	76.	0.3500	1.0000	0.00003000	0.				
246	267	251	252	268	3	76.	0.3500	1.0000	0.00003000	0.				

TABLE C-10. FINITE-ELEMENT ANALYSIS OF TYPICAL JOINT (continued)

COMPOSITE MATERIAL PROPERTIES

ELEM	ALPHA 1	ALPHA 2	ALPHA 12	C11	C12	C13	C22	C23	C33
48	0.0000900	0.0	0.0	1620.0	86.0	0.0	7641.0	0.0	670.0
49	0.0000900	0.0	0.0	1620.0	86.0	0.0	7641.0	0.0	670.0
50	0.0000900	0.0	0.0	1620.0	86.0	0.0	7641.0	0.0	670.0
51	0.0	0.0000900	0.0	7641.0	86.0	0.0	1620.0	0.0	670.0
52	0.0000900	0.0	0.0	1620.0	86.0	0.0	7641.0	0.0	670.0
53	0.0000900	0.0	0.0	1620.0	86.0	0.0	7641.0	0.0	670.0
54	0.0000900	0.0	0.0	1620.0	86.0	0.0	7641.0	0.0	670.0
55	0.0000900	0.0	0.0	1620.0	86.0	0.0	7641.0	0.0	670.0
56	0.0000900	0.0	0.0	1620.0	86.0	0.0	7641.0	0.0	670.0
57	0.0000900	0.0	0.0	1620.0	86.0	0.0	7641.0	0.0	670.0
58	0.0000900	0.0	0.0	1620.0	86.0	0.0	7641.0	0.0	670.0
59	0.0000900	0.0	0.0	1620.0	86.0	0.0	7641.0	0.0	670.0
60	0.0000900	0.0	0.0	1620.0	86.0	0.0	7641.0	0.0	670.0
61	0.0000900	0.0	0.0	1620.0	86.0	0.0	7641.0	0.0	670.0
62	0.0000900	0.0	0.0	1620.0	86.0	0.0	7641.0	0.0	670.0
63	0.0000900	0.0	0.0	1620.0	86.0	0.0	7641.0	0.0	670.0
64	0.0000900	0.0	0.0	1620.0	86.0	0.0	7641.0	0.0	670.0
65	0.0000900	0.0	0.0	1620.0	86.0	0.0	7641.0	0.0	670.0
66	0.0000900	0.0	0.0	1620.0	86.0	0.0	7641.0	0.0	670.0
67	0.0000900	0.0	0.0	1620.0	86.0	0.0	7641.0	0.0	670.0
68	0.0000900	0.0	0.0	1620.0	86.0	0.0	7641.0	0.0	670.0
69	0.0000900	0.0	0.0	1620.0	86.0	0.0	7641.0	0.0	670.0
70	0.0000900	0.0	0.0	1620.0	86.0	0.0	7641.0	0.0	670.0
71	0.0000900	0.0	0.0	1620.0	86.0	0.0	7641.0	0.0	670.0
72	0.0000900	0.0	0.0	1620.0	86.0	0.0	7641.0	0.0	670.0
73	0.0000900	0.0	0.0	1620.0	86.0	0.0	7641.0	0.0	670.0
74	0.0000900	0.0	0.0	1620.0	86.0	0.0	7641.0	0.0	670.0
75	0.0000900	0.0	0.0	1620.0	86.0	0.0	7641.0	0.0	670.0
76	0.0000900	0.0	0.0	1620.0	86.0	0.0	7641.0	0.0	670.0
77	0.0000900	0.0	0.0	1620.0	86.0	0.0	7641.0	0.0	670.0
78	0.0000900	0.0	0.0	1620.0	86.0	0.0	7641.0	0.0	670.0
79	0.0000900	0.0	0.0	1620.0	86.0	0.0	7641.0	0.0	670.0
80	0.0000900	0.0	0.0	1620.0	86.0	0.0	7641.0	0.0	670.0
81	0.0000900	0.0	0.0	1620.0	86.0	0.0	7641.0	0.0	670.0
82	0.0000900	0.0	0.0	1620.0	86.0	0.0	7641.0	0.0	670.0
83	0.0000900	0.0	0.0	1620.0	86.0	0.0	7641.0	0.0	670.0
84	0.0000900	0.0	0.0	1620.0	86.0	0.0	7641.0	0.0	670.0
85	0.0000900	0.0	0.0	1620.0	86.0	0.0	7641.0	0.0	670.0
86	0.0000900	0.0	0.0	1620.0	86.0	0.0	7641.0	0.0	670.0
87	0.0000900	0.0	0.0	1620.0	86.0	0.0	7641.0	0.0	670.0
88	0.0000900	0.0	0.0	1620.0	86.0	0.0	7641.0	0.0	670.0
89	0.0000900	0.0	0.0	1620.0	86.0	0.0	7641.0	0.0	670.0
90	0.0000900	0.0	0.0	1620.0	86.0	0.0	7641.0	0.0	670.0
91	0.0000900	0.0	0.0	1620.0	86.0	0.0	7641.0	0.0	670.0
92	0.0000900	0.0	0.0	1620.0	86.0	0.0	7641.0	0.0	670.0
93	0.0000900	0.0	0.0	1620.0	86.0	0.0	7641.0	0.0	670.0
94	0.0000900	0.0	0.0	1620.0	86.0	0.0	7641.0	0.0	670.0
95	0.0	0.0000900	0.0	7641.0	86.0	0.0	1620.0	0.0	670.0
96	0.0000900	0.0	0.0	1620.0	86.0	0.0	7641.0	0.0	670.0
97	0.0000900	0.0	0.0	1620.0	86.0	0.0	7641.0	0.0	670.0

TABLE C-10. FINITE-ELEMENT ANALYSIS OF TYPICAL JOINT (continued)

COMPOSITE MATERIAL PROPERTIES

ELEM	ALPHA 1	ALPHA 2	ALPHA 12	C11	C12	C13	C22	C23	C33
98	0.0000900	0.0	0.0	1620.0	86.0	0.0	7641.0	0.0	670.0
99	0.0000900	0.0	0.0	1620.0	86.0	0.0	7641.0	0.0	670.0
100	0.0000900	0.0	0.0	1620.0	86.0	0.0	7641.0	0.0	670.0
101	0.0000900	0.0	0.0	1620.0	86.0	0.0	7641.0	0.0	670.0
102	0.0000900	0.0	0.0	1620.0	86.0	0.0	7641.0	0.0	670.0
103	0.0000900	0.0	0.0	1620.0	86.0	0.0	7641.0	0.0	670.0
104	0.0000900	0.0	0.0	1620.0	86.0	0.0	7641.0	0.0	670.0
105	0.0000900	0.0	0.0	1620.0	86.0	0.0	7641.0	0.0	670.0
106	0.0000900	0.0	0.0	1620.0	86.0	0.0	7641.0	0.0	670.0
107	0.0000900	0.0	0.0	1620.0	86.0	0.0	7641.0	0.0	670.0
108	0.0000900	0.0	0.0	1620.0	86.0	0.0	7641.0	0.0	670.0
109	0.0000900	0.0	0.0	1620.0	86.0	0.0	7641.0	0.0	670.0
110	0.0000900	0.0	0.0	1620.0	86.0	0.0	7641.0	0.0	670.0
111	0.0000900	0.0	0.0	1620.0	86.0	0.0	7641.0	0.0	670.0
112	0.0000900	0.0	0.0	1620.0	86.0	0.0	7641.0	0.0	670.0
113	0.0000900	0.0	0.0	1620.0	86.0	0.0	7641.0	0.0	670.0
114	0.0000900	0.0	0.0	1620.0	86.0	0.0	7641.0	0.0	670.0
115	0.0000900	0.0	0.0	1620.0	86.0	0.0	7641.0	0.0	670.0
116	0.0000900	0.0	0.0	1620.0	86.0	0.0	7641.0	0.0	670.0
117	0.0000900	0.0	0.0	1620.0	86.0	0.0	7641.0	0.0	670.0
118	0.0000900	0.0	0.0	1620.0	86.0	0.0	7641.0	0.0	670.0
119	0.0000900	0.0	0.0	1620.0	86.0	0.0	7641.0	0.0	670.0
120	0.0000900	0.0	0.0	1620.0	86.0	0.0	7641.0	0.0	670.0
121	0.0000900	0.0	0.0	1620.0	86.0	0.0	7641.0	0.0	670.0
122	0.0000900	0.0	0.0	1620.0	86.0	0.0	7641.0	0.0	670.0
123	0.0000900	0.0	0.0	1620.0	86.0	0.0	7641.0	0.0	670.0
124	0.0000900	0.0	0.0	1620.0	86.0	0.0	7641.0	0.0	670.0
125	0.0000900	0.0	0.0	1620.0	86.0	0.0	7641.0	0.0	670.0
126	0.0000900	0.0	0.0	1620.0	86.0	0.0	7641.0	0.0	670.0
127	0.0000900	0.0	0.0	1620.0	86.0	0.0	7641.0	0.0	670.0
128	0.0000900	0.0	0.0	1620.0	86.0	0.0	7641.0	0.0	670.0
129	0.0000900	0.0	0.0	1620.0	86.0	0.0	7641.0	0.0	670.0
130	0.0000900	0.0	0.0	1620.0	86.0	0.0	7641.0	0.0	670.0
131	0.0000900	0.0	0.0	1620.0	86.0	0.0	7641.0	0.0	670.0
132	0.0000900	0.0	0.0	1620.0	86.0	0.0	7641.0	0.0	670.0
133	0.0000900	0.0	0.0	1620.0	86.0	0.0	7641.0	0.0	670.0
134	0.0000900	0.0	0.0	1620.0	86.0	0.0	7641.0	0.0	670.0
135	0.0	0.0000900	0.0	7641.0	86.0	0.0	1620.0	0.0	670.0
136	0.0000900	0.0	0.0	1620.0	86.0	0.0	7641.0	0.0	670.0
137	0.0000900	0.0	0.0	1620.0	86.0	0.0	7641.0	0.0	670.0
138	0.0000900	0.0	0.0	1620.0	86.0	0.0	7641.0	0.0	670.0
139	0.0000900	0.0	0.0	1620.0	86.0	0.0	7641.0	0.0	670.0
140	0.0000900	0.0	0.0	1620.0	86.0	0.0	7641.0	0.0	670.0
141	0.0000900	0.0	0.0	1620.0	86.0	0.0	7641.0	0.0	670.0
142	0.0000900	0.0	0.0	1620.0	86.0	0.0	7641.0	0.0	670.0
143	0.0000900	0.0	0.0	1620.0	86.0	0.0	7641.0	0.0	670.0
144	0.0000900	0.0	0.0	1620.0	86.0	0.0	7641.0	0.0	670.0
145	0.0000900	0.0	0.0	1620.0	86.0	0.0	7641.0	0.0	670.0
146	0.0000900	0.0	0.0	1620.0	86.0	0.0	7641.0	0.0	670.0
147	0.0000900	0.0	0.0	1620.0	86.0	0.0	7641.0	0.0	670.0

TABLE C-10. FINITE-ELEMENT ANALYSIS OF TYPICAL JOINT (continued)

COMPOSITE MATERIAL PROPERTIES

ELEM	ALPHA 1	ALPHA 2	ALPHA 12	C11	C12	C13	C22	C23	C33
148	0.0000900	0.0	0.0	1620.0	86.0	0.0	7641.0	0.0	670.0
149	0.0000900	0.0	0.0	1620.0	86.0	0.0	7641.0	0.0	670.0
150	0.0000900	0.0	0.0	1620.0	86.0	0.0	7641.0	0.0	670.0
151	0.0000900	0.0	0.0	1620.0	86.0	0.0	7641.0	0.0	670.0
152	0.0000900	0.0	0.0	1620.0	86.0	0.0	7641.0	0.0	670.0
153	0.0000900	0.0	0.0	1620.0	86.0	0.0	7641.0	0.0	670.0
154	0.0000900	0.0	0.0	1620.0	86.0	0.0	7641.0	0.0	670.0
155	0.0000900	0.0	0.0	1620.0	86.0	0.0	7641.0	0.0	670.0
156	0.0000900	0.0	0.0	1620.0	86.0	0.0	7641.0	0.0	670.0
157	0.0000900	0.0	0.0	1620.0	86.0	0.0	7641.0	0.0	670.0
158	0.0000900	0.0	0.0	1620.0	86.0	0.0	7641.0	0.0	670.0
159	0.0000900	0.0	0.0	1620.0	86.0	0.0	7641.0	0.0	670.0

TABLE C-10. FINITE-ELEMENT ANALYSIS OF TYPICAL JOINT (continued)

X DEFLECTION, CASE 1

	1	2	3	4	5	6	7	8	9	10
1	0.0	-1.058E-05	-1.779E-05	-3.549E-05	-4.185E-05	-5.486E-05	-5.779E-05	0.0	-7.055E-06	-1.333E-05
11	-2.723E-05	-3.325E-05	-4.571E-05	-4.863E-05	0.0	-6.780E-06	-1.283E-05	-2.584E-05	-3.167E-05	-4.377E-05
21	-4.662E-05	0.0	-5.067E-07	-2.330E-06	-4.978E-06	-3.975E-06	-8.220E-06	-1.729E-05	-1.998E-05	0.0
31	5.362E-06	5.665E-06	6.141E-06	3.362E-05	3.235E-05	3.536E-05	3.307E-05	0.0	3.082E-05	3.527E-05
41	3.780E-05	7.904E-05	7.992E-05	9.112E-05	8.927E-05	0.0	-2.166E-06	7.664E-06	8.254E-06	9.029E-06
51	3.334E-05	3.321E-05	3.278E-05	3.174E-05	0.0	-3.095E-06	2.736E-07	-7.453E-07	-1.805E-06	5.236E-09
61	-2.222E-06	-2.997E-06	-1.506E-05	-1.704E-05	0.0	-4.042E-06	5.939E-06	6.089E-06	4.412E-06	-2.199E-06
71	-4.522E-06	-6.328E-06	-7.991E-06	-1.087E-05	0.0	-4.987E-06	5.915E-07	1.720E-06	6.209E-06	3.199E-05
81	2.061E-05	2.088E-05	2.113E-05	3.261E-05	3.105E-05	0.0	-5.084E-06	5.771E-06	5.771E-06	5.460E-06
91	1.749E-05	1.445E-05	-5.953E-06	-7.988E-06	-8.675E-06	-1.018E-05	-9.452E-06	0.0	-5.416E-06	-6.083E-06
101	-7.473E-06	-8.775E-06	-8.967E-06	-1.296E-05	-3.452E-05	-3.683E-05	-3.816E-05	-5.329E-05	-5.658E-05	-5.354E-05
111	0.0	-5.603E-06	-1.825E-05	-2.152E-05	-2.473E-05	-3.618E-05	-4.164E-05	-6.103E-05	-6.355E-05	-6.619E-05
121	-9.540E-05	-9.637E-05	-9.659E-05	0.0	-5.638E-06	-2.504E-05	-2.930E-05	-3.350E-05	-5.210E-05	-5.886E-05
131	-9.223E-05	-9.688E-05	-9.699E-05	-9.295E-05	-1.210E-04	-1.227E-04	-1.238E-04	0.0	-5.547E-06	-2.486E-05
141	-2.893E-05	-3.282E-05	-4.970E-05	-5.665E-05	-6.203E-05	-6.421E-05	-6.610E-05	-6.476E-05	-6.695E-05	-8.952E-05
151	-9.191E-05	-9.358E-05	0.0	-5.391E-06	-2.128E-05	-2.464E-05	-2.775E-05	-4.016E-05	-4.744E-05	-5.010E-05
161	-5.143E-05	-5.256E-05	-5.275E-05	-5.549E-05	-6.694E-05	-6.835E-05	-6.947E-05	0.0	-5.236E-06	-1.842E-05
171	-2.127E-05	-2.392E-05	-3.416E-05	-4.169E-05	-4.843E-05	-5.035E-05	-5.215E-05	-5.652E-05	-6.015E-05	-5.968E-05
181	-5.972E-05	-6.010E-05	0.0	-5.114E-06	-1.737E-05	-2.006E-05	-2.261E-05	-3.283E-05	-4.052E-05	-5.115E-05
191	-5.366E-05	-5.608E-05	-6.547E-05	-6.993E-05	-8.085E-05	-8.167E-05	-8.126E-05	0.0	-4.979E-06	-1.719E-05
201	-1.986E-05	-2.242E-05	-3.315E-05	-4.096E-05	-5.285E-05	-5.544E-05	-5.751E-05	-6.802E-05	-7.248E-05	-7.583E-05
211	-7.642E-05	-7.683E-05	-7.813E-05	-6.989E-05	-7.614E-05	-7.677E-05	-7.723E-05	-7.871E-05	0.0	-4.799E-06
221	-1.639E-05	-1.893E-05	-2.139E-05	-3.174E-05	-3.957E-05	-4.982E-05	-5.200E-05	-5.402E-05	-6.202E-05	-6.679E-05
231	-7.429E-05	-7.500E-05	-7.563E-05	-7.763E-05	-5.978E-05	-6.690E-05	-6.756E-05	-6.810E-05	-6.987E-05	0.0
241	-4.622E-06	-1.388E-05	-1.600E-05	-1.804E-05	-2.616E-05	-3.394E-05	-4.048E-05	-4.197E-05	-4.329E-05	-4.761E-05
251	-5.262E-05	-5.567E-05	-5.606E-05	-5.643E-05	-5.915E-05	0.0	-4.543E-06	-1.253E-05	-1.443E-05	-1.625E-05
261	-2.315E-05	-3.088E-05	-3.576E-05	-3.693E-05	-3.795E-05	-4.054E-05	-4.566E-05	-4.217E-05	-4.204E-05	-4.197E-05
271	-4.226E-05									

TABLE C-10. FINITE-ELEMENT ANALYSIS OF TYPICAL JOINT (continued)

Y DEFLECTION, CASE 1

	1	2	3	4	5	6	7	8	9	10
1	3.391E-03	3.383E-03	3.386E-03	3.415E-03	3.419E-03	3.435E-03	3.437E-03	2.679E-03	2.679E-03	2.682E-03
11	2.722E-03	2.727E-03	2.747E-03	2.748E-03	2.413E-03	2.410E-03	2.415E-03	2.462E-03	2.471E-03	2.492E-03
21	2.495E-03	2.121E-03	2.137E-03	2.126E-03	2.145E-03	2.201E-03	2.221E-03	2.237E-03	2.248E-03	2.026E-03
31	1.949E-03	1.959E-03	1.966E-03	2.030E-03	2.054E-03	2.066E-03	2.085E-03	1.423E-03	1.756E-03	1.781E-03
41	1.790E-03	1.879E-03	1.884E-03	1.920E-03	1.919E-03	1.295E-03	1.255E-03	1.587E-03	1.610E-03	1.617E-03
51	1.725E-03	1.713E-03	1.771E-03	1.751E-03	1.204E-03	1.204E-03	1.430E-03	1.451E-03	1.459E-03	1.555E-03
61	1.538E-03	1.549E-03	1.600E-03	1.592E-03	1.128E-03	1.127E-03	1.289E-03	1.302E-03	1.308E-03	1.383E-03
71	1.390E-03	1.391E-03	1.435E-03	1.442E-03	1.061E-03	1.061E-03	1.160E-03	1.162E-03	1.137E-03	8.625E-04
81	1.202E-03	1.230E-03	1.236E-03	1.289E-03	1.294E-03	9.963E-04	9.966E-04	1.045E-03	1.041E-03	1.018E-03
91	7.727E-04	7.685E-04	1.060E-03	1.077E-03	1.076E-03	1.139E-03	1.120E-03	9.289E-04	9.290E-04	9.465E-04
101	9.383E-04	9.151E-04	7.136E-04	7.047E-04	9.302E-04	9.406E-04	9.370E-04	9.831E-04	9.623E-04	9.654E-04
111	8.600E-04	8.600E-04	8.567E-04	8.481E-04	8.283E-04	6.640E-04	6.526E-04	8.130E-04	8.161E-04	8.104E-04
121	8.307E-04	8.221E-04	8.132E-04	7.909E-04	7.909E-04	7.745E-04	7.673E-04	7.520E-04	6.169E-04	6.122E-04
131	6.994E-04	6.984E-04	6.755E-04	4.409E-04	6.534E-04	6.624E-04	6.639E-04	7.227E-04	7.226E-04	6.992E-04
141	6.936E-04	6.823E-04	5.713E-04	5.745E-04	6.049E-04	6.064E-04	5.916E-04	3.765E-04	3.781E-04	5.327E-04
151	5.427E-04	5.477E-04	6.559E-04	6.558E-04	6.300E-04	6.253E-04	6.165E-04	5.268E-04	5.304E-04	5.324E-04
161	5.292E-04	5.140E-04	3.366E-04	3.357E-04	4.366E-04	4.425E-04	4.447E-04	5.907E-04	5.906E-04	5.653E-04
171	5.610E-04	5.536E-04	4.819E-04	4.831E-04	4.687E-04	4.627E-04	4.478E-04	3.049E-04	2.995E-04	3.526E-04
181	3.520E-04	3.519E-04	5.271E-04	5.270E-04	5.035E-04	4.995E-04	4.931E-04	4.354E-04	4.350E-04	4.106E-04
191	4.038E-04	3.908E-04	2.753E-04	2.706E-04	2.722E-04	2.653E-04	2.472E-04	4.648E-04	4.647E-04	4.437E-04
201	4.400E-04	4.347E-04	3.874E-04	3.870E-04	3.567E-04	3.505E-04	3.400E-04	2.458E-04	2.455E-04	2.163E-04
211	2.122E-04	2.023E-04	2.017E-04	2.171E-04	1.832E-04	1.798E-04	1.745E-04	1.736E-04	3.441E-04	3.440E-04
221	3.281E-04	3.256E-04	3.221E-04	2.902E-04	2.905E-04	2.589E-04	2.545E-04	2.482E-04	1.867E-04	1.880E-04
231	1.578E-04	1.559E-04	1.534E-04	1.541E-04	1.427E-04	1.247E-04	1.246E-04	1.246E-04	1.266E-04	1.698E-04
241	1.698E-04	1.619E-04	1.608E-04	1.594E-04	1.446E-04	1.452E-04	1.263E-04	1.243E-04	1.219E-04	9.464E-05
251	9.601E-05	9.015E-05	9.160E-05	9.476E-05	9.780E-05	0.0	0.0	0.0	0.0	0.0
261	0.0	0.0	0.0	0.0	0.0	0.0	0.0	0.0	0.0	0.0
271	0.0									

TABLE C-10. FINITE-ELEMENT ANALYSIS OF TYPICAL JOINT (continued)

STRESS ELEM	XX	YY	XY	ON	OS	CASE	(TOTAL STRAIN)*1000000. XX	YY	XY	(MECH. STRAIN)*1000000. XX	YY	XY	CASE
1	1.1460	23.9926	-0.4055	8.3796	11.0550	1	-349.	1273.	-58.	-349.	1273.	-58.	1
2	-0.0666	16.8759	-0.2336	5.6031	7.9734	1	-293.	910.	-33.	-293.	910.	-33.	1
3	0.2618	14.2950	-0.1563	4.8522	6.6791	1	-231.	766.	-22.	-231.	766.	-22.	1
4	0.0798	12.3565	-0.1164	4.1454	5.8070	1	-207.	664.	-17.	-207.	664.	-17.	1
5	0.0702	11.9760	0.0542	4.0154	5.6293	1	-201.	644.	8.	-201.	644.	8.	1
6	0.0980	12.5646	0.0621	4.2209	5.9003	1	-210.	675.	9.	-210.	675.	9.	1
7	-0.0202	12.7957	0.0090	4.2585	6.0367	1	-220.	690.	1.	-220.	690.	1.	1
8	-0.1063	12.7844	-0.0120	4.2260	6.0518	1	-225.	691.	-2.	-225.	691.	-2.	1
9	-0.1402	12.6156	-0.0282	4.1585	5.9804	1	-224.	682.	-4.	-224.	682.	-4.	1
10	-0.1301	12.3588	-0.0352	4.0763	5.8570	1	-219.	668.	-5.	-219.	668.	-5.	1
11	-0.1064	12.0698	-0.0365	3.9878	5.7151	1	-213.	652.	-5.	-213.	652.	-5.	1
12	-0.0940	11.7853	-0.0341	3.8971	5.5780	1	-207.	637.	-5.	-207.	637.	-5.	1
13	-0.0826	11.5217	-0.0318	3.8130	5.4510	1	-202.	622.	-5.	-202.	622.	-5.	1
14	-0.0742	11.1802	-0.0261	3.7020	5.2880	1	-196.	604.	-4.	-196.	604.	-4.	1
15	-0.0768	10.7551	-0.0169	3.5594	5.0882	1	-188.	581.	-2.	-188.	581.	-2.	1
16	-0.0679	10.4847	-0.0057	3.4723	4.9586	1	-183.	566.	-1.	-183.	566.	-1.	1
17	1.5202	27.0059	-2.0803	9.5087	12.5038	1	-244.	915.	-189.	-244.	915.	-189.	1
18	-0.2778	17.0923	-1.0108	5.6049	8.1655	1	-197.	592.	-92.	-197.	592.	-92.	1
19	0.1013	14.1933	-0.6456	4.7649	6.6878	1	-152.	488.	-59.	-152.	488.	-59.	1
20	-0.1610	12.2670	-0.4036	4.0353	5.8303	1	-140.	425.	-37.	-140.	425.	-37.	1
21	-0.1508	12.0180	-0.4158	3.9557	5.7113	1	-137.	416.	-38.	-137.	416.	-38.	1
22	-0.0463	12.8327	-0.2879	4.2621	6.0649	1	-142.	443.	-26.	-142.	443.	-26.	1
23	-0.0462	13.3617	-0.1300	4.4385	6.3106	1	-148.	461.	-12.	-148.	461.	-12.	1
24	-0.0586	13.6961	-0.0633	4.5458	6.4705	1	-152.	473.	-6.	-152.	473.	-6.	1
25	-0.0775	13.8928	-0.0634	4.6051	6.5676	1	-155.	480.	-6.	-155.	480.	-6.	1
26	-0.0755	14.0201	-0.0898	4.6482	6.6274	1	-156.	484.	-8.	-156.	484.	-8.	1
27	-0.0585	14.0410	-0.0930	4.6608	6.6333	1	-156.	485.	-8.	-156.	485.	-8.	1
28	-0.0453	13.9927	-0.0388	4.6492	6.6070	1	-155.	483.	-4.	-155.	483.	-4.	1
29	1.0863	19.3552	-1.8022	6.8138	9.0003	1	-175.	656.	-164.	-175.	656.	-164.	1
30	-0.2156	11.9612	-1.0097	3.9152	5.7495	1	-139.	415.	-92.	-139.	415.	-92.	1
31	0.1120	9.7265	-0.6486	3.2795	4.5896	1	-103.	334.	-59.	-103.	334.	-59.	1
32	-0.0606	8.2403	-0.3433	2.7266	3.9090	1	-92.	285.	-31.	-92.	285.	-31.	1
33	-0.0616	7.9038	-0.2638	2.6141	3.7467	1	-89.	273.	-24.	-89.	273.	-24.	1
34	0.0388	8.2467	-0.3347	2.7618	3.8880	1	-89.	284.	-30.	-89.	284.	-30.	1
35	-0.1140	8.5251	-0.1324	2.8037	4.0473	1	-97.	295.	-12.	-97.	295.	-12.	1
36	-0.0915	8.4094	-0.0505	2.7726	3.9862	1	-95.	291.	-5.	-95.	291.	-5.	1
37	0.0261	8.7791	-0.2240	2.9350	4.1364	1	-95.	302.	-20.	-95.	302.	-20.	1
38	-0.0494	8.8843	-0.0907	2.9450	4.2004	1	-99.	307.	-8.	-99.	307.	-8.	1
39	-0.0362	9.0092	-0.2247	2.9910	4.2595	1	-100.	311.	-20.	-100.	311.	-20.	1
40	0.0091	9.1516	0.0409	3.0536	4.3121	1	-100.	315.	4.	-100.	315.	4.	1
41	-0.0220	9.2736	-0.2550	3.0839	4.3818	1	-102.	320.	-23.	-102.	320.	-23.	1
42	0.7174	13.2356	-1.1848	4.6510	6.1538	1	-120.	449.	-108.	-120.	449.	-108.	1
43	-0.1306	7.9766	-0.5746	2.6153	3.8203	1	-92.	276.	-52.	-92.	276.	-52.	1
44	-0.0317	5.8709	-0.2894	1.9464	2.7851	1	-65.	203.	-26.	-65.	203.	-26.	1
45	0.0221	5.4333	-0.0990	1.8185	2.5574	1	-59.	187.	-9.	-59.	187.	-9.	1
46	-0.2548	5.5958	0.0455	1.7803	2.7002	1	-70.	196.	4.	-70.	196.	4.	1
47	0.1976	9.3215	0.1507	3.1730	4.3501	1	-95.	319.	14.	-95.	319.	14.	1
48	-0.0204	13.4358	0.0236	4.4718	6.3385	1	-106.	1760.	35.	-106.	1760.	35.	1
49	-0.0032	13.6611	0.0394	4.5526	6.4407	1	-97.	1789.	59.	-97.	1789.	59.	1
50	0.0215	13.8096	0.0387	4.6104	6.5049	1	-83.	1808.	58.	-83.	1808.	58.	1

TABLE C-10. FINITE-ELEMENT ANALYSIS OF TYPICAL JOINT (continued)

STRESS ELEM	XX	YY	XY	ON	OS	CASE	(TOTAL STRAIN)*1000000. XX	YY	XY	(MECH. STRAIN)*1000000. XX	YY	XY	CASE
51	14.3545	0.0477	-0.0564	4.8007	9.7557	1	1879.	-70.	-84.	1879.	-70.	-84.	1
52	0.1052	14.1059	0.1022	4.7370	6.6255	1	-33.	1846.	152.	-33.	1846.	152.	1
53	0.2888	14.2874	0.1619	4.8588	6.6694	1	79.	1869.	242.	79.	1869.	242.	1
54	0.3579	12.9194	0.7580	4.4258	6.0395	1	131.	1689.	1131.	131.	1689.	1131.	1
55	0.1940	12.0090	0.5795	4.0677	5.6358	1	36.	1571.	865.	36.	1571.	865.	1
56	0.1533	11.0739	0.3571	3.7424	5.1927	1	18.	1449.	533.	18.	1449.	533.	1
57	0.1746	10.0657	0.2608	3.4134	4.7092	1	38.	1317.	389.	38.	1317.	389.	1
58	0.1297	8.9712	-0.0520	3.0336	4.1990	1	18.	1174.	-78.	18.	1174.	-78.	1
59	0.0515	7.7185	-0.0431	2.5900	3.6266	1	-22.	1010.	-64.	-22.	1010.	-64.	1
60	-0.0413	6.8731	-0.0890	2.2773	3.2506	1	-73.	900.	-133.	-73.	900.	-133.	1
61	-0.1219	6.2153	-0.1182	2.0312	2.9607	1	-118.	815.	-176.	-118.	815.	-176.	1
62	-0.1483	5.6797	-0.1371	1.8438	2.7154	1	-131.	745.	-205.	-131.	745.	-205.	1
63	-0.1302	5.2444	-0.1345	1.7047	2.5059	1	-117.	688.	-201.	-117.	688.	-201.	1
64	-0.1029	4.9215	-0.1157	1.6062	2.3465	1	-98.	645.	-173.	-98.	645.	-173.	1
65	-0.0883	4.7020	-0.0961	1.5379	2.2390	1	-87.	616.	-143.	-87.	616.	-143.	1
66	-0.0852	4.5509	-0.0822	1.4885	2.1667	1	-84.	597.	-123.	-84.	597.	-123.	1
67	-0.0832	4.3875	-0.0669	1.4348	2.0889	1	-82.	575.	-100.	-82.	575.	-100.	1
68	-0.0713	4.2080	-0.0430	1.3789	2.0010	1	-73.	552.	-64.	-73.	552.	-64.	1
69	-0.0561	4.1043	-0.0143	1.3494	1.9482	1	-63.	538.	-21.	-63.	538.	-21.	1
70	0.1199	13.7656	0.0611	4.6285	6.4613	1	-22.	1802.	91.	-22.	1802.	91.	1
71	0.2399	13.7928	-0.0549	4.6776	6.4463	1	52.	1805.	-82.	52.	1805.	-82.	1
72	0.2667	13.1870	0.4433	4.4846	6.1652	1	73.	1725.	662.	73.	1725.	662.	1
73	0.1520	12.0650	0.2871	4.0723	5.6569	1	10.	1579.	429.	10.	1579.	429.	1
74	0.0820	11.4455	0.1701	3.8425	5.3780	1	-29.	1498.	254.	-29.	1498.	254.	1
75	0.1764	11.3859	-0.0938	3.8541	5.3268	1	30.	1490.	-136.	30.	1490.	-136.	1
76	0.2097	9.1805	-0.5206	3.1301	4.3002	1	66.	1201.	-777.	66.	1201.	-777.	1
77	0.0473	7.8514	-0.4047	2.6329	3.7048	1	-25.	1028.	-604.	-25.	1028.	-604.	1
78	-0.0389	6.7607	-0.3522	2.2406	3.2091	1	-71.	886.	-526.	-71.	886.	-526.	1
79	-0.1213	5.9912	-0.3142	1.9567	2.8648	1	-117.	785.	-469.	-117.	785.	-469.	1
80	-0.1445	5.4670	-0.2843	1.7742	2.6222	1	-127.	717.	-424.	-127.	717.	-424.	1
81	-0.1207	5.1122	-0.2439	1.6638	2.4469	1	-110.	670.	-364.	-110.	670.	-364.	1
82	-0.0919	4.8547	-0.1948	1.5876	2.3160	1	-91.	636.	-291.	-91.	636.	-291.	1
83	-0.0800	4.6533	-0.1534	1.5244	2.2162	1	-82.	610.	-229.	-82.	610.	-229.	1
84	-0.0797	4.4955	-0.1248	1.4720	2.1407	1	-80.	589.	-186.	-80.	589.	-186.	1
85	-0.0790	4.3301	-0.0967	1.4170	2.0616	1	-79.	568.	-144.	-79.	568.	-144.	1
86	-0.0675	4.1644	-0.0594	1.3656	1.9798	1	-71.	546.	-89.	-71.	546.	-89.	1
87	-0.0525	4.0725	-0.0193	1.3400	1.9324	1	-61.	534.	-29.	-61.	534.	-29.	1
88	-0.0087	13.2252	0.0358	4.4055	6.2366	1	-97.	1732.	53.	-97.	1732.	53.	1
89	-0.0033	13.1120	0.0699	4.3696	6.1821	1	-93.	1717.	104.	-93.	1717.	104.	1
90	0.0182	13.0166	0.0563	4.3449	6.1320	1	-79.	1704.	84.	-79.	1704.	84.	1
91	0.0750	12.8960	-0.0302	4.3237	6.0617	1	-43.	1688.	-45.	-43.	1688.	-45.	1
92	0.1511	12.7648	-0.1890	4.3053	5.9841	1	5.	1671.	-282.	5.	1671.	-282.	1
93	0.1603	12.6375	0.3713	4.2659	5.9277	1	11.	1654.	554.	11.	1654.	554.	1
94	0.0866	12.5517	0.2055	4.2128	5.8990	1	-34.	1643.	307.	-34.	1643.	307.	1
95	12.8201	0.0577	-0.0640	4.2926	6.0301	1	1678.	-53.	-95.	1678.	-53.	-95.	1
96	0.0382	12.7344	0.1236	4.2582	5.9959	1	-65.	1668.	185.	-65.	1668.	185.	1
97	0.1519	12.7508	0.2370	4.3009	5.9785	1	5.	1669.	354.	5.	1669.	354.	1
98	0.2131	10.7325	0.7630	3.6485	5.0485	1	57.	1404.	1139.	57.	1404.	1139.	1
99	0.0854	9.7283	0.5900	3.2712	4.5913	1	-15.	1273.	881.	-15.	1273.	881.	1
100	0.0191	8.8374	0.4206	2.9521	4.1756	1	-50.	1157.	628.	-50.	1157.	628.	1

TABLE C-10. FINITE-ELEMENT ANALYSIS OF TYPICAL JOINT (continued)

STRESS ELEM	XX	YY	XY	ON	OS	CASE	(TOTAL STRAIN)*1000000. XX	YY	XY	(MECH. STRAIN)*1000000. XX	YY	XY	CASE
101	-0.0397	8.1352	0.3732	2.6985	3.8564	1	-81.	1066.	557.	-81.	1066.	557.	1
102	-0.0947	7.1143	-0.2047	2.3399	3.3804	1	-108.	932.	-306.	-108.	932.	-306.	1
103	-0.0256	5.7175	-0.1003	1.8973	2.7026	1	-56.	749.	-150.	-56.	749.	-150.	1
104	-0.0268	4.9660	-0.1066	1.6464	2.3490	1	-51.	650.	-159.	-51.	650.	-159.	1
105	-0.0625	4.4612	-0.1151	1.4662	2.1200	1	-70.	585.	-172.	-70.	585.	-172.	1
106	-0.0836	4.0935	-0.1249	1.3366	1.9523	1	-80.	537.	-186.	-80.	537.	-186.	1
107	-0.0799	3.6943	-0.1219	1.2048	1.7634	1	-75.	484.	-182.	-75.	484.	-182.	1
108	-0.0556	3.3420	-0.0883	1.0955	1.5903	1	-58.	438.	-132.	-58.	438.	-132.	1
109	-0.0317	3.1881	-0.0315	1.0521	1.5106	1	-42.	418.	-47.	-42.	418.	-47.	1
110	0.0633	12.1636	0.0757	4.0756	5.7195	1	-45.	1592.	113.	-45.	1592.	113.	1
111	0.1176	12.0410	-0.0604	4.0529	5.6489	1	-11.	1576.	-90.	-11.	1576.	-90.	1
112	0.1342	11.3660	0.3789	3.8334	5.3356	1	4.	1487.	566.	4.	1487.	566.	1
113	0.0495	10.0832	0.2644	3.3776	4.7465	1	-40.	1320.	395.	-40.	1320.	395.	1
114	-0.0258	9.1810	0.1929	3.0518	4.3369	1	-80.	1202.	288.	-80.	1202.	288.	1
115	-0.0191	8.5931	0.0403	2.8580	4.0555	1	-72.	1125.	60.	-72.	1125.	60.	1
116	0.0247	6.7145	-0.6099	2.2464	3.1984	1	-31.	879.	-910.	-31.	879.	-910.	1
117	-0.0102	5.9154	-0.4039	1.9684	2.8104	1	-47.	775.	-603.	-47.	775.	-603.	1
118	-0.0175	5.0622	-0.3217	1.6816	2.4049	1	-46.	663.	-480.	-46.	663.	-480.	1
119	-0.0577	4.4197	-0.2694	1.4540	2.1087	1	-66.	579.	-402.	-66.	579.	-402.	1
120	-0.0797	3.9718	-0.2351	1.2973	1.9011	1	-77.	521.	-351.	-77.	521.	-351.	1
121	-0.0739	3.5816	-0.1891	1.1692	1.7131	1	-71.	470.	-282.	-71.	470.	-282.	1
122	-0.0485	3.2625	-0.1159	1.0713	1.5524	1	-53.	428.	-173.	-53.	428.	-173.	1
123	-0.0244	3.1321	-0.0376	1.0359	1.4826	1	-37.	410.	-56.	-37.	410.	-56.	1
124	-0.0309	13.1432	0.0126	4.3808	6.1960	1	-92.	1721.	19.	-92.	1721.	19.	1
125	-0.0015	12.9152	0.0313	4.3046	6.0887	1	-91.	1691.	47.	-91.	1691.	47.	1
126	0.0027	12.7942	0.0296	4.2656	6.0306	1	-87.	1675.	44.	-87.	1675.	44.	1
127	0.0163	12.7325	-0.0295	4.2496	5.9984	1	-78.	1667.	-44.	-78.	1667.	-44.	1
128	0.0524	12.6966	-0.2182	4.2497	5.9756	1	-56.	1662.	-326.	-56.	1662.	-326.	1
129	0.0536	12.5486	0.2795	4.2007	5.9073	1	-54.	1643.	417.	-54.	1643.	417.	1
130	0.0182	12.2885	0.0942	4.1022	5.7891	1	-74.	1609.	141.	-74.	1609.	141.	1
131	0.0083	12.0339	0.0044	4.0141	5.6709	1	-79.	1576.	7.	-79.	1576.	7.	1
132	0.0704	11.8070	-0.1690	3.9591	5.5511	1	-39.	1546.	-252.	-39.	1546.	-252.	1
133	0.0334	11.5567	0.2184	3.8634	5.4430	1	-60.	1513.	326.	-60.	1513.	326.	1
134	0.0219	11.2844	0.0318	3.7688	5.3144	1	-65.	1478.	47.	-65.	1478.	47.	1
135	11.2803	0.0004	-0.0310	3.7602	5.3175	1	1477.	-78.	-46.	1477.	-78.	-46.	1
136	-0.0400	11.0360	0.0357	3.6653	5.2120	1	-101.	1445.	53.	-101.	1445.	53.	1
137	-0.0079	11.4123	0.2889	3.8015	5.3869	1	-84.	1495.	431.	-84.	1495.	431.	1
138	0.0160	9.2182	0.3027	3.0781	4.3487	1	-54.	1207.	452.	-54.	1207.	452.	1
139	-0.0057	7.5918	0.2704	2.5287	3.5869	1	-56.	994.	404.	-56.	994.	404.	1
140	0.0351	6.6366	0.1344	2.2239	3.1222	1	-24.	869.	201.	-24.	869.	201.	1
141	0.0067	5.9519	0.0835	1.9862	2.8050	1	-37.	779.	125.	-37.	779.	125.	1
142	-0.0246	4.1512	-0.2666	1.3789	1.9794	1	-44.	545.	-398.	-44.	545.	-398.	1
143	-0.0341	2.5011	-0.1558	0.8223	1.1939	1	-38.	328.	-233.	-38.	328.	-233.	1
144	-0.0473	1.8796	-0.1221	0.6108	0.9029	1	-42.	246.	-182.	-42.	246.	-182.	1
145	-0.0513	1.6335	-0.0743	0.5274	0.7848	1	-43.	214.	-111.	-43.	214.	-111.	1
146	-0.0339	1.7201	-0.0221	0.5621	0.8192	1	-33.	225.	-33.	-33.	225.	-33.	1
147	0.0124	2.3138	-0.0002	0.7754	1.0878	1	-8.	303.	-0.	-8.	303.	-0.	1
148	-0.0135	11.0259	0.0416	3.6708	5.2009	1	-85.	1444.	62.	-85.	1444.	62.	1
149	0.0011	10.4368	0.1136	3.4793	4.9206	1	-72.	1367.	170.	-72.	1367.	170.	1
150	0.0068	9.0469	0.0367	3.0179	4.2633	1	-59.	1185.	55.	-59.	1185.	55.	1

TABLE C-10. FINITE-ELEMENT ANALYSIS OF TYPICAL JOINT (continued)

STRESS ELEM	XX	YY	XY	ON	OS	CASE	(TOTAL STRAIN)*1000000. XX	YY	XY	(MECH. STRAIN)*1000000. XX	YY	XY	CASE
151	-0.0070	7.8581	0.0824	2.6170	3.7066	1	-59.	1029.	123.	-59.	1029.	123.	1
152	0.0150	6.9769	0.0611	2.3306	3.2858	1	-39.	914.	91.	-39.	914.	91.	1
153	-0.0064	6.7110	-0.1348	2.2348	3.1670	1	-51.	879.	-201.	-51.	879.	-201.	1
154	0.0437	3.7459	-0.6198	1.2632	1.8271	1	1.	490.	-925.	1.	490.	-925.	1
155	-0.0185	2.2964	-0.3160	0.7593	1.1171	1	-27.	301.	-472.	-27.	301.	-472.	1
156	-0.0364	1.7190	-0.1756	0.5609	0.8315	1	-34.	225.	-262.	-34.	225.	-262.	1
157	-0.0426	1.5245	-0.0870	0.4940	0.7324	1	-37.	200.	-130.	-37.	200.	-130.	1
158	-0.0285	1.6004	0.0148	0.5240	0.7613	1	-29.	210.	22.	-29.	210.	22.	1
159	0.0116	2.3725	0.0349	0.7947	1.1160	1	-9.	311.	52.	-9.	311.	52.	1
160	-0.0231	0.1255	0.0023	0.0341	0.0653	1	-882.	1758.	82.	-882.	1758.	82.	1
161	-0.0059	0.1334	-0.0049	0.0425	0.0645	1	-692.	1783.	-175.	-692.	1783.	-175.	1
162	0.0256	0.1523	0.0171	0.0593	0.0680	1	-364.	1886.	606.	-364.	1886.	606.	1
163	0.0639	0.1298	-0.0867	0.0646	0.0884	1	243.	1414.	-3079.	243.	1414.	-3079.	1
164	0.2776	0.3999	0.3560	0.2258	0.3354	1	1811.	3983.	12648.	1811.	3983.	12648.	1
165	0.3882	0.2480	0.8818	0.2121	0.7376	1	3966.	1476.	31326.	3966.	1476.	31326.	1
166	0.2353	0.1759	0.7295	0.1370	0.6040	1	2285.	1231.	25918.	2285.	1231.	25918.	1
167	0.1946	0.1507	0.5454	0.1151	0.4531	1	1866.	1087.	19378.	1866.	1087.	19378.	1
168	0.1680	0.1323	0.3692	0.1001	0.3100	1	1601.	967.	13115.	1601.	967.	13115.	1
169	0.0983	0.1023	0.2072	0.0669	0.1757	1	822.	894.	7361.	822.	894.	7361.	1
170	0.0694	0.0876	0.0950	0.0523	0.0863	1	509.	833.	3375.	509.	833.	3375.	1
171	-0.0336	0.0486	0.0218	0.0050	0.0381	1	-666.	794.	774.	-666.	794.	774.	1
172	-0.1159	0.0169	-0.0267	-0.0330	0.0629	1	-1602.	756.	-947.	-1602.	756.	-947.	1
173	-0.1459	0.0035	-0.0560	-0.0475	0.0833	1	-1936.	718.	-1990.	-1936.	718.	-1990.	1
174	-0.1318	0.0056	-0.0699	-0.0421	0.0854	1	-1760.	680.	-2482.	-1760.	680.	-2482.	1
175	-0.1062	0.0122	-0.0724	-0.0313	0.0795	1	-1454.	650.	-2573.	-1454.	650.	-2573.	1
176	-0.0911	0.0158	-0.0688	-0.0251	0.0733	1	-1272.	627.	-2443.	-1272.	627.	-2443.	1
177	-0.0874	0.0158	-0.0627	-0.0239	0.0684	1	-1223.	610.	-2228.	-1223.	610.	-2228.	1
178	-0.0852	0.0151	-0.0522	-0.0234	0.0614	1	-1190.	591.	-1856.	-1190.	591.	-1856.	1
179	-0.0731	0.0175	-0.0338	-0.0185	0.0480	1	-1043.	567.	-1199.	-1043.	567.	-1199.	1
180	-0.0579	0.0217	-0.0112	-0.0121	0.0349	1	-862.	553.	-399.	-862.	553.	-399.	1
181	-0.0155	0.1273	0.0477	0.0373	0.0749	1	-790.	1746.	1694.	-790.	1746.	1694.	1
182	-0.0050	0.1318	0.0608	0.0423	0.0805	1	-673.	1758.	2161.	-673.	1758.	2161.	1
183	0.0276	0.1440	0.0694	0.0572	0.0843	1	-300.	1768.	2466.	-300.	1768.	2466.	1
184	0.1146	0.1729	0.0772	0.0558	0.0955	1	712.	1747.	2741.	712.	1747.	2741.	1
185	0.2003	0.1979	0.0957	0.1327	0.1221	1	1724.	1681.	3398.	1724.	1681.	3398.	1
186	0.2191	0.2017	0.1502	0.1402	0.1579	1	1954.	1645.	5337.	1954.	1645.	5337.	1
187	0.1339	0.1701	0.1525	0.1013	0.1445	1	978.	1622.	5420.	978.	1622.	5420.	1
188	0.0616	0.1442	0.1234	0.0686	0.1168	1	146.	1613.	4384.	146.	1613.	4384.	1
189	0.0866	0.1587	0.0961	0.0817	0.1018	1	408.	1689.	3413.	408.	1689.	3413.	1
190	8.7822	3.1587	-0.2692	3.9803	3.6387	1	101009.	1117.	-9564.	101009.	1117.	-9564.	1
191	0.1964	0.1491	-0.7266	0.1152	0.5991	1	1898.	1057.	-25814.	1898.	1057.	-25814.	1
192	0.0758	0.0879	-0.6224	0.0545	0.5097	1	592.	807.	-22113.	592.	807.	-22113.	1
193	-0.0297	0.0415	-0.5088	0.0039	0.4164	1	-582.	683.	-18074.	-582.	683.	-18074.	1
194	-0.1115	0.0079	-0.4179	-0.0345	0.3456	1	-1503.	617.	-14848.	-1503.	617.	-14848.	1
195	-0.1362	-0.0039	-0.3468	-0.0467	0.2901	1	-1774.	576.	-12319.	-1774.	576.	-12319.	1
196	-0.1101	0.0033	-0.2844	-0.0356	0.2381	1	-1464.	551.	-10104.	-1464.	551.	-10104.	1
197	-0.0817	0.0124	-0.2284	-0.0231	0.1911	1	-1132.	539.	-8116.	-1132.	539.	-8116.	1
198	-0.0724	0.0153	-0.1824	-0.0190	0.1538	1	-1023.	535.	-6480.	-1023.	535.	-6480.	1
199	-0.0746	0.0143	-0.1476	-0.0201	0.1267	1	-1047.	532.	-5244.	-1047.	532.	-5244.	1
200	-0.0754	0.0135	-0.1116	-0.0206	0.0991	1	-1054.	525.	-3964.	-1054.	525.	-3964.	1

TABLE C-10. FINITE-ELEMENT ANALYSIS OF TYPICAL JOINT (continued)

STRESS ELEM	XX	YY	XY	ON	OS	CASE	(TOTAL STRAIN)*1000000. XX	YY	XY	(MECH. STRAIN)*1000000. XX	YY	XY	CASE
201	-0.0644	0.0165	-0.0662	-0.0160	0.0643	1	-924.	514.	-2351.	-924.	514.	-2351.	1
202	-0.0497	0.0211	-0.0210	-0.0095	0.0343	1	-751.	507.	-748.	-751.	507.	-748.	1
203	0.2326	0.1634	0.8775	0.1320	0.7231	1	2308.	1078.	31173.	2308.	1078.	31173.	1
204	0.1255	0.1136	0.7423	0.0797	0.6087	1	1128.	917.	26371.	1128.	917.	26371.	1
205	0.0558	0.0803	0.5583	0.0454	0.4571	1	364.	799.	19836.	364.	799.	19836.	1
206	-0.0707	0.0300	0.3674	-0.0136	0.3029	1	-1068.	720.	13052.	-1068.	720.	13052.	1
207	-0.1477	-0.0015	0.1609	-0.0497	0.1485	1	-1936.	661.	5715.	-1936.	661.	5715.	1
208	-0.0170	0.0384	0.0426	0.0071	0.0418	1	-401.	583.	1512.	-401.	583.	1512.	1
209	-0.0239	0.0338	-0.0184	0.0033	0.0280	1	-470.	555.	-655.	-470.	555.	-655.	1
210	-0.0591	0.0197	-0.0542	-0.0132	0.0555	1	-869.	531.	-1924.	-869.	531.	-1924.	1
211	-0.0321	0.0100	-0.0765	-0.0240	0.0749	1	-1126.	510.	-2719.	-1126.	510.	-2719.	1
212	-0.0812	0.0085	-0.0875	-0.0242	0.0820	1	-1107.	485.	-3107.	-1107.	485.	-3107.	1
213	-0.0587	0.0147	-0.0719	-0.0147	0.0667	1	-840.	463.	-2553.	-840.	463.	-2553.	1
214	-0.0358	0.0219	-0.0270	-0.0046	0.0324	1	-571.	453.	-960.	-571.	453.	-960.	1
215	-0.0028	0.1302	0.0247	0.0424	0.0652	1	-637.	1726.	879.	-637.	1726.	879.	1
216	-0.0016	0.1286	0.0286	0.0423	0.0653	1	-614.	1700.	1016.	-614.	1700.	1016.	1
217	0.0053	0.1300	0.0210	0.0451	0.0625	1	-529.	1686.	747.	-529.	1686.	747.	1
218	0.0381	0.1418	0.0063	0.0600	0.0601	1	-151.	1691.	223.	-151.	1691.	223.	1
219	0.0819	0.1552	0.0173	0.0790	0.0649	1	364.	1664.	615.	364.	1664.	615.	1
220	0.0865	0.1555	0.0841	0.0807	0.0936	1	422.	1647.	2989.	422.	1647.	2989.	1
221	0.0376	0.1379	0.0919	0.0585	0.0950	1	-141.	1642.	3264.	-141.	1642.	3264.	1
222	0.0320	0.1336	0.0700	0.0552	0.0807	1	-194.	1610.	2488.	-194.	1610.	2488.	1
223	0.0814	0.1452	0.0595	0.0756	0.0768	1	403.	1536.	2114.	403.	1536.	2114.	1
224	0.0962	0.1452	0.0950	0.0804	0.0982	1	597.	1467.	3374.	597.	1467.	3374.	1
225	0.0362	0.1197	0.0925	0.0520	0.0907	1	-75.	1409.	3287.	-75.	1409.	3287.	1
226	-0.0369	0.0882	0.0646	0.0171	0.0744	1	-892.	1330.	2297.	-892.	1330.	2297.	1
227	-0.0733	0.0793	0.0149	0.0020	0.0635	1	-1329.	1380.	530.	-1329.	1380.	530.	1
228	6.3445	2.1192	-0.0885	2.8212	2.6383	1	73721.	-1334.	-3145.	73721.	-1334.	-3145.	1
229	0.0436	0.0721	-0.6393	0.0386	0.5229	1	242.	747.	-22714.	242.	747.	-22714.	1
230	0.0228	0.0527	-0.5559	0.0251	0.4544	1	57.	588.	-19750.	57.	588.	-19750.	1
231	-0.0049	0.0354	-0.4502	0.0102	0.3680	1	-228.	489.	-15995.	-228.	489.	-15995.	1
232	-0.0465	0.0166	-0.3619	-0.0099	0.2967	1	-688.	433.	-12855.	-688.	433.	-12855.	1
233	-0.0723	0.0052	-0.2947	-0.0223	0.2432	1	-975.	402.	-10468.	-975.	402.	-10468.	1
234	-0.0670	0.0052	-0.2199	-0.0206	0.1826	1	-906.	377.	-7814.	-906.	377.	-7814.	1
235	-0.0423	0.0129	-0.1260	-0.0098	0.1056	1	-616.	364.	-4477.	-616.	364.	-4477.	1
236	-0.0190	0.0208	-0.0389	0.0006	0.0357	1	-346.	361.	-1382.	-346.	361.	-1382.	1
237	0.0130	0.0739	0.5061	0.0290	0.4145	1	-169.	913.	17981.	-169.	913.	17981.	1
238	0.0123	0.0577	0.3615	0.0233	0.2962	1	-104.	703.	12841.	-104.	703.	12841.	1
239	0.0536	0.0639	0.2194	0.0392	0.1813	1	412.	593.	7795.	412.	593.	7795.	1
240	0.0039	0.0394	0.0857	0.0134	0.0723	1	-169.	514.	3043.	-169.	514.	3043.	1
241	-0.0497	0.0134	-0.0392	-0.0121	0.0419	1	-715.	405.	-1391.	-715.	405.	-1391.	1
242	-0.0322	0.0121	-0.0892	-0.0067	0.0752	1	-480.	308.	-3170.	-480.	308.	-3170.	1
243	-0.0512	0.0028	-0.0911	-0.0162	0.0784	1	-687.	272.	-3237.	-687.	272.	-3237.	1
244	-0.0554	0.0005	-0.0692	-0.0183	0.0623	1	-731.	261.	-2458.	-731.	261.	-2458.	1
245	-0.0359	0.0080	-0.0352	-0.0093	0.0345	1	-509.	271.	-1251.	-509.	271.	-1251.	1
246	0.0113	0.0275	-0.0092	0.0130	0.0136	1	22.	310.	-327.	22.	310.	-327.	1

TABLE C-10. FINITE-ELEMENT ANALYSIS OF TYPICAL JOINT (continued)

X FORCE, CASE 1

	1	2	3	4	5	6	7	8	9	10
1	5.649E-03	5.960E-08	1.229E-07	5.960E-08	-1.267E-07	5.960E-08	-5.960E-08	4.034E-03	1.192E-07	-1.453E-07
11	1.192E-07	-1.825E-07	2.980E-07	-2.384E-07	-7.210E-04	2.384E-07	-2.049E-07	2.980E-07	-7.823E-08	-5.960E-08
21	-2.980E-07	-5.889E-03	0.0	-5.960E-08	-1.192E-07	1.788E-07	-1.155E-07	1.192E-07	0.0	-1.344E-02
31	5.960E-08	-5.960E-08	-7.451E-09	5.960E-08	-1.714E-07	0.0	-5.960E-08	-3.267E-02	1.192E-07	1.192E-07
41	2.608E-08	1.788E-07	6.706E-08	1.192E-07	5.960E-08	-2.683E-02	-1.267E-06	0.0	5.960E-08	5.588E-08
51	0.0	1.639E-07	-5.960E-08	1.192E-07	-1.771E-02	-3.003E-06	-5.960E-08	-5.960E-08	7.451E-08	-1.192E-07
61	-6.557E-07	-2.272E-07	5.960E-08	1.192E-07	-1.704E-02	-3.494E-06	5.960E-08	-1.789E-07	-6.706E-08	5.960E-08
71	0.0	3.353E-08	0.0	5.960E-08	-8.162E-03	-2.135E-06	-5.960E-08	-5.960E-08	-1.602E-07	4.508E-07
81	-1.192E-07	1.192E-07	2.012E-07	0.0	1.788E-07	-9.959E-03	-3.304E-06	0.0	0.0	2.980E-08
91	2.861E-06	-2.109E-06	-1.192E-07	-5.960E-08	-3.725E-09	0.0	0.0	-3.503E-03	-3.066E-06	0.0
101	5.960E-08	-5.588E-08	2.861E-06	-2.833E-06	0.0	-5.960E-08	-3.725E-09	-1.192E-07	2.384E-07	-1.192E-07
111	7.089E-03	-5.137E-06	5.960E-08	1.192E-07	-8.941E-08	1.907E-06	-4.369E-06	1.192E-07	-1.788E-07	-3.055E-07
121	-1.118E-08	4.843E-07	0.0	1.303E-02	-4.724E-06	0.0	0.0	-1.118E-08	1.907E-06	-4.135E-06
131	5.960E-08	1.788E-07	-2.645E-07	3.469E-07	5.215E-08	2.049E-07	0.0	1.389E-02	-3.275E-06	5.960E-08
141	-1.788E-07	9.313E-08	3.815E-06	-4.217E-06	1.192E-07	2.384E-07	-7.823E-08	6.676E-06	-9.889E-06	7.823E-08
151	-1.416E-07	-2.384E-07	1.181E-02	-3.904E-06	1.788E-07	-1.192E-07	-1.714E-07	4.768E-06	-2.891E-06	1.192E-07
161	0.0	-9.313E-08	0.0	-1.626E-06	8.568E-08	7.078E-08	-5.960E-08	9.822E-03	-3.181E-06	1.192E-07
171	-1.788E-07	7.078E-08	4.768E-06	-3.852E-06	5.960E-08	1.192E-07	-5.215E-08	3.815E-06	-5.486E-06	-7.078E-08
181	1.043E-07	-1.192E-07	8.954E-03	-4.426E-06	2.384E-07	0.0	-6.706E-08	3.815E-06	-3.826E-06	1.192E-07
191	5.960E-08	-1.467E-08	2.861E-06	-4.553E-06	-5.960E-08	9.686E-08	9.537E-07	1.317E-02	-2.053E-06	1.192E-07
201	-1.527E-07	2.608E-08	2.861E-06	-5.497E-07	7.078E-08	-1.490E-08	-1.173E-07	1.866E-06	-3.020E-06	1.080E-07
211	5.960E-07	1.979E-05	2.205E-06	-1.329E-06	1.527E-07	2.347E-07	1.132E-06	-2.980E-07	2.023E-02	-3.554E-06
221	1.416E-07	7.078E-08	-2.093E-07	4.292E-06	-5.084E-06	2.310E-07	-2.421E-07	-6.799E-08	-1.494E-06	-1.787E-06
231	1.229E-07	3.949E-07	1.311E-06	-2.231E-06	-9.688E-07	3.055E-07	-1.676E-07	3.755E-06	-2.727E-06	1.982E-02
241	-5.625E-07	5.960E-08	-9.686E-08	-1.863E-08	2.861E-06	-3.595E-06	2.384E-07	-1.788E-07	-7.451E-08	4.131E-06
251	-1.710E-06	-1.192E-07	1.192E-07	1.907E-06	-1.907E-06	8.615E-03	5.588E-08	5.960E-08	0.0	-2.235E-08
261	9.537E-07	-1.688E-06	5.960E-08	-5.960E-08	-6.706E-08	9.537E-07	-1.013E-06	-5.960E-08	5.960E-08	3.052E-05
271	-3.052E-05									

TABLE C-10. FINITE-ELEMENT ANALYSIS OF TYPICAL JOINT (continued)

Y FORCE, CASE 1

	1	2	3	4	5	6	7	8	9	10
1	-1.788E-07	4.240E-01	4.240E-01	4.240E-01	4.240E-01	2.120E-01	2.120E-01	0.0	0.0	-2.980E-07
11	-1.907E-06	1.371E-06	-1.907E-06	2.574E-06	-1.192E-07	9.537E-07	1.431E-06	0.0	2.205E-06	-1.907E-06
21	1.356E-06	5.960E-08	-2.289E-05	1.144E-05	7.853E-06	0.0	6.519E-07	0.0	1.192E-06	-5.960E-08
31	-5.537E-07	2.861E-06	3.498E-06	1.907E-06	9.947E-07	0.0	2.861E-06	-8.941E-07	-1.907E-06	3.815E-06
41	3.431E-06	9.537E-07	7.674E-07	9.537E-07	2.384E-06	0.0	3.248E-05	-9.537E-07	3.815E-06	4.403E-06
51	1.907E-06	1.233E-06	-9.537E-07	1.967E-06	-2.193E-05	2.604E-05	-4.172E-07	3.278E-06	2.004E-06	-6.914E-06
61	8.593E-06	-3.736E-06	-9.537E-07	2.861E-06	6.676E-06	1.563E-05	-2.384E-07	1.848E-06	1.352E-06	-7.749E-07
71	3.576E-07	2.958E-06	-1.311E-06	2.086E-06	-3.910E-05	6.415E-06	-2.384E-06	1.848E-06	-3.800E-07	-1.814E-06
81	7.153E-07	1.609E-06	1.471E-06	-8.941E-07	1.073E-06	-1.049E-05	6.560E-06	-1.788E-07	2.384E-07	-2.719E-07
91	-2.861E-06	8.035E-06	-4.172E-07	4.172E-07	1.956E-06	-1.192E-07	8.941E-07	-6.676E-06	-6.977E-06	-1.788E-07
101	5.364E-07	-6.035E-07	9.537E-07	3.553E-05	1.371E-06	1.788E-07	1.639E-07	1.132E-06	-1.407E-05	2.325E-06
111	-1.431E-05	9.052E-06	1.729E-06	1.192E-07	2.258E-06	-1.049E-05	-2.816E-06	1.431E-06	2.384E-07	3.058E-06
121	-5.537E-07	1.371E-06	1.132E-06	-1.243E-05	-1.609E-06	4.768E-07	1.609E-06	1.535E-06	9.537E-07	6.191E-06
131	0.0	3.576E-07	-1.676E-07	-8.307E-07	-9.537E-07	2.980E-07	7.153E-07	-8.583E-06	-1.350E-05	5.960E-07
141	8.345E-07	-3.949E-07	-1.907E-06	2.831E-07	-1.132E-06	1.848E-06	1.062E-06	-2.384E-05	1.330E-05	-8.941E-07
151	7.749E-07	1.132E-06	9.537E-07	-4.284E-07	-5.364E-07	1.311E-06	-5.960E-07	1.907E-06	1.047E-06	-7.153E-07
161	1.192E-06	9.127E-07	-2.861E-06	6.340E-06	-1.431E-06	1.967E-06	5.960E-07	1.907E-06	-3.044E-06	-5.364E-07
171	-7.749E-07	-1.229E-07	0.0	2.049E-06	5.960E-08	5.364E-07	-8.568E-08	-2.861E-06	3.077E-06	-2.027E-06
181	2.384E-07	1.252E-06	4.768E-06	-3.111E-06	0.0	0.0	1.118E-08	3.815E-06	1.539E-06	-1.192E-07
191	1.550E-06	-1.229E-07	2.861E-06	-5.849E-07	-1.132E-06	2.980E-07	-1.080E-07	1.907E-06	-1.632E-06	-3.576E-07
201	5.960E-08	9.537E-07	1.907E-06	1.453E-07	0.0	-1.371E-06	4.992E-07	5.186E-06	-2.913E-06	0.0
211	-7.153E-07	-1.717E-05	6.676E-06	4.549E-06	-1.788E-07	-6.557E-07	-1.907E-06	1.311E-06	-9.537E-06	-3.092E-06
221	-1.013E-06	4.768E-07	7.488E-07	-1.907E-06	2.388E-06	0.0	-1.073E-06	2.682E-07	3.576E-07	1.907E-06
231	-1.192E-07	-2.980E-07	9.537E-07	3.695E-06	3.047E-06	-5.960E-08	-2.980E-07	-1.550E-06	3.040E-06	1.285E-06
241	3.883E-07	2.496E-07	-7.343E-07	2.065E-07	-2.205E-06	2.615E-06	4.843E-08	-6.706E-08	2.380E-07	-1.073E-06
251	2.884E-06	-1.863E-08	-8.605E-07	-9.537E-07	2.205E-06	-1.304E-01	-1.307E-01	-6.497E-02	-1.295E-01	-6.476E-02
261	-3.423E-01	-3.570E-01	-4.995E-02	-9.988E-02	-5.017E-02	-1.946E-01	-2.693E-01	-1.790E-02	-4.065E-02	5.190E-01
271	-6.973E-01									

CHECKS, SUM		X-FORCES	Y-FORCES	Z-MOMENTS	CASE
		1.363D-04	-2.489D-04	-1.467D-04	1
NZE	BARK	4710			
	+RHS	4716			
	REDU	4356			

UPPER PLATE

Introduction

Three finite-element models were used to analyze the upper plate. Each model was of moderate size with a fine mesh of elements in a specific region of interest. The first model was used to determine the stresses at the hole for the lead-lag pin; the second, the stresses at the center hole; and the third strains during the fatigue test of the model hub.

Lugs at Lead-Lag Pin

The load pattern for the analysis is shown in Figure C-23. Figure C-24 shows the finite-element model for the analysis of the joint at the lead-lag pin. This model has 269 nodes and 338 elements. Nodes 1 - 149 and elements 1 - 216 are identical to those in the finite-element model for the element specimen. The elements perform the same roles as described for the element specimen. Table C-11 presents the results of the analysis using this model for the calculated ultimate loads of Condition TW7F1, which produces the highest lug load of 89.97 kips, as shown in Table C-6.

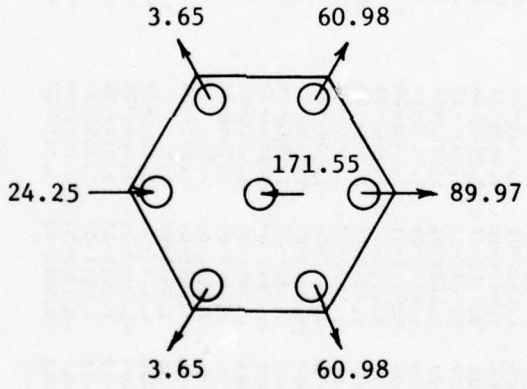


Figure C-23. Load pattern for upper plate, condition TW7F1 ultimate.

The following comparisons establish that the critical stresses in the upper plate in the immediate vicinity of the outer holes are similar within a few percent to those in the element specimens. The margins of safety for the upper plate are then found by direct use of the experimental results from the element tests. In general, this is conservative because the strain gage results, shown in Figure 34, indicated that measured loads in the upper plate were lower than the analytical predictions. In addition, the clamp-up of the upper and pan plates by the bearing housing allows a partial transfer of load by friction, which reduces the load transferred by the pins in the lug.

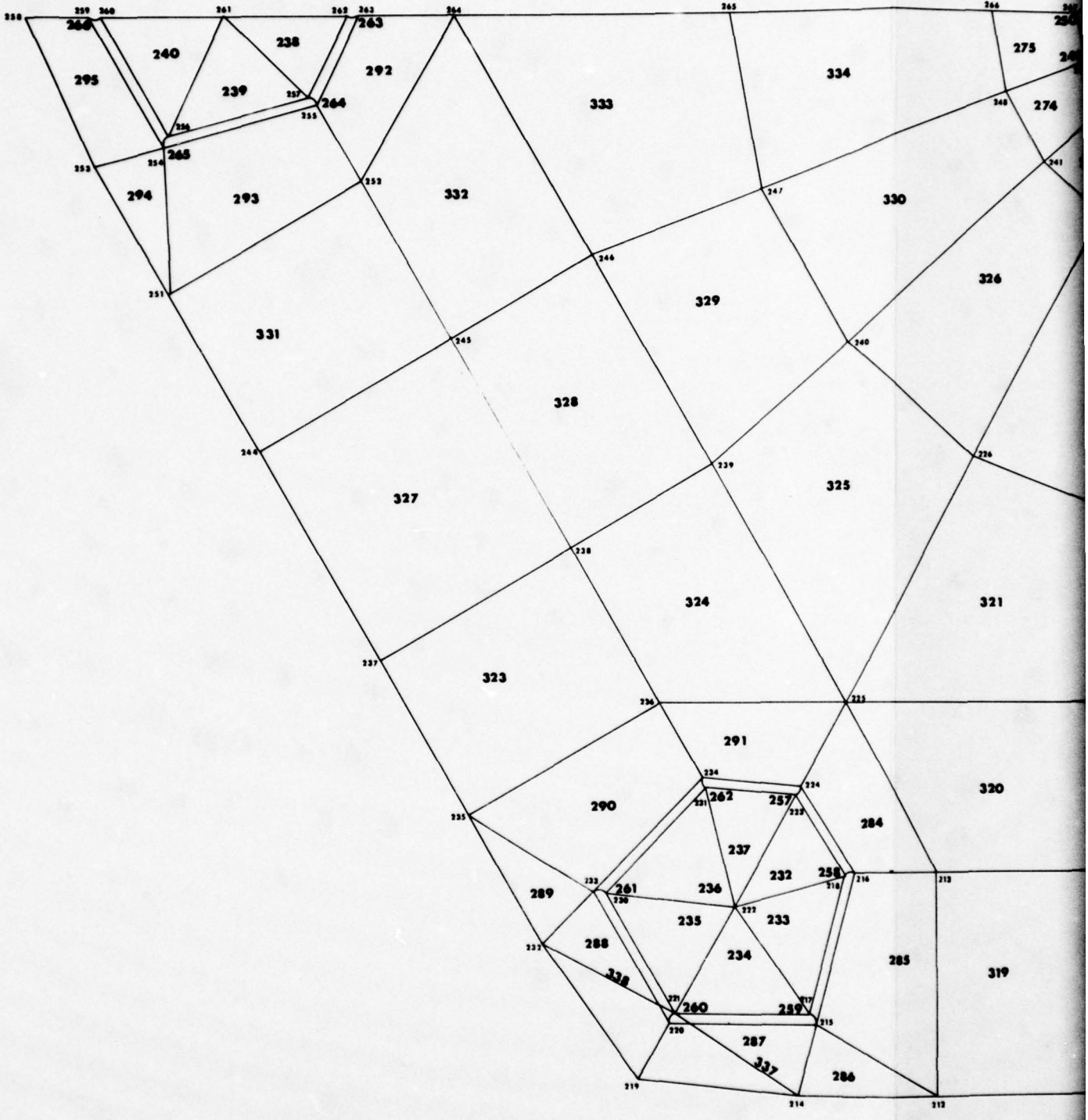
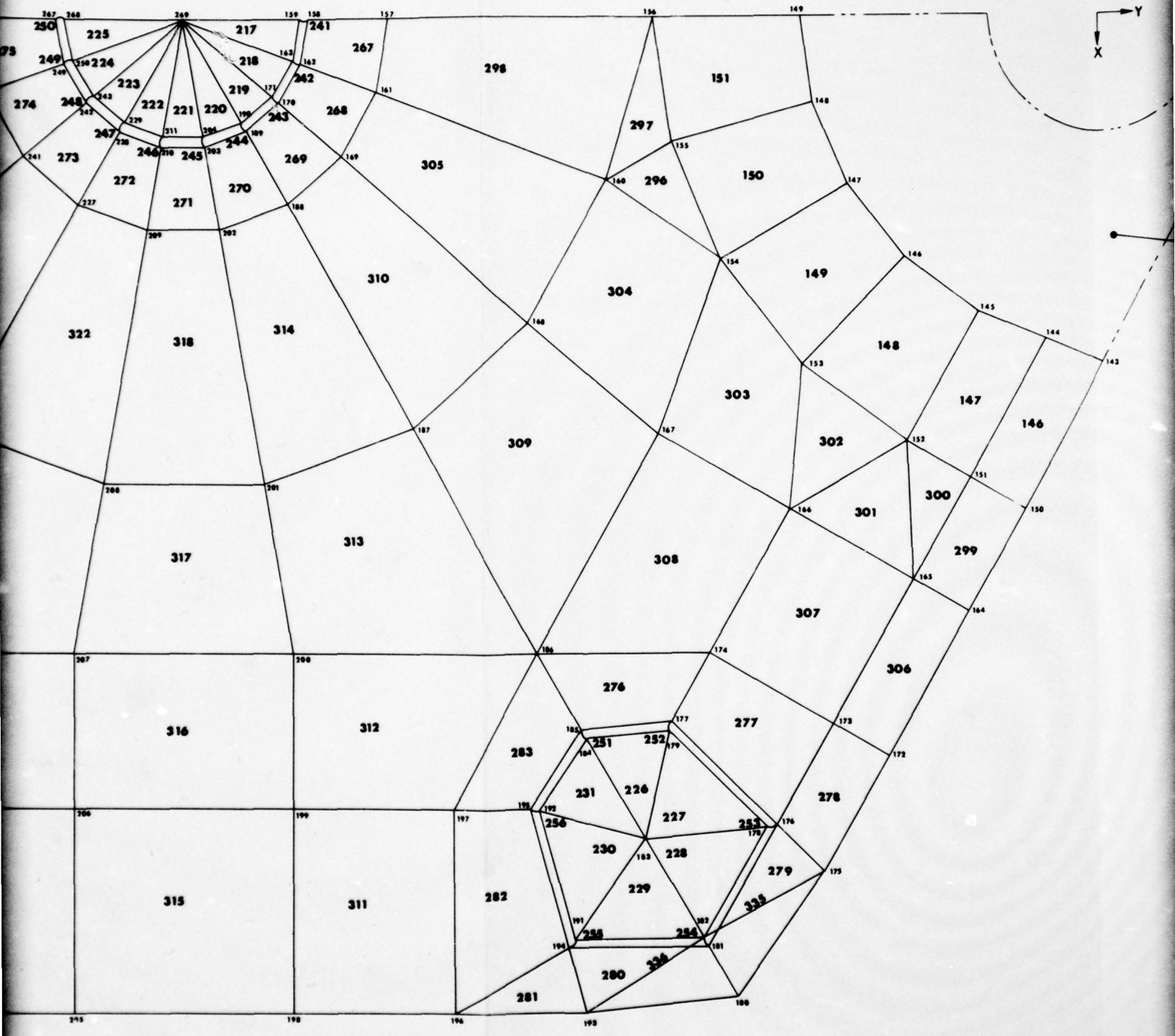


Figure C-24. Finite-element model for lead-lag joints in upper plate.


Y
X
225
217
224
218
223
219
222
221
220
241
242
243
244
245
246
247
248
249
250
267
268
269
159
158
157
156
149
163
162
161
171
170
169
168
167
166
165
164
163
162
161
160
159
158
157
156
155
154
153
152
151
150
149
148
147
146
145
144
143
142
141
140
139
138
137
136
135
134
133
132
131
130
129
128
127
126
125
124
123
122
121
120
119
118
117
116
115
114
113
112
111
110
109
108
107
106
105
104
103
102
101
100
99
98
97
96
95
94
93
92
91
90
89
88
87
86
85
84
83
82
81
80
79
78
77
76
75
74
73
72
71
70
69
68
67
66
65
64
63
62
61
60
59
58
57
56
55
54
53
52
51
50
49
48
47
46
45
44
43
42
41
40
39
38
37
36
35
34
33
32
31
30
29
28
27
26
25
24
23
22
21
20
19
18
17
16
15
14
13
12
11
10
9
8
7
6
5
4
3
2
1
267
298
151
297
268
305
296
150
269
272
271
270
310
304
149
322
318
314
148
303
147
146
309
302
301
300
317
313
308
299
307
306
276
316
312
277
283
278
231
226
227
279
230
228
229
282
315
311
280
281
251
252
253
254
255
256
257
258
259
260
261
262
263
264
265
266

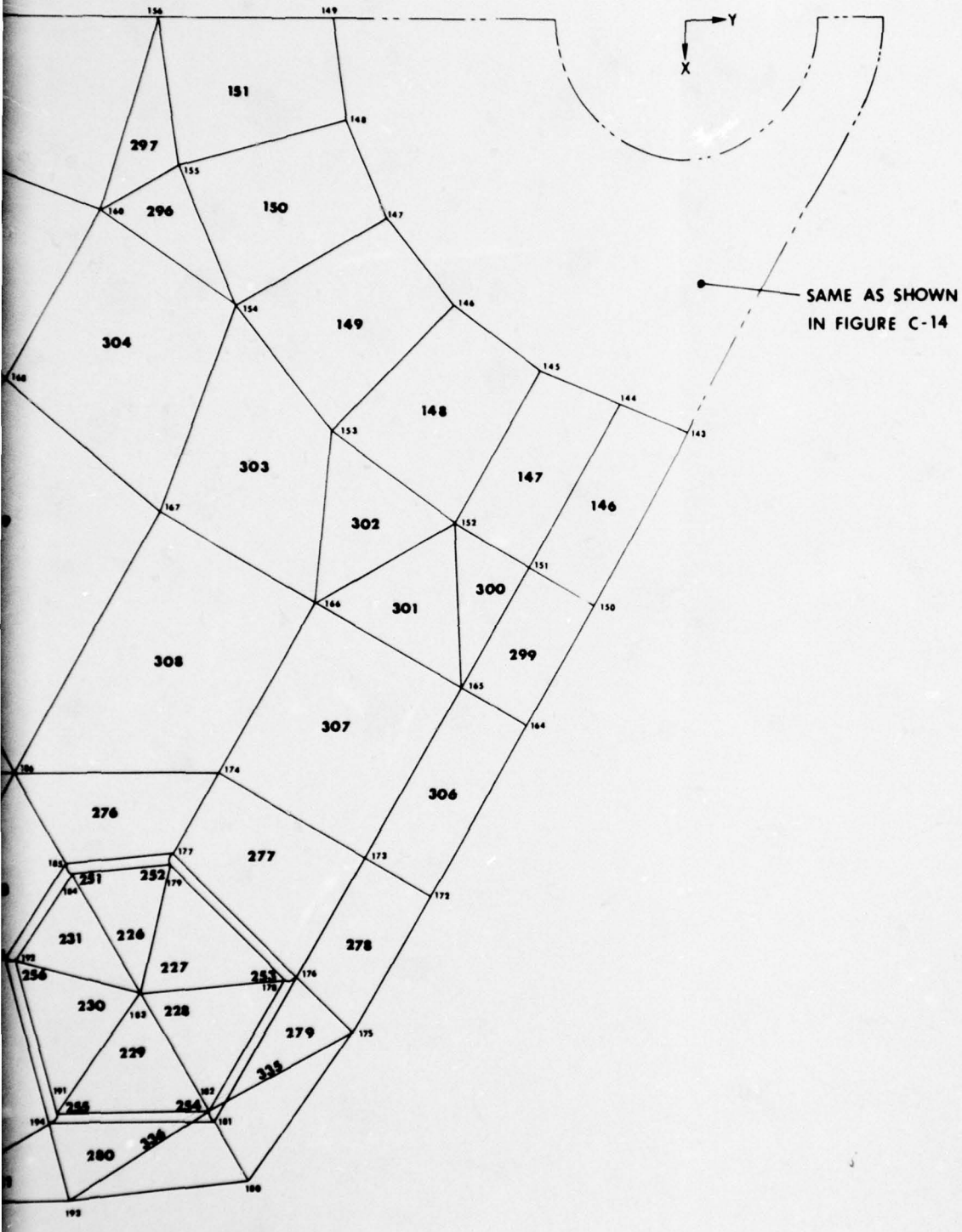

Y
X
SAME AS SHOWN
IN FIGURE C-14
151
297
150
296
304
149
148
303
147
146
302
301
300
299
308
307
306
276
277
278
231
226
227
230
228
279
229
280
156
149
148
155
160
147
154
146
145
144
143
153
152
151
150
167
166
165
164
174
173
172
177
179
176
175
191
182
181
190
193

TABLE C-11. FINITE-ELEMENT ANALYSIS OF LEAD-LAG JOINT IN UPPER PLATE FOR ULTIMATE LOADS OF CONDITION TW7F1

X COORDINATES AND SUPPORTS

	1	2	3	4	5	6	7	8	9	10
1	0.0 S	0.0 S	0.8310	1.5800	2.1750	2.3950	2.5560	2.6550	2.6880	2.6550
11	2.5560	2.1750	1.5800	0.8310	0.0 S	0.0 S	0.8310	1.5800	2.1750	2.3950
21	2.5560	2.6550	2.6880	2.6550	2.5560	2.1750	1.5800	0.8310	0.0 S	0.0 S
31	0.8660	1.6480	2.2680	2.4980	2.6670	2.7690	2.8040	2.7690	2.6670	2.2680
41	1.6480	0.8660	0.0 S	0.0 S	0.9020	1.7160	2.3620	2.6020	2.7770	2.8840
51	2.9200	2.8840	2.7770	2.3620	1.7160	0.9020	0.0 S	0.0 S	0.9270	1.7630
61	2.4270	2.6730	2.8530	2.9630	3.0000	2.9630	2.8530	2.4270	1.7630	0.9270
71	0.0 S	0.0 S	0.9700	1.8460	2.5400	2.7980	2.9860	3.1010	3.1400	3.1010
81	2.9860	2.5400	1.8460	0.9700	0.0 S	0.0 S	1.0570	2.0100	2.7670	3.0470
91	3.2530	3.3780	3.4200	3.3780	3.2530	2.7670	2.0100	1.0560	0.0 S	0.0 S
101	1.3700	2.6000	3.5100	4.0000	4.1700	4.2000	4.1200	3.9600	3.7000	2.4900
111	2.0900	4.1900	4.5500	4.5200	4.0700	3.2900	2.2600	1.1700	0.0 S	4.7300
121	4.9500	4.9100	4.4200	3.5700	2.4800	1.3700	0.0 S	5.2400	5.3500	5.3100
131	4.7800	3.8600	2.6800	1.3800	0.0 S	6.1400	6.1000	5.4900	4.4400	3.0900
141	1.5900	0.0 S	8.7800	8.1600	7.4700	6.0800	4.2300	2.1800	0.0 S	11.9300
151	11.6600	10.7300	8.7600	6.1000	3.1500	0.0 S	0.0 S	0.0 S	0.0 S	4.0900
161	1.8500	1.1287	1.0603	15.3600	14.2200	12.4200	10.4700	7.6900	3.4700	2.1212
171	1.9926	18.7000	17.8600	16.0200	21.6600	20.4100	17.7800	20.4300	17.9742	24.7800
181	23.4900	23.3167	20.7500	18.1529	17.9800	16.0200	10.3600	4.6800	2.8579	2.6847
191	23.3676	19.9837	25.1800	23.5300	19.9300	25.1800	19.9300	25.1800	19.9300	16.0200
201	11.7500	5.3200	3.2499	3.0529	25.1800	19.9300	16.0200	11.7500	5.3200	3.2499
211	3.0529	25.1800	19.9300	25.1800	23.5300	19.9300	23.3676	19.9837	24.7800	23.4900
221	23.3167	20.7500	18.1529	17.9800	16.0200	10.3600	4.6800	2.8579	2.6847	20.4300
231	17.9742	21.6600	20.4100	17.7800	18.7000	16.0200	15.0600	12.4200	10.4700	7.6900
241	3.4700	2.1212	1.9926	10.1500	7.5400	5.5700	4.0500	1.8500	1.1287	1.0603
251	6.4700	3.8600	3.5000	3.0400	2.0600	2.7800	1.8800	0.0 S	0.0 S	0.0 S
261	0.0 S	0.0 S	0.0 S	0.0 S	0.0 S	0.0 S	0.0 S	0.0 S	0.0 S	

TABLE C-11. FINITE-ELEMENT ANALYSIS OF LEAD-LAG JOINT IN UPPER PLATE FOR ULTIMATE LOADS OF CONDITION TW7F1 (continued)

Y COORDINATES AND SUPPORTS

	1	2	3	4	5	6	7	8	9	10
1	0.0	2.6880	2.5560	2.1750	1.5800	1.2200	0.8310	0.4200	0.0	-0.4200
11	-0.8310	-1.5800	-2.1750	-2.5560	-2.6880	2.6880	2.5560	2.1750	1.5800	1.2200
21	0.8310	0.4200	0.0	-0.4200	-0.8310	-1.5800	-2.1750	-2.5560	-2.6880	2.8040
31	2.6670	2.2680	1.6480	1.2730	0.8670	0.4390	0.0	-0.4390	-0.8670	-1.6480
41	-2.2680	-2.6670	-2.8040	2.9200	2.7770	2.3620	1.7160	1.3260	0.9020	0.4570
51	0.0	-0.4570	-0.9020	-1.7160	-2.3620	-2.7770	-2.9200	3.0000	2.8530	2.4270
61	1.7630	1.3620	0.9270	0.4690	0.0	-0.4690	-0.9270	-1.7630	-2.4270	-2.8530
71	-3.0000	3.1400	2.9860	2.5400	1.8460	1.4260	0.9700	0.4910	0.0	-0.4910
81	-0.9700	-1.8460	-2.5400	-2.9860	-3.1400	3.4200	3.2530	2.7670	2.0100	1.5530
91	1.0570	0.5350	0.0	-0.5350	-1.0570	-2.0100	-2.7670	-3.2530	-3.4200	4.4000
101	4.2000	3.5900	3.0400	2.0200	1.2600	0.6500	-0.0400	-0.6500	-1.2400	-2.2100
111	-2.9000	2.6600	1.3600	-0.0700	-1.4000	-2.4700	-3.2500	-3.7000	-3.8500	2.3400
121	1.4000	-0.1400	-1.9600	-2.7500	-3.5800	-4.0900	-4.2500	2.0500	1.4400	-0.2100
131	-1.7700	-3.0300	-3.9400	-4.4800	-4.6500	1.5200	-0.3500	-2.1400	-3.5900	-4.6300
141	-5.2600	-5.4700	0.0	-1.5400	-3.2900	-5.1900	-6.6300	-7.4800	-7.7600	-2.1200
151	-3.5400	-5.1700	-7.8200	-9.8900	-11.1200	-11.5300	-10.6000	-20.7000	-20.9000	-12.7800
161	-18.9300	-20.8990	-21.0870	-3.6000	-5.0200	-8.1600	-11.5400	-14.8500	-19.8600	-21.4721
171	-21.6253	-5.7000	-7.1400	-10.2500	-7.4200	-8.6200	-11.2700	-8.8190	-11.3177	-9.6700
181	-10.4200	-10.5199	-12.0000	-13.5035	-13.6100	-14.7400	-16.0900	-21.3000	-22.3500	-22.4500
191	-13.8832	-14.7474	-13.5300	-14.0000	-14.9400	-17.0100	-17.0100	-21.1800	-21.1800	-21.1800
201	-21.9300	-23.0600	-23.4270	-23.4617	-26.8200	-26.8200	-26.8200	-26.0700	-24.9400	-24.5730
211	-24.5383	-30.9900	-30.9900	-34.4700	-34.0000	-33.0600	-34.1168	-33.2526	-38.3300	-37.5800
221	-37.4801	-36.0000	-34.4905	-34.3900	-33.2600	-29.9700	-26.7000	-25.6500	-25.5500	-39.1810
231	-36.6822	-40.5800	-39.3800	-36.7300	-42.3000	-37.7500	-44.4000	-39.8400	-36.4600	-33.1500
241	-26.1400	-26.5279	-26.3747	-47.2000	-47.6400	-34.2800	-35.2200	-29.0700	-27.4010	-26.9130
251	-49.3300	-44.7800	-51.0500	-49.4000	-45.7900	-49.2800	-45.9800	-52.6600	-51.1800	-50.8700
261	-48.3000	-45.0600	-44.8200	-42.5200	-39.9400	-29.4000	-27.3000	-27.1000	-24.0000 S	

LOADS, CASE 1

1	X	0.0
1	Y	44.985
183	X	52.810
183	Y	30.490
222	X	3.161
222	Y	-1.825
261	X	0.0
261	Y	12.125

TABLE C-11. FINITE-ELEMENT ANALYSIS OF LEAD-LAG JOINT IN UPPER PLATE FOR ULTIMATE LOADS OF CONDITION TW7F1 (continued)

ELEM	P	Q	R	S	TYPE	E	PR	THICK-AREA	ALPHA	TEM 1	TEM 2	TEM 3	TEM 4	TEM 5
1	2	3	1	0	2	29000.	0.3180	0.5000	0.00000560	0.				
2	3	4	1	0	2	29000.	0.3180	0.5000	0.00000560	0.				
3	4	5	1	0	2	29000.	0.3180	0.5000	0.00000560	0.				
4	5	6	1	0	2	29000.	0.3180	0.5000	0.00000560	0.				
5	6	7	1	0	2	29000.	0.3180	0.5000	0.00000560	0.				
6	7	8	1	0	2	29000.	0.3180	0.5000	0.00000560	0.				
7	8	9	1	0	2	29000.	0.3180	0.5000	0.00000560	0.				
8	9	10	1	0	2	29000.	0.3180	0.5000	0.00000560	0.				
9	10	11	1	0	2	29000.	0.3180	0.5000	0.00000560	0.				
10	11	12	1	0	2	29000.	0.3180	0.5000	0.00000560	0.				
11	12	13	1	0	2	29000.	0.3180	0.5000	0.00000560	0.				
12	13	14	1	0	2	29000.	0.3180	0.5000	0.00000560	0.				
13	14	15	1	0	2	29000.	0.3180	0.5000	0.00000560	0.				
14	17	16	30	31	3	16200.	0.3180	0.5000	0.00000490	0.				
15	16	17	31	32	3	16200.	0.3180	0.5000	0.00000490	0.				
16	19	18	32	33	3	16200.	0.3180	0.5000	0.00000490	0.				
17	20	19	33	34	3	16200.	0.3180	0.5000	0.00000490	0.				
18	21	20	34	35	3	16200.	0.3180	0.5000	0.00000490	0.				
19	22	21	35	36	3	16200.	0.3180	0.5000	0.00000490	0.				
20	23	22	36	37	3	16200.	0.3180	0.5000	0.00000490	0.				
21	24	23	37	38	3	16200.	0.3180	0.5000	0.00000490	0.				
22	25	24	38	39	3	16200.	0.3180	0.5000	0.00000490	0.				
23	26	25	39	40	3	16200.	0.3180	0.5000	0.00000490	0.				
24	27	26	40	41	3	16200.	0.3180	0.5000	0.00000490	0.				
25	28	27	41	42	3	16200.	0.3180	0.5000	0.00000490	0.				
26	29	28	42	43	3	16200.	0.3180	0.5000	0.00000490	0.				
27	31	30	44	45	3	16200.	0.3180	0.5000	0.00000490	0.				
28	32	31	45	46	3	16200.	0.3180	0.5000	0.00000490	0.				
29	33	32	46	47	3	16200.	0.3180	0.5000	0.00000490	0.				
30	34	33	47	48	3	16200.	0.3180	0.5000	0.00000490	0.				
31	35	34	48	49	3	16200.	0.3180	0.5000	0.00000490	0.				
32	36	35	49	50	3	16200.	0.3180	0.5000	0.00000490	0.				
33	37	36	50	51	3	16200.	0.3180	0.5000	0.00000490	0.				
34	38	37	51	52	3	16200.	0.3180	0.5000	0.00000490	0.				
35	39	38	52	53	3	16200.	0.3180	0.5000	0.00000490	0.				
36	40	39	53	54	3	16200.	0.3180	0.5000	0.00000490	0.				
37	41	40	54	55	3	16200.	0.3180	0.5000	0.00000490	0.				
38	42	41	55	56	3	16200.	0.3180	0.5000	0.00000490	0.				
39	43	42	56	57	3	16200.	0.3180	0.5000	0.00000490	0.				
40	2	30	0	0	1	29000.	0.3180	0.2300	0.00000560	0.				
41	3	31	0	0	1	29000.	0.3180	0.4600	0.00000560	0.				
42	4	32	0	0	1	29000.	0.3180	0.4600	0.00000560	0.				
43	5	33	0	0	1	29000.	0.3180	0.3450	0.00000560	0.				
44	6	34	0	0	1	29000.	0.3180	0.2300	0.00000560	0.				
45	7	35	0	0	1	29000.	0.3180	0.2300	0.00000560	0.				
46	8	36	0	0	1	29000.	0.3180	0.2300	0.00000560	0.				
47	9	37	0	0	1	1.	0.3180	0.2300	0.00000560	0.				
48	10	38	0	0	1	1.	0.3180	0.2300	0.00000560	0.				
49	11	39	0	0	1	1.	0.3180	0.3450	0.00000560	0.				
50	12	40	0	0	1	1.	0.3180	0.4600	0.00000560	0.				

TABLE C-11. FINITE-ELEMENT ANALYSIS OF LEAD-LAG JOINT IN UPPER PLATE FOR ULTIMATE LOADS OF CONDITION TW7F1 (continued)

ELEM	P	Q	R	S	TYPE	E	PR	THICK-AREA	ALPHA	TEM 1	TEM 2	TEM 3	TEM 4	TEM 5
51	13	41	0	0	1	1.	0.3180	0.4600	0.00000560	0.				
52	14	42	0	0	1	1.	0.3180	0.4600	0.00000560	0.				
53	15	43	0	0	1	1.	0.3180	0.2300	0.00000560	0.				
54	30	58	0	0	1	29000.	0.3180	0.2300	0.00000560	0.				
55	31	59	0	0	1	29000.	0.3180	0.4600	0.00000560	0.				
56	32	60	0	0	1	29000.	0.3180	0.4600	0.00000560	0.				
57	33	61	0	0	1	29000.	0.3180	0.3450	0.00000560	0.				
58	34	62	0	0	1	29000.	0.3180	0.2300	0.00000560	0.				
59	35	63	0	0	1	29000.	0.3180	0.2300	0.00000560	0.				
60	36	64	0	0	1	29000.	0.3180	0.2300	0.00000560	0.				
61	37	65	0	0	1	29000.	0.3180	0.2300	0.00000560	0.				
62	38	66	0	0	1	29000.	0.3180	0.2300	0.00000560	0.				
63	39	67	0	0	1	29000.	0.3180	0.3450	0.00000560	0.				
64	40	68	0	0	1	29000.	0.3180	0.4600	0.00000560	0.				
65	41	69	0	0	1	1.	0.3180	0.4600	0.00000560	0.				
66	42	70	0	0	1	1.	0.3180	0.4600	0.00000560	0.				
67	43	71	0	0	1	1.	0.3180	0.2300	0.00000560	0.				
68	59	58	72	73	5	0.	0.0	0.3300	0.0	0.				
69	60	59	73	74	5	0.	0.0	0.3300	0.0	0.				
70	61	60	74	75	5	0.	0.0	0.3300	0.0	0.				
71	62	61	75	76	5	0.	0.0	0.3300	0.0	0.				
72	63	62	76	77	5	0.	0.0	0.3300	0.0	0.				
73	64	63	77	78	5	0.	0.0	0.3300	0.0	0.				
74	65	64	78	79	5	0.	0.0	0.3300	0.0	0.				
75	66	65	79	80	5	0.	0.0	0.3300	0.0	0.				
76	67	66	80	81	5	0.	0.0	0.3300	0.0	0.				
77	68	67	81	82	5	0.	0.0	0.3300	0.0	0.				
78	69	68	82	83	5	0.	0.0	0.3300	0.0	0.				
79	70	69	83	84	5	0.	0.0	0.3300	0.0	0.				
80	71	70	84	85	5	0.	0.0	0.3300	0.0	0.				
81	73	72	86	87	5	0.	0.0	0.3300	0.0	0.				
82	74	73	87	88	5	0.	0.0	0.3300	0.0	0.				
83	75	74	88	89	5	0.	0.0	0.3300	0.0	0.				
84	76	75	89	90	5	0.	0.0	0.3300	0.0	0.				
85	77	76	90	91	5	0.	0.0	0.3300	0.0	0.				
86	78	77	91	92	5	0.	0.0	0.3300	0.0	0.				
87	79	78	92	93	5	0.	0.0	0.3300	0.0	0.				
88	80	79	93	94	5	0.	0.0	0.3300	0.0	0.				
89	81	80	94	95	5	0.	0.0	0.3300	0.0	0.				
90	83	81	95	96	5	0.	0.0	0.3300	0.0	0.				
91	83	82	96	97	5	0.	0.0	0.3300	0.0	0.				
92	84	83	97	98	5	0.	0.0	0.3300	0.0	0.				
93	85	84	98	99	5	0.	0.0	0.3300	0.0	0.				
94	87	86	100	101	5	0.	0.0	0.3300	0.0	0.				
95	88	87	101	102	5	0.	0.0	0.3300	0.0	0.				
96	89	88	102	103	5	0.	0.0	0.3300	0.0	0.				
97	90	89	103	104	5	0.	0.0	0.3300	0.0	0.				
98	91	90	104	105	5	0.	0.0	0.3300	0.0	0.				
99	92	91	105	106	5	0.	0.0	0.3300	0.0	0.				
100	93	92	106	107	5	0.	0.0	0.3300	0.0	0.				

TABLE C-11. FINITE-ELEMENT ANALYSIS OF LEAD-LAG JOINT IN UPPER PLATE FOR ULTIMATE LOADS OF CONDITION TW7F1 (continued)

ELEM	P	Q	R	S	TYPE	E	PR	THICK-AREA	ALPHA	TEM 1	TEM 2	TEM 3	TEM 4	TEM 5
101	94	93	107	108	5	0.	0.0	0.3300	0.0	0.				
102	95	94	108	109	5	0.	0.0	0.3300	0.0	0.				
103	96	95	109	110	5	0.	0.0	0.3300	0.0	0.				
104	97	96	110	111	5	0.	0.0	0.3300	0.0	0.				
105	98	97	111	0	4	0.	0.0	0.3300	0.0	0.				
106	104	103	112	0	4	0.	0.0	0.3300	0.0	0.				
107	112	113	104	0	4	0.	0.0	0.3300	0.0	0.				
108	105	104	113	0	4	0.	0.0	0.3300	0.0	0.				
109	106	105	113	0	4	0.	0.0	0.3300	0.0	0.				
110	113	114	106	0	4	0.	0.0	0.3300	0.0	0.				
111	107	106	114	0	4	0.	0.0	0.3300	0.0	0.				
112	108	107	114	0	4	0.	0.0	0.3300	0.0	0.				
113	115	114	108	0	4	0.	0.0	0.3300	0.0	0.				
114	109	108	115	0	4	0.	0.0	0.3300	0.0	0.				
115	110	109	115	116	5	0.	0.0	0.3300	0.0	0.				
116	111	110	116	117	5	0.	0.0	0.3300	0.0	0.				
117	98	111	117	118	5	0.	0.0	0.3300	0.0	0.				
118	99	98	118	119	5	0.	0.0	0.3300	0.0	0.				
119	113	112	120	121	5	0.	0.0	0.3300	0.0	0.				
120	114	113	121	122	5	0.	0.0	0.3300	0.0	0.				
121	115	114	122	123	5	0.	0.0	0.3300	0.0	0.				
122	116	115	123	124	5	0.	0.0	0.3300	0.0	0.				
123	117	116	124	125	5	0.	0.0	0.3300	0.0	0.				
124	118	117	125	126	5	0.	0.0	0.3300	0.0	0.				
125	119	118	126	127	5	0.	0.0	0.3300	0.0	0.				
126	121	120	128	129	5	0.	0.0	0.3300	0.0	0.				
127	122	121	129	130	5	0.	0.0	0.3300	0.0	0.				
128	123	122	130	131	5	0.	0.0	0.3300	0.0	0.				
129	124	123	131	132	5	0.	0.0	0.3300	0.0	0.				
130	125	124	132	133	5	0.	0.0	0.3300	0.0	0.				
131	126	125	133	134	5	0.	0.0	0.3300	0.0	0.				
132	127	126	134	135	5	0.	0.0	0.3300	0.0	0.				
133	129	128	136	0	4	0.	0.0	0.3300	0.0	0.				
134	130	129	136	137	5	0.	0.0	0.3300	0.0	0.				
135	131	130	137	138	5	0.	0.0	0.3300	0.0	0.				
136	132	131	138	139	5	0.	0.0	0.3300	0.0	0.				
137	133	132	139	140	5	0.	0.0	0.3300	0.0	0.				
138	134	133	140	141	5	0.	0.0	0.3300	0.0	0.				
139	135	134	141	142	5	0.	0.0	0.3300	0.0	0.				
140	144	137	136	143	5	0.	0.0	0.3300	0.0	0.				
141	145	138	137	144	5	0.	0.0	0.3300	0.0	0.				
142	139	138	145	146	5	0.	0.0	0.3300	0.0	0.				
143	140	139	146	147	5	0.	0.0	0.3300	0.0	0.				
144	141	140	147	148	5	0.	0.0	0.3300	0.0	0.				
145	142	141	148	149	5	0.	0.0	0.3300	0.0	0.				
146	151	144	143	150	5	0.	0.0	0.3300	0.0	0.				
147	152	145	144	151	5	0.	0.0	0.3300	0.0	0.				
148	146	145	152	153	5	0.	0.0	0.3300	0.0	0.				
149	147	146	153	154	5	0.	0.0	0.3300	0.0	0.				
150	148	147	154	155	5	0.	0.0	0.3300	0.0	0.				

TABLE C-11. FINITE-ELEMENT ANALYSIS OF LEAD-LAG JOINT IN UPPER PLATE FOR ULTIMATE LOADS OF CONDITION TW7F1 (continued)

ELEM	P	Q	R	S	TYPE	E	PR	THICK-AREA	ALPHA	TEM 1	TEM 2	TEM 3	TEM 4	TEM 5
151	149	148	155	156	5	0.	0.0	0.3300	0.0	0.				
152	59	58	72	73	3	29000.	0.3180	0.2960	0.00000560	0.				
153	60	59	73	74	3	29000.	0.3180	0.2960	0.00000560	0.				
154	61	60	74	75	3	29000.	0.3180	0.2960	0.00000560	0.				
155	62	61	75	76	3	29000.	0.3180	0.2960	0.00000560	0.				
156	63	62	76	77	3	29000.	0.3180	0.2960	0.00000560	0.				
157	64	63	77	78	3	29000.	0.3180	0.2960	0.00000560	0.				
158	65	64	78	79	3	29000.	0.3180	0.2960	0.00000560	0.				
159	66	65	79	80	3	29000.	0.3180	0.2960	0.00000560	0.				
160	67	66	80	81	3	29000.	0.3180	0.2960	0.00000560	0.				
161	68	67	81	82	3	29000.	0.3180	0.2960	0.00000560	0.				
162	69	68	82	83	3	29000.	0.3180	0.2960	0.00000560	0.				
163	70	69	83	84	3	29000.	0.3180	0.2960	0.00000560	0.				
164	71	70	84	85	3	29000.	0.3180	0.2960	0.00000560	0.				
165	73	72	86	87	3	29000.	0.3180	0.2960	0.00000560	0.				
166	74	73	87	88	3	29000.	0.3180	0.2960	0.00000560	0.				
167	75	74	88	89	3	29000.	0.3180	0.2960	0.00000560	0.				
168	76	75	89	90	3	29000.	0.3180	0.2960	0.00000560	0.				
169	77	76	90	91	3	29000.	0.3180	0.2960	0.00000560	0.				
170	78	77	91	92	3	29000.	0.3180	0.2960	0.00000560	0.				
171	79	78	92	93	3	29000.	0.3180	0.2960	0.00000560	0.				
172	80	79	93	94	3	29000.	0.3180	0.2960	0.00000560	0.				
173	81	80	94	95	3	29000.	0.3180	0.2960	0.00000560	0.				
174	82	81	95	96	3	29000.	0.3180	0.2960	0.00000560	0.				
175	83	82	96	97	3	29000.	0.3180	0.2960	0.00000560	0.				
176	84	83	97	98	3	29000.	0.3180	0.2960	0.00000560	0.				
177	85	84	98	99	3	29000.	0.3180	0.2960	0.00000560	0.				
178	87	86	100	101	3	29000.	0.3180	0.2960	0.00000560	0.				
179	88	87	101	102	3	29000.	0.3180	0.2960	0.00000560	0.				
180	89	88	102	103	3	29000.	0.3180	0.2960	0.00000560	0.				
181	90	89	103	104	3	29000.	0.3180	0.2960	0.00000560	0.				
182	91	90	104	105	3	29000.	0.3180	0.2960	0.00000560	0.				
183	92	91	105	106	3	29000.	0.3180	0.2960	0.00000560	0.				
184	93	92	106	107	3	29000.	0.3180	0.2960	0.00000560	0.				
185	94	93	107	108	3	29000.	0.3180	0.2960	0.00000560	0.				
186	95	94	108	109	3	29000.	0.3180	0.2960	0.00000560	0.				
187	96	95	109	110	3	29000.	0.3180	0.2960	0.00000560	0.				
188	97	96	110	111	3	29000.	0.3180	0.2960	0.00000560	0.				
189	98	97	111	0	2	29000.	0.3180	0.2960	0.00000560	0.				
190	104	103	112	0	2	29000.	0.3180	0.2320	0.00000560	0.				
191	112	113	104	0	2	29000.	0.3180	0.2320	0.00000560	0.				
192	105	104	113	0	2	29000.	0.3180	0.2320	0.00000560	0.				
193	106	105	113	0	2	29000.	0.3180	0.2320	0.00000560	0.				
194	113	114	106	0	2	29000.	0.3180	0.2320	0.00000560	0.				
195	107	106	114	0	2	29000.	0.3180	0.2320	0.00000560	0.				
196	108	107	114	0	2	29000.	0.3180	0.2320	0.00000560	0.				
197	115	114	108	0	2	29000.	0.3180	0.2320	0.00000560	0.				
198	109	108	115	0	2	29000.	0.3180	0.2320	0.00000560	0.				
199	110	109	115	116	3	29000.	0.3180	0.2320	0.00000560	0.				
200	111	110	116	117	3	29000.	0.3180	0.2320	0.00000560	0.				

TABLE C-11. FINITE-ELEMENT ANALYSIS OF LEAD-LAG JOINT IN UPPER PLATE FOR ULTIMATE LOADS OF CONDITION TW7F1 (continued)

ELEM	P	Q	R	S	TYPE	E	PR	THICK-AREA	ALPHA	TEM 1	TEM 2	TEM 3	TEM 4	TEM 5
201	98	111	117	118	3	29000.	0.3180	0.2320	0.00000560	0.				
202	99	98	118	119	3	29000.	0.3180	0.2320	0.00000560	0.				
203	113	112	120	121	3	29000.	0.3180	0.2320	0.00000560	0.				
204	114	113	121	122	3	29000.	0.3180	0.1320	0.00000560	0.				
205	115	114	122	123	3	29000.	0.3180	0.1320	0.00000560	0.				
206	116	115	123	124	3	29000.	0.3180	0.1320	0.00000560	0.				
207	117	116	124	125	3	29000.	0.3180	0.1320	0.00000560	0.				
208	118	117	125	126	3	29000.	0.3180	0.1320	0.00000560	0.				
209	119	118	126	127	3	29000.	0.3180	0.1320	0.00000560	0.				
210	121	120	128	129	3	29000.	0.3180	0.0320	0.00000560	0.				
211	122	121	129	130	3	29000.	0.3180	0.0320	0.00000560	0.				
212	123	122	130	131	3	29000.	0.3180	0.0320	0.00000560	0.				
213	124	123	131	132	3	29000.	0.3180	0.0320	0.00000560	0.				
214	125	124	132	133	3	29000.	0.3180	0.0320	0.00000560	0.				
215	126	125	133	134	3	29000.	0.3180	0.0320	0.00000560	0.				
216	127	126	134	135	3	29000.	0.3180	0.0320	0.00000560	0.				
217	269	159	163	0	2	29000.	0.3180	0.5000	0.00000560	0.				
218	269	163	171	0	2	29000.	0.3180	0.5000	0.00000560	0.				
219	269	171	190	0	2	29000.	0.3180	0.5000	0.00000560	0.				
220	269	190	204	0	2	29000.	0.3180	0.5000	0.00000560	0.				
221	269	204	211	0	2	29000.	0.3180	0.5000	0.00000560	0.				
222	269	211	229	0	2	29000.	0.3180	0.5000	0.00000560	0.				
223	269	229	243	0	2	29000.	0.3180	0.5000	0.00000560	0.				
224	269	243	250	0	2	29000.	0.3180	0.5000	0.00000560	0.				
225	269	250	268	0	2	29000.	0.3180	0.5000	0.00000560	0.				
226	183	184	179	0	2	29000.	0.3180	0.5000	0.00000560	0.				
227	183	179	178	0	2	29000.	0.3180	0.5000	0.00000560	0.				
228	183	178	182	0	2	29000.	0.3180	0.5000	0.00000560	0.				
229	183	182	191	0	2	29000.	0.3180	0.5000	0.00000560	0.				
230	183	191	192	0	2	29000.	0.3180	0.5000	0.00000560	0.				
231	183	192	184	0	2	29000.	0.3180	0.5000	0.00000560	0.				
232	232	223	218	0	2	29000.	0.3180	0.5000	0.00000560	0.				
233	232	218	217	0	2	29000.	0.3180	0.5000	0.00000560	0.				
234	232	217	221	0	2	29000.	0.3180	0.5000	0.00000560	0.				
235	232	221	230	0	2	29000.	0.3180	0.5000	0.00000560	0.				
236	232	230	231	0	2	29000.	0.3180	0.5000	0.00000560	0.				
237	232	231	223	0	2	29000.	0.3180	0.5000	0.00000560	0.				
238	261	262	257	0	2	29000.	0.3180	0.5000	0.00000560	0.				
239	261	257	256	0	2	29000.	0.3180	0.5000	0.00000560	0.				
240	261	256	260	0	2	29000.	0.3180	0.5000	0.00000560	0.				
241	159	158	0	0	1	29000.	0.3180	0.2800	0.00000560	0.				
242	163	162	0	0	1	29000.	0.3180	0.5600	0.00000560	0.				
243	171	170	0	0	1	29000.	0.3180	0.5600	0.00000560	0.				
244	190	189	0	0	1	29000.	0.3180	0.5600	0.00000560	0.				
245	204	203	0	0	1	29000.	0.3180	0.5600	0.00000560	0.				
246	211	210	0	0	1	29000.	0.3180	0.5600	0.00000560	0.				
247	229	228	0	0	1	29000.	0.3180	0.5600	0.00000560	0.				
248	243	242	0	0	1	29000.	0.3180	0.5600	0.00000560	0.				
249	250	249	0	0	1	29000.	0.3180	0.5600	0.00000560	0.				
250	268	267	0	0	1	29000.	0.3180	0.2800	0.00000560	0.				

TABLE C-11. FINITE-ELEMENT ANALYSIS OF LEAD-LAG JOINT IN UPPER PLATE FOR ULTIMATE LOADS OF CONDITION TW7F1 (continued)

ELEM	P	J	R	S	TYPE	E	PR	THICK-AREA	ALPHA	TEM 1	TEM 2	TEM 3	TEM 4	TEM 5
251	184	185	0	0	1	1.	0.3180	1.5700	0.00000560	0.				
252	179	177	0	0	1	1.	0.3180	1.5700	0.00000560	0.				
253	178	176	0	0	1	29000.	0.3180	1.5700	0.00000560	0.				
254	182	181	0	0	1	29000.	0.3180	1.5700	0.00000560	0.				
255	191	194	0	0	1	29000.	0.3180	1.5700	0.00000560	0.				
256	192	195	0	0	1	1.	0.3180	1.5700	0.00000560	0.				
257	223	224	0	0	1	1.	0.3180	1.5700	0.00000560	0.				
258	218	216	0	0	1	1.	0.3180	1.5700	0.00000560	0.				
259	217	215	0	0	1	29000.	0.3180	1.5700	0.00000560	0.				
260	221	220	0	0	1	29000.	0.3180	1.5700	0.00000560	0.				
261	230	233	0	0	1	29000.	0.3180	1.5700	0.00000560	0.				
262	231	234	0	0	1	1.	0.3180	1.5700	0.00000560	0.				
263	262	263	0	0	1	29000.	0.3180	0.7850	0.00000560	0.				
264	257	255	0	0	1	29000.	0.3180	1.5700	0.00000560	0.				
265	256	254	0	0	1	1.	0.3180	1.5700	0.00000560	0.				
266	260	259	0	0	1	1.	0.3180	0.7850	0.00000560	0.				
267	162	158	157	161	3	29000.	0.3180	0.5000	0.00000560	0.				
268	170	162	161	169	3	29000.	0.3180	0.3000	0.00000560	0.				
269	189	170	169	188	3	29000.	0.3180	0.3000	0.00000560	0.				
270	203	189	188	202	3	29000.	0.3180	0.2000	0.00000560	0.				
271	210	203	202	209	3	29000.	0.3180	0.3000	0.00000560	0.				
272	228	210	209	227	3	29000.	0.3180	0.3000	0.00000560	0.				
273	242	228	227	241	3	29000.	0.3180	0.3000	0.00000560	0.				
274	249	242	241	248	3	29000.	0.3180	0.2000	0.00000560	0.				
275	267	249	248	266	3	29000.	0.3180	0.3000	0.00000560	0.				
276	186	174	177	185	3	29000.	0.3180	0.2000	0.00000560	0.				
277	177	174	173	176	3	29000.	0.3180	0.2000	0.00000560	0.				
278	176	173	172	175	3	29000.	0.3180	0.2000	0.00000560	0.				
279	181	176	175	180	3	29000.	0.3180	0.3000	0.00000560	0.				
280	194	191	180	193	3	29000.	0.3180	0.3000	0.00000560	0.				
281	192	196	194	0	2	29000.	0.3180	0.2000	0.00000560	0.				
282	197	195	194	196	3	29000.	0.3180	0.2000	0.00000560	0.				
283	197	186	185	195	3	29000.	0.3180	0.2000	0.00000560	0.				
284	225	213	216	224	3	29000.	0.3180	0.2000	0.00000560	0.				
285	216	210	212	215	3	29000.	0.3180	0.2000	0.00000560	0.				
286	214	212	215	0	2	29000.	0.3180	0.2000	0.00000560	0.				
287	220	219	214	219	3	29000.	0.3180	0.2000	0.00000560	0.				
288	233	220	219	232	3	29000.	0.3180	0.3000	0.00000560	0.				
289	232	235	233	0	2	29000.	0.3180	0.2000	0.00000560	0.				
290	236	234	233	235	3	29000.	0.3180	0.2000	0.00000560	0.				
291	234	225	224	234	3	29000.	0.3180	0.2000	0.00000560	0.				
292	264	252	255	263	3	29000.	0.3180	0.2000	0.00000560	0.				
293	255	252	251	254	3	29000.	0.3180	0.2000	0.00000560	0.				
294	253	251	254	0	2	29000.	0.3180	0.2000	0.00000560	0.				
295	259	254	253	258	3	29000.	0.3180	0.3000	0.00000560	0.				
296	155	154	160	0	4	0.	0.0	0.3300	0.0	0.				
297	156	155	160	0	4	0.	0.0	0.3300	0.0	0.				
298	161	157	156	160	5	0.	0.0	0.3300	0.0	0.				
299	165	161	150	164	5	0.	0.0	0.3300	0.0	0.				
300	152	151	165	0	4	0.	0.0	0.3300	0.0	0.				

TABLE C-11. FINITE-ELEMENT ANALYSIS OF LEAD-LAG JOINT IN UPPER PLATE FOR ULTIMATE LOADS OF CONDITION TW7F1 (continued)

ELEM	P	Q	R	S	TYPE	E	PR	THICK-AREA	ALPHA	TEM 1	TEM 2	TEM 3	TEM 4	TEM 5
301	165	166	152	0	4	0.	0.0	0.3300	0.0	0.				
302	153	152	166	0	4	0.	0.0	0.3300	0.0	0.				
303	167	154	153	166	5	0.	0.0	0.3300	0.0	0.				
304	168	160	154	167	5	0.	0.0	0.3300	0.0	0.				
305	169	161	160	168	5	0.	0.0	0.3300	0.0	0.				
306	173	165	164	172	5	0.	0.0	0.3200	0.0	0.				
307	174	166	165	173	5	0.	0.0	0.3300	0.0	0.				
308	186	167	166	174	5	0.	0.0	0.3300	0.0	0.				
309	187	168	167	186	5	0.	0.0	0.3300	0.0	0.				
310	188	169	168	187	5	0.	0.0	0.3300	0.0	0.				
311	195	197	196	198	5	0.	0.0	0.3300	0.0	0.				
312	200	186	197	199	5	0.	0.0	0.3300	0.0	0.				
313	201	187	186	200	5	0.	0.0	0.3300	0.0	0.				
314	202	188	187	201	5	0.	0.0	0.3300	0.0	0.				
315	206	199	198	205	5	0.	0.0	0.3300	0.0	0.				
316	207	200	199	206	5	0.	0.0	0.3300	0.0	0.				
317	209	201	200	207	5	0.	0.0	0.3300	0.0	0.				
318	209	202	201	208	5	0.	0.0	0.3300	0.0	0.				
319	213	206	205	212	5	0.	0.0	0.3300	0.0	0.				
320	225	207	206	213	5	0.	0.0	0.3300	0.0	0.				
321	226	208	207	225	5	0.	0.0	0.3300	0.0	0.				
322	227	209	208	226	5	0.	0.0	0.3300	0.0	0.				
323	238	236	235	237	5	0.	0.0	0.3300	0.0	0.				
324	239	225	236	238	5	0.	0.0	0.3300	0.0	0.				
325	240	226	225	239	5	0.	0.0	0.3300	0.0	0.				
326	241	227	226	240	5	0.	0.0	0.3300	0.0	0.				
327	245	238	237	244	5	0.	0.0	0.3300	0.0	0.				
328	246	239	238	245	5	0.	0.0	0.3300	0.0	0.				
329	247	240	239	246	5	0.	0.0	0.3300	0.0	0.				
330	248	241	240	247	5	0.	0.0	0.3300	0.0	0.				
331	252	245	244	251	5	0.	0.0	0.3300	0.0	0.				
332	264	246	245	252	5	0.	0.0	0.3300	0.0	0.				
333	265	247	246	264	5	0.	0.0	0.3300	0.0	0.				
334	266	249	247	265	5	0.	0.0	0.3300	0.0	0.				
335	175	182	0	0	1	100.	0.3180	0.1000	0.00000560	0.				
336	182	193	0	0	1	100.	0.3180	0.1000	0.00000560	0.				
337	214	221	0	0	1	100.	0.3180	0.1000	0.00000560	0.				
338	221	232	0	0	1	100.	0.3180	0.1000	0.00000560	0.				

TABLE C-11. FINITE-ELEMENT ANALYSIS OF LEAD-LAG JOINT IN UPPER PLATE FOR ULTIMATE LOADS OF CONDITION TW7F1 (continued)

COMPOSITE MATERIAL PROPERTIES									
ELEM	ALPHA 1	ALPHA 2	ALPHA 12	C11	C12	C13	C22	C23	C33
68	0.0	0.0	0.0	8288.0	2494.0	0.0	8288.0	0.0	2897.0
69	0.0	0.0	0.0	8288.0	2494.0	0.0	8288.0	0.0	2897.0
70	0.0	0.0	0.0	8288.0	2494.0	0.0	8288.0	0.0	2897.0
71	0.0	0.0	0.0	8288.0	2494.0	0.0	8288.0	0.0	2897.0
72	0.0	0.0	0.0	8288.0	2494.0	0.0	8288.0	0.0	2897.0
73	0.0	0.0	0.0	8288.0	2494.0	0.0	8288.0	0.0	2897.0
74	0.0	0.0	0.0	8288.0	2494.0	0.0	8288.0	0.0	2897.0
75	0.0	0.0	0.0	8288.0	2494.0	0.0	8288.0	0.0	2897.0
76	0.0	0.0	0.0	8288.0	2494.0	0.0	8288.0	0.0	2897.0
77	0.0	0.0	0.0	8288.0	2494.0	0.0	8288.0	0.0	2897.0
78	0.0	0.0	0.0	8288.0	2494.0	0.0	8288.0	0.0	2897.0
79	0.0	0.0	0.0	8288.0	2494.0	0.0	8288.0	0.0	2897.0
80	0.0	0.0	0.0	8288.0	2494.0	0.0	8288.0	0.0	2897.0
81	0.0	0.0	0.0	8288.0	2494.0	0.0	8288.0	0.0	2897.0
82	0.0	0.0	0.0	8288.0	2494.0	0.0	8288.0	0.0	2897.0
83	0.0	0.0	0.0	8288.0	2494.0	0.0	8288.0	0.0	2897.0
84	0.0	0.0	0.0	8288.0	2494.0	0.0	8288.0	0.0	2897.0
85	0.0	0.0	0.0	8288.0	2494.0	0.0	8288.0	0.0	2897.0
86	0.0	0.0	0.0	8288.0	2494.0	0.0	8288.0	0.0	2897.0
87	0.0	0.0	0.0	8288.0	2494.0	0.0	8288.0	0.0	2897.0
88	0.0	0.0	0.0	8288.0	2494.0	0.0	8288.0	0.0	2897.0
89	0.0	0.0	0.0	8288.0	2494.0	0.0	8288.0	0.0	2897.0
90	0.0	0.0	0.0	8288.0	2494.0	0.0	8288.0	0.0	2897.0
91	0.0	0.0	0.0	8288.0	2494.0	0.0	8288.0	0.0	2897.0
92	0.0	0.0	0.0	8288.0	2494.0	0.0	8288.0	0.0	2897.0
93	0.0	0.0	0.0	8288.0	2494.0	0.0	8288.0	0.0	2897.0
94	0.0	0.0	0.0	8288.0	2494.0	0.0	8288.0	0.0	2897.0
95	0.0	0.0	0.0	8288.0	2494.0	0.0	8288.0	0.0	2897.0
96	0.0	0.0	0.0	8288.0	2494.0	0.0	8288.0	0.0	2897.0
97	0.0	0.0	0.0	8288.0	2494.0	0.0	8288.0	0.0	2897.0
98	0.0	0.0	0.0	8288.0	2494.0	0.0	8288.0	0.0	2897.0
99	0.0	0.0	0.0	8288.0	2494.0	0.0	8288.0	0.0	2897.0
100	0.0	0.0	0.0	8288.0	2494.0	0.0	8288.0	0.0	2897.0
101	0.0	0.0	0.0	8288.0	2494.0	0.0	8288.0	0.0	2897.0
102	0.0	0.0	0.0	8288.0	2494.0	0.0	8288.0	0.0	2897.0
103	0.0	0.0	0.0	8288.0	2494.0	0.0	8288.0	0.0	2897.0
104	0.0	0.0	0.0	8288.0	2494.0	0.0	8288.0	0.0	2897.0
105	0.0	0.0	0.0	8288.0	2494.0	0.0	8288.0	0.0	2897.0
106	0.0	0.0	0.0	8288.0	2494.0	0.0	8288.0	0.0	2897.0
107	0.0	0.0	0.0	8288.0	2494.0	0.0	8288.0	0.0	2897.0
108	0.0	0.0	0.0	8288.0	2494.0	0.0	8288.0	0.0	2897.0
109	0.0	0.0	0.0	8288.0	2494.0	0.0	8288.0	0.0	2897.0
110	0.0	0.0	0.0	8288.0	2494.0	0.0	8288.0	0.0	2897.0
111	0.0	0.0	0.0	8288.0	2494.0	0.0	8288.0	0.0	2897.0
112	0.0	0.0	0.0	8288.0	2494.0	0.0	8288.0	0.0	2897.0
113	0.0	0.0	0.0	8288.0	2494.0	0.0	8288.0	0.0	2897.0
114	0.0	0.0	0.0	8288.0	2494.0	0.0	8288.0	0.0	2897.0
115	0.0	0.0	0.0	8288.0	2494.0	0.0	8288.0	0.0	2897.0
116	0.0	0.0	0.0	8288.0	2494.0	0.0	8288.0	0.0	2897.0
117	0.0	0.0	0.0	8288.0	2494.0	0.0	8288.0	0.0	2897.0

TABLE C-11. FINITE-ELEMENT ANALYSIS OF LEAD-LAG JOINT IN UPPER PLATE FOR ULTIMATE LOADS OF CONDITION TW7F1 (continued)

COMPOSITE MATERIAL PROPERTIES									
ELEM	ALPHA 1	ALPHA 2	ALPHA 12	C11	C12	C13	C22	C23	C33
118	0.0	0.0	0.0	8288.0	2494.0	0.0	8288.0	0.0	2897.0
119	0.0	0.0	0.0	8288.0	2494.0	0.0	8288.0	0.0	2897.0
120	0.0	0.0	0.0	8288.0	2494.0	0.0	8288.0	0.0	2897.0
121	0.0	0.0	0.0	8288.0	2494.0	0.0	8288.0	0.0	2897.0
122	0.0	0.0	0.0	8288.0	2494.0	0.0	8288.0	0.0	2897.0
123	0.0	0.0	0.0	8288.0	2494.0	0.0	8288.0	0.0	2897.0
124	0.0	0.0	0.0	8288.0	2494.0	0.0	8288.0	0.0	2897.0
125	0.0	0.0	0.0	8288.0	2494.0	0.0	8288.0	0.0	2897.0
126	0.0	0.0	0.0	8288.0	2494.0	0.0	8288.0	0.0	2897.0
127	0.0	0.0	0.0	8288.0	2494.0	0.0	8288.0	0.0	2897.0
128	0.0	0.0	0.0	8288.0	2494.0	0.0	8288.0	0.0	2897.0
129	0.0	0.0	0.0	8288.0	2494.0	0.0	8288.0	0.0	2897.0
130	0.0	0.0	0.0	8288.0	2494.0	0.0	8288.0	0.0	2897.0
131	0.0	0.0	0.0	8288.0	2494.0	0.0	8288.0	0.0	2897.0
132	0.0	0.0	0.0	8288.0	2494.0	0.0	8288.0	0.0	2897.0
133	0.0	0.0	0.0	8288.0	2494.0	0.0	8288.0	0.0	2897.0
134	0.0	0.0	0.0	8288.0	2494.0	0.0	8288.0	0.0	2897.0
135	0.0	0.0	0.0	8288.0	2494.0	0.0	8288.0	0.0	2897.0
136	0.0	0.0	0.0	8288.0	2494.0	0.0	8288.0	0.0	2897.0
137	0.0	0.0	0.0	8288.0	2494.0	0.0	8288.0	0.0	2897.0
138	0.0	0.0	0.0	8288.0	2494.0	0.0	8288.0	0.0	2897.0
139	0.0	0.0	0.0	8288.0	2494.0	0.0	8288.0	0.0	2897.0
140	0.0	0.0	0.0	8288.0	2494.0	0.0	8288.0	0.0	2897.0
141	0.0	0.0	0.0	8288.0	2494.0	0.0	8288.0	0.0	2897.0
142	0.0	0.0	0.0	8288.0	2494.0	0.0	8288.0	0.0	2897.0
143	0.0	0.0	0.0	8288.0	2494.0	0.0	8288.0	0.0	2897.0
144	0.0	0.0	0.0	8288.0	2494.0	0.0	8288.0	0.0	2897.0
145	0.0	0.0	0.0	8288.0	2494.0	0.0	8288.0	0.0	2897.0
146	0.0	0.0	0.0	8288.0	2494.0	0.0	8288.0	0.0	2897.0
147	0.0	0.0	0.0	8288.0	2494.0	0.0	8288.0	0.0	2897.0
148	0.0	0.0	0.0	8288.0	2494.0	0.0	8288.0	0.0	2897.0
149	0.0	0.0	0.0	8288.0	2494.0	0.0	8288.0	0.0	2897.0
150	0.0	0.0	0.0	8288.0	2494.0	0.0	8288.0	0.0	2897.0
151	0.0	0.0	0.0	8288.0	2494.0	0.0	8288.0	0.0	2897.0
296	0.0	0.0	0.0	8288.0	2494.0	0.0	8288.0	0.0	2897.0
297	0.0	0.0	0.0	8288.0	2494.0	0.0	8288.0	0.0	2897.0
298	0.0	0.0	0.0	8288.0	2494.0	0.0	8288.0	0.0	2897.0
299	0.0	0.0	0.0	8288.0	2494.0	0.0	8288.0	0.0	2897.0
300	0.0	0.0	0.0	8288.0	2494.0	0.0	8288.0	0.0	2897.0
301	0.0	0.0	0.0	8288.0	2494.0	0.0	8288.0	0.0	2897.0
302	0.0	0.0	0.0	8288.0	2494.0	0.0	8288.0	0.0	2897.0
303	0.0	0.0	0.0	8288.0	2494.0	0.0	8288.0	0.0	2897.0
304	0.0	0.0	0.0	8288.0	2494.0	0.0	8288.0	0.0	2897.0
305	0.0	0.0	0.0	8288.0	2494.0	0.0	8288.0	0.0	2897.0
306	0.0	0.0	0.0	8288.0	2494.0	0.0	8288.0	0.0	2897.0
307	0.0	0.0	0.0	8288.0	2494.0	0.0	8288.0	0.0	2897.0
308	0.0	0.0	0.0	8288.0	2494.0	0.0	8288.0	0.0	2897.0
309	0.0	0.0	0.0	8288.0	2494.0	0.0	8288.0	0.0	2897.0
310	0.0	0.0	0.0	8288.0	2494.0	0.0	8288.0	0.0	2897.0
311	0.0	0.0	0.0	8288.0	2494.0	0.0	8288.0	0.0	2897.0

TABLE C-11. FINITE-ELEMENT ANALYSIS OF LEAD-LAG JOINT IN UPPER PLATE FOR ULTIMATE LOADS OF CONDITION TW7F1 (continued)

COMPOSITE MATERIAL PROPERTIES

ELEM	ALPHA 1	ALPHA 2	ALPHA 12	C11	C12	C13	C22	C23	C33
312	0.0	0.0	0.0	8288.0	2494.0	0.0	8288.0	0.0	2897.0
313	0.0	0.0	0.0	8288.0	2494.0	0.0	8288.0	0.0	2897.0
314	0.0	0.0	0.0	8288.0	2494.0	0.0	8288.0	0.0	2897.0
315	0.0	0.0	0.0	8288.0	2494.0	0.0	8288.0	0.0	2897.0
316	0.0	0.0	0.0	8288.0	2494.0	0.0	8288.0	0.0	2897.0
317	0.0	0.0	0.0	8288.0	2494.0	0.0	8288.0	0.0	2897.0
318	0.0	0.0	0.0	8288.0	2494.0	0.0	8288.0	0.0	2897.0
319	0.0	0.0	0.0	8288.0	2494.0	0.0	8288.0	0.0	2897.0
320	0.0	0.0	0.0	8288.0	2494.0	0.0	8288.0	0.0	2897.0
321	0.0	0.0	0.0	8288.0	2494.0	0.0	8288.0	0.0	2897.0
322	0.0	0.0	0.0	8288.0	2494.0	0.0	8288.0	0.0	2897.0
323	0.0	0.0	0.0	8288.0	2494.0	0.0	8288.0	0.0	2897.0
324	0.0	0.0	0.0	8288.0	2494.0	0.0	8288.0	0.0	2897.0
325	0.0	0.0	0.0	8288.0	2494.0	0.0	8288.0	0.0	2897.0
326	0.0	0.0	0.0	8288.0	2494.0	0.0	8288.0	0.0	2897.0
327	0.0	0.0	0.0	8288.0	2494.0	0.0	8288.0	0.0	2897.0
328	0.0	0.0	0.0	8288.0	2494.0	0.0	8288.0	0.0	2897.0
329	0.0	0.0	0.0	8288.0	2494.0	0.0	8288.0	0.0	2897.0
330	0.0	0.0	0.0	8288.0	2494.0	0.0	8288.0	0.0	2897.0
331	0.0	0.0	0.0	8288.0	2494.0	0.0	8288.0	0.0	2897.0
332	0.0	0.0	0.0	8288.0	2494.0	0.0	8288.0	0.0	2897.0
333	0.0	0.0	0.0	8288.0	2494.0	0.0	8288.0	0.0	2897.0
334	0.0	0.0	0.0	8288.0	2494.0	0.0	8288.0	0.0	2897.0

TABLE C-11. FINITE-ELEMENT ANALYSIS OF LEAD-LAG JOINT IN UPPER PLATE FOR ULTIMATE LOADS OF CONDITION TW7F1 (continued)

X DEFLECTION, CASE 1

	1	2	3	4	5	6	7	8	9	10
1	0.0	0.0	-8.786E-05	-3.178E-04	-6.999E-04	-8.459E-04	-8.929E-04	-8.306E-04	-7.048E-04	-7.147E-04
11	-7.929E-04	-9.408E-04	-8.754E-04	-5.298E-04	0.0	0.0	4.204E-04	6.061E-04	3.292E-04	9.392E-05
21	-1.542E-04	-3.676E-04	-3.486E-04	8.109E-04	2.983E-03	8.177E-03	5.691E-03	1.876E-03	0.0	0.0
31	4.664E-04	6.869E-04	3.900E-04	1.256E-04	-1.481E-04	-3.848E-04	-4.000E-04	8.350E-04	3.249E-03	8.365E-03
41	4.953E-03	1.097E-03	0.0	0.0	5.170E-04	7.630E-04	4.528E-04	1.577E-04	-1.408E-04	-4.041E-04
51	-4.158E-04	8.762E-04	3.552E-03	8.473E-03	4.196E-03	3.221E-04	0.0	0.0	2.833E-03	4.544E-03
61	4.585E-03	3.864E-03	2.747E-03	1.253E-03	-4.047E-04	-1.419E-03	-1.814E-03	-2.465E-03	-1.666E-03	-7.865E-04
71	0.0	0.0	2.924E-03	4.684E-03	4.606E-03	3.816E-03	2.622E-03	1.071E-03	-5.590E-04	-1.573E-03
81	-1.989E-03	-2.358E-03	-1.407E-03	-5.562E-04	0.0	0.0	3.160E-03	4.977E-03	4.798E-03	3.750E-03
91	2.423E-03	8.071E-04	-7.731E-04	-1.794E-03	-2.248E-03	-2.195E-03	-1.020E-03	-1.822E-04	0.0	0.0
101	4.185E-03	6.965E-03	6.999E-03	4.597E-03	2.343E-03	5.832E-04	-1.173E-03	-2.040E-03	-2.554E-03	-2.087E-03
111	-7.940E-04	6.501E-03	2.509E-03	-1.370E-03	-2.759E-03	-1.918E-03	-3.964E-04	2.266E-04	0.0	5.708E-03
121	2.569E-03	-1.485E-03	-2.864E-03	-1.856E-03	-1.997E-04	3.690E-04	0.0	4.935E-03	2.745E-03	-1.490E-03
131	-2.967E-03	-2.035E-03	-4.485E-04	2.618E-04	0.0	3.142E-03	-1.377E-03	-3.165E-03	-2.595E-03	-1.237E-03
141	-3.219E-04	0.0	-2.971E-04	-2.424E-03	-3.364E-03	-3.087E-03	-2.030E-03	-1.008E-03	0.0	-2.343E-03
151	-2.524E-03	-2.285E-03	-1.771E-03	-1.983E-03	-1.245E-03	0.0	0.0	0.0	0.0	-1.542E-03
161	-1.714E-03	-1.580E-03	-4.235E-04	-2.404E-03	-8.598E-04	1.079E-03	4.351E-04	-7.533E-04	-2.667E-03	-2.397E-03
171	-4.244E-04	2.057E-03	5.865E-03	6.865E-03	1.131E-02	1.175E-02	7.509E-03	2.472E-02	2.663E-02	2.370E-02
181	2.509E-02	2.479E-02	2.765E-02	2.801E-02	7.645E-03	7.453E-03	2.912E-04	-2.153E-03	-2.031E-03	-4.714E-04
191	2.647E-02	2.810E-02	1.754E-02	1.720E-02	1.018E-02	1.072E-02	9.544E-03	5.211E-03	5.437E-03	4.297E-03
201	2.845E-03	-4.992E-04	-6.217E-04	-2.079E-05	3.611E-03	4.113E-03	4.491E-03	4.197E-03	1.664E-03	1.178E-03
211	5.326E-04	4.592E-03	4.823E-03	5.797E-03	5.540E-03	5.504E-03	6.399E-03	6.021E-03	7.813E-03	7.635E-03
221	7.691E-03	7.257E-03	6.581E-03	5.952E-03	5.766E-03	5.697E-03	3.166E-03	2.532E-03	9.222E-04	8.552E-03
231	7.537E-03	7.713E-03	7.234E-03	6.251E-03	7.691E-03	6.546E-03	6.496E-03	6.434E-03	6.197E-03	5.738E-03
241	3.381E-03	2.775E-03	4.572E-04	3.532E-03	4.628E-03	4.437E-03	3.742E-03	2.149E-03	1.792E-03	6.045E-04
251	9.526E-04	2.328E-03	1.031E-04	6.516E-04	1.881E-03	-6.825E-05	1.198E-04	0.0	0.0	0.0
261	0.0	0.0	0.0	0.0	0.0	0.0	0.0	0.0	0.0	

TABLE C-11. FINITE-ELEMENT ANALYSIS OF LEAD-LAG JOINT IN UPPER PLATE FOR ULTIMATE LOADS OF CONDITION TW7F1 (continued)

Y DEFLECTION, CASE 1

	1	2	3	4	5	6	7	8	9	10
1	7.445E-02	7.085E-02	7.075E-02	7.048E-02	7.025E-02	7.023E-02	7.031E-02	7.044E-02	7.060E-02	7.078E-02
11	7.102E-02	7.162E-02	7.229E-02	7.281E-02	7.301E-02	7.074E-02	7.048E-02	6.968E-02	6.865E-02	6.815E-02
21	6.771E-02	6.731E-02	6.679E-02	6.605E-02	6.477E-02	6.223E-02	6.530E-02	7.112E-02	7.396E-02	7.073E-02
31	7.045E-02	6.959E-02	6.853E-02	6.804E-02	6.761E-02	6.725E-02	6.694E-02	6.654E-02	6.567E-02	6.232E-02
41	6.474E-02	7.096E-02	7.407E-02	7.071E-02	7.041E-02	6.951E-02	6.840E-02	6.792E-02	6.751E-02	6.718E-02
51	6.709E-02	6.703E-02	6.656E-02	6.246E-02	6.418E-02	7.077E-02	7.413E-02	7.053E-02	6.947E-02	6.655E-02
61	6.234E-02	6.017E-02	5.797E-02	5.582E-02	5.375E-02	5.185E-02	5.006E-02	4.728E-02	4.426E-02	4.221E-02
71	4.143E-02	7.025E-02	6.915E-02	6.611E-02	6.177E-02	5.955E-02	5.736E-02	5.525E-02	5.337E-02	5.174E-02
81	5.016E-02	4.749E-02	4.451E-02	4.225E-02	4.139E-02	6.977E-02	6.858E-02	6.532E-02	6.059E-02	5.849E-02
91	5.628E-02	5.427E-02	5.270E-02	5.140E-02	5.020E-02	4.781E-02	4.486E-02	4.234E-02	4.133E-02	5.861E-02
101	6.706E-02	6.237E-02	5.777E-02	5.418E-02	5.251E-02	5.163E-02	5.089E-02	5.037E-02	4.980E-02	4.793E-02
111	4.499E-02	5.373E-02	5.112E-02	4.988E-02	4.934E-02	4.793E-02	4.511E-02	4.238E-02	4.128E-02	5.086E-02
121	4.953E-02	4.868E-02	4.850E-02	4.753E-02	4.504E-02	4.242E-02	4.117E-02	4.835E-02	4.774E-02	4.713E-02
131	4.723E-02	4.649E-02	4.426E-02	4.194E-02	4.093E-02	4.424E-02	4.404E-02	4.410E-02	4.364E-02	4.218E-02
141	4.049E-02	3.975E-02	3.884E-02	3.776E-02	3.806E-02	3.791E-02	3.702E-02	3.590E-02	3.541E-02	3.399E-02
151	3.400E-02	3.399E-02	3.320E-02	3.129E-02	2.881E-02	2.742E-02	9.122E-03	5.836E-03	5.580E-03	2.586E-02
161	9.977E-03	6.434E-03	5.757E-03	3.535E-02	3.477E-02	3.386E-02	3.140E-02	2.796E-02	1.168E-02	7.952E-03
171	6.199E-03	4.282E-02	4.033E-02	3.855E-02	4.957E-02	4.859E-02	4.008E-02	5.000E-02	4.972E-02	5.055E-02
181	5.117E-02	5.205E-02	5.191E-02	5.031E-02	3.886E-02	3.778E-02	2.841E-02	1.357E-02	9.656E-03	6.674E-03
191	5.304E-02	5.130E-02	4.054E-02	4.033E-02	3.976E-02	3.818E-02	4.001E-02	3.534E-02	3.743E-02	3.481E-02
201	2.976E-02	1.469E-02	1.072E-02	6.946E-03	3.450E-02	3.396E-02	3.208E-02	2.819E-02	1.456E-02	1.063E-02
211	6.860E-03	3.356E-02	3.219E-02	3.314E-02	3.266E-02	3.196E-02	3.161E-02	3.003E-02	3.214E-02	3.155E-02
221	3.161E-02	3.037E-02	2.924E-02	3.032E-02	2.954E-02	2.519E-02	1.305E-02	9.402E-03	6.425E-03	3.021E-02
231	2.918E-02	3.086E-02	3.034E-02	2.949E-02	2.962E-02	2.868E-02	2.747E-02	2.627E-02	2.484E-02	2.185E-02
241	1.086E-02	7.552E-03	5.819E-03	2.624E-02	2.557E-02	2.335E-02	1.994E-02	8.894E-03	5.944E-03	5.300E-03
251	2.744E-02	2.823E-02	2.864E-02	2.878E-02	2.939E-02	3.147E-02	3.111E-02	2.930E-02	2.922E-02	3.194E-02
261	3.205E-02	3.062E-02	3.054E-02	2.852E-02	1.887E-02	8.154E-03	5.310E-03	5.097E-03	0.0	

TABLE C-11. FINITE-ELEMENT ANALYSIS OF LEAD-LAG JOINT IN UPPER PLATE FOR ULTIMATE LOADS OF CONDITION TW7F1 (continued)

STRESS ELEM	XX	YY	XY	ON	OS	CASE	(TOTAL STRAIN)*1000000. XX	YY	XY	(MECH. STRAIN)*1000000. XX	YY	XY	CASE
1	-44.8025	-16.6785	-0.6798	-20.4937	18.4967	1	-1362.	-84.	-62.	-1362.	-84.	-62.	1
2	-43.7148	-16.8242	-2.0033	-20.1797	19.0777	1	-1323.	-101.	-182.	-1323.	-101.	-182.	1
3	-40.7908	-16.6853	-4.0242	-19.1590	17.2014	1	-1224.	-128.	-439.	-1224.	-128.	-439.	1
4	-35.8826	-15.5736	-9.6150	-17.1854	16.6536	1	-1065.	-147.	-874.	-1065.	-147.	-874.	1
5	-30.9849	-15.6784	-14.0811	-15.5544	17.0938	1	-897.	-201.	-1280.	-897.	-201.	-1280.	1
6	-24.3669	-15.5907	-17.8261	-13.3192	17.7107	1	-669.	-270.	-1621.	-669.	-270.	-1621.	1
7	-16.5848	-15.6316	-19.4521	-10.7308	17.6088	1	-401.	-357.	-1768.	-401.	-357.	-1768.	1
8	-9.4220	-15.5715	-14.9029	-8.3312	13.8082	1	-154.	-434.	-1362.	-154.	-434.	-1362.	1
9	-3.8841	-15.5578	-11.4939	-6.4806	11.4798	1	37.	-494.	-1043.	37.	-494.	-1045.	1
10	2.0735	-15.7248	-7.8631	-4.5505	10.2146	1	244.	-565.	-714.	244.	-565.	-714.	1
11	7.2661	-15.6062	-4.3718	-2.7800	10.1880	1	422.	-618.	-397.	422.	-618.	-397.	1
12	10.0439	-15.5437	-2.1603	-1.8333	10.6730	1	517.	-646.	-196.	517.	-646.	-196.	1
13	11.2441	-15.5110	-0.6656	-1.4223	10.9824	1	558.	-658.	-60.	558.	-658.	-60.	1
14	0.1344	9.1083	0.0178	3.0809	4.2624	1	-171.	560.	3.	-171.	560.	3.	1
15	0.1873	10.5442	0.1565	3.5772	4.9289	1	-195.	647.	27.	-195.	647.	27.	1
16	0.2107	10.2092	0.1890	3.4733	4.7663	1	-188.	626.	31.	-188.	626.	31.	1
17	0.3589	11.0693	0.0493	3.8094	5.1258	1	-195.	676.	8.	-195.	676.	8.	1
18	0.2688	11.4490	0.1211	3.9126	5.3452	1	-208.	703.	20.	-208.	703.	20.	1
19	0.2825	11.3926	0.1729	4.0583	5.5426	1	-216.	729.	28.	-216.	729.	28.	1
20	0.6716	15.7063	2.8279	5.4593	7.6097	1	-267.	956.	460.	-267.	956.	460.	1
21	0.1802	16.2634	-0.6482	6.1479	8.5836	1	-347.	1124.	-105.	-347.	1124.	-105.	1
22	3.1589	20.3002	2.2463	7.8199	9.1057	1	-204.	1191.	366.	-204.	1191.	366.	1
23	-1.6219	4.6223	-13.3737	1.0001	11.2394	1	-191.	317.	-2177.	-191.	317.	-2177.	1
24	-3.5457	1.5491	9.2813	-0.6655	7.8724	1	-249.	165.	1510.	-249.	165.	1510.	1
25	1.6457	13.4233	5.6472	5.0230	7.5495	1	-162.	796.	919.	-162.	796.	919.	1
26	2.0496	14.6739	1.9011	7.2412	8.9664	1	-259.	1174.	310.	-259.	1174.	310.	1
27	-0.3139	9.3163	-0.1050	3.0675	4.5626	1	-207.	594.	-17.	-207.	594.	-17.	1
28	-0.1236	10.8979	0.1062	3.5914	5.1675	1	-222.	675.	17.	-222.	675.	17.	1
29	-0.2582	9.9419	0.1873	3.2279	4.7511	1	-211.	619.	31.	-211.	619.	31.	1
30	-0.1030	9.7449	-0.0310	3.2139	4.6183	1	-198.	604.	-5.	-198.	604.	-5.	1
31	-0.1150	9.9748	0.0547	3.2879	4.7316	1	-203.	618.	9.	-203.	618.	9.	1
32	-0.4316	9.8113	0.0891	3.1265	4.7307	1	-219.	614.	15.	-219.	614.	15.	1
33	0.2542	7.1555	2.4773	2.4699	3.8833	1	-125.	437.	403.	-125.	437.	403.	1
34	-0.2000	4.7449	-0.4670	1.5150	2.3169	1	-105.	297.	-76.	-105.	297.	-76.	1
35	1.9714	2.8794	2.2295	1.6169	2.1814	1	65.	139.	363.	65.	139.	363.	1
36	-1.1575	18.2263	-12.4048	5.6896	13.4682	1	-429.	1148.	-2018.	-429.	1148.	-2018.	1
37	-4.7368	21.1489	8.4172	5.4707	13.1862	1	-707.	1398.	1370.	-707.	1398.	1370.	1
38	1.4333	10.1072	5.3857	3.8468	6.2671	1	-110.	596.	877.	-110.	596.	877.	1
39	1.6181	4.1363	1.6052	1.9181	2.1481	1	19.	223.	261.	19.	223.	261.	1
40	-29.7427					1	-1026.			-1026.			1
41	-29.5398					1	-1019.			-1019.			1
42	-30.7206					1	-1059.			-1059.			1
43	-34.4490					1	-1188.			-1188.			1
44	-35.5383					1	-1225.			-1225.			1
45	-30.8171					1	-1063.			-1063.			1
46	-21.2072					1	-731.			-731.			1
47	0.3026					1	2628.			2628.			1
48	0.0192					1	19265.			19265.			1
49	0.0471					1	47095.			47095.			1
50	0.1128					1	112843.			112843.			1

TABLE C-11. FINITE-ELEMENT ANALYSIS OF LEAD-LAG JOINT IN UPPER PLATE FOR ULTIMATE LOADS OF CONDITION TW7F1 (continued)

STRESS ELEM	XX	YY	XY	ON	OS	CASE	(TOTAL STRAIN)*1000000. XX	YY	XY	(MECH. STRAIN)*1000000. XX	YY	XY	CASE
51	0.9828					1	82805.			82805.			1
52	0.0194					1	19377.			19377.			1
53	-0.0091					1	-9144.			-9144.			1
54	-29.0676					1	-1002.			-1002.			1
55	-28.7343					1	-991.			-991.			1
56	-29.9278					1	-1032.			-1032.			1
57	-33.7266					1	-1163.			-1163.			1
58	-34.6598					1	-1195.			-1195.			1
59	-29.9345					1	-1032.			-1032.			1
60	-19.0514					1	-657.			-657.			1
61	-0.6980					1	-24.			-24.			1
62	2.4319					1	84.			84.			1
63	-4.1348					1	-143.			-143.			1
64	6.2630					1	216.			216.			1
65	0.7648					1	64782.			64782.			1
66	0.1366					1	136554.			136554.			1
67	0.1665					1	166519.			166519.			1
68	-9.2356	20.8650	-0.0566	3.8764	12.5936	1	-2059.	3137.	-19.	-2059.	3137.	-19.	1
69	-9.4491	19.8676	-0.1130	3.4828	12.2316	1	-2048.	3017.	-39.	-2048.	3017.	-39.	1
70	-10.0785	20.6113	0.5156	3.5109	12.7796	1	-2160.	3137.	178.	-2160.	3137.	178.	1
71	-11.4242	19.6777	0.4722	2.7512	12.8513	1	-2301.	3067.	163.	-2301.	3067.	163.	1
72	-10.4902	21.6199	0.3796	3.7099	13.3724	1	-2255.	3287.	131.	-2255.	3287.	131.	1
73	-8.1342	24.5305	0.7451	5.4654	13.8973	1	-2059.	3579.	257.	-2059.	3579.	257.	1
74	-2.7052	27.9126	1.1838	8.4025	13.8736	1	-1473.	3811.	409.	-1473.	3811.	409.	1
75	1.5681	29.2903	-0.1443	10.2861	13.4537	1	-961.	3823.	-50.	-961.	3823.	-50.	1
76	-0.3969	27.0986	-0.9734	8.9006	12.8935	1	-1135.	3611.	-336.	-1135.	3611.	-336.	1
77	0.3543	21.1204	0.2266	7.3249	9.7629	1	-730.	2768.	78.	-730.	2768.	78.	1
78	1.8310	12.3599	-2.1345	4.7303	5.7185	1	-251.	1567.	-737.	-251.	1567.	-737.	1
79	-3.5536	1.4564	-1.0447	0.3009	1.2026	1	-132.	215.	-361.	-132.	215.	-361.	1
80	-0.2132	-4.2767	-0.4134	-1.4966	1.9973	1	143.	-559.	-145.	143.	-559.	-145.	1
81	-7.4290	21.1531	-0.2516	4.5747	12.1104	1	-1830.	3103.	-87.	-1830.	3103.	-87.	1
82	-7.3366	20.0167	-0.0857	4.2267	11.5602	1	-1772.	2949.	-30.	-1772.	2949.	-30.	1
83	-8.3565	20.4035	0.1743	4.0490	12.0464	1	-1910.	3036.	60.	-1910.	3036.	60.	1
84	-9.1442	17.2322	0.5331	2.6960	10.9442	1	-1901.	2651.	184.	-1901.	2651.	184.	1
85	-8.2771	20.2434	1.5105	3.9888	12.3435	1	-1906.	3016.	521.	-1906.	3016.	521.	1
86	-5.8605	22.3081	1.5627	5.4825	12.2026	1	-1668.	3194.	539.	-1668.	3194.	539.	1
87	-1.2495	23.3056	1.4685	7.2520	11.2154	1	-1084.	3102.	507.	-1084.	3102.	507.	1
88	2.2463	23.3154	-0.3579	8.5206	10.5057	1	-633.	3004.	-123.	-633.	3004.	-123.	1
89	1.2369	21.8088	-1.5476	7.6819	10.0815	1	-707.	2844.	-534.	-707.	2844.	-534.	1
90	1.9450	17.6933	-1.3781	6.5461	8.0017	1	-448.	2270.	-476.	-448.	2270.	-476.	1
91	2.0509	10.5456	-3.5431	4.1984	5.4073	1	-149.	1317.	-1225.	-149.	1317.	-1225.	1
92	0.1611	2.4805	-2.5004	0.8805	2.3350	1	-78.	323.	-863.	-78.	323.	-863.	1
93	-0.1135	-1.6843	-0.8174	-0.5993	1.0179	1	52.	-219.	-282.	52.	-219.	-282.	1
94	-2.7144	22.7196	-0.2620	6.6684	11.4059	1	-1267.	3123.	-90.	-1267.	3123.	-90.	1
95	-3.0791	22.6279	-0.9874	6.5162	11.4901	1	-1312.	3125.	-341.	-1312.	3125.	-341.	1
96	-1.7644	19.3186	-1.5248	5.8514	9.6308	1	-1005.	2633.	-526.	-1005.	2633.	-526.	1
97	-4.1597	14.8479	-0.4820	3.5627	4.1680	1	-1145.	2136.	-166.	-1145.	2136.	-166.	1
98	-3.0254	15.3467	0.0535	4.1071	8.0431	1	-1014.	2157.	18.	-1014.	2157.	18.	1
99	-1.3873	15.7119	0.6424	4.7749	7.7721	1	-811.	2140.	222.	-811.	2140.	222.	1
100	0.5817	15.4241	0.5020	5.3353	7.1496	1	-539.	2023.	173.	-539.	2023.	173.	1

TABLE C-11. FINITE-ELEMENT ANALYSIS OF LEAD-LAG JOINT IN UPPER PLATE FOR ULTIMATE LOADS OF CONDITION TW7F1 (continued)

STRESS ELEM	XX	YY	XY	ON	OS	CASE	(TOTAL STRAIN)*1000000. XX	YY	XY	(MECH. STRAIN)*1000000. XX	YY	XY	CASE
101	2.7196	15.3574	-1.6917	6.0257	6.8324	1	-252.	1929.	-584.	-252.	1929.	-584.	1
102	2.9811	14.5144	-2.3688	5.8318	6.55.0	1	-134.	1807.	-818.	-184.	1807.	-818.	1
103	2.9604	12.8447	-3.5136	5.2683	6.1960	1	-120.	1586.	-1213.	-120.	1586.	-1213.	1
104	1.7418	8.1108	-4.2939	3.2842	4.9443	1	-93.	1007.	-1482.	-93.	1007.	-1482.	1
105	0.5532	2.9641	-2.1079	1.1724	2.1490	1	-45.	371.	-728.	-45.	371.	-728.	1
106	2.8569	15.4967	-4.6675	6.1179	7.7373	1	-240.	1942.	-1611.	-240.	1942.	-1611.	1
107	-1.9647	7.5231	-2.9722	1.8861	4.7283	1	-548.	1073.	-1026.	-548.	1073.	-1026.	1
108	-0.3831	10.8830	-0.9241	3.5000	5.2772	1	-485.	1459.	-319.	-485.	1459.	-319.	1
109	0.1792	9.8517	-2.8115	3.3436	5.1432	1	-370.	1300.	-971.	-370.	1300.	-971.	1
110	2.3990	7.6505	-1.9858	3.3498	3.5828	1	13.	919.	-686.	13.	919.	-686.	1
111	0.9201	10.4521	-0.6277	3.7907	4.7530	1	-295.	1350.	-217.	-295.	1350.	-217.	1
112	2.5483	9.4746	-4.8943	4.0076	5.6565	1	-40.	1155.	-1689.	-40.	1155.	-1689.	1
113	6.4182	7.0941	-3.8650	4.5041	4.4926	1	568.	685.	-1335.	568.	685.	-1335.	1
114	2.7405	9.2611	-2.5740	4.3005	4.4165	1	-6.	1119.	-888.	-6.	1119.	-889.	1
115	5.1457	7.1953	-5.0528	4.1137	5.1168	1	395.	749.	-1744.	395.	749.	-1744.	1
116	4.7086	5.3421	-5.6642	3.3502	5.2172	1	411.	521.	-1962.	411.	521.	-1962.	1
117	2.6723	2.9366	-4.2234	1.8696	3.6947	1	237.	283.	-1458.	237.	283.	-1458.	1
118	0.7819	1.3658	-1.3860	0.7259	1.2677	1	48.	154.	-478.	48.	154.	-478.	1
119	1.0775	6.8177	-2.7812	2.6317	3.7565	1	-129.	861.	-960.	-129.	861.	-960.	1
120	2.3407	6.5130	-2.5109	2.9512	3.3852	1	51.	771.	-867.	51.	771.	-867.	1
121	5.6797	5.5597	-4.6932	3.7465	4.6588	1	532.	511.	-1620.	532.	511.	-1620.	1
122	7.5794	4.7847	-6.5953	4.1214	6.2285	1	815.	332.	-2277.	815.	332.	-2277.	1
123	6.5392	4.0842	-7.0638	3.5411	6.3870	1	705.	281.	-2438.	705.	281.	-2438.	1
124	4.9674	4.3715	-5.5138	3.1130	5.0172	1	485.	382.	-1903.	485.	382.	-1903.	1
125	2.7237	3.4219	-2.2188	2.0486	2.3370	1	225.	345.	-766.	225.	345.	-766.	1
126	1.7812	4.3076	-3.0193	2.0296	3.0333	1	64.	500.	-1042.	64.	500.	-1042.	1
127	4.2270	5.2192	-4.5382	3.1487	4.3419	1	352.	524.	-1566.	352.	524.	-1566.	1
128	9.3515	4.9498	-7.6010	4.7671	7.2876	1	1043.	283.	-2624.	1043.	283.	-2624.	1
129	12.5893	4.6405	-10.2054	5.7432	9.8212	1	1485.	113.	-3523.	1485.	113.	-3523.	1
130	12.5383	4.4826	-10.9641	5.6737	10.3608	1	1485.	94.	-3791.	1485.	94.	-3791.	1
131	8.7622	5.4076	-8.5892	4.7233	7.8875	1	947.	368.	-2965.	947.	368.	-2965.	1
132	7.8456	4.7842	-2.9130	4.2099	4.3101	1	850.	322.	-1006.	850.	322.	-1006.	1
133	0.7805	2.8218	-2.2190	1.2008	2.1675	1	-9.	343.	-766.	-9.	343.	-766.	1
134	4.5090	3.3360	-4.8567	2.6817	4.4105	1	457.	289.	-1676.	457.	289.	-1676.	1
135	10.6987	5.1434	-8.2627	5.2807	8.0375	1	1214.	255.	-2852.	1214.	255.	-2852.	1
136	15.2807	4.7319	-11.2904	6.6708	11.2151	1	1838.	18.	-3897.	1838.	18.	-3897.	1
137	15.1035	4.6890	-11.7260	6.9308	11.7217	1	1949.	-21.	-4048.	1949.	-21.	-4048.	1
138	14.3041	4.4348	-8.9281	6.2463	9.4278	1	1721.	17.	-3082.	1721.	17.	-3082.	1
139	13.0861	4.3907	-3.3286	5.8256	6.0792	1	1561.	60.	-1149.	1561.	60.	-1149.	1
140	0.8399	4.5686	1.5041	1.8028	2.3346	1	-71.	573.	519.	-71.	573.	519.	1
141	1.5705	8.7248	4.4509	3.4318	5.2561	1	-140.	1095.	1536.	-140.	1095.	1536.	1
142	11.5160	3.5030	-7.1041	5.0063	7.5418	1	1388.	5.	-2452.	1388.	5.	-2452.	1
143	14.0051	3.2989	-7.3470	5.7680	8.4690	1	1726.	-121.	-2536.	1726.	-121.	-2536.	1
144	14.8042	3.1557	-5.8810	5.9866	7.9744	1	1838.	-172.	-2030.	1838.	-172.	-2030.	1
145	15.2421	2.4102	-2.2829	5.8841	6.9447	1	1926.	-289.	-788.	1926.	-289.	-788.	1
146	-0.3041	1.4615	0.1244	0.3858	0.7774	1	-99.	206.	43.	-99.	206.	43.	1
147	1.2491	5.0047	1.6169	2.0846	2.5033	1	-34.	614.	558.	-34.	614.	558.	1
148	8.0067	2.7631	-2.8040	3.5900	4.0334	1	952.	47.	-968.	952.	47.	-968.	1
149	10.4769	4.3118	-3.4914	4.9295	5.1586	1	1218.	154.	-1205.	1218.	154.	-1205.	1
150	12.8944	3.3898	-4.0814	5.4281	6.3948	1	1575.	-65.	-1409.	1575.	-65.	-1409.	1

TABLE C-11. FINITE-ELEMENT ANALYSIS OF LEAD-LAG JOINT IN UPPER PLATE FOR ULTIMATE LOADS OF CONDITION TW7F1 (continued)

STRESS ELEM	XX	YY	XY	ON	OS	CASE	(TOTAL STRAIN)*1000000. XX	YY	XY	(MECH. STRAIN)*1000000. XX	YY	XY	CASE
151	15.5257	1.8590	-1.9542	5.8282	7.1496	1	1999.	-377.	-675.	1999.	-377.	-675.	1
152	-24.2457	50.0872	-0.2148	15.2805	47.9108	1	-2059.	3137.	-19.	-2059.	3137.	-19.	1
153	-35.1181	76.3313	-0.4307	13.7377	46.5258	1	-2048.	3017.	-39.	-2048.	3017.	-39.	1
154	-37.5014	79.0442	1.9563	13.8476	48.6029	1	-2160.	3137.	178.	-2160.	3137.	178.	1
155	-42.7810	75.3323	1.7915	10.8504	48.8490	1	-2301.	3067.	163.	-2301.	3067.	163.	1
156	-39.0215	82.9158	1.4404	14.6314	50.8580	1	-2255.	3287.	131.	-2255.	3287.	131.	1
157	-29.6897	94.3555	2.8311	21.5553	52.9357	1	-2059.	3579.	257.	-2059.	3579.	257.	1
158	-8.4307	107.8420	4.4983	33.1371	53.0636	1	-1473.	3811.	409.	-1473.	3811.	409.	1
159	8.2119	113.4883	-0.5457	40.5667	51.6741	1	-961.	3823.	-50.	-961.	3823.	-50.	1
160	0.4463	104.8623	-3.6978	35.1029	49.4200	1	-1135.	3611.	-336.	-1135.	3611.	-336.	1
161	4.8474	81.3132	0.8596	28.8869	37.4834	1	-730.	2768.	78.	-730.	2768.	78.	1
162	7.9877	47.9763	-8.1077	18.6547	22.0076	1	-251.	1567.	-737.	-251.	1567.	-737.	1
163	-2.0403	5.5991	-3.9680	1.1863	4.5746	1	-132.	215.	-361.	-132.	215.	-361.	1
164	-1.1423	-16.5691	-1.5920	-5.9038	7.6669	1	143.	-559.	-145.	143.	-559.	-145.	1
165	-27.2072	81.3319	-0.9552	18.0416	46.1174	1	-1830.	3103.	-87.	-1830.	3103.	-87.	1
166	-26.9328	76.9414	-0.3303	16.6695	44.0150	1	-1772.	2949.	-30.	-1772.	2949.	-30.	1
167	-30.4639	78.3691	0.6611	15.9684	45.8464	1	-1910.	3036.	60.	-1910.	3036.	60.	1
168	-34.1348	66.0310	2.0217	10.6321	41.6106	1	-1901.	2651.	184.	-1901.	2651.	184.	1
169	-30.5588	77.7505	5.7339	15.7305	45.8344	1	-1906.	3016.	521.	-1906.	3016.	521.	1
170	-21.0557	85.9182	5.9331	21.6208	45.5235	1	-1668.	3194.	539.	-1668.	3194.	539.	1
171	-3.1548	88.9558	5.5764	28.6003	42.9393	1	-1084.	3102.	507.	-1084.	3102.	507.	1
172	10.3994	90.4102	-1.3591	33.6032	40.4076	1	-633.	3004.	-123.	-633.	3004.	-123.	1
173	6.3826	84.5029	-5.8757	30.2955	38.7181	1	-707.	2844.	-534.	-707.	2844.	-534.	1
174	8.8227	68.6267	-5.2329	25.8165	30.7829	1	-448.	2270.	-476.	-448.	2270.	-476.	1
175	8.7102	40.9700	-13.4771	16.5601	20.7763	1	-149.	1317.	-1225.	-149.	1317.	-1225.	1
176	0.8039	9.6130	-9.4949	3.4723	8.8918	1	-78.	323.	-863.	-78.	323.	-863.	1
177	-0.5620	-6.5267	-3.1037	-2.3629	3.8914	1	52.	-219.	-262.	52.	-219.	-282.	1
178	-5.8450	87.7416	-0.9947	26.2989	43.6039	1	-1267.	3123.	-90.	-1267.	3123.	-90.	1
179	-10.2654	87.3601	-3.7500	25.6982	43.9093	1	-1312.	3125.	-341.	-1312.	3125.	-341.	1
180	-5.4173	74.6465	-5.7905	23.0764	35.8372	1	-1005.	2633.	-526.	-1005.	2633.	-526.	1
181	-15.0155	57.1655	-1.8331	14.0500	31.1333	1	-1145.	2136.	-166.	-1145.	2136.	-166.	1
182	-10.5879	59.1809	0.2036	16.1977	30.7000	1	-1014.	2157.	18.	-1014.	2157.	18.	1
183	-4.2209	60.7153	2.4397	18.8315	29.7332	1	-811.	2140.	222.	-811.	2140.	222.	1
184	3.3792	59.7451	1.9065	21.0414	27.4486	1	-539.	2023.	173.	-539.	2023.	173.	1
185	11.6497	59.6423	-6.4241	23.7640	26.3393	1	-252.	1929.	-584.	-252.	1929.	-584.	1
186	12.6001	56.3994	-8.9958	22.9998	25.2621	1	-184.	1807.	-818.	-184.	1807.	-818.	1
187	12.3992	49.9343	-13.3430	20.7778	23.8614	1	-120.	1586.	-1213.	-120.	1586.	-1213.	1
188	7.3324	31.5222	-16.3096	12.9515	18.9402	1	-93.	1007.	-1482.	-93.	1007.	-1482.	1
189	2.3555	11.5168	-8.0054	4.6241	8.2100	1	-45.	371.	-728.	-45.	371.	-728.	1
190	12.1885	60.1917	-17.7239	24.1267	29.7409	1	-240.	1942.	-1611.	-240.	1942.	-1611.	1
191	-6.6658	28.9836	-11.2671	7.4393	18.0116	1	-548.	1073.	-1026.	-548.	1073.	-1026.	1
192	-0.6882	42.6962	-8.5107	13.8027	22.2128	1	-485.	1459.	-319.	-485.	1459.	-319.	1
193	1.4133	38.1455	-10.6775	13.1863	19.6431	1	-370.	1300.	-971.	-370.	1300.	-971.	1
194	9.8449	29.7890	-7.5420	13.2113	13.8378	1	13.	919.	-686.	13.	919.	-686.	1
195	4.3247	40.5235	-2.3850	14.9494	18.2737	1	-295.	1350.	-217.	-295.	1350.	-217.	1
196	10.5579	36.8582	-18.5864	15.8053	21.6908	1	-40.	1155.	-1689.	-40.	1155.	-1689.	1
197	25.3596	27.9280	-14.6812	17.7625	17.3938	1	568.	685.	-1335.	568.	685.	-1335.	1
198	11.2837	36.0457	-9.7754	15.7764	17.0395	1	-6.	1119.	-888.	-6.	1119.	-888.	1
199	20.4441	28.2273	-19.1890	16.2238	19.6769	1	395.	749.	-1744.	395.	749.	-1744.	1
200	18.6160	21.0220	-21.5859	13.2127	19.9722	1	411.	521.	-1962.	411.	521.	-1962.	1

TABLE C-11. FINITE-ELEMENT ANALYSIS OF LEAD-LAG JOINT IN UPPER PLATE FOR ULTIMATE LOADS OF CONDITION TW7F1 (continued)

STRESS ELEM	XX	YY	XY	ON	CS	CASE	(TOTAL STRAIN)*1000000. XX	YY	XY	(MECH. STRAIN)*1000000. XX	YY	XY	CASE
201	10.5589	11.5615	-16.0381	7.3734	14.1007	1	237.	283.	-1456.	237.	283.	-1458.	1
202	3.1296	5.4595	-5.2636	2.8630	4.8449	1	48.	154.	-478.	48.	154.	-478.	1
203	4.6685	26.4673	-10.5625	10.3786	14.4025	1	-129.	861.	-960.	-129.	861.	-960.	1
204	9.5361	25.3809	-9.5354	11.6390	13.0457	1	51.	771.	-867.	51.	771.	-867.	1
205	22.3909	21.9348	-17.8228	14.7752	17.9152	1	532.	511.	-1620.	532.	511.	-1620.	1
206	29.6886	19.0742	-25.0491	16.2543	23.8555	1	815.	332.	-2277.	815.	332.	-2277.	1
207	25.6116	16.2871	-26.8247	13.9662	24.3255	1	705.	281.	-2438.	705.	281.	-2438.	1
208	19.5472	17.2235	-20.9388	12.2769	19.1965	1	485.	382.	-1903.	485.	382.	-1903.	1
209	10.7925	13.4447	-8.4262	8.0791	9.0079	1	225.	345.	-766.	225.	345.	-766.	1
210	7.2085	16.8042	-11.4673	8.0042	11.6209	1	64.	500.	-1042.	64.	500.	-1042.	1
211	16.7428	20.5110	-17.2344	12.4179	16.6579	1	352.	524.	-1566.	352.	524.	-1566.	1
212	36.5590	19.8425	-28.8662	18.8005	27.9071	1	1043.	283.	-2624.	1043.	283.	-2624.	1
213	49.0686	18.8823	-38.7561	22.6503	37.5466	1	1485.	113.	-3523.	1485.	113.	-3523.	1
214	48.8613	18.2678	-41.7124	22.3764	39.5764	1	1435.	94.	-3791.	1485.	94.	-3791.	1
215	34.3102	21.5715	-32.6176	18.6272	30.1630	1	947.	368.	-2965.	947.	368.	-2965.	1
216	30.7178	19.0915	-11.8623	16.6331	15.5545	1	850.	322.	-1006.	850.	322.	-1006.	1
217	5.3975	53.9161	5.3295	19.7712	24.6219	1	-405.	1800.	484.	-405.	1800.	484.	1
218	2.9073	50.1585	-1.5233	17.6886	23.0240	1	-450.	1698.	-138.	-450.	1698.	-138.	1
219	0.4341	40.7973	-8.3053	13.7438	20.2969	1	-432.	1402.	-755.	-432.	1402.	-755.	1
220	-1.6583	26.8723	-14.0561	8.4047	17.3983	1	-352.	945.	-1278.	-352.	945.	-1278.	1
221	-3.1134	10.1028	-18.0503	2.3298	15.7808	1	-218.	383.	-1641.	-218.	383.	-1641.	1
222	-3.8069	-7.4475	-19.9554	-3.7515	15.5748	1	-50.	-215.	-1814.	-50.	-215.	-1814.	1
223	-3.6180	-23.7320	-19.4366	-9.1167	18.9958	1	135.	-779.	-1767.	135.	-779.	-1767.	1
224	-2.5556	-36.7599	-16.5096	-13.1052	21.5075	1	315.	-1240.	-1501.	315.	-1240.	-1501.	1
225	-0.7650	-44.9037	-11.5977	-15.2229	23.0270	1	466.	-1540.	-1054.	466.	-1540.	-1054.	1
226	-3.3091	3.7030	3.4109	0.1313	3.9949	1	-155.	164.	310.	-155.	164.	310.	1
227	-16.1409	-0.3409	-0.9970	-5.4939	7.5737	1	-553.	165.	-91.	-553.	165.	-91.	1
228	-24.8799	-22.4401	-6.4763	-15.7733	12.3836	1	-612.	-501.	-589.	-612.	-501.	-589.	1
229	-17.9678	-29.3040	-3.4340	-15.7573	12.3865	1	-298.	-813.	-312.	-298.	-813.	-312.	1
230	-1.4875	-15.0462	4.1784	-5.5112	7.5806	1	114.	-503.	380.	114.	-503.	380.	1
231	-3.3125	3.6851	3.4214	0.1242	3.9966	1	-155.	163.	311.	-155.	163.	311.	1
232	-0.1704	0.1106	0.1011	-0.0199	0.1421	1	-7.	6.	9.	-7.	6.	9.	1
233	0.1022	0.1508	0.2283	0.0843	0.1957	1	2.	4.	21.	2.	4.	21.	1
234	-2.1624	-0.4312	-0.7867	-0.8645	1.1339	1	-70.	9.	-72.	-70.	9.	-72.	1
235	-0.1360	-2.4597	0.1297	-0.8652	1.1338	1	22.	-83.	12.	22.	-83.	12.	1
236	-0.0037	0.2573	0.1902	0.0845	0.1976	1	-3.	9.	17.	-3.	9.	17.	1
237	-0.1331	0.0688	0.1334	-0.0214	0.1407	1	-5.	4.	13.	-5.	4.	13.	1
238	-2.9664	-15.1288	0.2823	-6.0351	6.5543	1	64.	-489.	26.	64.	-489.	26.	1
239	-1.1875	-6.7549	1.9026	-2.6474	3.3292	1	33.	-220.	173.	33.	-220.	173.	1
240	-0.8677	1.4568	1.9062	0.1964	1.8282	1	-46.	60.	173.	-46.	60.	173.	1
241	37.1803					1	1282.			1282.			1
242	35.2062					1	1214.			1214.			1
243	29.5070					1	1017.			1017.			1
244	20.4037					1	704.			704.			1
245	9.1912					1	317.			317.			1
246	-2.5211					1	-87.			-87.			1
247	-13.7104					1	-473.			-473.			1
248	-22.9176					1	-790.			-790.			1
249	-28.8520					1	-995.			-995.			1
250	-30.8888					1	-1065.			-1065.			1

TABLE C-11. FINITE-ELEMENT ANALYSIS OF LEAD-LAG JOINT IN UPPER PLATE FOR ULTIMATE LOADS OF CONDITION TW7F1 (continued)

STRESS ELEM	XX	YY	XY	ON	OS	CASE	(TOTAL STRAIN)*1000000. XX	YY	XY	(MECH. STRAIN)*1000000. XX	YY	XY	CASE
251	0.1168					1	116824.			116824.			1
252	0.0813					1	81345.			81345.			1
253	-15.4772					1	-534.			-534.			1
254	-25.8969					1	-893.			-893.			1
255	-15.4614					1	-533.			-533.			1
256	0.0797					1	79667.			79667.			1
257	0.0054					1	5445.			5445.			1
258	0.0100					1	9961.			9961.			1
259	0.0464					1	2.			2.			1
260	-2.3456					1	-81.			-81.			1
261	0.0492					1	2.			2.			1
262	0.0059					1	5879.			5879.			1
263	-9.2462					1	-319.			-319.			1
264	-4.2615					1	-147.			-147.			1
265	0.0262					1	6221.			6221.			1
266	0.0088					1	8783.			8783.			1
267	40.0589	-21.8923	0.3638	6.0355	25.6531	1	1621.	-1194.	33.	1621.	-1194.	33.	1
268	36.5585	-19.4824	3.4406	5.6920	23.3992	1	1474.	-1073.	313.	1474.	-1073.	313.	1
269	28.2847	-12.7069	5.0928	5.1926	17.6302	1	1115.	-748.	463.	1115.	-748.	463.	1
270	17.3967	-4.6349	6.0606	4.2543	10.6974	1	651.	-351.	551.	651.	-351.	551.	1
271	5.5167	3.5532	6.2232	3.1566	5.5864	1	147.	76.	566.	147.	76.	566.	1
272	-6.4723	13.5712	6.3508	2.3663	9.8308	1	-372.	539.	577.	-372.	539.	577.	1
273	-17.7223	21.8183	5.2487	1.3654	16.7294	1	-850.	947.	477.	-850.	947.	477.	1
274	-25.6282	28.2661	3.1239	0.8793	22.1563	1	-1194.	1256.	284.	-1194.	1256.	284.	1
275	-29.7114	31.0903	1.0724	0.4596	24.8308	1	-1365.	1398.	97.	-1365.	1398.	97.	1
276	10.9989	13.7980	6.6271	8.2656	8.0464	1	228.	355.	602.	228.	355.	602.	1
277	39.3921	16.0982	-20.4406	18.4934	23.2392	1	1182.	123.	-1858.	1182.	123.	-1858.	1
278	1.3710	25.1198	-15.4625	8.8303	17.7196	1	-228.	851.	-1496.	-228.	851.	-1496.	1
279	-10.7466	73.9400	-4.3553	21.0645	37.8128	1	-1181.	2667.	-396.	-1181.	2667.	-396.	1
280	-10.5621	75.3808	6.2452	21.6052	38.6053	1	-1191.	2715.	568.	-1191.	2715.	568.	1
281	-4.3196	18.2711	20.8726	4.6505	19.6548	1	-349.	677.	1897.	-349.	677.	1897.	1
282	31.9149	18.9939	16.3463	16.9696	18.7067	1	892.	305.	1486.	892.	305.	1486.	1
283	13.4478	16.4277	-9.2534	9.9585	10.3995	1	284.	419.	-841.	284.	419.	-841.	1
284	1.7258	5.0246	-4.1723	2.2501	3.9938	1	4.	154.	-379.	4.	154.	-379.	1
285	-0.0273	4.0817	-0.8716	1.3515	2.0576	1	-46.	141.	-79.	-46.	141.	-79.	1
286	1.1125	3.8257	-0.2210	1.6461	1.6169	1	-4.	120.	-20.	-4.	120.	-20.	1
287	-0.9993	7.0577	-0.6171	2.0195	3.6211	1	-112.	254.	-56.	-112.	254.	-56.	1
288	-1.1016	6.6789	0.1364	1.8591	3.4395	1	-111.	242.	12.	-111.	242.	12.	1
289	0.7695	5.6474	0.4733	2.1390	2.5303	1	-35.	186.	43.	-35.	186.	43.	1
290	0.9470	3.7870	-0.5148	1.5780	1.6631	1	-9.	120.	-47.	-9.	120.	-47.	1
291	1.4403	7.6761	3.0857	3.0388	4.1768	1	-35.	249.	280.	-35.	249.	280.	1
292	-14.3226	15.2020	-7.3660	0.2931	13.4721	1	-661.	681.	-670.	-661.	681.	-670.	1
293	1.6734	0.2540	1.5820	0.6425	1.4868	1	55.	-10.	144.	55.	-10.	144.	1
294	0.8877	1.4124	1.2054	0.7667	1.1439	1	15.	39.	110.	15.	39.	110.	1
295	0.2387	0.6504	0.3956	0.2963	0.4201	1	1.	20.	36.	1.	20.	36.	1
296	12.4246	4.3871	-4.5174	5.6039	6.3304	1	1473.	86.	-1559.	1473.	86.	-1559.	1
297	14.3288	1.8079	-2.1204	5.3789	6.6025	1	1829.	-332.	-732.	1829.	-332.	-732.	1
298	14.2411	1.1081	1.0939	6.7830	8.8659	1	2508.	-621.	378.	2508.	-621.	378.	1
299	0.3225	0.6982	0.0423	0.3402	0.2874	1	15.	80.	15.	15.	80.	15.	1
300	2.8438	0.4428	1.1259	1.0955	1.5511	1	360.	-55.	389.	360.	-55.	389.	1

TABLE C-11. FINITE-ELEMENT ANALYSIS OF LEAD-LAG JOINT IN UPPER PLATE FOR ULTIMATE LOADS OF CONDITION TW7F1 (continued)

STRESS ELEM	XX	YY	XY	ON	OS	CASE	(TOTAL STRAIN)*1000000. XX	YY	XY	(MECH. STRAIN)*1000000. XX	YY	XY	CASE
301	5.3484	1.2555	-0.2606	2.2013	2.2935	1	659.	-47.	-90.	659.	-47.	-90.	1
302	6.5936	2.7232	1.1078	3.1056	2.8526	1	766.	98.	382.	766.	98.	382.	1
303	6.1471	6.4830	0.2784	4.2100	2.9688	1	557.	615.	96.	557.	615.	96.	1
304	9.9690	5.1281	1.0996	5.0323	4.1682	1	1118.	282.	380.	1118.	282.	380.	1
305	17.1311	2.2851	1.8371	6.4721	7.7413	1	2132.	-381.	634.	2182.	-381.	634.	1
306	0.7566	3.0427	-0.4293	1.2664	1.3401	1	-21.	373.	-148.	-21.	373.	-148.	1
307	2.6474	5.6994	-3.6755	2.8489	3.8505	1	116.	677.	-1269.	116.	677.	-1269.	1
308	8.0412	6.4872	-4.3208	4.8428	4.9573	1	808.	540.	-1491.	808.	540.	-1491.	1
309	10.9906	3.3461	-0.8694	4.7789	4.6543	1	1325.	5.	-300.	1325.	5.	-300.	1
310	13.8780	1.7053	2.8093	5.1944	6.5915	1	1773.	-328.	970.	1773.	-328.	970.	1
311	2.2193	5.1166	2.3943	2.4453	2.8654	1	90.	590.	826.	90.	590.	826.	1
312	6.5735	6.0077	4.3431	4.1937	4.6284	1	632.	535.	1499.	632.	535.	1499.	1
313	9.2341	2.3277	2.3358	3.8540	4.3604	1	1132.	-60.	806.	1132.	-60.	806.	1
314	9.7384	1.7935	3.4922	3.8440	5.1028	1	1220.	-151.	1205.	1220.	-151.	1205.	1
315	0.4869	3.3603	0.4587	1.2831	1.5269	1	-69.	426.	158.	-69.	426.	158.	1
316	2.1765	4.7961	1.9624	2.3242	2.5322	1	97.	549.	677.	97.	549.	677.	1
317	2.7772	4.1073	2.5280	2.2948	2.6812	1	204.	434.	873.	204.	434.	873.	1
318	4.3943	3.1543	4.4752	2.5162	4.0955	1	457.	243.	1545.	457.	243.	1545.	1
319	0.2326	2.5223	-0.0617	0.9183	1.1393	1	-70.	325.	-21.	-70.	325.	-21.	1
320	0.0592	3.0983	0.7981	1.0525	1.5868	1	-116.	409.	275.	-116.	409.	275.	1
321	-0.4949	4.2217	0.7732	1.2423	2.2086	1	-234.	580.	267.	-234.	580.	267.	1
322	-1.2690	3.6427	3.5671	0.7912	3.5801	1	-314.	534.	1231.	-314.	534.	1231.	1
323	0.0482	3.0949	-0.5620	1.0477	1.5187	1	-117.	409.	-194.	-117.	409.	-194.	1
324	-0.5734	2.1685	-1.0034	0.5317	1.4372	1	-163.	311.	-346.	-163.	311.	-346.	1
325	-2.1171	2.3391	0.2806	0.2573	2.2651	1	-396.	468.	99.	-396.	468.	99.	1
326	-5.3992	3.6485	2.7653	-0.5836	4.3488	1	-862.	700.	955.	-862.	700.	955.	1
327	-0.5580	3.2386	0.1875	0.8935	1.6803	1	-203.	452.	65.	-203.	452.	65.	1
328	-2.2052	2.1311	0.7779	-0.0247	1.8809	1	-378.	371.	269.	-378.	371.	269.	1
329	-3.5436	2.8373	1.0892	-0.2354	2.7576	1	-583.	518.	376.	-583.	518.	376.	1
330	-8.9089	3.6760	2.2217	-1.7443	5.5865	1	-1329.	843.	767.	-1329.	843.	767.	1
331	-0.1965	1.9765	1.3579	0.5933	1.4868	1	-105.	270.	472.	-105.	270.	472.	1
332	-2.1786	0.6462	3.7436	-0.5108	3.2868	1	-315.	173.	1292.	-315.	173.	1292.	1
333	-7.3023	3.7972	1.5517	-1.1684	4.7771	1	-1120.	795.	536.	-1120.	795.	536.	1
334	-10.6931	4.5811	0.8309	-2.1373	6.5704	1	-1641.	1047.	287.	-1641.	1047.	287.	1
335	0.1168					1	1168.			1168.			1
336	0.1688					1	1688.			1688.			1
337	0.0086					1	86.			86.			1
338	0.0187					1	187.			187.			1

TABLE C-11. FINITE-ELEMENT ANALYSIS OF LEAD-LAG JOINT IN UPPER PLATE FOR ULTIMATE LOADS OF CONDITION TW7F1 (continued)

X FORCE, CASE 1

	1	2	3	4	5	6	7	8	9	10
1	2.021E 01	1.019E 01	-2.441E-04	-2.930E-03	-1.221E-03	0.0	-2.441E-04	-7.324E-04	3.013E-05	-6.515E-04
11	9.169E-04	-1.219E-04	2.990E-04	5.301E-04	1.035E 01	-2.058E-01	-2.441E-04	-6.866E-04	-6.409E-04	-4.158E-04
21	-3.815E-04	-1.526E-05	4.578E-05	3.815E-04	3.815E-04	4.120E-04	2.441E-04	1.389E-03	-2.782E 00	-5.322E-01
31	-1.465E-03	1.709E-02	-2.197E-03	-4.883E-04	-1.221E-03	-2.441E-04	4.196E-05	9.766E-04	9.766E-04	9.766E-04
41	1.973E-04	-6.446E-04	-6.743E-01	-3.138E-01	2.136E-04	4.883E-04	7.477E-04	9.918E-04	9.766E-04	4.578E-05
51	-9.155E-05	-1.678E-04	-1.038E-03	-9.766E-04	-9.613E-04	-4.883E-04	1.957E 00	-1.267E 00	-4.883E-04	-4.883E-04
61	7.629E-05	1.965E-04	6.256E-04	6.104E-05	3.052E-05	2.899E-04	-6.866E-04	6.409E-04	6.561E-04	4.578E-04
71	1.444E 00	-6.671E 00	5.493E-04	-5.035E-04	6.981E-04	5.646E-04	4.425E-04	1.373E-04	1.526E-05	-6.561E-04
81	-7.629E-05	-3.052E-05	-1.526E-05	-4.272E-04	1.134E 00	-2.218E 01	4.578E-05	1.068E-04	4.120E-04	6.256E-04
91	1.068E-04	0.0	-4.578E-05	-1.526E-05	-7.019E-04	1.526E-05	4.883E-04	-1.373E-04	1.613E-01	-1.525E 01
101	3.204E-04	5.951E-04	5.951E-04	-2.441E-04	3.052E-05	1.526E-05	-1.526E-05	0.0	-2.136E-04	-2.289E-04
111	-8.411E-04	4.578E-04	1.526E-05	-5.341E-04	-2.441E-04	-4.578E-05	2.325E-06	0.0	-1.113E 00	0.0
121	0.0	0.0	-3.357E-04	-8.850E-04	-2.879E-04	-3.052E-05	-1.444E 00	1.526E-05	3.052E-05	-7.629E-05
131	1.526E-05	7.629E-06	8.583E-06	-2.575E-05	-1.244E 00	3.147E-05	-4.766E-06	2.861E-06	-1.335E-05	-1.049E-05
141	-1.240E-05	-1.786E 00	2.003E-05	6.676E-06	-2.193E-05	-1.335E-05	-3.242E-05	-2.480E-05	-1.715E 00	4.768E-06
151	-1.526E-05	-3.052E-05	-2.766E-05	7.629E-06	0.0	-1.706E 00	5.514E 00	7.859E 00	-2.518E 00	4.959E-05
161	4.673E-05	3.052E-05	0.0	8.583E-06	-1.144E-05	-2.098E-05	-1.621E-05	-1.431E-05	1.240E-05	-6.104E-05
171	-7.629E-05	1.144E-05	-3.052E-05	-1.049E-05	-3.593E-05	1.967E-04	-1.526E-05	-2.136E-04	7.629E-05	-7.629E-05
181	8.392E-04	4.053E-03	5.281E 01	-1.068E-04	-1.717E-05	-6.580E-05	-1.431E-05	3.624E-05	-2.441E-04	3.052E-05
191	0.0	1.792E-04	-1.678E-04	-1.602E-03	3.052E-05	0.0	0.0	-5.341E-05	2.575E-05	-2.098E-05
201	2.861E-06	-1.068E-04	2.599E-05	-3.636E-05	-4.292E-05	8.583E-06	1.144E-05	2.956E-05	-4.196E-05	2.289E-05
211	-1.526E-05	-4.578E-05	-4.578E-05	-5.277E-05	-5.280E-03	-1.526E-05	-2.747E-04	-3.052E-05	-1.526E-05	-1.373E-04
221	8.964E-05	3.161E 00	1.526E-05	0.0	-1.544E-05	-5.722E-06	-3.338E-05	2.136E-04	-6.104E-05	-2.441E-04
231	2.178E-04	1.335E-05	6.046E-04	-4.578E-05	5.722E-06	2.861E-05	5.722E-06	-3.624E-05	4.959E-05	-2.688E-05
241	1.621E-05	2.480E-05	-6.104E-05	3.815E-06	1.144E-05	3.529E-05	6.485E-05	4.673E-05	6.104E-05	-1.812E-05
251	-1.526E-05	3.052E-05	1.526E-05	1.526E-05	-5.932E-04	3.052E-05	4.578E-04	7.845E-01	-1.290E 00	1.602E 00
261	1.358E 00	1.631E 00	-4.459E 00	-8.235E 00	-9.468E 00	-1.558E 01	-1.174E 01	-2.517E 00	-5.479E 00	

TABLE C-11. FINITE-ELEMENT ANALYSIS OF LEAD-LAG JOINT IN UPPER PLATE FOR ULTIMATE LOADS OF CONDITION TW7F1 (continued)

Y FORCE, CASE 1

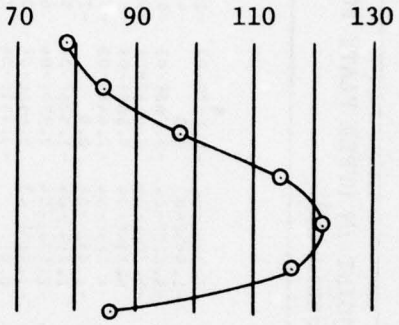
	1	2	3	4	5	6	7	8	9	10
1	4.498E 01	-2.441E-03	-7.813E-03	-7.813E-03	-2.197E-03	-3.906E-03	-7.324E-04	-2.182E-03	-2.686E-03	-3.554E-03
11	4.548E-04	-1.444E-03	1.680E-04	1.274E-03	-1.290E-04	-2.441E-04	-1.953E-03	0.0	-4.730E-04	-6.104E-05
21	3.052E-05	-3.052E-04	-6.866E-04	-7.477E-04	-4.883E-04	-4.883E-04	-4.883E-04	-9.766E-03	-1.221E-03	3.662E-03
31	0.0	1.416E-02	-9.766E-04	-2.441E-04	-3.967E-04	-1.526E-05	-3.204E-04	7.019E-04	-9.308E-04	-2.197E-03
41	-1.862E-03	-2.673E-04	2.165E-03	4.883E-04	3.174E-03	-4.883E-04	6.714E-04	9.308E-04	1.053E-03	8.698E-04
51	1.160E-03	8.087E-04	9.766E-04	1.221E-03	9.766E-04	1.953E-03	-4.883E-04	-2.441E-03	-7.568E-03	-1.025E-02
61	2.441E-04	1.221E-04	-4.730E-04	-5.951E-04	-8.850E-04	-6.561E-04	-2.441E-04	0.0	-7.324E-04	-4.883E-04
71	-2.441E-04	1.221E-03	6.545E-03	3.021E-03	4.120E-04	1.831E-04	2.289E-04	-1.526E-04	5.951E-04	1.526E-04
81	2.441E-04	7.324E-04	4.883E-04	4.883E-04	4.883E-04	2.441E-04	-2.136E-04	7.324E-04	6.561E-04	9.003E-04
91	7.477E-04	4.883E-04	4.425E-04	1.526E-04	2.441E-04	4.883E-04	-1.465E-03	5.646E-04	0.0	1.526E-05
101	5.951E-04	9.308E-04	2.899E-04	3.510E-04	4.883E-04	-1.526E-05	0.0	-2.441E-04	2.441E-04	7.324E-04
111	1.129E-03	1.984E-04	3.662E-04	4.425E-04	2.594E-04	5.646E-04	1.373E-04	5.798E-04	0.0	7.629E-05
121	3.510E-04	1.068E-03	7.324E-04	2.747E-04	6.409E-04	3.357E-04	0.0	3.052E-05	1.221E-04	2.289E-04
131	6.256E-04	6.104E-04	5.646E-04	5.798E-04	2.594E-04	0.0	1.526E-05	3.052E-05	3.052E-05	-1.068E-04
141	4.578E-05	3.052E-05	-1.526E-05	4.578E-05	4.578E-05	1.526E-05	3.052E-05	0.0	2.593E-05	-3.052E-05
151	-8.239E-05	3.052E-05	6.104E-05	3.052E-05	9.155E-05	3.052E-05	-4.578E-05	-2.508E-04	-1.221E-04	-8.583E-06
161	-1.526E-05	1.221E-04	2.899E-04	-3.052E-05	3.052E-05	0.0	7.629E-05	-1.526E-05	0.0	7.629E-05
171	-6.104E-05	-1.831E-04	3.052E-05	6.104E-05	-6.663E-04	-6.104E-03	-2.136E-04	3.906E-03	-4.883E-04	-3.662E-04
181	-2.522E-03	1.764E-04	3.049E 01	4.730E-04	-4.272E-04	1.373E-04	4.578E-05	1.526E-05	-1.221E-04	-4.578E-05
191	-1.221E-03	6.928E-04	-6.104E-05	1.740E-03	-2.441E-04	4.578E-05	5.798E-04	1.526E-05	4.578E-05	4.578E-05
201	4.578E-05	4.578E-05	3.052E-05	-2.441E-04	1.526E-05	2.670E-05	4.959E-05	5.341E-05	6.962E-05	1.526E-05
211	-9.155E-05	0.0	-3.662E-04	-2.325E-06	1.907E-05	5.188E-04	-2.136E-04	-2.747E-04	-2.899E-04	2.289E-04
221	-2.112E-04	-1.275E 00	-7.324E-04	-1.373E-04	6.485E-05	2.098E-05	-1.240E-05	-1.373E-04	-3.052E-05	-3.906E-03
231	3.624E-04	-6.676E-06	5.676E-03	-1.221E-04	-3.815E-06	9.727E-05	1.717E-05	1.144E-05	6.390E-05	1.812E-05
241	-6.676E-06	-3.204E-04	1.068E-04	2.003E-05	3.242E-05	3.052E-05	6.580E-05	1.907E-05	-3.271E-04	4.730E-04
251	1.431E-05	-1.831E-04	-1.526E-04	3.204E-04	-1.984E-04	0.0	7.324E-04	-2.441E-04	-7.486E-05	-1.068E-04
261	1.212E 01	-2.441E-04	3.052E-05	-5.722E-06	2.338E-05	1.621E-05	9.155E-05	0.0	-8.595E 01	

CHECKS, SUM		X-FORCES	Y-FORCES	Z-MOMENTS	CASE
		-1.471D-02	-1.904D-01	-1.446D 00	1
NZE	BARK	4220			
	*RHS	4226			
	REDU	3857			

Steel Tangential Stress at Inner Edge of Hole

Figure C-25 shows a plot of steel stresses from the data in Table C-11. The maximum stress in the steel is 1.347 ksi/kip of axial load. The corresponding maximum stress is 3.5 percent lower, at 1.300 ksi/kip of axial load, for the element specimen as shown in Figure C-16.

Elements	2nd	1st	i-edge
168, 155	66.03	75.33	78.43
169, 156	77.75	82.92	84.64
170, 157	85.92	94.36	97.17
171, 158	88.96	107.84	114.13
172, 159	90.41	113.49	121.18
173, 160	84.50	104.86	111.65
174, 161	68.63	81.81	86.20



Use Peak $\sigma = \frac{121.2}{89.97} = 1.347$ ksi/kip of axial load

Figure C-25. Tangential stress at inner edge of hole for upper plate, Condition TW7F1 Ultimate.

Composite Tangential Stress at Inner Edge of Hole

Elements	2nd	1st	i-edge
86, 73	22.31	24.53	25.27
87, 74	23.01	27.91	29.54
88, 75	23.32	29.29	31.28
89, 76	21.81	27.10	28.87

Use Peak $\sigma = \frac{31.3}{89.97} = .3479$ ksi/kip of axial load

The corresponding maximum stress for the element specimen is 3.9 percent lower.

Steel Tangential Stress at Outer Edge of Lug (Point A in Figure 17)

Elements	2nd	3rd	0-edge
165, 178	81.33	87.74	92.73
166, 179	76.94	87.36	95.46

$$\text{Use Peak } \sigma = \frac{95.7}{89.97} = 1.064 \text{ ksi/kip of axial load}$$

The corresponding maximum stress for the element specimen is 3.3 percent higher.

Composite Stress at Outer Edge of Lug (Point A in Figure 17)

Elements	2nd	1st	0-edge
81, 94	21.15	22.72	23.94
82, 95	20.02	22.63	24.66

$$\text{Use Peak } \sigma = \frac{24.7}{89.97} = .2745 \text{ ksi/kip of axial load}$$

The corresponding maximum stress for the element specimen is 3.3 percent higher.

Ultimate Margins of Safety

From Table C-6, the largest load at the lead-lag of the upper plate is 89.97 kips. The scaled failure load from the test of the element test was 176 kips.

$$\text{Ultimate M.S.} = \frac{176}{89.97} - 1 = +\underline{.95}$$

Fatigue Margins of Safety

Figure 20 summarized the results of the fatigue tests of element specimens and related them to the S-N curve for the present titanium hub. The specimens were 7 and 14 percent higher than the mean fatigue strength of the titanium hub.

$$\text{Fatigue M.S.} = \left(\frac{.07 + .14}{2}\right) = +\underline{.10}$$

The following calculations relate the test loads to the head moment shown in Figure 20 for the case of head moment = 800 in.-kips. Table C-6 shows that for the fatigue design condition, which has a head moment of 800 in.-kips, the maximum and minimum loads at the lead-lag pin of the upper plate are 43.95 and 4.95 kips, respectively, corresponding to 24.45 $\pm$ 19.5 kips. The corresponding test condition was step 1 in which the scaled loads were

.25 x 176 = 44.0 kips maximum, and .025 x 176 = 4.4 kips minimum, or 24.2 $\pm$ 19.8 kips, providing a close match. The vibratory loads are similarly matched for steps 2 and 3 shown in Figure 20.

Buckling

Table C-6 shows that a compressive load of 24.34 kips ultimate occurs at maximum flapping upward during condition TW7F1. Considering the central region of the upper plate as a pin-ended column with an effective length = 9 inches and an effective width = 11 inches, its critical buckling load is:

$$P_{cr} = \frac{\pi^2 EI}{L^2} = \frac{\pi^2 Ebt^3}{12\,L^2} = \frac{\pi^2\,(7540)(11)(.330)^3}{12\,(9)^2} = 30.26 \text{ kips}$$

$$\text{Ultimate Buckling M.S.} = \frac{30.26}{24.34} - 1 = +\,\underline{.24}$$

Center hole

The center hole in the upper plate was preloaded radially when the hub was assembled. Figure 2 shows the final assembled position and makes it apparent how the preload was generated. The cone at the center was designed so that its top sat, initially, .037 inch (full-scale) above the end of the rotor shaft. Then, as the bolts were tightened, the cone was forced down inducing a radial expansion and a tight radial fit into the upper plate. The nominal fits were chosen so that radial compression existed up to a head moment corresponding to 170 percent of the fatigue design moment. These fits and the corresponding stresses were established from analyses using the finite-element model shown in Figure C-26. The results from these analyses are summarized herein.

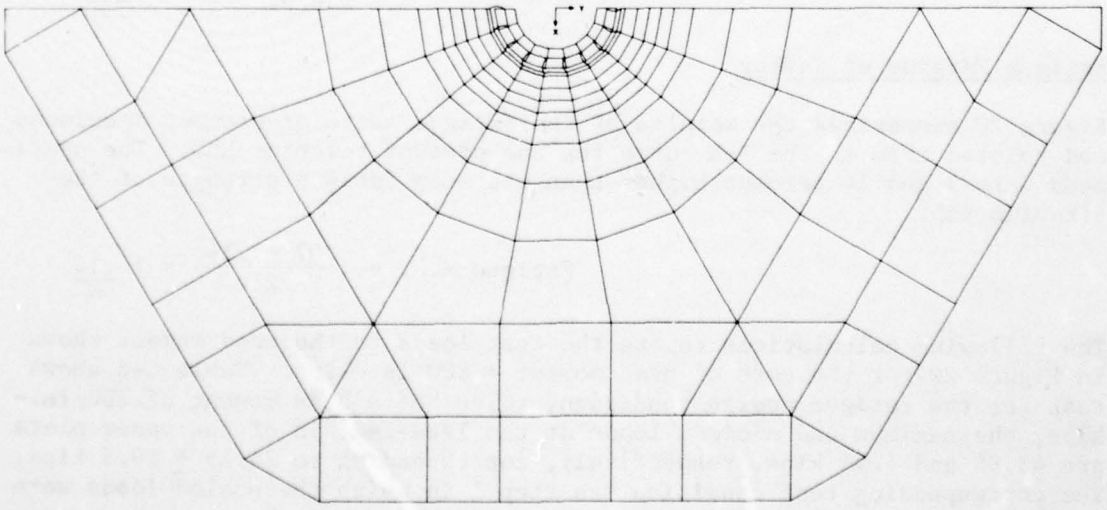
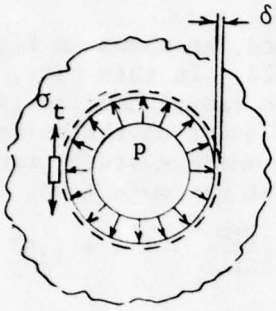


Figure C-26. Finite-element model for center hole in upper plate.

The first analysis established the radial stiffness of the center hole in the upper plate when subjected to a uniformly distributed radial force. Figure C-27 shows the results.



p = radial force/unit length, kip/inch

δ = radial expansion of hole, inch

σ_t = tangential stress in steel, ksi

$\delta/p = .0006662$ in.^{2}/kip

$\sigma_t/p = 5.027$ inch^{-1}

Figure C-27. Deflections and stresses for uniform radial load at center hole of upper plate.

The second analysis established the radial forces that exist for the fatigue design loads (shown in Table C-6) assuming radial continuity at the center hole to the rotor mast. Figure C-28 shows the results.

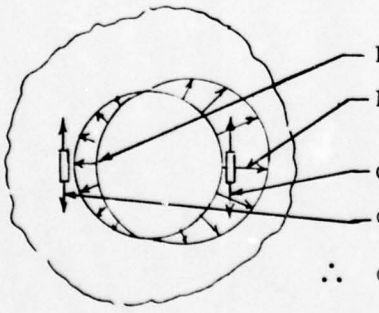


Figure C-28. Stresses and force intensities at center hole of upper plate for fatigue design loads.

Sufficient preload is applied to maintain radial continuity at the center hole, thus:

$$\text{Fatigue M.S.} = \frac{25.0}{13.8} - 1 = +\underline{.81}$$

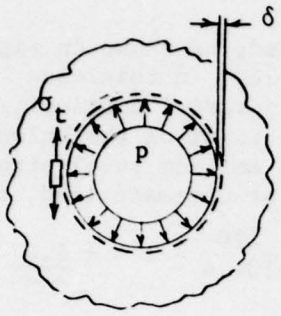
AD-A060 313 KAMAN AEROSPACE CORP BLOOMFIELD CONN F/G 1/3
DESIGN, FABRICATION AND LABORATORY TESTING OF A HELICOPTER COMP--ETC(U)
AUG 78 R J MAYERJAK DAAJ02-75-C-0013
UNCLASSIFIED USARTL-TR-78-16 NL

3 OF 3
ADA
060313



END
DATE
FILMED
12-78
DDC

The first analysis established the radial stiffness of the center hole in the upper plate when subjected to a uniformly distributed radial force. Figure C-27 shows the results.



p = radial force/unit length, kip/inch

δ = radial expansion of hole, inch

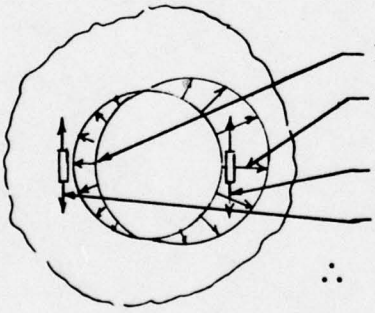
σ_t = tangential stress in steel, ksi

$\delta/p = .0006662$ in.^{2}/kip

$\sigma_t/p = 5.027$ inch^{-1}

Figure C-27. Deflections and stresses for uniform radial load at center hole of upper plate.

The second analysis established the radial forces that exist for the fatigue design loads (shown in Table C-6) assuming radial continuity at the center hole to the rotor mast. Figure C-28 shows the results.



Maximum compression = -3.748 kips/inch

Maximum tension = 6.067 kips/inch

σ_t = -10.283 ksi

σ_t = 17.249 ksi

$\therefore$ $\sigma_t = \pm 13.766$ ksi

Figure C-28. Stresses and force intensities at center hole of upper plate for fatigue design loads.

Sufficient preload is applied to maintain radial continuity at the center hole, thus:

$$\text{Fatigue M.S.} = \frac{25.0}{13.8} - 1 = +\underline{.81}$$

For radial continuity to exist, a radial preload of at least 6.067 kips/inch is required. The design provides 1.7 x 6.067 = 10.31 kips/inch to provide positive assurance of continuity. The maximum steady stress in the steel corresponding to this preload is:

$$10.31 \times 5.027 = 51.83 \text{ ksi}$$

In the third analysis, the ultimate loads were applied, as shown in Figure C-23, to the finite-element model shown in Figure C-26. In this case, it was assumed that preload was insufficient to maintain radial continuity around the hole and the natural gap was permitted to exist on the unloaded side of the hole. The analysis established that the maximum steel stress in the laminae at the edge of the hole is 101.6 ksi at ultimate load, thus:

$$\text{Ultimate M.S.} = \frac{210}{101.6} - 1 = +\underline{1.07}$$

Strains During Fatigue Test of Model

The analytical predictions of strains in the upper plate shown in Figure 34 were calculated by applying appropriate loads for the fatigue test to the finite-element model shown in Figure C-29.

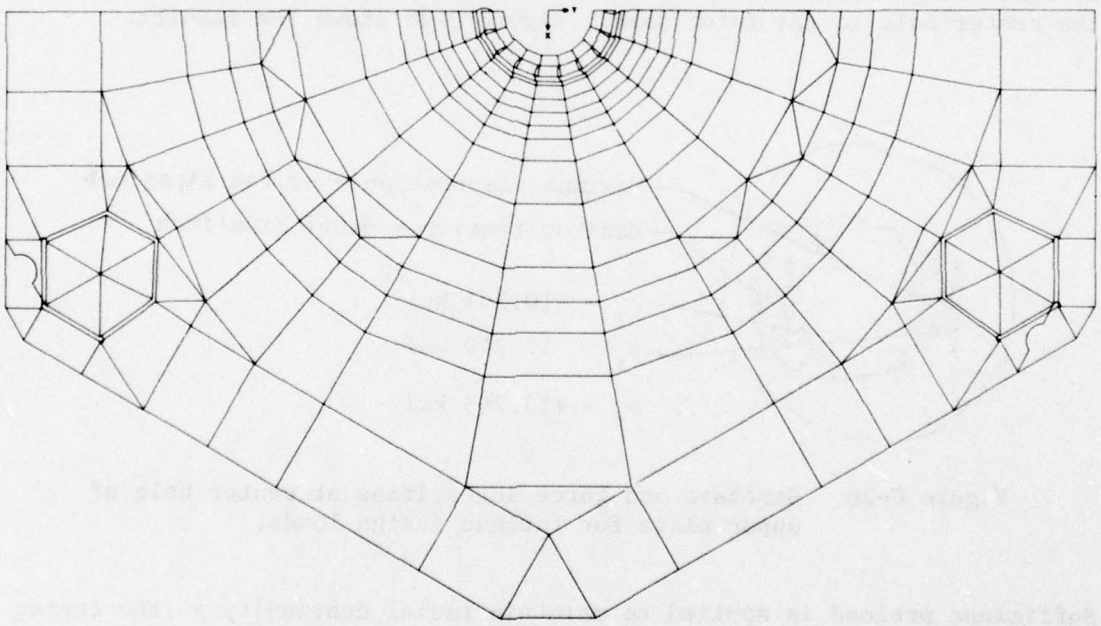


Figure C-29. Finite-element model of upper plate for prediction of strains during fatigue test of model hub.

LOWER PLATE

Lugs at Lead-Lag Pin

Figure C-30 shows the finite-element model that was used for the analysis of the lower plate. It has 222 nodes and 272 elements. In the vicinity of the hole, this model was very similar to those already described for the element specimen and the upper plate. In the case of the lower plate, Table C-6 shows that the loads are nearly uniform at all azimuth positions. Because of this near symmetry of loading, the plate was analyzed assuming it to be symmetrically loaded, and thus, only one-eighth of the surface was needed in the model.

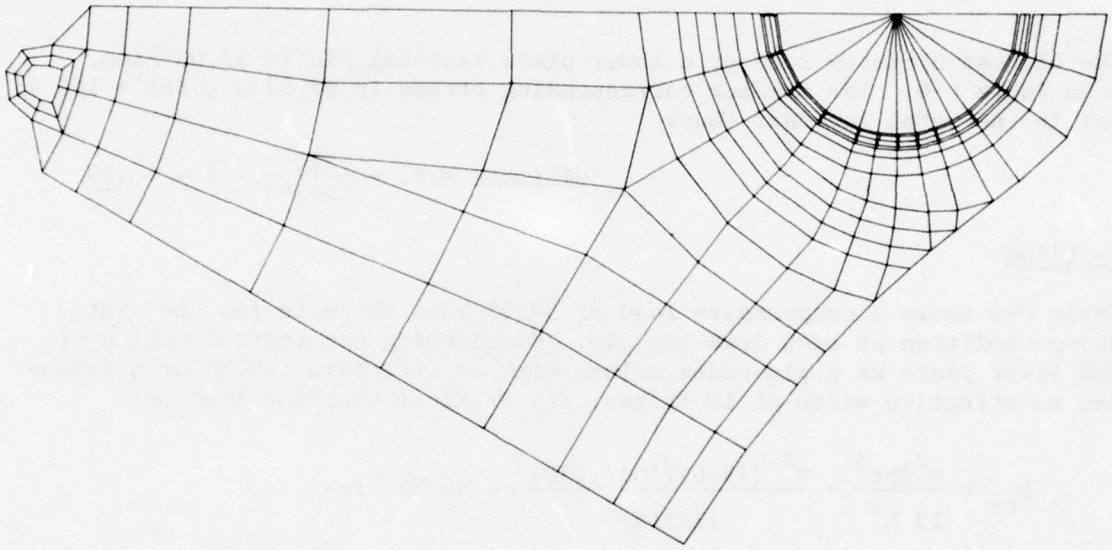


Figure C-30. Finite-element model for analysis of lower plate.

The analysis showed that the tangential stress in the steel at the edge of the hole was 1.561 ksi/kip of axial load. Thus, for the fatigue condition, the stress varied from a high of 1.561 x 49.33 = 77.00 ksi to a low of 1.561 x 45.04 = 70.31, corresponding to 73.66 $\pm$ 3.35 ksi. From Figure C-31, the allowable alternating stress is 18.44 ksi, thus:

$$\text{Fatigue M.S.} = \frac{18.44}{3.35} - 1 = \underline{4.50}$$

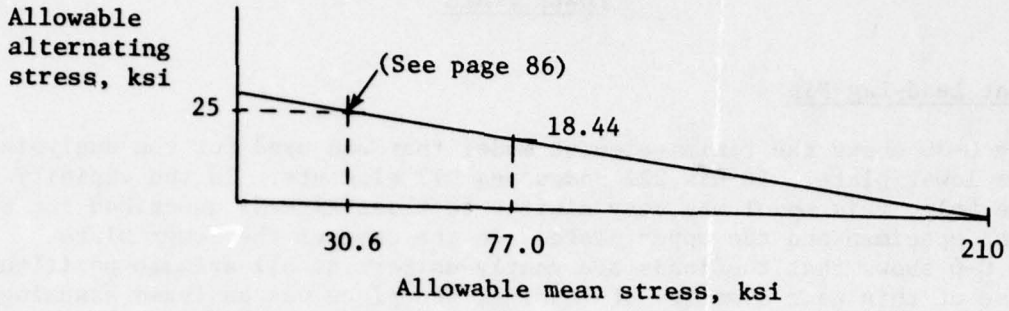


Figure C-31. Allowable alternating stress versus mean stress for steel laminae.

The highest ultimate load at a lower plate lead-lag pin is 97.02 kips, from Table C-6. The maximum corresponding stress is 97.02 x 1.561 = 151.45 ksi in the metal laminae, thus:

$$\text{Ultimate M.S.} = \frac{210}{151.45} - 1 = +\underline{.39}$$

Buckling

Table C-6 shows a compressive load of 30.55 kips ultimate for the static droop condition at each lead-lag pin. Considering the central region of the lower plate as a pin-ended column with an effective length of 8 inches and an effective width of 10 inches, its critical buckling load is:

$$P_{cr} = \frac{\pi^2 Ebt^3}{12\,L^2} = \frac{\pi^2\,(7540)(10)(.330)^3}{(12)(8)^2} = 34.82 \text{ kips}$$

$$\text{Ultimate Buckling M.S.} = \frac{34.82}{30.55} - 1 = +\underline{.14}$$

Scalloped Lug at Inner Hole

The bolt holes were sized and positioned so that the lower plate could deform in response to the centrifugal forces without inducing radial loads at the bolts. Thus, the primary load on the lug was torque. Table C-3 shows the ultimate torque to be 2480 x 1.5 = 3720 in.-kips. Assuming that the torque divides equally to the lower and pan plates, the force per bolt = 3720/(12 x 6.2 x 2) = 25 kips. Figure C-32 shows the geometry of the scalloped lugs on the fitting at the center of the lower plate and the scalloped flange on the rotor shaft.

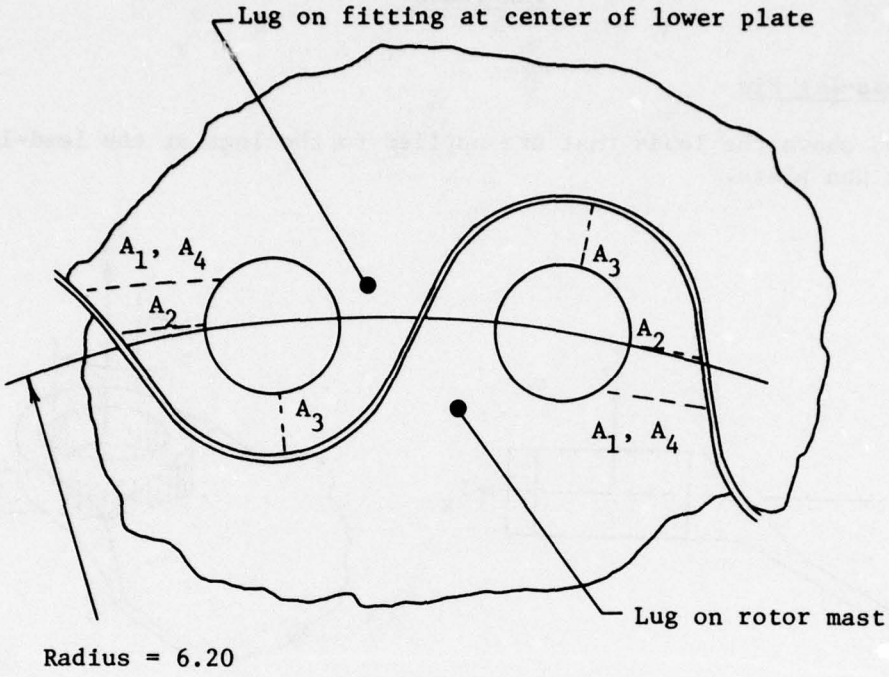


Figure C-32. Lug geometry at scalloped flanges.

Using Reference 18, the ultimate strength for transverse loading, P_{tru}, is calculated as:

$A_1 = .72\ t$
$A_2 = .46\ t$
$A_3 = .31\ t$
$A_4 = .72\ t$
$D = .75$
$t = .35$

$$\frac{A_{av}}{A_{br}} = \left(\frac{6}{3/A_1 + 1/A_2 + 1/A_3 + 1/A_4}\right)\frac{1}{Dt}$$

$$\frac{A_{av}}{A_{br}} = \left(\frac{6}{3/.72 + 1/.46 + 1/.31 + 1/.72}\right)\frac{1}{.75} = .730$$

$$P_{tru} = K_{tru}\ Dt\ F_{tu} = .957 \times .75 \times .35 \times 130 = 32.66 \text{ kips}$$

Ultimate lug shear, M.S. $= \frac{32.66}{25.00} - 1 = +\underline{.31}$

18. Melcon, M. A., and Hoblit, F. M., DEVELOPMENTS IN THE ANALYSIS OF LUGS AND SHEAR PINS, Product Engineering, June 1953.

PAN PLATE

Lugs at Lead-Lag Pin

Figure C-33 shows the loads that are applied to the lugs at the lead-lag pin in the pan plate.

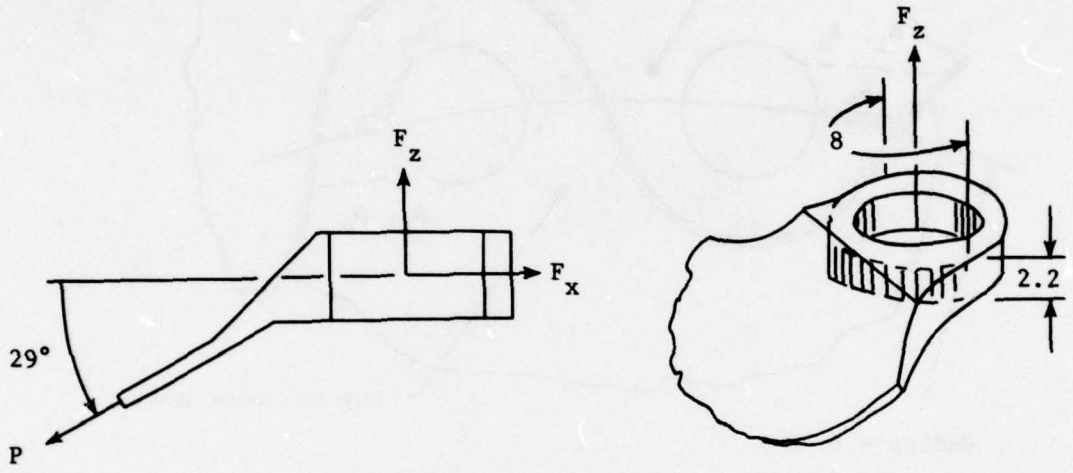


Figure C-33. Lug at lead-lag pin of pan plate.

The margins of safety for the F_x component of load are established by comparison of loads to those of the upper plate. Each lug in the pan plate contains the same number and thickness of steel laminae as the lugs in the upper plate. In addition, the pan plate lugs have many more plies of composite to help support the load. Thus, for F_x components, it is conservative to assume for the pan plate that the steel stresses at the edge of the hole are the same as would be present in the upper plate for the same load. Use, from Figure C-25, the maximum tangential stress at the inner edge of the hole = 1.347 ksi/kips of F_x component of load. From Table C-6, for the fatigue condition, the alternating stress is then:

$$\pm (\cos 29°)(37.15)(1.347)/2 = \pm 21.88 \text{ ksi}$$

$$\text{Fatigue M.S.} = \frac{25.00}{21.88} - 1 = +\underline{.14}$$

NOTE: The - 11.16 kips load in Table C-6 for the fatigue condition produces a positive stress at the critical section, and thus, the greatest range of stress occurs between loads 0 and 37.15 kips.

The stress at ultimate load is similarly found from Table C-6 loads as:

$$(\cos 29°)(106.36)(1.347) = 125.3 \text{ ksi}$$

$$\text{Ultimate M.S.} = \frac{210}{125.3} - 1 = +\underline{.67}$$

The force F_z is assumed to produce a transverse shear that causes interlaminar shear. The shear area is considered to be 8.0 x 2.2 = 17.60 in., as shown in Figure C-32. The maximum shear is assumed to be 1.4 times the average shear. For the fatigue condition, Table C-5 shows that F_z varies from - 5.41 to 18.01 kips, corresponding to $F_z = 6.3 \pm 11.71$ kips. The alternating shear stress is:

$$\pm 1.40\ F_z/A = \pm 1.40 \times 11.71/17.6 = .93 \text{ ksi}$$

$$\text{Fatigue, composite interlaminar, M.S.} = \frac{2.5}{.93} - 1 = +\underline{1.69}$$

$$\text{Fatigue, adhesive, M.S.} = \frac{1.0}{.93} - 1 = +\underline{.07}$$

At the ultimate load (from Table C-6), the shear stress is:

$$1.40\ F_z/A = 1.40 \times \sin 29° \times 106.36/17.6 = 4.10 \text{ ksi}$$

$$\text{Ultimate, composite interlaminar, M.S.} = \frac{10.0}{4.1} - 1 = +\underline{1.44}$$

$$\text{Ultimate, adhesive, M.S.} = \frac{5.0}{4.1} - 1 = +\underline{.22}$$

Scarf Joint

The most important load on the scarf joint is the alternating membrane force produced by hub moment. These forces are found using the general solution given in Reference 19 for a conical shell loaded at its vertex. Figure C-34 shows the geometry and equations for the composite plate hub.

For the fatigue design condition:

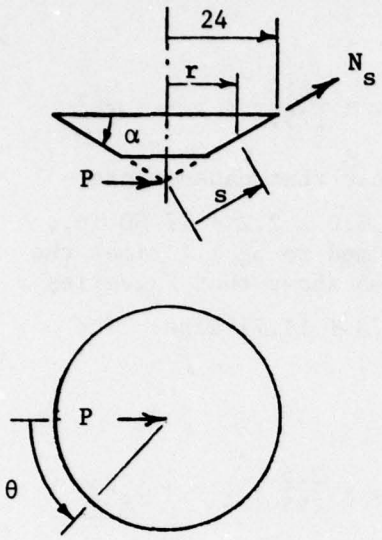
$$M = 800 \text{ in.-kips from Table C-3}$$

$$N_s = \pm .002487 \times 800 = 1.99 \text{ kip/inch}$$

$$\text{Shear stress} = \frac{N_s}{A} = \pm \frac{1.99}{5} = \pm .398 \text{ ksi}$$

$$\text{Fatigue M.S.} = \frac{.80}{.398} - 1 = +\underline{1.01}$$

19. Flugge, W., STRESSES IN SHELLS, Berlin, Springer-Verlag, 1960.



$$N_s = \frac{P \cos \theta}{\pi r \cos \alpha}$$, force/unit width

M = Hub moment

$$P = \frac{M}{24 \tan \alpha}$$

$$N_s = \frac{M \cos \theta}{24 \pi r \sin \alpha}$$

For: $\alpha = 29°$, $\theta = 0°$ and $180°$, $r = 11$ inches

Peak $N_s = \pm .002487$ M, kip/inch at scarf joint of pan plate

Figure C-34. Membrane forces in conical shell loaded at its vertex.

For the ultimate TW7F2 condition:

M = 1500 x 1.5 = 2250 in.-kips (ult) from Table C-3

Thrust = 85.8 x 1.5 = 128.7 kips (ult)

$(N_s)_{\text{hub moment}}$ = .002487 x 2250 = 5.60 in.-kips (ult)

$$(N_s)_{\text{thrust}} = \frac{128.7}{2\pi r \sin 29°} = \frac{128.7}{2\pi \times 11 \times \sin 29°} = 3.84 \text{ in.-kips (ult)}$$

$$\text{Shear stress} = \frac{N_s}{A} = \frac{5.60 + 3.84}{5} = 1.89 \text{ ksi}$$

$$\text{Ultimate M.S.} = \frac{4.00}{1.89} - 1 = +\underline{1.12}$$

For the ultimate load burst condition:

Rotor torque on pan plate = .5 x 2480 x 1.5 = 1860 in.-kips (ult)

$$\text{Shear stress} = \frac{\text{Torque}}{\text{Area} \times r} = \frac{1860}{2\pi \times 11 \times 5 \times 11} = .49 \text{ ksi}$$

$$\text{Ultimate M.S.} = \frac{4.00}{.49} - 1 = +\underline{7.16}$$

ROTOR SHAFT AND ATTACHMENTS

Shaft

The fatigue condition produces a horizontal shear of 800/(24 tan 29°) = 60.13 kips at the top of the shaft. Table C-12 presents the margins of safety for bending and shear at increments of 1 inch below the upper plate. The margins of safety were calculated using an allowable stress of 25 ksi in bending and 17.672 ksi in shear. These allowables are compatible; they produce equal octahedral shears, as shown below:

$$\text{In tension test, } \tau_{oct} = \frac{\sigma}{\sqrt{3}} = \frac{25}{\sqrt{3}} = 14.43 \text{ ksi}$$

$$\text{In pure shear test, } \tau_{oct} = \sqrt{\frac{2}{3}}\,\tau = \sqrt{\frac{2}{3}} \times 17.672 = 14.43 \text{ ksi}$$

The stresses were calculated using elementary beam formulas:

$$\sigma = \frac{Mc}{I} = \frac{10.186\ MD}{(D^4 - d^4)} \qquad \text{and,} \qquad \tau = 1.4\,\frac{V}{A} = \frac{1.783\ V}{(D^2 - d^2)}$$

where

D = outer diameter

d = inner diameter

M = moment

V = shear = 60.13 kips for fatigue condition

The ultimate margins of safety can be conservatively calculated using the formula derived below:

$$(M.S.)_{ult} = \frac{(Allow.)_{ult}}{(Actual)_{ult}} \times \frac{(Actual)_{fatigue}}{(Allow.)_{fatigue}} \times \frac{(Allow.)_{fatigue}}{(Actual)_{fatigue}} - 1$$

$$(M.S.)_{ult} = \frac{(Allow.)_{ult}}{(Allow.)_{fatigue}} \times \frac{(Actual)_{fatigue}}{(Actual)_{ult}} \times \frac{(Allow.)_{fatigue}}{(Actual)_{fatigue}} - 1$$

Thus:

$$(M.S.)_{ult} = \frac{150}{25} \times \frac{800}{1500} \times \frac{(Allow.)_{fatigue}}{(Actual)_{fatigue}} - 1$$

$$(M.S.)_{ult} = 3.2 \times (M.S.)_{fatigue} + 2.2$$

TABLE C-12. MARGINS OF SAFETY FOR ROTOR SHAFT, FATIGUE

x	M	D	d	σ	τ	M.S., σ	M.S., τ
0	0	6.08	4.18	0	5.50	High	+ 2.21
1	60.13	6.61	4.18	2.53	4.09	High	+ 3.32
2	120.36	7.00	6.41	12.04	13.56	+ 1.08	+ .30
3	180.39	7.40	6.90	18.59	15.00	+ .35	+ .18
4	240.52	7.80	7.25	20.37	12.96	+ .23	+ .36
5	300.65	8.20	7.60	21.20	11.31	+ .18	+ .56
6	360.78	8.60	7.98	22.35	10.43	+ .12	+ .69
7	420.91	9.00	8.30	21.27	8.86	+ .18	+ 1.00
8	481.04	9.40	8.37	15.89	5.86	+ .57	+ 2.02
9	541.17	9.80	8.37	12.52	4.13	+ 1.00	+ 3.28

The lowest ultimate margins of safety are then:

Bending, Ultimate M.S. = 3.2 x .12 + 2.2 = 2.58

Shear, Ultimate M.S. = 3.2 x .18 + 2.2 = 2.78

Main Attachment Bolts

Ultimate torque = 2480 x 1.5 = 3720 in.-kips (ult)

12 - 3/4-in. diam. bolts on 6.2 in. radius

$$\text{Force/bolt} = \frac{T}{nR} = \frac{3720}{12 \times 6.2} = 50.00 \text{ kips (ult)}$$

Use 180-ksi bolts, double shear strength = 95.4 kips

$$\text{Ultimate M.S.} = \frac{95.4}{50.0} - 1 = + .91$$

Lug, Torque

Figure C-32 shows the geometry of the lug. From preceding bolt calculation, the ultimate load per hole is 50 kips. Using Reference 18, the ultimate strength for transverse loading, P_{tru}, is calculated as:

$$A_1 = .58\ t \qquad \frac{A_{av}}{A_{br}} = \left(\frac{6}{3/A_1 + 1/A_2 + 1/A_3 + 1/A_4}\right)\frac{1}{Dt}$$

$$A_2 = .38\ t$$

$$A_3 = .33\ t$$

$$A_4 = .58\ t \qquad \frac{A_{av}}{A_{br}} = \left(\frac{6}{3/.58 + 1/.38 + 1/.33 + 1/.58}\right)\frac{1}{.75} = .637$$

$$D = .75$$

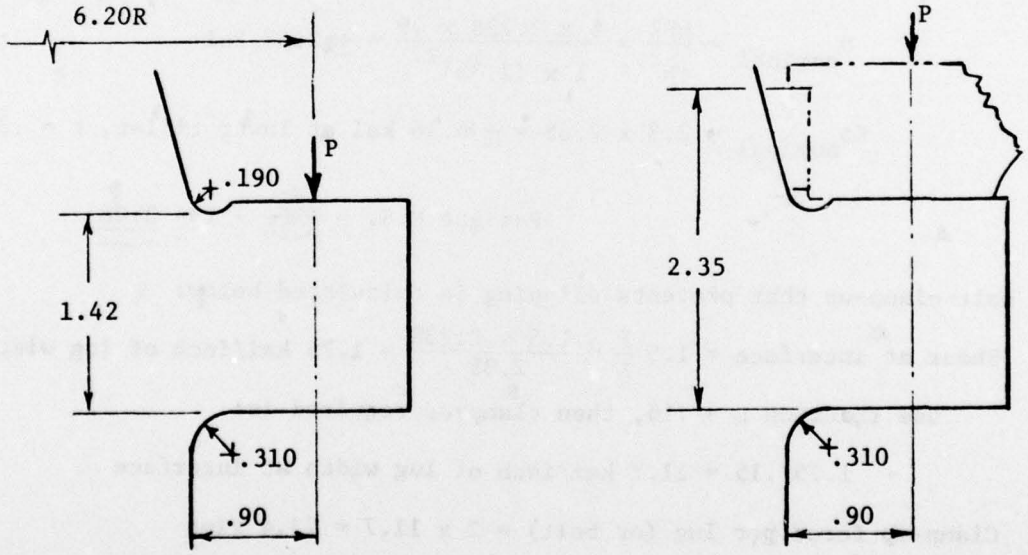
$$t = 1.55$$

$$P_{tru} = K_{tru} Dt\ F_{tu} = .835 \times .75 \times 1.55 \times 160 = 155.31 \text{ kips}$$

$$\text{Ultimate M.S.} = \frac{155.31}{50.0} - 1 = \underline{2.11}$$

Lug, Bending

First, the bending stresses are calculated assuming no clamp-up pressure between the pan plate and the lug. It is found, even with this very conservative assumption, that the bending stresses are well below the endurance limit. Then, the bending stress and margins of safety are calculated assuming clamp-up that prevents slipping between the pan plate and the lug. The bolt clamp-up to prevent slipping is shown to be an attainable 33 percent of the ultimate strength of the bolt. Figure C-35 shows the geometry at the lug.



Without bolt clamp-up

With bolt clamp-up

Figure C-35. Attachment lug on rotor shaft.

Using the equation for N_s from Figure C-34, the fatigue condition without bolt clamp-up produces:

$$\text{Alternating } N_s = \frac{M \cos \theta}{24\pi \, r \sin \alpha} = \pm \frac{800}{24\pi \times 6.2 \times \sin 29^\circ}$$

$$= \pm 3.53 \text{ kips/inch}$$

Use, $$P = 3.53 \times \sin 29 \times \frac{3.2}{2.0} = 2.738 \text{ kips/inch of lug width}$$

($\frac{3.2}{2.0}$ ← ratio of loaded arc to lug width)

$\sigma_{nominal}$ = bending stress without stress concentration factor, K

$$\sigma_{nominal} = \frac{6P\ell}{th^2} = \frac{6 \times 2.738 \times .9}{1 \times (1.42)^2} = \pm 7.33 \text{ ksi}$$

$K\sigma_{nominal} = 2.3 \times 7.33 = \pm 16.86$ ksi at upper fillet, r = .19

$K\sigma_{nominal} = 1.92 \times 7.33 = \pm 14.07$ ksi at lower fillet, r = .31

Assuming bolt clamp-up, the fatigue condition produces:

$$\sigma_{nominal} = \frac{6P\ell}{th^2} = \frac{6 \times 2.738 \times .9}{1 \times (2.35)^2} = \pm 2.68 \text{ ksi}$$

$K\sigma_{nominal} = 2.3 \times 2.68 = \pm 6.16$ ksi at lower fillet, r = .31

$$\text{Fatigue M.S.} = \frac{25}{6.16} - 1 = \underline{3.06}$$

The bolt clamp-up that prevents slipping is calculated below:

$$\text{Shear at interface} \simeq 1.5 \frac{P}{A} = \frac{1.5 \times 2.738}{2.35} = 1.75 \text{ ksi/inch of lug width}$$

Use friction $\mu = .15$, then clamp-up required is:

$1.75/.15 = 11.7$ ksi/inch of lug width at interface

Clamp-up force per lug (or bolt) = $2 \times 11.7 = 23.4$ kips

The ultimate tensile strength of a 3/4-inch bolt at 180 ksi is 71.2 kips. Thus, a clamp-up of 33 percent of the ultimate bolt strength prevents slippage.

Bolts at Top of Shaft

The axial force required to seat the cone provides the design loads for the bolts and the ring at the top of the rotor shaft. The axial force is estimated from the free-body diagram of the cone shown in Figure C-36.

Use friction coefficient, $\mu = .15$, thus, $\phi = \tan^{-1} .15 = 8.53°$. The radial force, 10.31 kips/inch, was established on page 190.

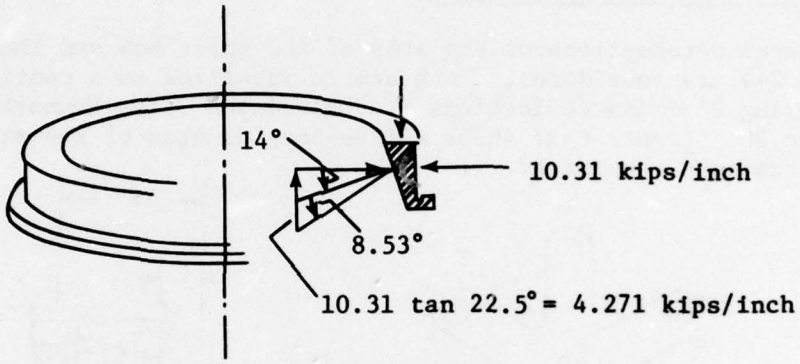


Figure C-36. Cone at top of rotor shaft.

The total axial force = $4.271 \times 6.6 \times \pi = 88.56$ kips.

Force/bolt = 88.56/12 = 7.38 kips (LIMIT)

Use 180-ksi bolts, 3/8-inch diameter, ultimate tensile strength = 17.1 kips.

$$\text{Ultimate M.S.} = \frac{17.1}{7.38 \times 1.5} - 1 = +\underline{.54}$$

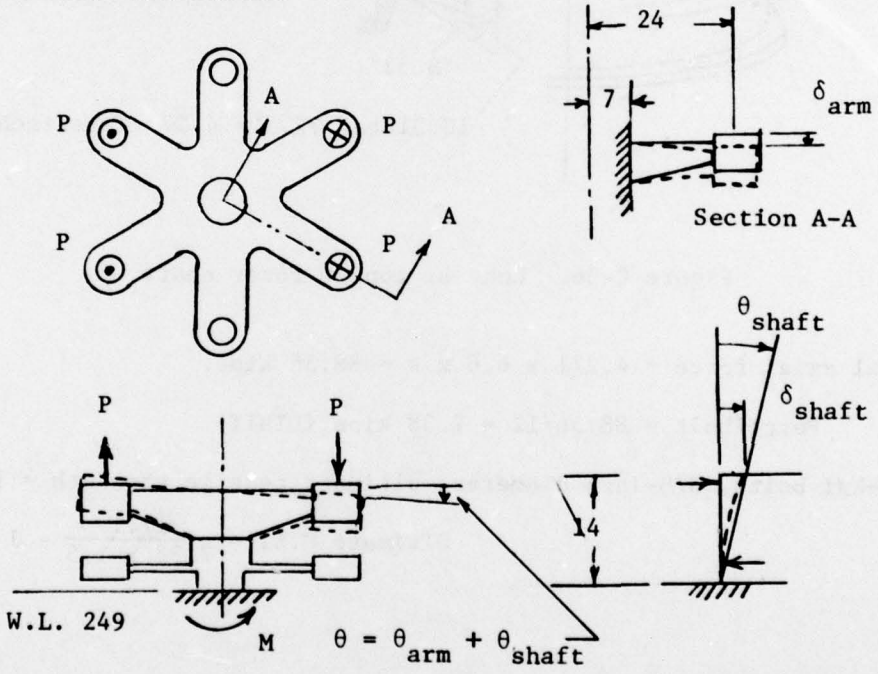
DYNAMIC COMPATIBILITY

Introduction

This section presents the calculations for the stiffnesses shown in Table 6. The stiffnesses for the titanium hub are theoretical stiffnesses. Those for the composite plate hub are experimental stiffnesses calculated from the deflection gage data presented in Figure 12.

Moment Stiffness for Titanium Hub

The flexural deformations of the arms of the upper hub and the rotor shaft above WL 249 are considered. Each arm is idealized as a cantilevered beam with varying EI. Its deflections are calculated using Newmark's Method, Reference 20. Figure C-37 shows a free-body diagram of the structure and the deformations considered.



$$\theta_{arm} = \delta_{arm}/(.866 \times 24) \qquad \theta_{shaft} = \delta_{shaft}/14$$

$$\text{Moment stiffness} = M/\theta = M/(\theta_{arm} + \theta_{shaft})$$

Figure C-37. Deformations of titanium hub from head moment.

20. Newmark, N. M., NUMERICAL PROCEDURE FOR COMPUTING DEFLECTIONS, MOMENTS AND BUCKLING LOADS, Transactions of the American Society of Civil Engineers, New York, 1943.

Figure C-38 shows approximate dimensions for the present hub scaled from Reference 21.

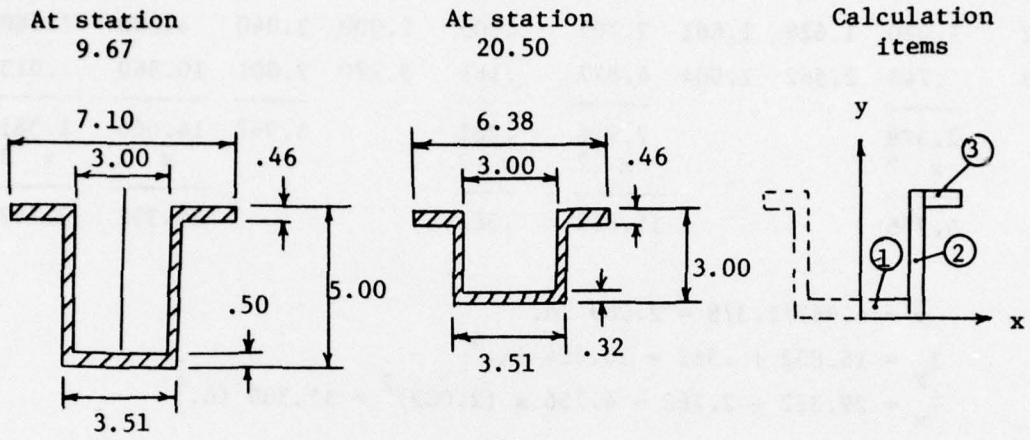


Figure C-38. Approximate sections for present titanium hub.

Station 9.67 Section Properties

Item	A	x	Ax	Ax^2	$I_{y\ elem}$	y	Ay	Ay^2	$I_{x\ elem}$
1	.750	.750	.562	.422	.141	.250	.187	.047	.016
2	1.275	1.628	2.076	3.379	.007	2.500	3.187	7.969	2.656
3	.826	2.653	2.191	5.814	.222	4.770	3.940	18.794	.015
	2.851			9.615	.370		7.314	26.810	2.687
	x 2			x 2	x 2			x 2	x 2
	5.702			19.230	.740			53.620	5.374

$\bar{y} = 7.314/2.851 = 2.565$ in.

$I_y = 19.230 + .740 = 19.970$ in.^{4}

$I_x = 53.62 + 5.374 - 5.702 \times (2.565)^2 = 21.479$ in.^{4}

21. Drawings Number 65100-1100, Sheet 4, and 65103-11000, Sheet 5, Sikorsky Aircraft Division , United Aircraft Corporation, Stratford, Connecticut, 1963.

Station 15.08 Section Properties

Item	A	x	Ax	Ax^2	$I_{y\ elem}$	y	Ay	Ay^2	$I_{x\ elem}$
1	.615	.750	.461	.346	.115	.205	.126	.026	.008
2	1.020	1.628	1.661	2.703	.005	2.000	2.040	4.080	1.360
3	.743	2.562	1.904	4.877	.161	3.770	2.801	10.560	.013
	2.378			7.926	.281		4.967	14.666	1.381
	x 2			x 2	x 2			x 2	x 2
	4.756			15.852	.562			29.332	2.762

$\bar{y} = 4.967/2.378 = 2.089$ in.

$I_y = 15.852 + .562 = 16.414$ in.^{4}

$I_x = 29.332 + 2.762 - 4.756 \times (2.089)^2 = 11.339$ in.^{4}

Station 20.50 Section Properties

Item	A	x	Ax	Ax^2	$I_{y\ elem}$	y	Ay	Ay^2	$I_{x\ elem}$
1	.480	.750	.360	.270	.090	.160	.077	.012	.004
2	.765	1.628	1.245	2.028	.004	1.500	1.147	1.721	.574
3	.660	2.472	1.632	4.033	.113	2.770	1.828	5.064	.012
	1.905			6.331	.207		3.052	6.797	.590
	x 2			x 2	x 2			x 2	x 2
	3.810			12.662	.414			13.594	1.180

$\bar{y} = 3.052/1.905 = 1.602$ in.

$I_y = 12.662 + .414 = 13.076$ in.^{4}

$I_x = 13.594 + 1.180 - 3.810 \times (1.602)^2 = 4.996$ in.^{4}

Figure C-39 shows curves of approximate moments of inertia for an arm of the present titanium hub.

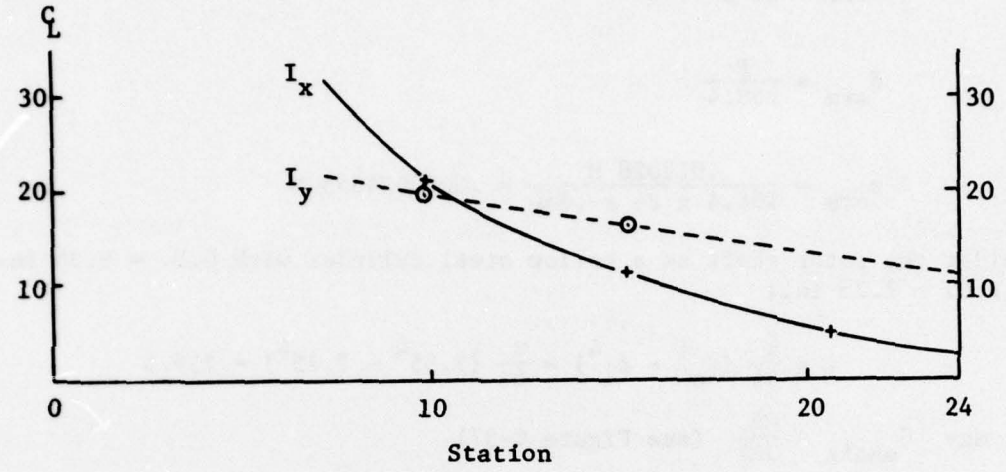
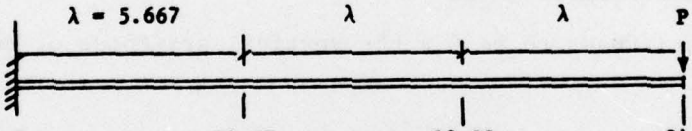


Figure C-39. Approximate I_x and I_y for arm of titanium hub.

Consider the hub arm as a simple beam cantilevered at station 7.



Sta.	7		12.67		18.33	24	
I_x	32		15.5		7.4	2.5	
M	3		2		1	0	$P\lambda$
α	.09375		.12903		.13514	0	$P\lambda/E$
$\bar{\alpha}$	.64765		1.51919		1.48043	.34091	$P\lambda^2/12E$
ϕ	0	.64765		2.16684		3.64727	3.98818 $P\lambda^2/12E$
δ	0		.64765		2.81449	6.46176	$P\lambda^3/12E$

$$\text{Vertical stiffness of arm} = \frac{P}{\delta} = \frac{12\,E}{6.46176\,\lambda^3} = \frac{12 \times 16500}{6.46176\,(5.667)^3} = 168.4 \text{ kips/in.}$$

Head Moment = 4 P x 24 x .866 (see Figure C-37)

$$\therefore P = .012028\ M$$

$$\theta_{arm} = \frac{\delta_{arm}}{24 \times 8.66}$$

$$\delta_{arm} = \frac{P}{168.4}$$

$$\therefore \theta_{arm} = \frac{.012028\ M}{168.4 \times 24 \times .866} = .0000034655\ M$$

Consider the rotor shaft as a hollow steel cylinder with O.D. = 9.35 in. and I.D. = 7.25 in.:

$$I = \frac{\pi}{64}(d_o^4 - d_i^4) = \frac{\pi}{64}(9.35^4 - 7.25^4) = 239.5$$

Say $\theta_{shaft} \simeq \frac{M\ell}{3EI}$ (see Figure C-37)

$$\theta_{shaft} = \frac{14\ M}{3 \times 29000 \times 239.5} = .000000672\ M$$

$$\theta = \theta_{arm} + \theta_{shaft} = .000004137\ M$$

$$\text{Moment stiffness} = \frac{M}{\theta} = 241700.\ \text{in.-kips/rad.}$$

Thrust Stiffness for Titanium Hub

Consider thrust stiffness to be 6 x the vertical stiffness of an individual arm:

$$\therefore \text{Thrust stiffness} = 6 \times 168.4 = 1010.\ \text{kips/in.}$$

Torque Stiffness for Titanium Hub

Torque causes flexural deflections of the arms of the upper hub and the lower plate and, in addition, a twist of the rotor shaft. Both components of deformation are considered in the calculation of the torque stiffness. Figure C-40 shows the deformations. The angle β will be different for the upper hub and the lower plate. The torque stiffness is calculated using the average β.

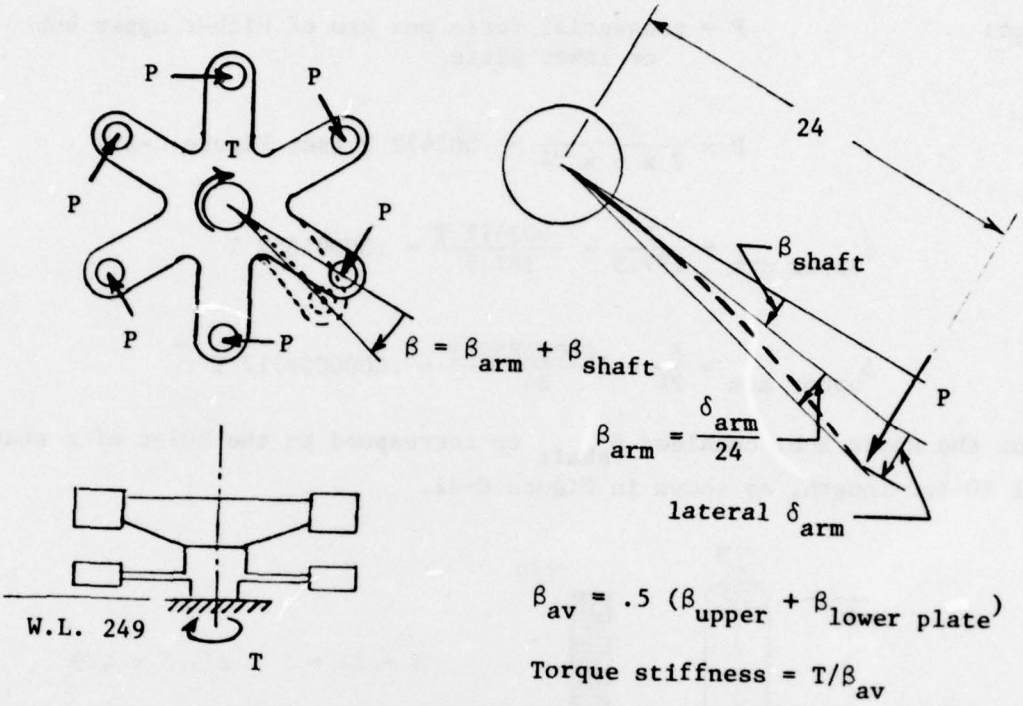
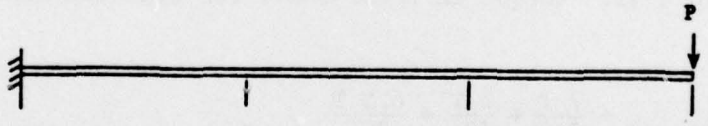


Figure C-40. Deformations of titanium hub from torque.

Consider the upper hub as a simple beam cantilevered at station 7.



I_y		21.5		18.		14.5		11.0		
M		3		2		1		0		$P\lambda$
α		.1395		.1111		.0690		0		$P\lambda/E$
$\bar{\alpha}$		.78705		1.3195		.8011		.1514		$P\lambda^2/12E$
ϕ	0		.78705		2.10655		2.90765		3.05905	$P\lambda^2/12E$
δ		0		.78705		2.8936		5.80125		$P\lambda^3/12E$

Tangential stiffness of upper arm (torque loading) $= \frac{P}{\delta} = \frac{12\ E}{5.80125\ \lambda^3} = \frac{12 \times 16500}{5.80125(5.667)^3} = 187.5$ kips/in.

Consider the total torque, T, to divide equally to the upper hub and the lower plate.

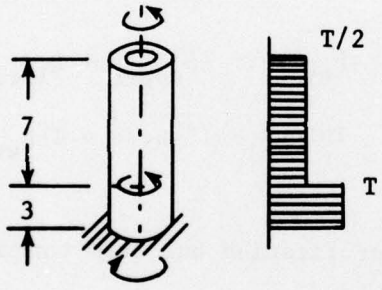
Let: P = tangential force per arm of either upper hub or lower plate

$$P = \frac{T}{2 \times 6 \times 24} = .003472\ T \text{ (see Figure C-39)}$$

$$\delta_{\text{upper arm}} = \frac{P}{187.5} = \frac{.003472\ T}{187.5} = .00001852\ T$$

$$\delta_{\text{upper arm}} = \frac{\delta}{24} = \frac{.00001852\ T}{24} = .0000007717\ T$$

For the upper hub, consider β_{shaft} to correspond to the twist of a shaft of 10-in. length, as shown in Figure C-41.



$$J = 2I = 2 \times 239.5 = 479$$

Figure C-41. Torque in rotor shaft for titanium hub.

$$\beta_{\text{shaft upper arm}} = \frac{7\ T}{2JG} + \frac{3\ T}{JG} = \frac{6.5\ T}{JG}$$

$$\beta_{\text{shaft upper arm}} = \frac{6.5\ T}{479 \times 11000} = .000001234\ T$$

$$\beta_{\text{upper hub}} = \beta_{\text{upper arm}} + \beta_{\text{shaft upper arm}}$$

$$\beta_{\text{upper hub}} = .000002005\ T$$

Consider the lower plate to consist of radial beams cantilevered from station 10.0.

Consider the beams to be of constant width = .375 in. and constant depth = 6.0 in. (for tangential loadings):

$$I = \frac{1}{12} bd^3 = \frac{1}{12} (.375)(6)^3 = 6.75$$

$$\delta_{\text{lower arm}} = \frac{PL^3}{3EI} = \frac{(.003472)\ T\ (14)^3}{(3)(16500)(6.75)} = .00002851\ T$$

$$\beta_{\text{lower arm}} = \frac{\delta}{24} = .000001188\ T$$

For lower plate, consider β_{shaft} to correspond to the twist of a shaft of 3-in. length:

$$\beta_{\text{shaft lower arm}} = \frac{3\ T}{JG}$$

$$\beta_{\text{shaft lower arm}} = \frac{3\ T}{479 \times 11000} = .0000005694\ T$$

$$\beta_{\text{lower plate}} = \beta_{\text{lower arm}} + \beta_{\text{shaft lower arm}}$$

$$\beta_{\text{lower plate}} = .000001757\ T$$

$$\beta_{av} = .5\ (\beta_{\text{upper hub}} + \beta_{\text{lower plate}})$$

$$\beta_{av} = .5\ (.000002005 + .000001757)\ T$$

$$\beta_{av} = .000001881\ T$$

$$\text{torque stiffness} = \frac{T}{\beta_{av}} = 531632\ \text{in.-kips/rad.}$$

Moment Stiffness for Composite Plate Hub

gage 3, .0625 - .0180 = .0445 in.

gage 4, - .023 - .0205 = - .0435 in.

α = tilt angle = (.0445 - [- .0435]) ÷ 20.78

= .004235 rad.

moment stiffness = M/α = 164.25 ÷ .004235 = 38784 in.-kips/rad. (model)

corresponding full scale = 38784 x 8 = 310270 in.-kips/rad. (prototype)

Thrust Stiffness for Composite Plate Hub

gage 3, upper plate .0180 (conservatively adjusted from raw .011)

gage 4, upper plate .0205

average = .0385 ÷ 2 = .01925 in.

vertical stiffness = Thrust/δ = 21.45 ÷ .01925 = 1114 kips/in. (model) assembly

corresponding full scale = 114 x 2 = 2228 kips/in. (prototype) assembly

Torque Stiffness for Composite Plate Hub

gage 1, pan plate .015

gage 2, lower plate .0215

average = .0365 ÷ 2 = .01825 in.

average twist = θ = .01825 ÷ 12 = .001521 rad.

torsional stiffness = T/θ = 296.6 ÷ .001521 = 195000 in.-kips/rad. (model)

corresponding full scale = T/θ = 195000 x 8 = 1,560,000 in.-kips/rad. (prototype)